

Report No. FHWA-RD-77-66

PB296607



# OVERLAY DESIGN AND REFLECTION CRACKING ANALYSIS FOR RIGID PAVEMENTS

Vol. 1 Development of New Design Criteria



August 1977

Final Report

Document is available to the public through  
the National Technical Information Service,  
Springfield, Virginia 22161

Prepared for

**FEDERAL HIGHWAY ADMINISTRATION**  
**Offices of Research & Development**  
**Washington, D.C. 20590**

REPRODUCED BY  
**NATIONAL TECHNICAL  
INFORMATION SERVICE**  
U. S. DEPARTMENT OF COMMERCE  
SPRINGFIELD, VA. 22161



1. Report No. FHWA-RD-77-66		2. Government Accession No.		3. Recipient's Catalog No. <b>PB296607</b>	
4. Title and Subtitle Overlay Design and Reflection Cracking Analysis for Rigid Pavements Vol. 1. Development of New Design Criteria				5. Report Date August 1977	
				6. Performing Organization Code	
7. Author(s) Harvey J. Treybig, B. Frank McCullough, Phil Smith and Harold Von Quintus				8. Performing Organization Report No.	
9. Performing Organization Name and Address Austin Research Engineers Inc 2600 Dellana Lane Austin, Texas 78746				10. Work Unit No. (TRAIS) FCP 35D2-202	
				11. Contract or Grant No. DOT-FH-11-8544	
12. Sponsoring Agency Name and Address Offices of Research and Development Federal Highway Administration U.S. Department of Transportation Washington, D.C. 20590				13. Type of Report and Period Covered Phases II and III Final Report	
				14. Sponsoring Agency Code <b>S0856</b>	
15. Supplementary Notes FHWA Contract Manager: R. A. McComb (HRS-14)					
16. Abstract Fatigue cracking and reflection cracking criteria were developed and incorporated into a design procedure for flexible and rigid overlays of rigid pavements. Linear elastic layered theory is the basic model used to compute stresses and strains in the pavement system, which are then input to the fatigue and reflection cracking models. The fatigue criteria developments resulted from analyses of the performance of rigid pavements at the AASHO Road Test. A regression analysis was performed to obtain a fatigue equation relating stress and wheel load repetitions prior to Class 3 and 4 cracking. The effects of voids beneath the pavement as well as the condition of joints are also considered in the fatigue criteria. The reflection cracking criteria developed resulted from a study of the mechanics of reflection cracking and literature reviews. Mechanistic equations were derived and incorporated into an analysis model for use in design. This volume is the first in a series. The other is: Overlay Design and Reflection Cracking Analysis for Rigid Pavements - Vol. 2. Design Procedures, FHWA Report No. FHWA-RD-77-67.					
17. Key Words pavement, overlays, fatigue cracking, reflection cracking, rigid overlays, flexible overlays, deflection analysis, pavement design, pavement evaluation			18. Distribution Statement No restrictions. This document is available to the public through the National Technical Information Service, Springfield, Virginia 22161.		
19. Security Classif. (of this report) Unclassified		20. Security Classif. (of this page) Unclassified			

## PREFACE

This is the first of a two-volume series concerning the design of flexible and rigid overlays for rigid pavements and analyses of flexible overlays for reflection cracking. Volume 2 which has been published separately, is a user manual for the design procedure developed and reported in this volume.

The work presented in these two reports was accomplished by a team including Harvey J. Treybig, B. F. McCullough, Phil Smith, Harold Von Quintus, Frank Carmichael, Jack O'Quin, Peter Jordahl, and Stephen Seeds. Appreciation is extended to W. Ronald Hudson for his technical assistance in certain phases of the project and also for review of the manuscript.

Support for the project was provided by the Federal Highway Administration, Office of Research and Development, Contract No. DOT-FH-11-8544. We are grateful for the technical coordination provided by Mr. Richard McComb, Contract Manager during this phase of the contract.

Austin Research Engineers Inc

TABLE OF CONTENTS

	Page
<b>CHAPTER I. INTRODUCTION</b>	
Background . . . . .	1
Need for New Criteria . . . . .	2
Current State-of-the-Art . . . . .	2
Objectives . . . . .	3
Scope of Study . . . . .	4
Outline of Report . . . . .	4
<b>CHAPTER II. CONCEPTS FOR UNIVERSAL OVERLAY DESIGN PROCEDURE</b>	
Evaluation of Existing Pavement . . . . .	8
Design Inputs . . . . .	10
Analysis for Overlay of Rigid Pavements . . . . .	12
Analysis for Overlay of Flexible Pavements . . . . .	22
Conclusion . . . . .	26
<b>CHAPTER III. DEVELOPMENT OF DESIGN CRITERIA</b>	
Effective Moduli for Cracked Layers . . . . .	27
Stress Adjustments for Corner and Edge Loads . . . . .	36
Consideration of Voids . . . . .	38
Fatigue Curve Development . . . . .	45
Evaluation of New Materials . . . . .	56
Summary . . . . .	69
<b>CHAPTER IV. REFLECTION CRACKING</b>	
Failure Mechanisms . . . . .	71
Preventative Methods Used . . . . .	77
Model Development . . . . .	100
Maintaining Reflection Cracks . . . . .	144
Guidelines for Data Collection and Analysis . . . . .	147
Treatment and Material Selection . . . . .	155
Summary . . . . .	155
<b>CHAPTER V. VERIFICATION OF DESIGN CONCEPTS</b>	
Verification of Deflection Concepts . . . . .	156
Illustrative Overlay Design Problem . . . . .	182
Application of Reflection Cracking Model . . . . .	203
<b>CHAPTER VI. SUMMARY, CONCLUSIONS, AND RECOMMENDATIONS</b>	
Summary . . . . .	213
Conclusions . . . . .	213
Recommendations . . . . .	215
<b>APPENDIXES</b>	
Appendix A. Derivation of Selected Reflection Cracking Equations . . . . .	217
<b>REFERENCES . . . . .</b>	229

1. The first part of the document discusses the importance of maintaining accurate records of all transactions and activities. It emphasizes that this is crucial for ensuring transparency and accountability in the organization's operations.

2. The second part of the document outlines the various methods and tools used to collect and analyze data. It highlights the need for consistent data collection procedures and the use of advanced analytical techniques to derive meaningful insights from the data.

3. The third part of the document focuses on the role of technology in data management and analysis. It discusses how modern software solutions can streamline data collection, storage, and processing, thereby improving efficiency and accuracy.

4. The fourth part of the document addresses the challenges associated with data management, such as data quality, security, and privacy. It provides strategies to mitigate these risks and ensure that the data remains reliable and secure throughout its lifecycle.

5. The fifth part of the document concludes by summarizing the key findings and recommendations. It stresses the importance of a data-driven approach in decision-making and the need for continuous monitoring and improvement of the data management process.

CHAPTER I  
INTRODUCTION  
Background

In 1970 the Comptroller General reported to the Congress relative to problems resulting from deterioration of pavements on the Interstate Highway system (Ref 1).<sup>1</sup> This report concluded that there were significant differences among the states regarding the methods used for evaluating the conditions of highway surfaces and the design procedures used to establish overlay thicknesses. It also stated that more precise procedures were necessary to insure that overlays were placed at proper times and to the proper thickness for providing the desired surface quality. This report also called for adoption of uniform overlay design standards by the Federal Highway Administration to insure that all states establish proper overlay design methods.

The structural rehabilitation of existing pavements is usually achieved through the application of an overlay of either asphaltic or portland cement concrete. This application results in the restoration of riding quality and/or skid properties, and prolongs the useful life of the pavement structure. It also increases the present worth of the initial investment in the facility at a smaller total cost than complete reconstruction of the pavement. The engineering procedures necessary to accomplish complete rehabilitation require the determination of whether or not an overlay is necessary and also a prediction of the load carrying capacity remaining in the existing pavement. Finally, the type and amount of overlay necessary to extend the pavement life for the desired time period must be determined.

This report is one of a series which has been prepared on the development of pavement and rehabilitation design procedures, and is part of the Federal Highway Administration's FCP project 5D (Structural Rehabilitation of Pavement Systems). Prior to the initiation of this contract, the Federal Highway Administration conducted a pavement rehabilitation workshop in 1973. This workshop was attended by highway engineers from all over the United States who were experts in the field of pavement design technology. The proceedings from this workshop provide a key reference for the design procedure developed in this report (Ref 2).<sup>2</sup> Likewise, the first report prepared on this project is a keystone reference for the development of overlay design procedures

---

<sup>1</sup>"Pavement Rehabilitation Design Procedures" RFP-237, Federal Highway Administration, Washington, D.C., March 12, 1974.

<sup>2</sup>"Pavement Rehabilitation: Proceedings of a Workshop", Federal Highway Administration Report No. FHWA-RD-74-60, June 1974.

using elastic layer theory (Ref. 3)<sup>1</sup>.

#### Need for New Criteria

The need for reliable design criteria for portland cement concrete overlays has existed for many years. Actually, a good theoretical basis has never been formulated for the rigid pavement overlays, much less for the many slab detail combinations that may exist for rigid pavement overlays. Another vital need for overlay design criteria is an increase in load restrictions and a change in legal limitations to truck operations. Recent and future changes in legal loadings for trucks may have a significant impact on the serviceability of pavements, thus emphasizing the need for rational criteria applicable on a nationwide basis.

It is projected that an increased percentage of the highway construction dollars will be required for rehabilitation of existing pavements. If this rehabilitation is to be done with federal tax monies, design criteria will be necessary to provide assurance that all states are applying proper overlays for the existing conditions.

Until recently, the Federal Highway Administration did not approve funding of highway maintenance or rehabilitation. The policy committee of the American Association of State Highway and Transportation Officials (AASHTO) recommended that the definition of construction be expanded to include pavement overlays (Ref. 2). The 1976 Federal Aid Highway Act included passages that expanded the FHWA's role in resurfacing. As a result, the FHWA has instituted the "Three-R Program (Resurfacing, Rehabilitation, and Restoration) for funding programs on the Interstate System. In addition, consideration must presently be given to expand the funding to the Primary and Secondary Systems. Since rehabilitation has always been a state responsibility, this would involve the FHWA in a new role of responsibility. Because funds are always available in limited supply, it is most important that existing rehabilitation methodologies be evaluated and criteria be established to insure optimum use of the available financial resources.

#### Current State-of-the-Art

The development of a new overlay design procedure must be preceded by a review of the current state-of-the-art if the new procedure is to be an improvement and an addition to overlay design. Thus, a review and evaluation of several existing design procedures was undertaken and their shortcomings were outlined.

---

<sup>1</sup>Austin Research Engineers Inc, "Asphalt Concrete Overlays of Flexible Pavements - Volume 1, Development of New Design Criteria, "Federal Highway Administration Report No. FHWA-RD-75-75, June, 1975.



## Review of Existing Procedures

A review of several existing overlay design methods which were presented in a paper by McComb (Ref. 4)<sup>1</sup> was undertaken to establish what input they might have for the development of an overlay design method. Methods for concrete resurfacing of pavements which have been published by the Portland Cement Association, American Concrete Institute and the Corps of Engineers were also reviewed (Ref. 5, 6, 7).<sup>2,3,4</sup>

## Shortcomings of Existing Procedures

The existing procedures mentioned above are all modifications of existing design procedures for determining the thickness of the PCC overlay required as if a single slab were used. The determination of this thickness is arrived at by using normal PCC pavement design procedures and is independent of the overlay design. The present procedures consider existing pavements only in a global sense without any rational pavement evaluation scheme. Designs have historically been based on a stress criterion using slab theory. Thus with the existing methods it is not possible to make a mechanistic analysis of the layered system of existing slab and rigid overlay.

In summary, the current design procedures and criteria are lacking in consideration of the structural value of the existing pavements, its remaining life and an evaluation of the layers as they will function in an overlaid pavement. Furthermore, they are not based on fatigue criteria which is one of the primary failure modes or mechanisms.

## Objectives

The general objectives of the contract under which this work was done were two-fold.

1. To develop pavement overlay thickness design procedures for the rehabilitation of all common pavement types.

---

<sup>1</sup>McComb, Richard A. and John J. Labra, "A Review of Structural Evaluation and Overlay Design for Highway Pavements," Pavement Rehabilitation: Proceedings of a Workshop--Report No. FHWA-RD-74-60, June 1974.

<sup>2</sup>The Design and Construction of Concrete Resurfacing for Old Pavements. PCS, NO. 1S 115.01P, 1965.

<sup>3</sup>Design of Concrete Overlays for Pavements, ACI Journal, Vol. 64, 1967.

<sup>4</sup>Hutchinson, R. Basis for Rigid Pavement Design for Military Airfields Corps of Engineers, Ohio River Div. Laboratories, Misc. Paper 5-7, May 1966.

2. To develop design procedures for eliminating or reducing the reflection cracking of pavement overlays.

The specific objectives of Phases II and III reported herein were to develop an overlay design procedure for rigid and flexible overlays of rigid pavements and to develop methods for reducing reflection cracking. The results of these studies are reported herein.

#### Scope of Study

The technical scope and funding for this contract provided for the development of a state-of-the-art design procedure for flexible and rigid overlays over rigid pavements using elastic layered theory as an analytical model for the design analysis. The design procedure developed includes a series of computer programs to perform various aspects of the analysis required for the design. The report describes the experimental investigations and research conducted relative to flexible and rigid overlays of rigid pavements. The analytical methods used to perform the analyses in the design procedures are carefully documented. To adequately develop the working design procedures in line with the conceptual model, new design criteria were developed and are documented.

This report does not include the details of the design procedures necessary to perform design analyses itself. A separate report was prepared for the practicing engineer to use as a guide for design purposes. Since the reports were prepared as independent documents, it will not be necessary for the user to have this report to use the design procedure.

#### Outline of Report

This report presents the methodology and development of the overlay design procedure which is given in the user's manual, Report No. FHWA-RD-77-67 (Ref. 8).<sup>1</sup> Chapter II contains the concepts for a universal overlay design procedure that encompasses flexible and rigid overlays of both flexible and rigid pavements. Chapter III contains the detailed design criteria developments and discusses the determination of effective modulus values for cracked concrete, stress adjustments for corner and edge loads, effects of voids beneath pavements, the development of fatigue cracking criteria, and an evaluation of new paving materials. Chapter IV is a discussion of the reflection cracking research and describes the development of the design model to reduce reflection cracking. Chapter V contains a comparison and evaluation of field measured deflections and computed deflections using elastic layered theory. Chapter VI contains conclusions and recommendations for further research.

---

<sup>1</sup>Austin Research Engineers Inc, "Overlay Design and Reflection Cracking Analysis for Rigid Pavements, Volume 2--Design Procedures" Report FHWA-RD-77-67, August 1977.

## CHAPTER 2

### CONCEPTS FOR UNIVERSAL OVERLAY DESIGN PROCEDURE

The overlay design concepts presented in this chapter apply to both rigid and flexible pavements. Although this phase of the contract deals primarily with overlays of rigid pavements, it is necessary to include flexible pavements when describing a universal procedure. The remaining chapters of the report deal only with overlays of existing rigid pavements. The flexible pavement procedures were reported in Phase I of this contract (Refs. 3, 9)<sup>1</sup>. The design concepts are essentially the same for both flexible and rigid pavements, with some variation in the overlay thickness analysis.

Efforts were made to use and improve the most up to date concepts and theories available. Work done by McCullough (Ref. 10)<sup>2</sup> and McComb (Ref. 4) provided useful information on review of existing overlay design concepts. The new concepts developed account for rehabilitation of existing portland cement concrete and asphaltic concrete pavements by overlaying with either portland cement concrete or asphaltic concrete. There are three basic steps: (1) evaluation of the existing pavement, (2) determination of design inputs, and (3) overlay thickness analysis. The procedures are illustrated in flow chart form in Figure 1. Evaluation of the existing pavement is accomplished by a condition survey and deflection measurements. This information enables the designer to distinguish between different segments of the existing pavement based on their condition. Each segment becomes a "design section" and is analyzed separately. Thus, the most economical rehabilitation is accomplished by varying overlay thickness along the roadway according to the existing pavement condition.

Determination of the design inputs includes both past and projected future traffic, environmental considerations, and materials testing and analysis. Results of the deflection measurements also serve as an aid in establishing properties of the subgrade material.

The overlay thickness analysis is based on the concepts of failure by excessive rutting and fatigue cracking for flexible pavements and excessive reflection and fatigue cracking for rigid pavements. Stresses

---

<sup>1</sup>Austin Research Engineers Inc, "Asphalt Concrete Overlays of Flexible Pavements, Volume 2 - Design Procedures" Report FHWA-RD-75-76, August 1975.

<sup>2</sup>McCullough, B. F., "A Pavement Overlay Design System Considering Wheel Loads, Temperature Changes, and Performance," Institute of Transportation and Traffic Engineering Graduate Report, University of California, Berkeley, July 1969.

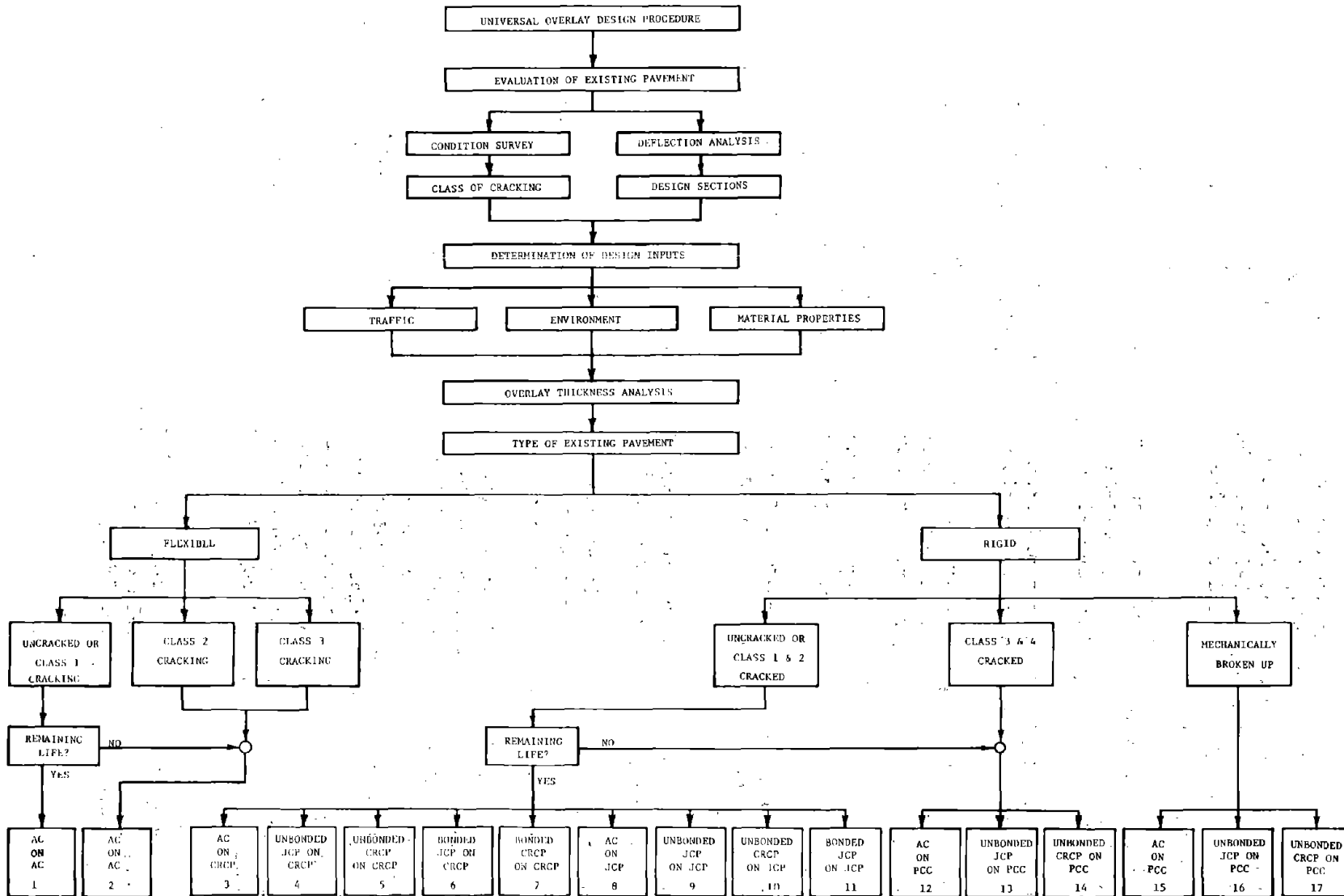


Figure 1. Flow chart of universal overlay design procedure.

and strains in the pavement are computed using linear elastic layered theory. (Ref. 11)<sup>1</sup> The overlay life is determined by entering these stresses into a fatigue or rutting equation that relates stress or strain magnitude and repetitions to failure. The overlay thickness that satisfies the fatigue, rutting, and/or reflection cracking criteria is selected as the design thickness.

After a study of the two available mechanistic approaches, elastic layered theory and plate theory, elastic layered theory was selected as the basic analysis model for several reasons:

1. It is desirable for a universal procedure that the same basic model be used for both flexible and rigid pavements,
2. Since rutting can occur in any layer of a flexible pavement, a knowledge of stress and strains in the sublayers is required, thus, layered theory must be used,
3. Elastic layered theory solutions are inexpensive to obtain as compared to finite or discrete element solutions,
4. Elastic layered theory is the most universally available analysis technique for computing stress, strain, and deflection.
5. The layers of the pavement system are more accurately characterized by separate modulus and thickness values, and
6. The applied stress is spread throughout the layers in a realistic manner, the stress at the bottom of a layer being smaller than at the surface.

The application of linear elastic layered theory implies that pavement materials can be characterized by the elastic constants of Poisson's Ratio and Modulus of Elasticity which is not the case in a "pure sense". Thus, it is essential that the laboratory and field procedures characterize the materials under stress, temperature, and moisture conditions that simulate those in the field. Elastic constants obtained with unrealistic material characterization procedures and used in linear elastic layered theory may result in erroneous predictions of stress and strain. Many of the techniques described in this chapter and subsequent chapters were developed to simulate field conditions of stress, temperature, and moisture,

---

<sup>1</sup>Warren, H. and W. S. Dieckman, "Numerical Computation of Stresses and Strains in a Multiple-Layered Asphalt Pavement System," California Research Company, September 1963.

thus maximizing the reliability of the overlay design procedure.

The three basic steps in the design procedure are presented in more detail in the remainder of this chapter.

### Evaluation of Existing Pavement

Evaluation of the existing pavement is accomplished by a condition survey and deflection measurements. The laboratory sampling and testing plan is set up based on an analysis of the condition survey and deflections.

#### Condition Survey

The main purpose of the condition survey is the determination of the type and amount of cracking present. The cracking is classified as Class 1, 2, 3, or 4 for rigid pavements and Class 1, 2, or 3, for flexible pavements according to the definitions adopted during the AASHO Road Test. (Ref. 12)<sup>1</sup> This information becomes decision criterion relative to the method of characterization of the existing pavement and the kind of overlay analysis performed. The condition survey should also include other relevant information such as rutting, drainage areas, soil changes, and cut-fill transition areas.

#### Deflection Analysis

The deflection measurements provide data necessary for dividing the pavement into segments that behave differently under load. These are termed "design sections" and each is analyzed separately for overlay thickness. The deflections may be measured with any conventional device and should be spaced along the pavement at intervals that will adequately describe its behavior. The deflection measurements are input as data to a computer program that plots deflection versus distance along the pavement, as shown in Figure 2. The designer must then visually divide the plot into sections of different structural capacity, such as those designated as Section 1, Section 2, and Section 3 in Figure 2. These sections are then compared for significant difference by using the Student's "t" test. If they prove to be significantly different, they are analyzed separately for overlay thickness, but if they are not significantly different the data are combined and analyzed as one section.

The deflection measurements also serve another purpose by aiding in characterization of the subgrade material. Since the subgrade has the largest variability of any of the layers and its effect on performance is substantial, adequate sampling for accurate characterization is essential.

---

<sup>1</sup>"The AASHO Road Test, Report 5, Pavement Research," Special Report 61E Highway Research Board, 1962.

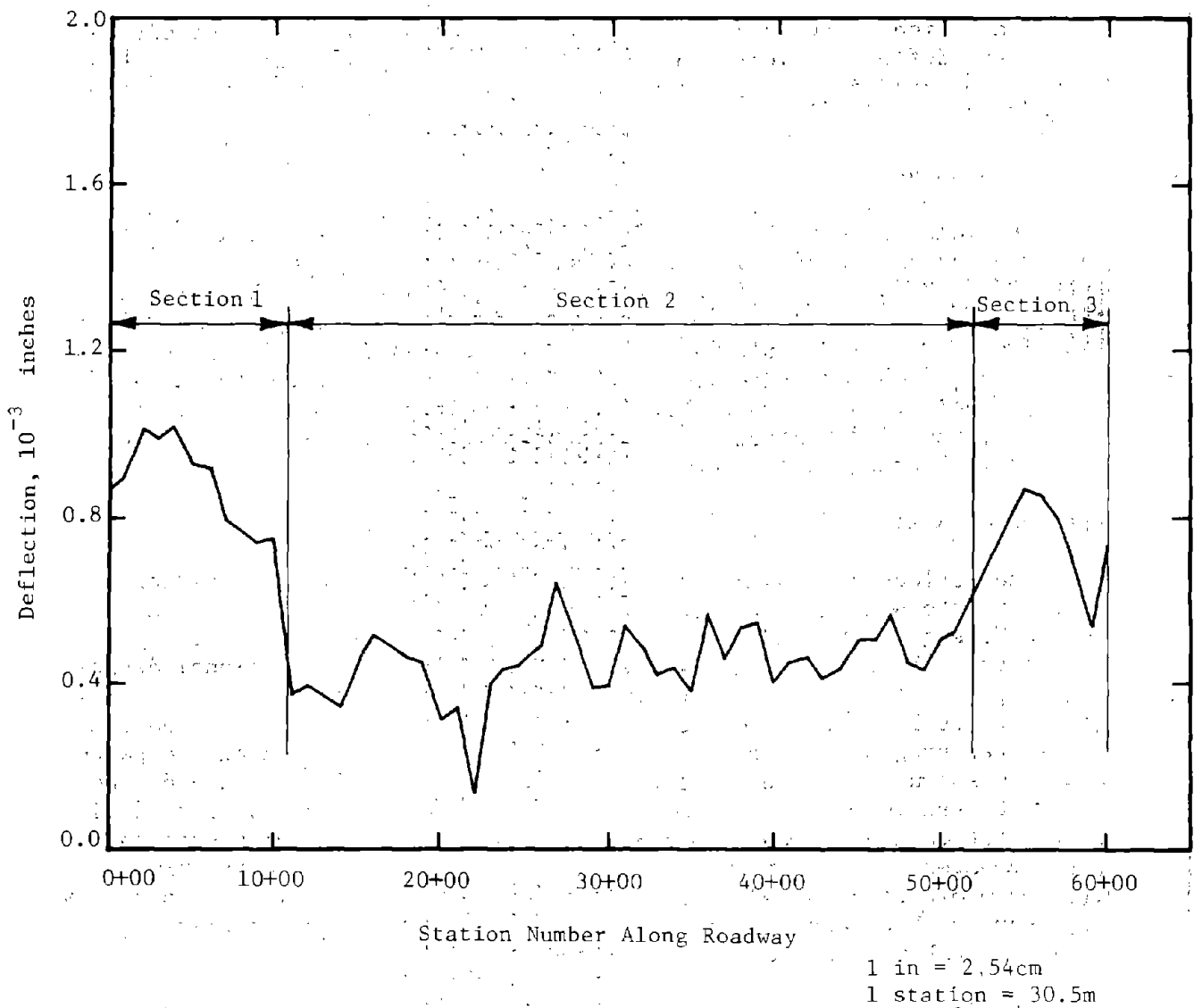


Figure 2. A typical deflection profile illustrating the variability along a roadway that requires characterization of independent design sections.

The subgrade can be characterized more thoroughly by using deflections along the entire roadway in conjunction with laboratory tests, than it can be using laboratory test values alone. This is discussed in more detail under the section on Design Inputs.

#### Classification of Existing Pavement

Based on the condition of the existing pavement, it must be classified according to one of the following categories:

##### Flexible Pavements

1. Uncracked or Class 1 cracking
2. Class 2 cracking
3. Class 3 cracking

##### Rigid Pavements

1. Uncracked or Class 1 and 2 cracking
2. Class 3 and 4 cracking,
3. Mechanically broken up

Each of these categories is treated differently in the overlay analysis. If the pavement is classified in Category 1, it is checked for remaining life. If there is any remaining life it is accounted for in design, thus allowing some reduction in the overlay thickness. If the existing pavement is classified in Category 2, it is said to have no remaining life. It is therefore assigned a reduced surface modulus to help model this deteriorated condition. If it is classified in Category 3, this condition is modeled by an even lower surface modulus for use in the overlay analysis. The overlay analysis performed in each of these three categories is discussed in more detail under the section on Overlay Analysis.

#### Design Inputs

The design inputs consist primarily of traffic in the form of equivalent axle loads, environmental considerations such as rainfall, temperature, and season, and material properties such as modulus of elasticity and Poisson's ratio.

##### Traffic

The design load used in the procedure is an 18-kip (8172kg) single axle, since most agencies base their data storage and projections on this value. Thus, mixed traffic must be converted to 18-kip (8172kg) equivalent axle load applications using AASHO equivalency factors. The traffic prior to the overlay should be determined for use in remaining life computations and the projected future traffic.



should be determined for the overlay thickness analysis. The traffic analysis should also determine the distribution between directions and lanes. The following equation is used in traffic computations:

$$N_{\text{design}} = N_{\text{total}} \times \text{DDF} \times \text{LDF} \dots \dots \dots (1)$$

where:

$N_{\text{design}}$  = design traffic,

$N_{\text{total}}$  = total traffic expressed as 18-kip (8172kg) single axle loads for both directions and all lanes,

DDF = directional distribution factor expressed as a ratio, and

LDF = lane distribution factor expressed as a ratio.

#### Environmental Considerations

It is desirable to consider the rainfall for the area and drainage for the highway being overlaid, since moisture can have significant effects on material properties. In some cases, the material strengths should be reduced due to excessive rainfall or poor drainage. The designer should also consider environmental effects in selecting the season for making deflection measurements. They should be made during the season that produces the highest deflections. This will insure a conservative approach when characterizing the subgrade material. An alternative to this step is to correct the deflection taken at any time to the poorest condition based on previous correlations.

#### Material Properties

Material properties in the form of linear elastic properties (modulus of elasticity and Poisson's Ratio) must be established for each layer in the pavement system as inputs to the linear elastic layered theory analysis. In the remainder of the report the term "modulus" will be used in lieu of modulus of elasticity since many of the tests used are approximations. Some of these values are determined directly from laboratory tests, some are derived from deflection measurements, and some have been permanently set based on previous studies.

The moduli for the overlay material, the existing surfacing material, and base or subbase material are determined directly from laboratory tests. For the existing surface materials, the modulus may be derived from splitting tensile tests on specimens prepared from cores taken in the field. The modulus for the base and/or subbase may be determined by resilient modulus testing on samples reconstituted at field density and moisture contents.

The modulus for the subgrade is based on deflection measurements in conjunction with laboratory tests. The process is shown in flow chart form in Figure 3. Linear elastic layered theory is used to develop a relation between subgrade modulus and surface deflection as shown in Figure 4. The deflection measured in the field is entered into this relation, and corresponding modulus selected. If the deflection measurement load is different than the design load, the modulus must be adjusted for stress sensitivity. This is accomplished by developing a laboratory relationship between deviator stress and modulus, and adjusting the laboratory test results as shown in Figure 5. The deviator stress in the subgrade for the design load is then used in conjunction with the adjusted laboratory curve to determine the final subgrade modulus.

The modulus of an existing PCC pavement is automatically set at 500,000 psi (3,450,000kN/m<sup>2</sup>) if it exhibits Class 3 or 4 cracking or 70,000 psi (483,000kN/m<sup>2</sup>) if it is to be mechanically broken up. An existing flexible pavement is assigned a modulus of 70,000 psi (483,000kN/m<sup>2</sup>) if it exhibits Class 2 cracking and 20,000 psi (138,000kN/m<sup>2</sup>) if it exhibits Class 3 cracking. These values were established from stress and deflection analyses of AASHO Road Test rigid pavements using elastic layered theory and discrete element theory (Ref. 13)<sup>1</sup>.

#### Analysis for Overlay of Rigid Pavements

After evaluation of the existing pavement, designation of "design sections", and determination of design inputs the analysis for overlay thickness is performed. This includes designation of the existing pavement and overlay type, stress computations, and a fatigue analysis and/or reflection cracking analysis. The rigid pavement overlay analysis procedure is shown in flow chart form in Figure 6.

#### Pavement Type

Figure 6 indicates there are a total of 15 different analyses depending on the type of existing pavement, bonding characteristics between overlay and existing pavement, and overlay type. A distinction is made between jointed and continuous pavement, because the stress computations differ in each case. A jointed pavement should be designed for a corner load condition, whereas a continuous pavement should be designed for an edge load condition. The fatigue analysis is performed for all 15 cases, but the reflection cracking analysis is performed only in cases where the existing pavement is jointed, badly cracked, or mechanically broken up. The proper case is keyed in the computer program by simply indicating in the input data the type of existing pavement, bond, and overlay.

---

<sup>1</sup>Treybig, Harvey J., W. R. Hudson, and Adnan Abou-Ayyash, "Application of Slab Analysis Methods to Rigid Pavement Problems," Research Report 56-26, Center for Highway Research, University of Texas, May 1972.

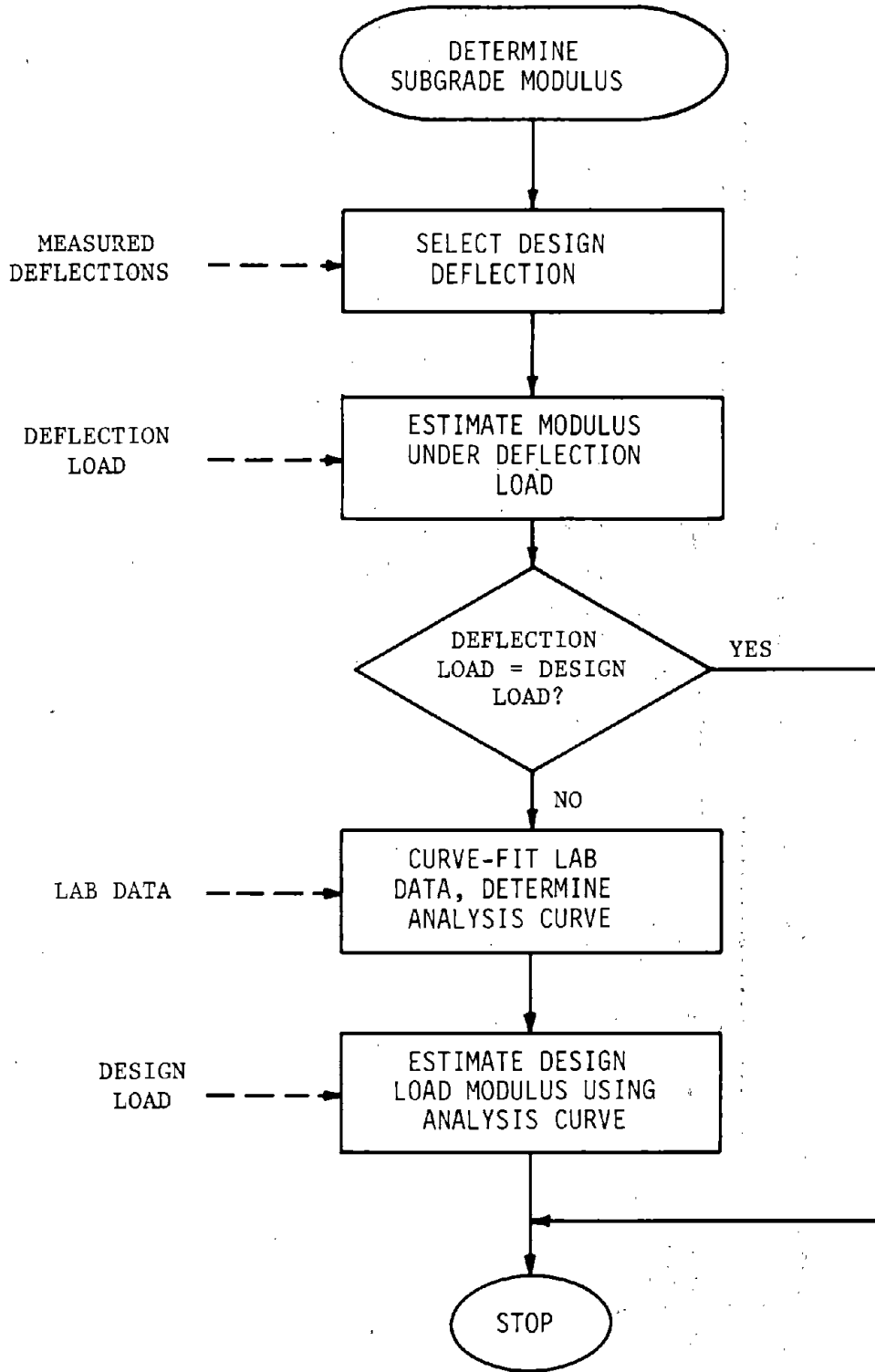
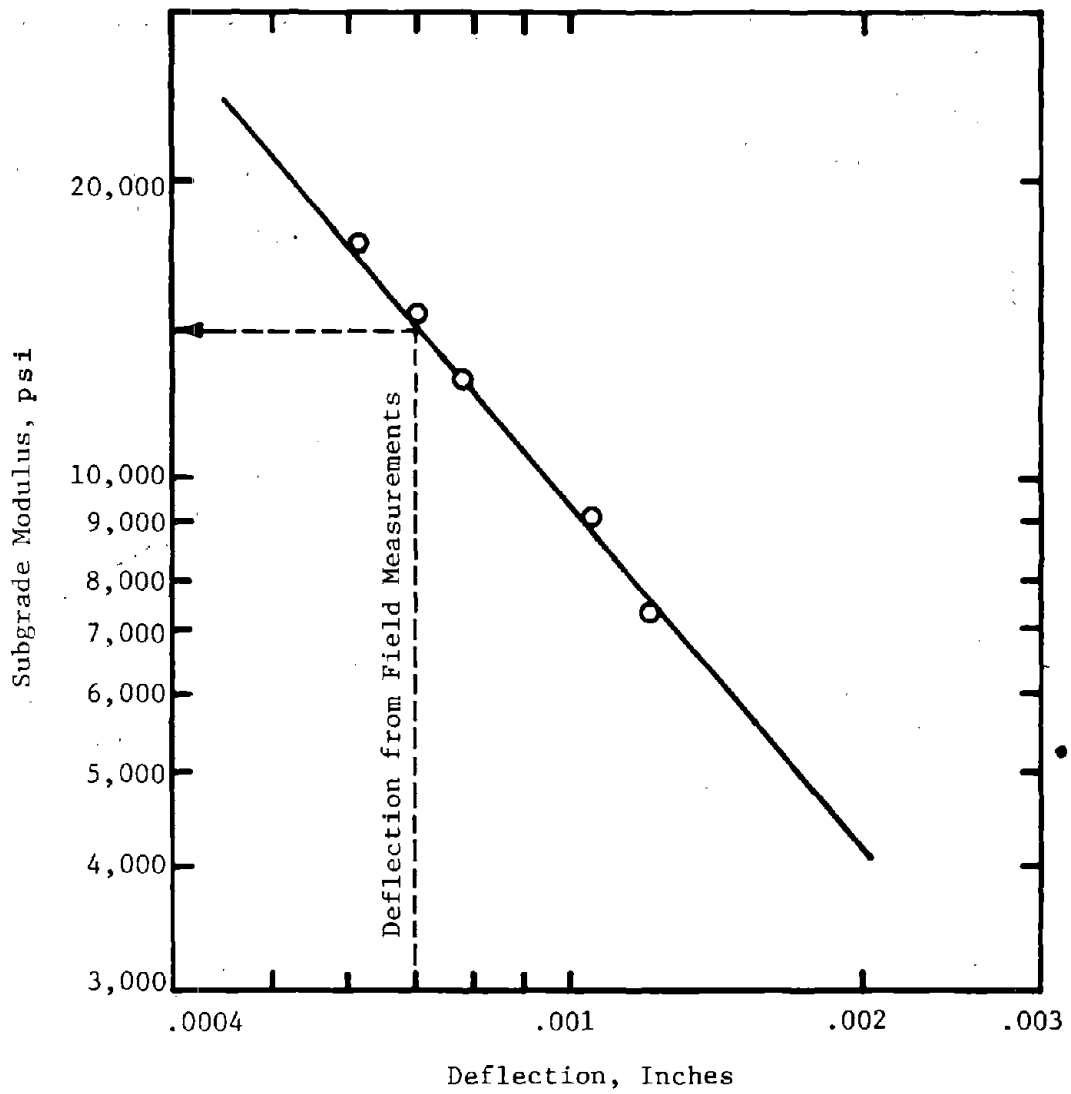


Figure 3. Flow chart for determining the subgrade modulus of elasticity.



1 in. = 254cm  
 1 psi = 6.9kN/m<sup>2</sup>

Figure 4: Relation of computed deflection for the Dynaflect load and subgrade modulus.

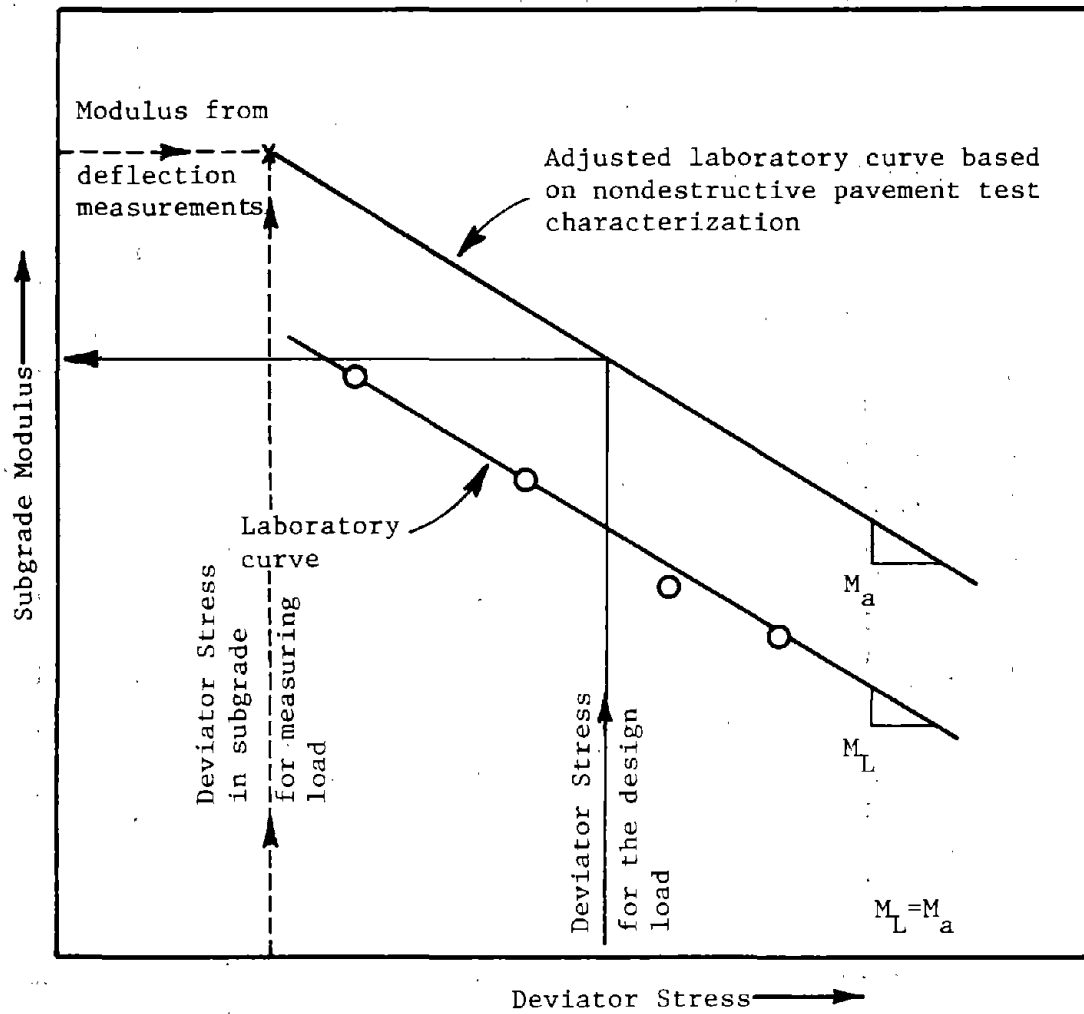


Figure 5. Relation of subgrade modulus and deviator stress used in determining subgrade modulus.

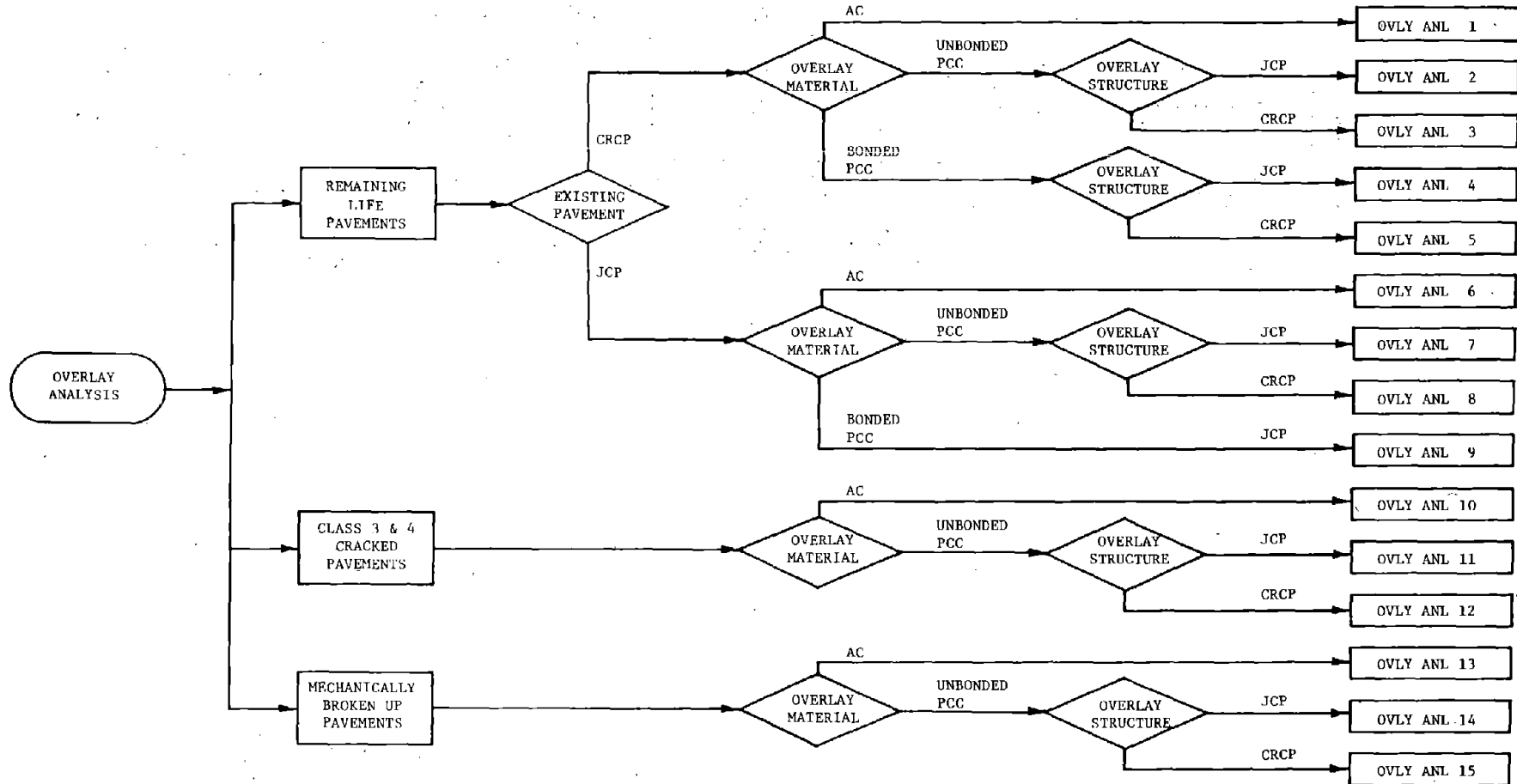


Figure 6. Analysis system for determining overlay thickness of existing rigid pavements considering wheel load repetitions.

## Stress Computations

The wheel load stresses in each layer should be checked against the criteria for the layer, and the one resulting in the maximum overlay thickness should be used. The overlay design procedure developed herein considers only the tensile stresses in the "bound layers" since criteria were available for these layers only. Tensile stresses are used since the primary mode of failure for the two currently used materials i.e. asphalt concrete and portland cement concrete is tensile cracking. Future development of the design procedures should consider the possibility of failure occurring in other layers.

The stresses needed for the fatigue analysis are computed by the linear elastic layered theory program ELSYM5 (Ref. 14)<sup>1</sup>, which is the primary subroutine in the overlay design computer program. Figure 7 shows that almost every phase of the design procedure is keyed to ELSYM5. A thorough review was made of elastic layer analysis programs before finally selecting this one as being best for the design procedure. Reasons for selecting ELSYM5 are given in Reference 3.

The horizontal tensile stress due to the design load, an 18-kip (8172kg) single axle, is computed at either the bottom of the overlay or the bottom of the existing pavement depending on which analysis is being performed. If the existing pavement has remaining life, the critical stress is at the bottom of this layer, whereas if the existing pavement has no remaining life the critical stress is at the bottom of the overlay. The stress is automatically computed at the proper location in the pavement system, depending on which analysis has been designated in the program input data.

The stress computed by ELSYM5 is adjusted so that it is equivalent to the stress resulting from the design load position, that is, an edge or corner load. A continuous pavement is designed for edge loading and a jointed pavement for a corner loading. For urban conditions, where curbs are used, consideration may be given to interior and edge loadings for continuous and jointed pavements, respectively. The current versions of the design procedure do not consider this latter feature at the present time, but this feature could be added in subsequent developments and improvements of the procedure. Deflection measurements on jointed pavements should be made at the interior and corner of the same panel. The ratio of these deflections is calculated and used in selecting the exact stress adjustment factor. This concept allows the actual condition of load transfer at joints in the existing pavement to be considered in the design procedure.

---

<sup>1</sup>Ahlborn, Gale, "Elastic Layered System with Normal Loads," The Institute of Transportation and Traffic Engineering, University of California, Berkeley, California, May 1972.

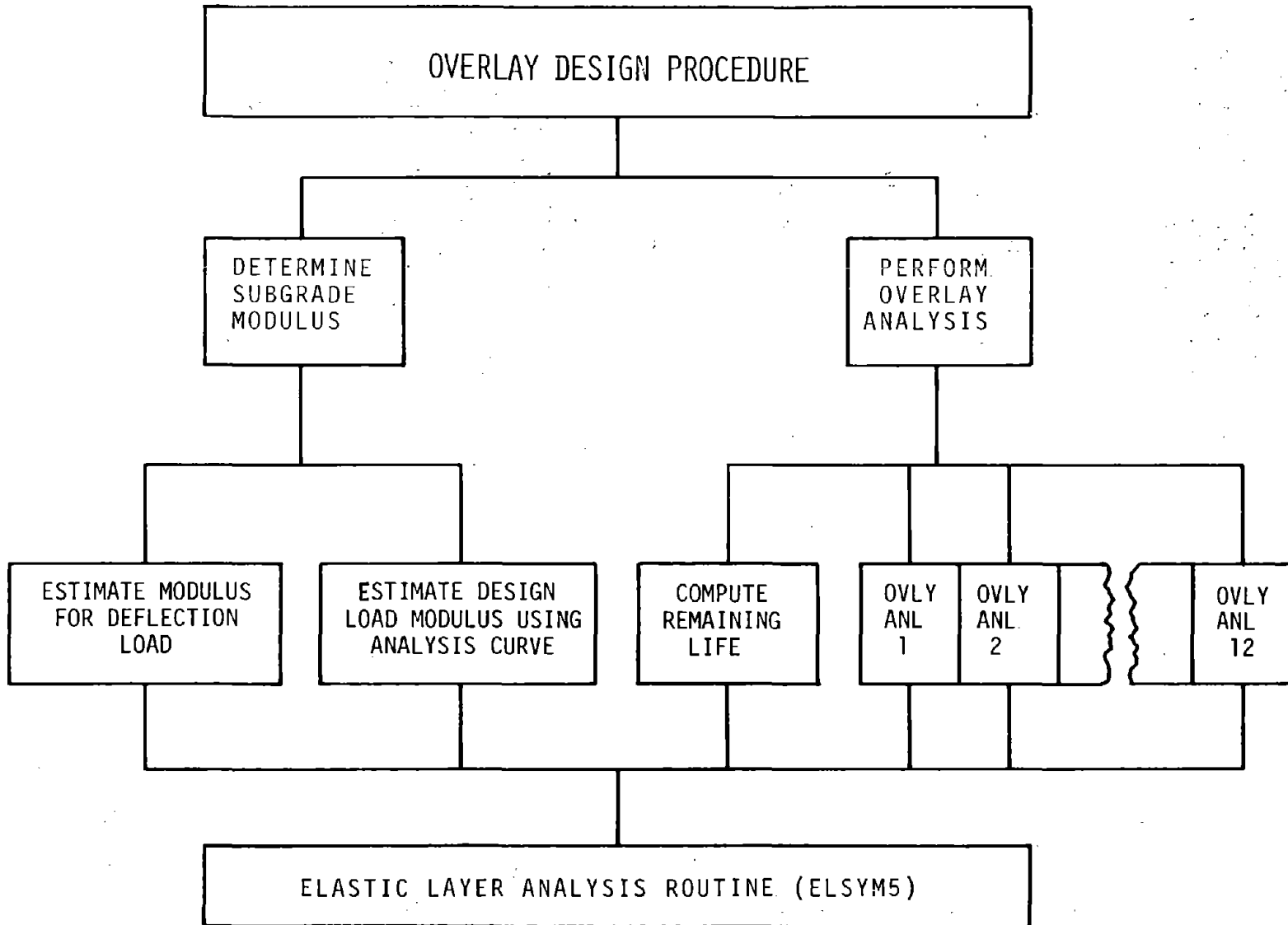


Figure 7. Overlay analysis program hierarchy.



An extensive investigation of stresses and deflections led to the development of a stress-deflection relation as shown in Figure 8. The ratio of corner deflection to interior deflection is entered on the abscissa, projected to the curve, and then to the ordinate to determine the stress adjustment. For an edge load stress adjustment, a constant value is used. These adjusted stresses are then used as the design stresses in the fatigue analysis.

### Fatigue Analysis

The fatigue analysis consists of the development of a relation between overlay thickness and axle applications until Class 3 and 4 cracking occurs. The number of axle loads is computed using a fatigue equation of the following form:

$$N = A (f/\sigma)^B \dots \dots \dots (2)$$

where:

N = number of axle loads until Class 3 and 4 cracking occurs, (fatigue life)

f = flexural strength of concrete, psi,

$\sigma$  = computed stress due to design load, psi, and

A, B = constants .

(1 psi = 6.9kN/m<sup>2</sup>)

The fatigue life is computed for a range of overlay thicknesses and a plot is made of overlay thickness versus fatigue life as shown in Figure 9. The projected future traffic or desired life of the overlay is entered on the abscissa, projected to the curve and then to the ordinate to determine the overlay thickness. This concept allows the designer to evaluate the relation of overlay cost, as a function of thickness and life of the overlay so that he can make tradeoffs between them if available funding requires or permits it.

### Reflection Cracking Analysis

The reflection cracking analysis consists of evaluating overlay thickness using the following concept:

$$C_R = f (E_o, E_o', D, \Delta T, \alpha, F_1, w_d, X_{BB} \dots \dots \dots (3)$$

where:

C<sub>R</sub> = reflection cracking,

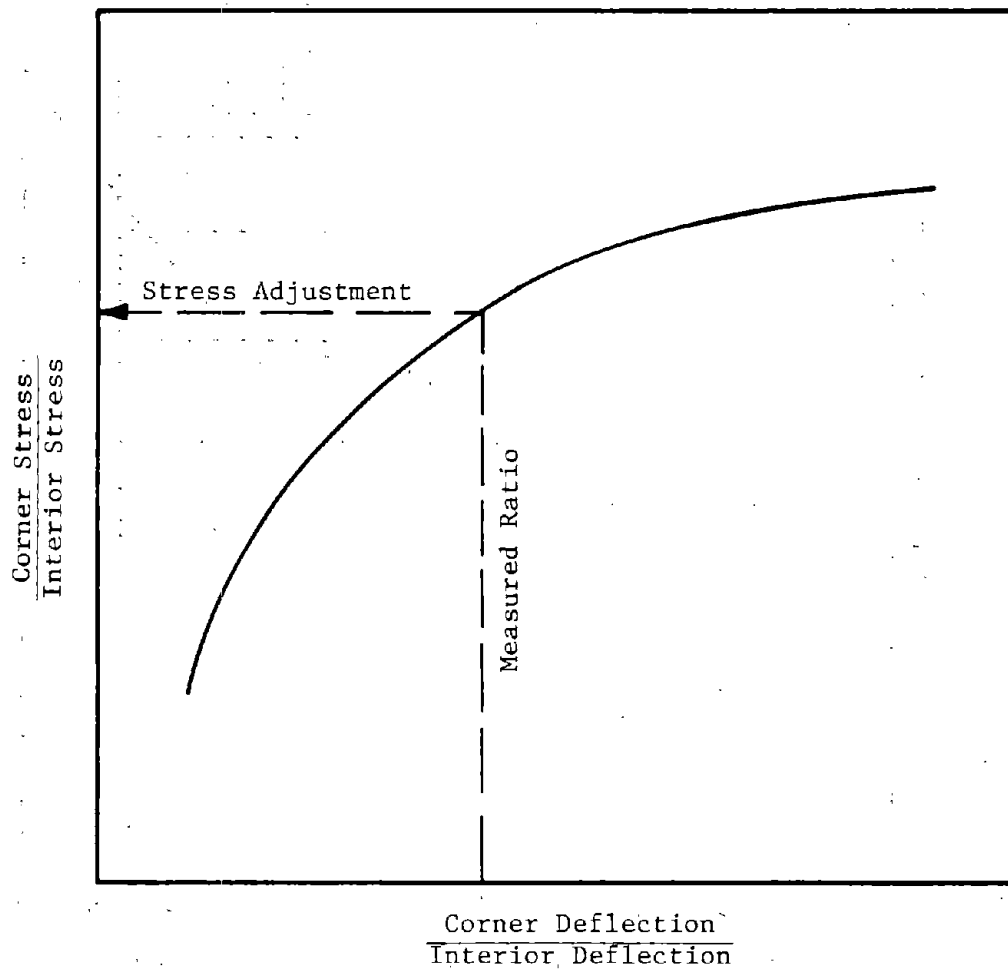


Figure 8. Selection of stress adjustment factor for jointed concrete pavements based on ratio of measured deflections.

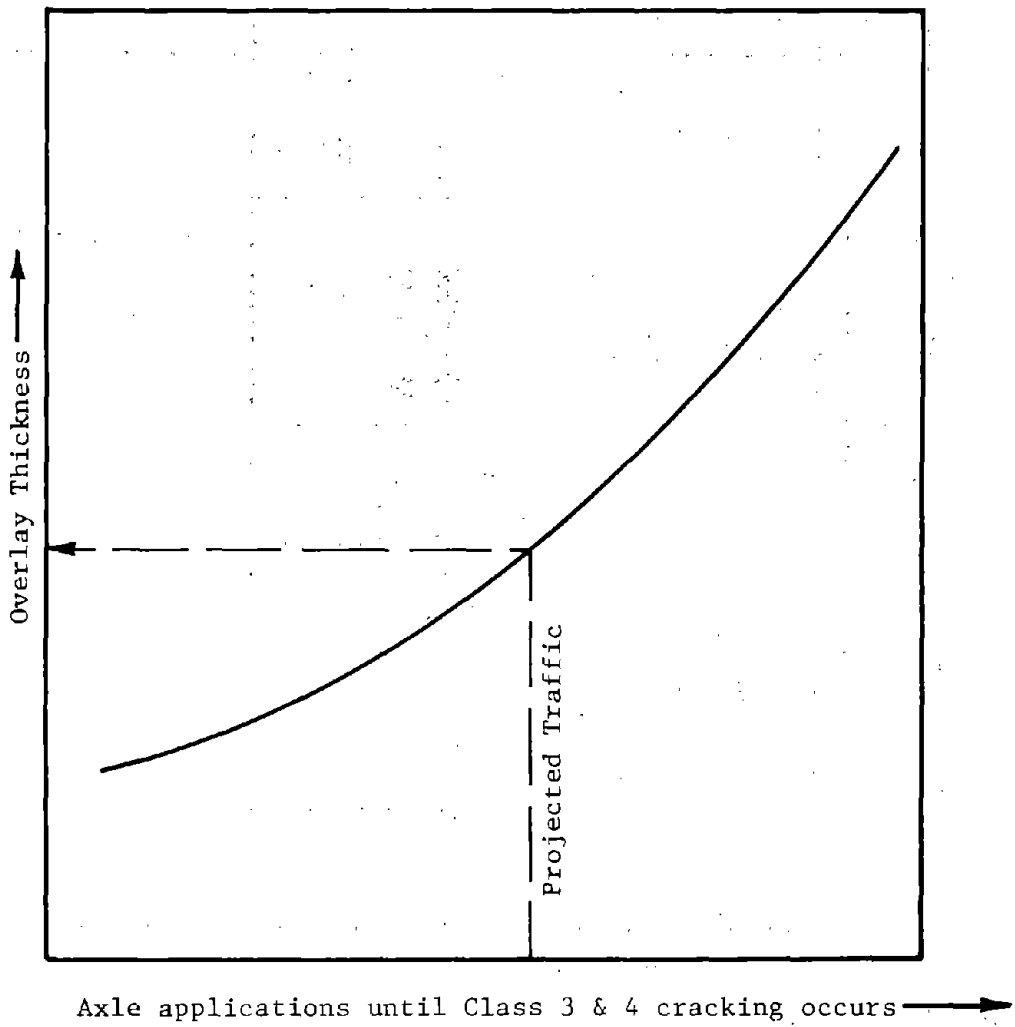


Figure 9. Relation of thickness and fatigue life used in selecting overlay thickness for rigid pavements.

- $E'_o$  = dynamic modulus of asphalt or concrete,
- $E_o$  = creep modulus of asphalt or concrete,
- $D$  = thickness of existing pavement or overlay,
- $\Delta T$  = temperature change of pavement materials,
- $\alpha$  = coefficient of volume change for pavement materials,
- $F_i$  = force-movement relationship between pavement layers resulting from friction, adhesion, bearing, etc.,
- $w_d$  = differential deflection at crack or joint, and
- $X_{BB}$  = width of bond breaker.

The overlay thickness as well as any other type of treatment necessary to minimize or prevent reflection cracking is selected based on these factors. Reflection cracking is discussed in more detail in Chapter 4.

#### Selection of Overlay Thickness

The final overlay thickness or other rehabilitation selected should satisfy both the fatigue and reflection cracking criteria.

#### Analysis for Overlay of Flexible Pavements

The concepts for design of overlays on flexible pavements are very similar to those for rigid pavements. They account for flexible overlays only, since rigid overlays on flexible pavements may be considered as new pavement design. After evaluation of the existing pavement, designation of "design sections", and determination of design inputs, the analysis for overlay thickness is performed. This includes designation of the existing pavement condition, stress and strain computations, and fatigue and rutting analyses. The flexible pavement overlay analysis procedure is shown in flow chart form in Figure 10.

#### Existing Pavement Condition

There are two different analyses depending on the condition of the existing pavement. If the existing pavement is uncracked or has Class 1 cracking, the analysis includes a check for remaining life. If it has Class 2 or Class 3 cracking it is assigned the appropriate modulus value and then analyzed without remaining life.

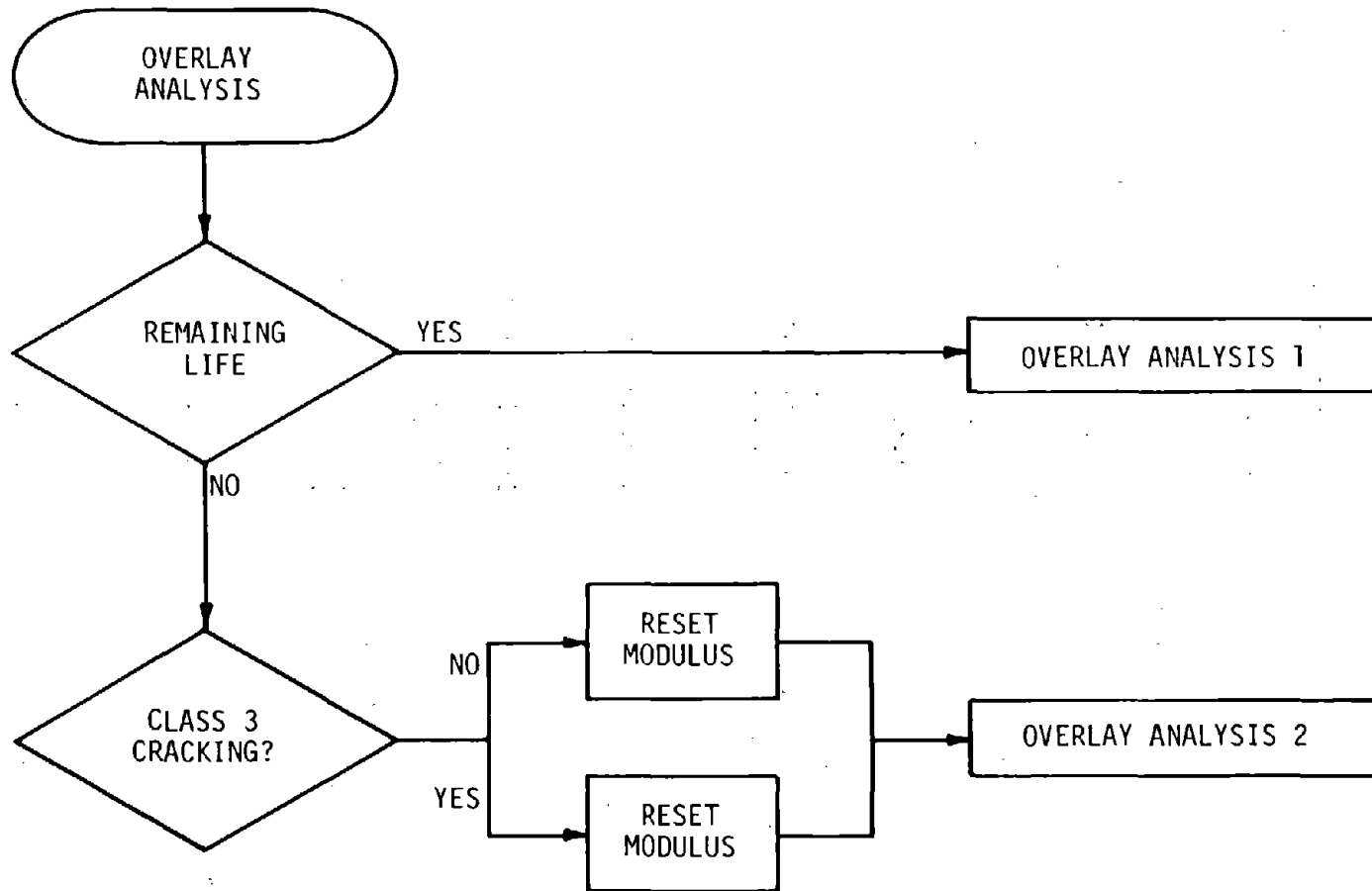


FIGURE 10. Analysis system for overlay of flexible pavements

## Stress and Strain Computations

The stresses and strains needed for the fatigue and rutting criteria are computed using elastic layered theory, the same as for rigid pavements. For the fatigue check the horizontal tensile strain is computed at the bottom of the existing pavement or the overlay depending on which analysis is being performed. If the existing pavement has remaining life the critical strain is at the bottom of this layer, whereas if it has no remaining life, the critical strain is at the bottom of the overlay. For the rutting check, stresses and strains are computed at various points in the pavement system for use in the rutting model.

## Fatigue Analysis

The fatigue analysis consists of the development of a relation between overlay thickness and axle applications until Class 2 cracking occurs. The number of axle loads is computed using a fatigue equation of the following form:

$$N = A(1/\epsilon)^B \dots \dots \dots (4)$$

where:

N = number of axle loads until Class 2 cracking occurs,  
(fatigue life)

$\epsilon$  = computed strain due to design load, and

A, B = constants.

The fatigue life is computed for a range of overlay thicknesses and a plot is made of overlay thickness versus fatigue life as shown in Figure 11.

## Rutting Analysis

This analysis, like the fatigue analysis, consists of development of a relation between axle applications to a specified rut depth and overlay thickness. The number of axle loads is computed using a rutting function such as follows:

$$N = f(R, \sigma_i, \epsilon_i, d_T) \dots \dots \dots (5)$$

where:

N = the number of equivalent 18-kip (8172kg) axle loads until a specified rut depth, R, occurs (rutting life)

R = the allowable rut depth for design,

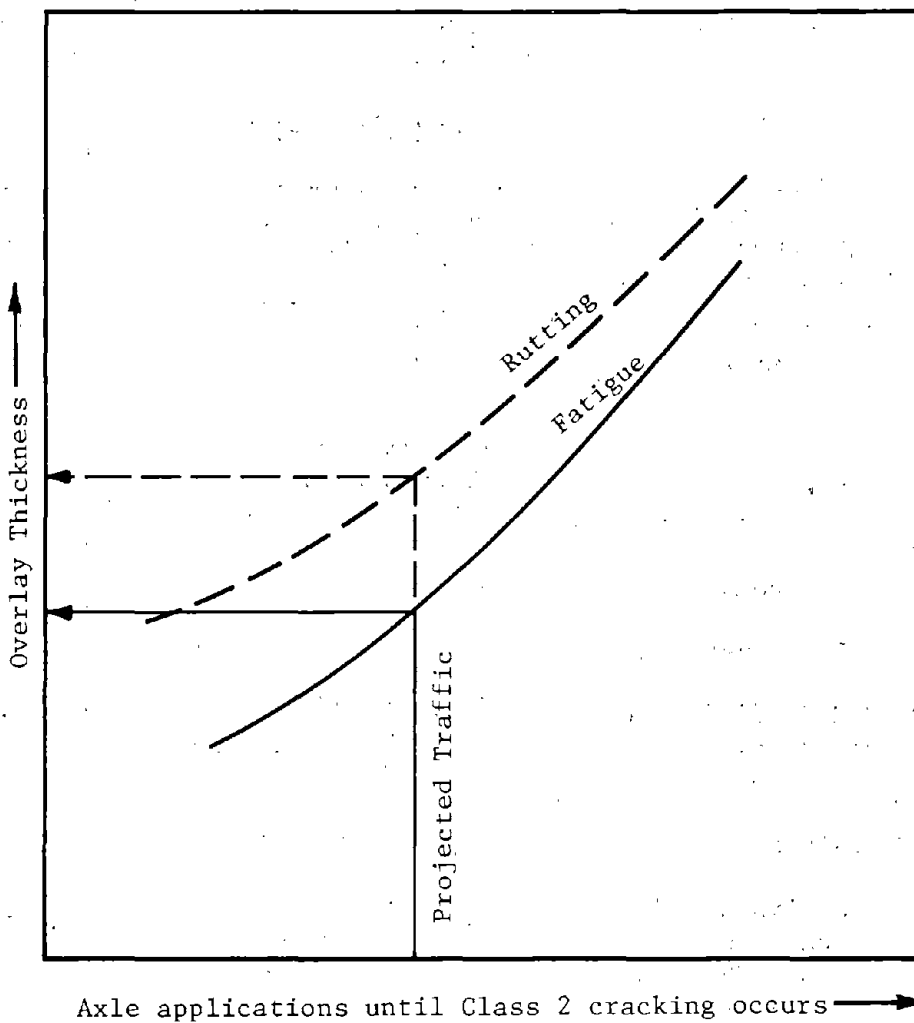


FIGURE 11. Relation of thickness and life used in selecting overlay thickness for flexible pavements.

$\sigma_i$  = stress in the  $i^{\text{th}}$  pavement layer,

$\epsilon_i$  = strain in the  $i^{\text{th}}$  pavement layer,

$d_T$  = number of days in year air temperature exceeds a set value.

The rutting life is computed for a range of overlay thicknesses and a plot is made of overlay thickness versus fatigue life as shown in Figure 11.

#### Selection of Overlay Thickness

The projected design traffic is entered in Figure 11 to determine the required thickness for both fatigue and rutting. The larger of the two is selected as the overlay design thickness.

#### Conclusion

Actual working design procedures have been developed that are based on the concepts presented in this chapter. However, they are not combined into the computerized universal procedure as described. The flexible pavement procedure (Refs. 3, 9) consists of the use of computer programs along with hand computations. The rigid pavement procedure, which is described in the remainder of this report, is almost completely automated. Thus, actual working procedures exist which could be refined and combined into a computerized universal working overlay design procedure.



## CHAPTER 3

### DEVELOPMENT OF DESIGN CRITERIA

This chapter presents the development of design criteria necessary to produce a working rigid pavement overlay design procedure from the concepts given in Chapter 2. These criteria were developed through the use of field data, elastic layered theory analysis, discrete element analysis, and finite element analysis. The developments include the determination of effective modulus values for cracked concrete layers, elastic layered theory stress adjustments, effects of voids, concrete fatigue equation, and evaluation of new materials.

#### Effective Moduli for Cracked Layers

Analysis of an existing rigid pavement for overlay thickness design requires that the existing PCC be represented by an effective elastic modulus based on its structural condition. If it is uncracked it can be assigned the same modulus as when it was initially constructed, but if it is cracked or will be mechanically broken up, it should be represented by a reduced modulus. To determine this reduced value a deflection analysis was made which was based on the AASHO Road Test rigid pavements (Ref 12).

#### Determination of Effective Elastic Modulus for Cracked Portland Cement Concrete Pavement

During the Road Test, static deflection measurements were made on the rigid pavements prior to cracking and after cracking. These data provided inputs for the analysis which led to a distinction between the uncracked and cracked condition of the pavements. The analysis consisted essentially of matching measured and computed deflections, first for determining the proper subgrade support (k-value) beneath the slab, and second for determining the effective modulus for the cracked slab.

Deflection Data Analysis. To determine the k-value and effective modulus, deflection data from 49 AASHO sections were used with slab thicknesses ranging from 8 inches (20.3cm) to 12½ inches (31.8cm) and subbase thicknesses of either 6 inches (15.2cm) or 9 inches (22.9cm). The deflections were measured during the Road Test with a Benkleman Beam. The axle load used was the same as the normal test load that ran on the specific section and loop. Both corner and edge measurements were made, but the edge measurements were selected for this analysis because the computer program used can model the edge load condition more accurately than the corner load condition. Figure 12 is a comparison of the load configuration used for the field measurements and the one modeled for the computer program.

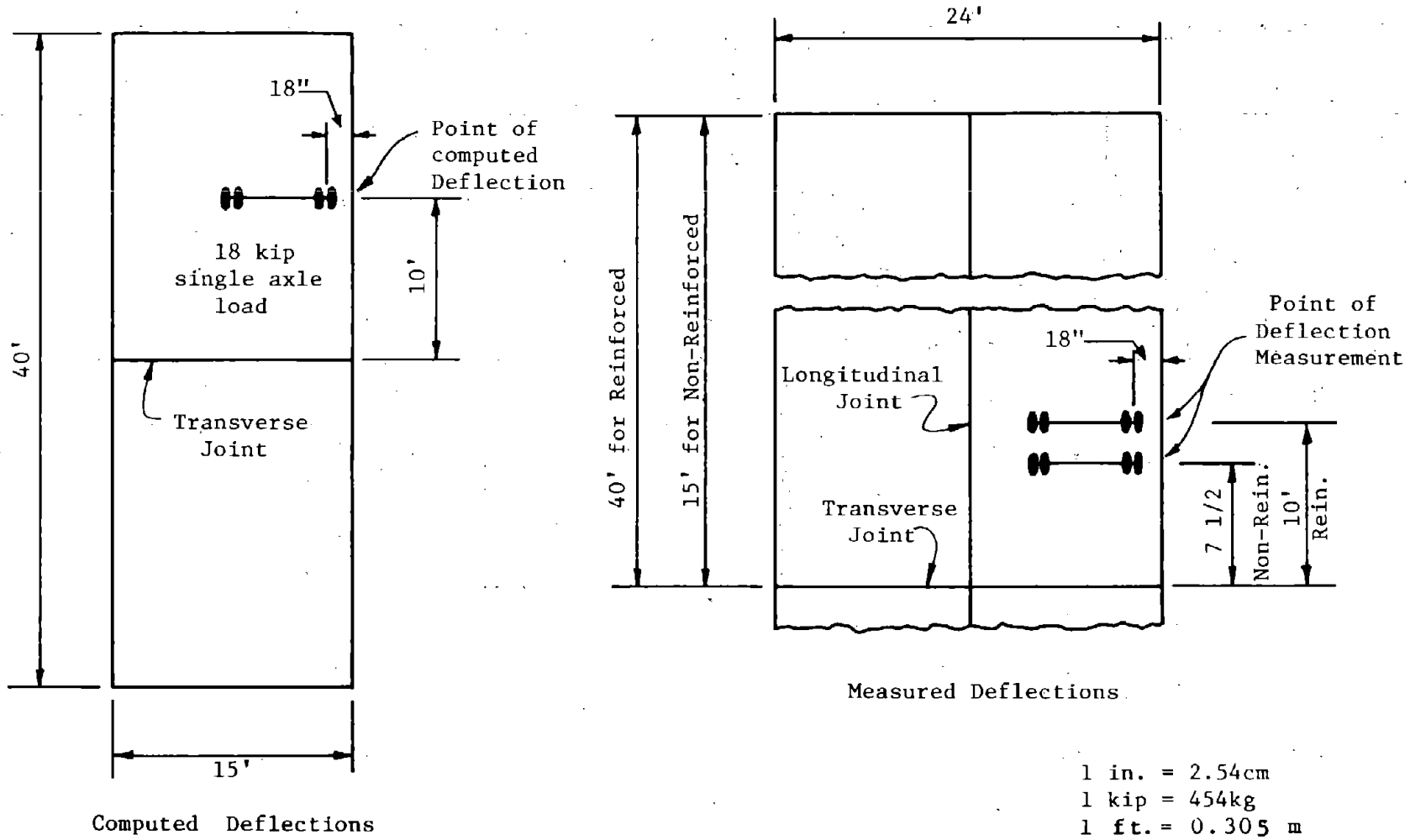


FIGURE 12. Comparison of load configurations for computed and measured deflections.



A Class 3 crack is defined as a crack opened or slapped at the surface to a width of 1/4 inch (.64cm) or more over a distance equal to at least one-half the crack length, except that any portion of the crack opened less than 1/4 inch (.64cm) at the surface for a distance of 3 feet (.92m) or more is classified separately. A Class 4 crack is defined as any crack which has been sealed.

Table 1. Summary of Data from 49 AASHO Sections

	<u>Uncracked Pavement</u>	<u>Class 1 &amp; 2 Cracked</u>	<u>Class 3 &amp; 4 Cracked</u>
Mean Deflection (in.)	$10.8 \times 10^{-3}$	$10.6 \times 10^{-3}$	$14.0 \times 10^{-3}$
Standard Deviation (in.)	$4.0 \times 10^{-3}$	$3.2 \times 10^{-3}$	$4.4 \times 10^{-3}$
Mean Surface Thickness (in.)	9.3	9.3	9.3
Mean Subbase Thickness (in.)	7.1	7.1	7.1

1 in=2.54cm

Figure 13 is a plot of the mean deflection data for the three pavement conditions. It can be seen that there is essentially no difference in deflection between the uncracked and Class 1 and 2 cracked condition. Thus, these two conditions were considered structurally the same. However, there is a significant difference between the deflection for the uncracked condition and the deflection for the Class 3 and 4 cracked condition. A "student-t" analysis showed them to be significantly different at a 97.5% confidence level. This left two distinct structural conditions to be carried forward in the analysis (1) Class 1 and 2 or uncracked and (2) Class 3 and 4 cracked. The deflections for the uncracked condition were used to determine the modulus of subgrade reaction (k-value) and the deflections for the Class 3 and 4 cracked condition were used to determine the effective modulus for cracked concrete.

Determination of k-value - The discrete element computer program SLAB49 (Ref. 13) was used to compute edge deflections of the 9.3 inch (23.6cm) thick slab. Since the slab condition for this analysis was uncracked, the modulus of elasticity for the concrete was selected as  $5.25 \times 10^6$  psi, ( $36.23 \text{ kN/m}^2$ ) which is the value that has been reported for the Road Test concrete. The 18-kip (8172kg) single axle load was modeled as shown in Figure 12. Three different k-values were used in the analysis, 150 psi/in, 200 psi/in, and 250 psi/in, (4155g/cc, 5540g/cc, 6925g/cc). Results of the deflections computed for each k-value are given in Table 2. The relation of computed edge deflection versus k-value is shown in Figure 14.

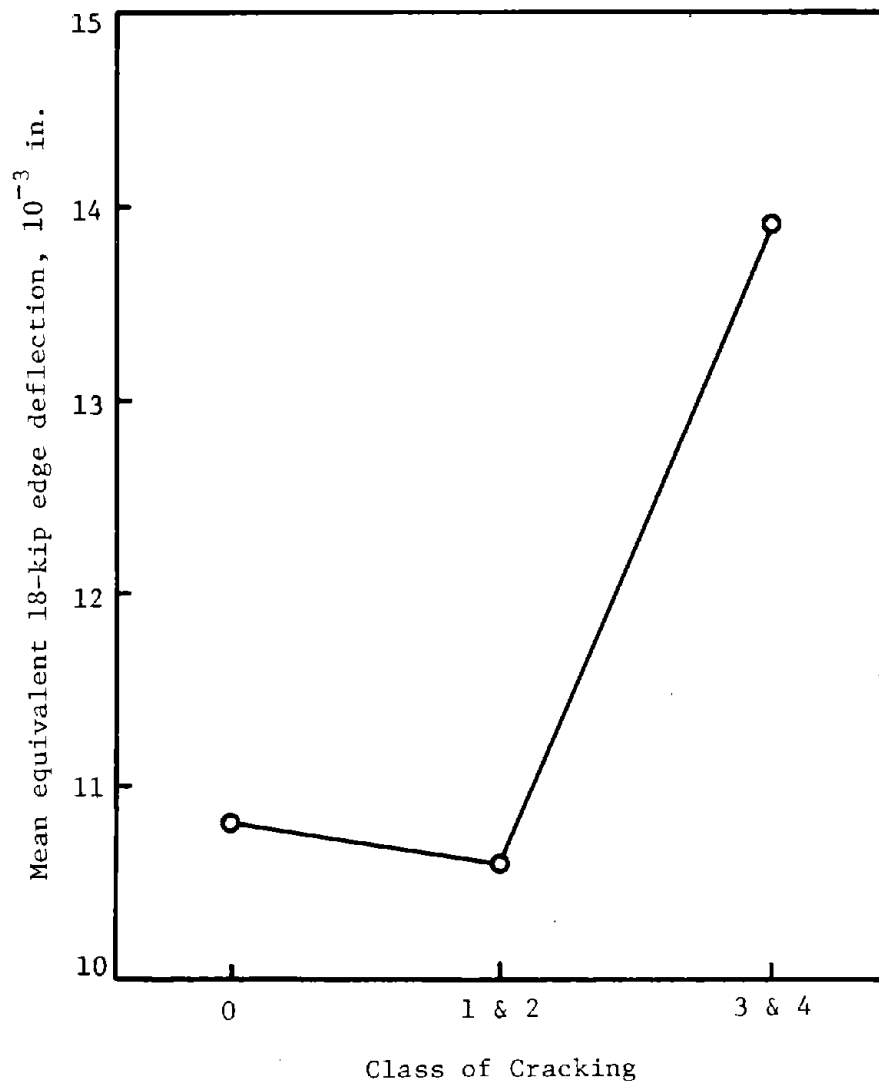


FIGURE 13. Normalized edge deflection versus cracking for AASHO Road Test Rigid Pavements.

1 in = 2.54cm  
 1 kip = 454kg

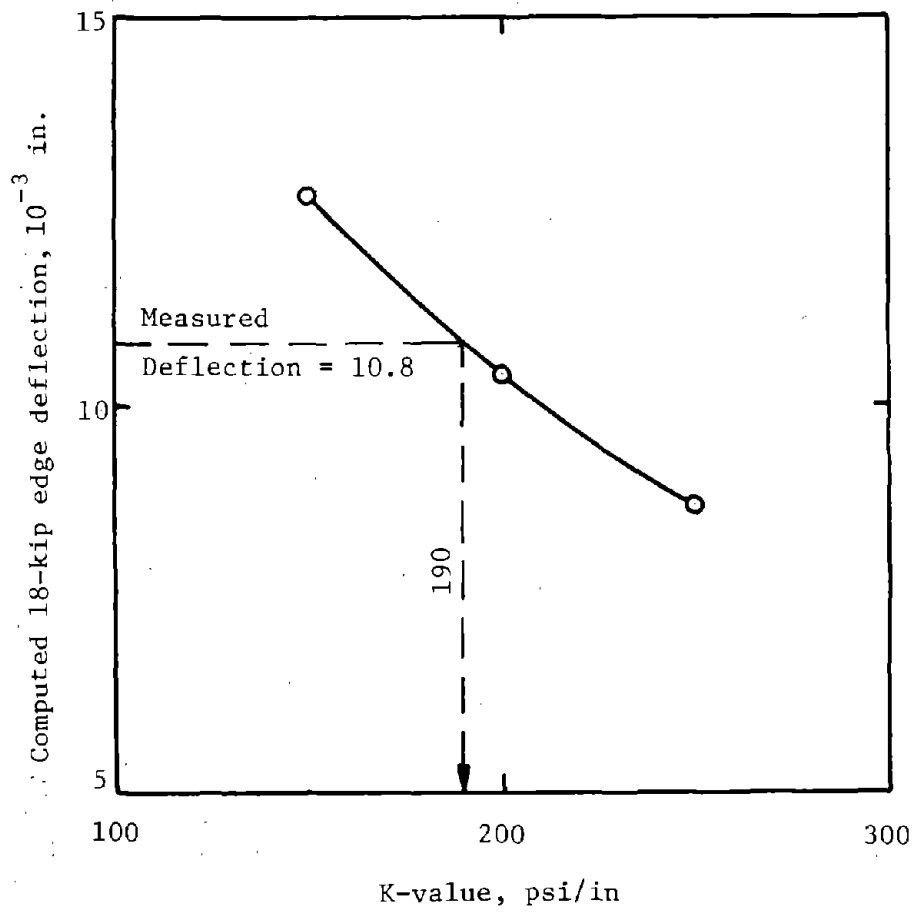


FIGURE 14. Determination of K-value by matching measured and computed deflections.

1 in = 2.54cm  
 1 psi = 27.7kN/m<sup>2</sup>  
 1 kip = 454kg

Table 2. Computed Edge Deflections for Various k-values

<u>k-value, psi/in</u>	<u>Computed Edge Deflection, mils</u>
150	12.7
200	10.3
250	8.8

1 mil = .0025cm  
1 psi/in = 27.7g/cc

To determine the proper k-value, the mean normalized measured deflection for the uncracked condition,  $10.8 \times 10^{-3}$  inches ( $27.4 \times 10^{-3}$ cm) was entered in the graph and projected down to the abscissa. The resulting k-value was 190 psi/in. ( $.007\text{kg/m}^3$ ). This value was then fixed in the next analysis for determining the effective modulus of the cracked concrete.

Determination of Effective Modulus - The principle of matching measured and computed deflections was again used. The mean measured deflection increased from 10.8 mils (.03cm) for the uncracked condition to 14.0 mils (0.4cm) for the Class 3 and 4 cracked condition. This deflection increase was due to a reduced stiffness, i.e., a lower effective concrete modulus. An investigation was made to determine if the deflection increase might be due in part to increase in moisture content with time or in part to the season of deflection measurement. These were found to have only a minor connection with the increased deflection. Thus, it was assumed valid to correlate the deflection increase with a reduced effective concrete modulus.

The SLAB49 computer program was used to compute edge deflections with the same load configuration (Figure 12) and slab thickness as in the previous analysis. The k-value of 190 psi/in. ( $.007\text{kg/m}^3$ ) was held constant and the surface modulus was varied. Seven values were used ranging from 200,000 psi to 5.25 million psi (1,380,000 to 36.225 million  $\text{kN/m}^2$ ). The edge deflections computed for each of these modulus values are shown in the modulus versus deflection relation, Figure 15.

In this case the deflection entered in Figure 15 to determine the modulus was not the mean value. Data from the AASHTO Road Test Report 5 (Ref. 12) indicate that the mean deflection is not truly representative of the severe Class 3 and 4 cracked condition which is being characterized. The deflection measurements were made on panel 4 for the reinforced sections and panel 5 for the nonreinforced sections, whereas the cracking survey was made on the entire section. The AASHTO data shows that the cracking was not uniformly distributed among the panels within a section. In fact, there was usually one panel in each section that had considerably more cracking than any other panel. Consequently, panels 4 and 5 were not always the severely cracked ones within each section. Thus, some of the deflection measurements are representative of uncracked or mildly cracked panels. This results in the mean value being lower than that which would be truly representative of a severely cracked condition.

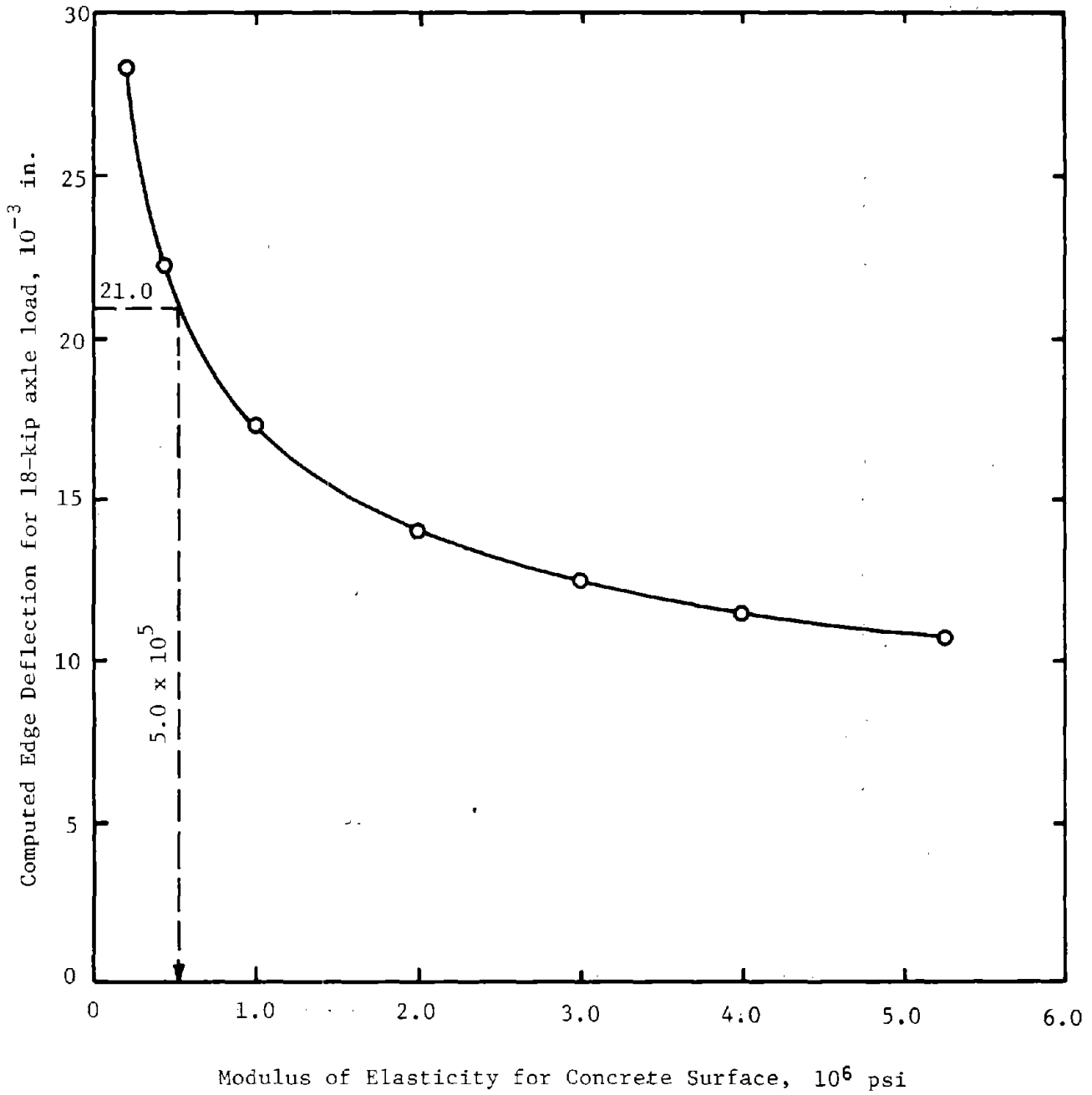


FIGURE 15. Determination of modulus for cracked concrete by matching measured and computed deflections.

1 in = 2.54cm  
 1 psi = 6.9 kN/m<sup>2</sup>  
 1 kip = 454kg



Because of this fact and also because it is desirable to select a modulus that will give a conservative overlay design, it was decided to use the 90<sup>th</sup> percentile deflection as being representative of the severely cracked condition. Entering the 90<sup>th</sup> percentile deflection, 21 mils, (.05cm) in Figure 15 and projecting to the modulus scale, results in a modulus of 500,000 psi (3,450,000kN/m<sup>2</sup>). Thus, this value is considered as the effective modulus of a Class 3 and 4 cracked concrete pavement.

#### Selection of Effective Elastic Modulus for Mechanically Broken-up Concrete

If an existing pavement is cracked badly enough, the decision may be made to mechanically break it up into small pieces so that it completely loses integrity and functions more like a base material than a surface layer. It is necessary to use an effective elastic modulus in the overlay analysis that is representative of this condition.

An uncracked pavement is assigned an effective modulus based on the strength of the concrete at time of construction or on a strength that has increased with age. This will usually be in the range of two to five million psi. A Class 3 and 4 cracked pavement is assigned an effective modulus of 500,000 psi (3,450,000kN/m<sup>2</sup>) as has been previously discussed. The modulus for a mechanically broken-up concrete must logically be a value less than 500,000 psi (3,450,000kN/m<sup>2</sup>) since the pavement has much less structural integrity than a Class 3 or 4 cracked pavement.

In the flexible overlay design procedure of Phase I (Ref. 9), a Class 2 cracked asphaltic concrete was assigned an effective modulus of 70,000 psi (483,000kN/m<sup>2</sup>). A field inspection of a mechanically broken-up concrete showed it can be expected to exhibit a load carrying capacity very near that of a Class 2 cracked asphalt. Thus, it was assigned a modulus of 70,000 psi (483,000kN/m<sup>2</sup>).

The resulting modulus of elasticity values for the three conditions of the existing pavement considered in the overlay design procedure may be described as follows:

$$E_e = f \text{ (Condition of existing surface)}$$

where:

$$E_e = \text{Effective modulus of elasticity for existing concrete surface, psi.}$$

The value of  $E_e$  for use in the stress analysis procedures may be derived from the following:

<u>Pavement Condition</u>	<u><math>E_e</math></u>
Uncracked or Class 1 and 2 cracked	Same as new pavement, usually 2 to 5 million psi
Class 3 and 4 cracked	500,000 psi
Mechanically broken up	70,000 psi

1 psi=6.9kNm/2

#### Stress Adjustments for Corner and Edge Loads

The stresses and deflections predicted using elastic layered theory are for an interior loading condition away from a joint or crack, where the slab is assumed homogeneous in all directions. However, the design of CRCP and JCP is normally based on edge and corner stresses, respectively, which are more critical than interior loading stress conditions. In order to conform to existing practice, it is necessary to increase stresses computed by elastic layered theory so that they will be representative of edge and corner stresses in concrete slabs. The development of these stress adjustment factors is discussed in this section.

An extensive series of problems were solved for interior, edge, and corner deflections and stresses using the discrete element theory program, SLAB49 (Ref. 13), as well as Westergaard (Ref. 15)<sup>1</sup> and Pickett theory (Ref. 16)<sup>2</sup>. A relation between the ratio of corner to interior stress and the ratio of corner to interior deflection was developed and is given in Figure 16. The purpose for developing this curve was to allow consideration of the joint condition of an existing jointed concrete pavement in the design of the overlay. The designer can measure interior and corner deflections, compute their ratio, and then use the curve in Figure 16 to determine the relation between interior and corner stress. The stress computed by elastic layered theory is then multiplied by this stress ratio to determine the design stress. If the deflection ratio is less than 2.3 the stress ratio is fixed at a constant value equal to the minimum value on the curve.

<sup>1</sup>Westergaard, H. M., "Theory of Concrete Pavement Design," Proceedings Highway Research Board, 1927.

<sup>2</sup>Pickett, Gerald, M. E. Raville, W. C. Jones, and F. J. McCormick, Deflections, Movements and Reactive Pressures for Concrete Pavements, Kansas State College Bulletin No. 65, October 1951.

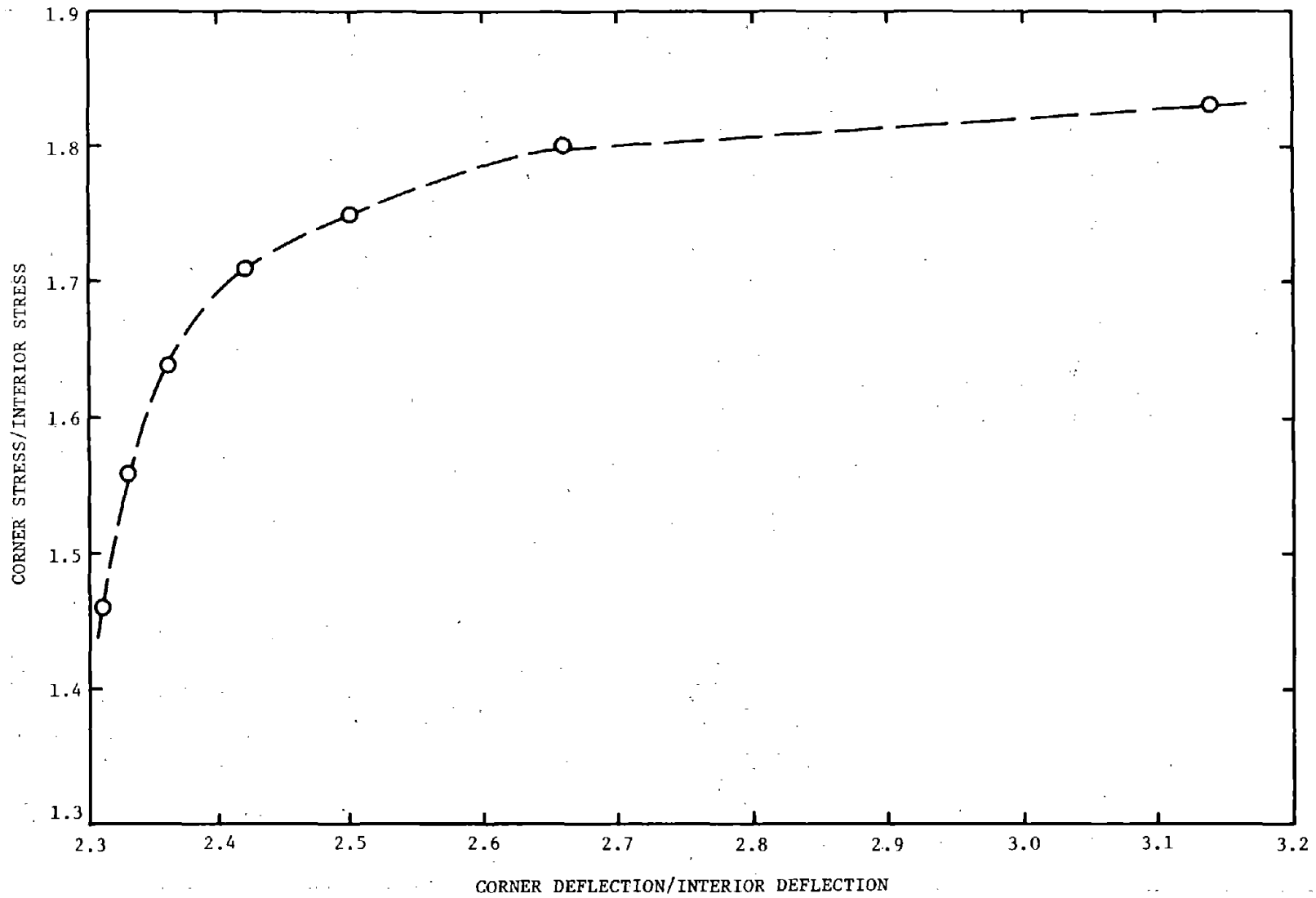


Figure 16. Stress ratio curve for relating interior to corner stresses for a given Deflection Ratio

Further stress and deflection analyses finally led to stress adjustment factors,  $C_L$ , for each of the combinations of existing pavement type and overlay type. These are given in Table 3. The stress computed by elastic layered theory is adjusted by these factors and the resulting stress is used in determining the overlay thickness.

The relationship described in this section may be mathematically described as follows:

$$\sigma_L = C_L \sigma_i \dots\dots\dots (8)$$

where:

$\sigma_L$  = the simulated stress in the pavement at the critical point (maximum stress) for a given combination of pavement types, psi,

$C_L$  = stress adjustment factor taken from Table 3 or Figure 16 to correct interior stress to critical loading condition,

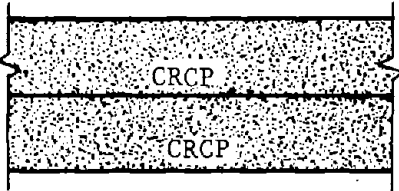
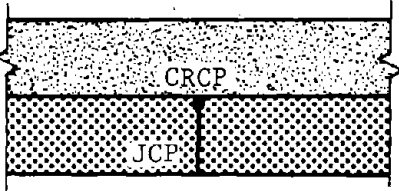
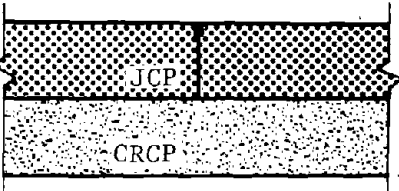
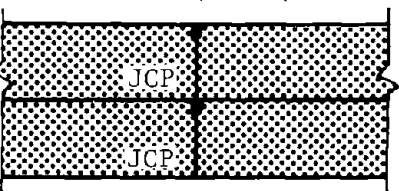
$\sigma_i$  = stress simulating an interior loading condition as predicted by ELSYM5, psi.

$$1 \text{ psi} = 6.9 \text{ kN/m}^2$$

#### Consideration of Voids

There are two primary causes of voids beneath a pavement; 1) pumping of the subbase, and 2) differential vertical movements such as may be caused by expansive soils. This analysis considers different sizes of edge and corner voids and applies slab theory for calculating moments produced by the 18-kip (8172kg) single axle load. When voids exist beneath a pavement there is an increase in the applied stress, resulting in a reduction of allowable load applications. This increase in stress (or moment), due to voids, is defined as the void factor,  $C_v$ . It can be shown that the shape of the void has a definite effect on the void factor. Figure 17 illustrates the analytical effect of void size, and void shape and composite support value on an increase in stress due to the presence of a void. Based on engineering judgement only the shapes of voids shown in Figure 18 were considered. The results are graphically illustrated in Figure 19, and the computed void factors are tabulated in Table 4. For this analysis all support was removed, but as a real pavement deflects under load, some support is obtained as the slabs' curvature takes the shape of the void. This would reduce the resulting void factor. This was considered by removing only a percentage of the total support, Figure 20. The percent of support removed is a function of void depth, shape, slab stiffness, and other variables, although a value of 50% support removed was selected to represent all conditions. This results in a 25% reduction of the values given in Table 4. Based on the above analysis, the void factors were selected for use in the design procedure.

TABLE 3. Stress adjustment factors selected for various overlay-existing pavement combinations to convert interior stresses to stresses for use in design.

Overlay-Existing Pavement Combinations		Stress Adjustment Factor- $C_L$
Overlay		1.2
Overlay		1.2
Overlay		1.3
Overlay		1.4 - 1.8 based on field deflections measured and Figure 16

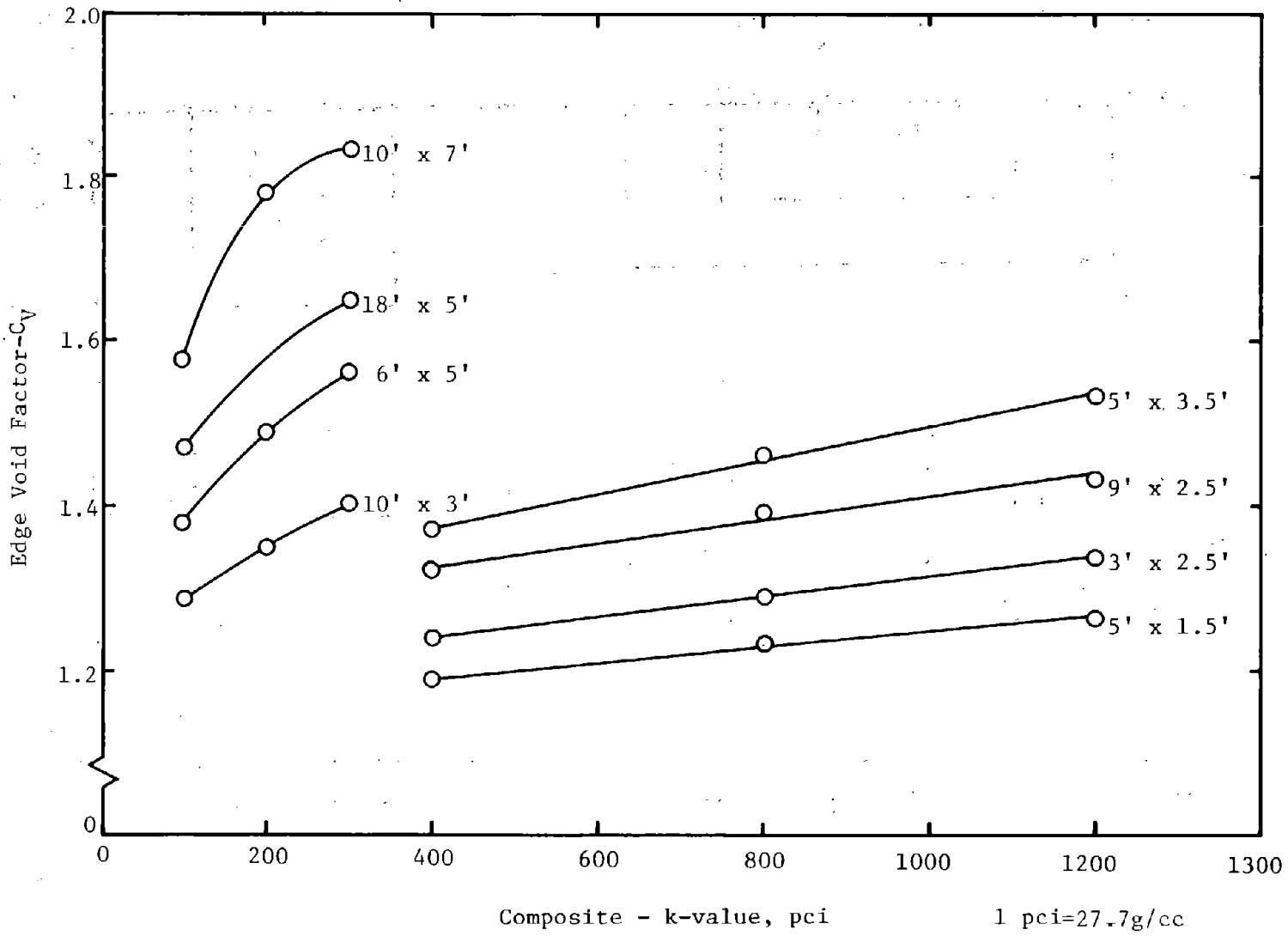


FIGURE 17. Effect of composite support, void size and shape on the void factor.  
 1 ft = 0.305 m

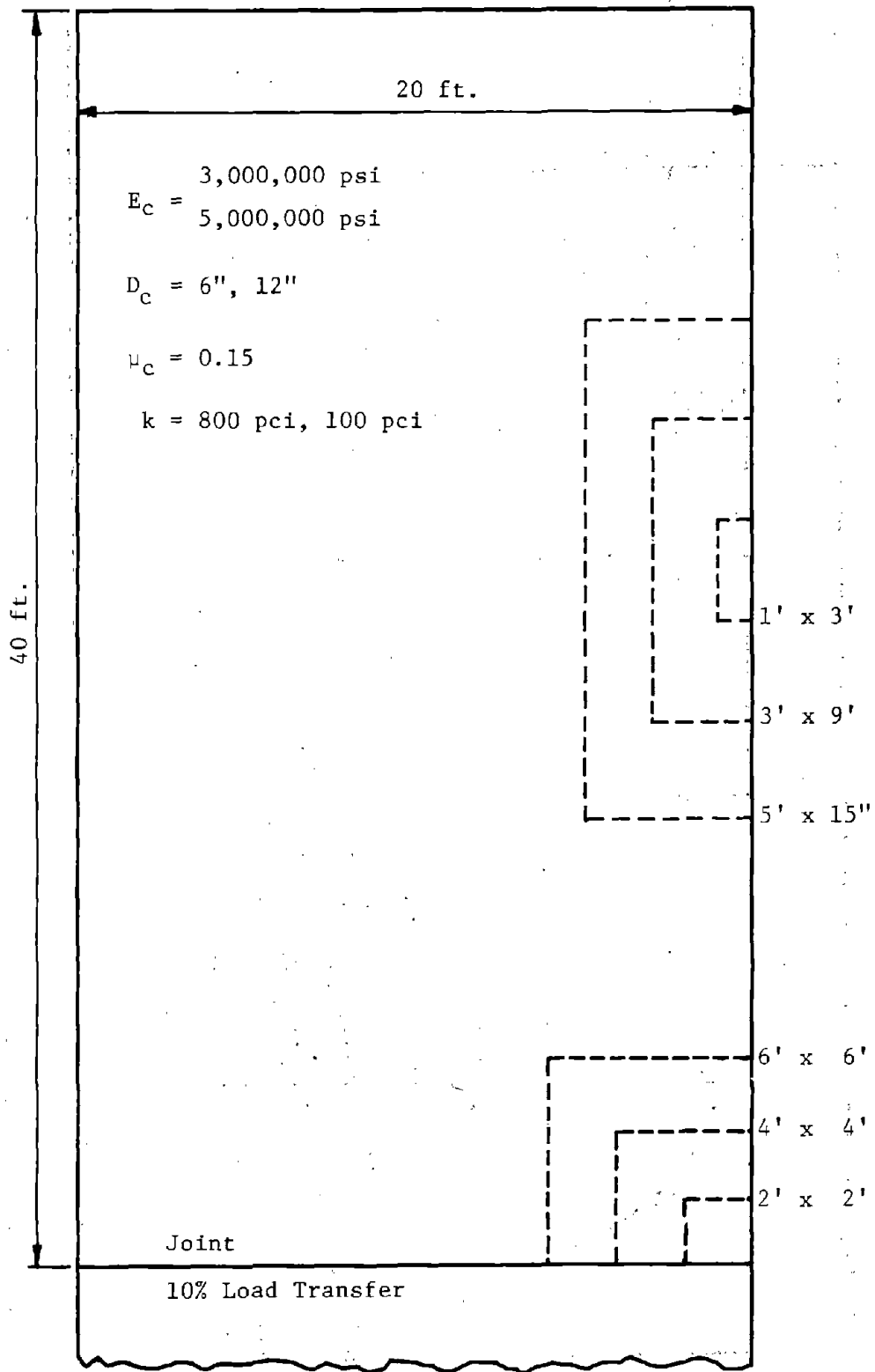


Figure 18. Size and shape of voids used in developing void factors.

1 pci = 27.7g/cc  
 1 psi = 6.9kN/m<sup>2</sup>  
 1 ft = .305m  
 1 in = 25.4 mm

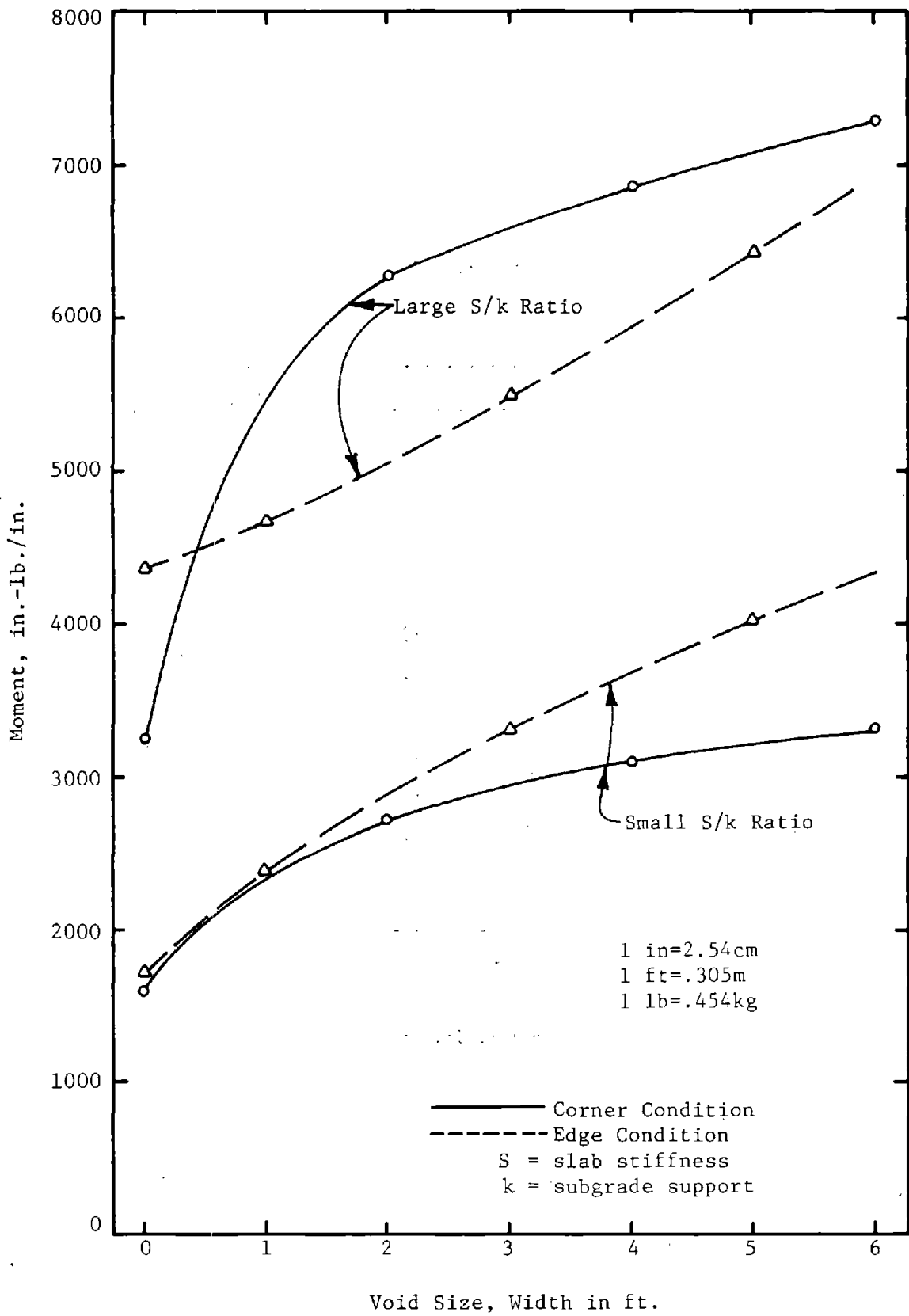


FIGURE 19. Effect of void size on maximum principal moment for edge and corner loading conditions.



Table 4. Summary of void factors where full support was removed in the analysis

Void Location	Void Size (ft. x ft.)	Void Factor	
		$S/k^* = 6.9 \times 10^4$	$S/k^* = 7.36 \times 10^6$
Edge	0 x 0	1.0	1.0
	1 x 3	1.39	1.07
	3 x 9	1.93	1.26
	5 x 15	2.35	1.47
Corner	0 x 0	1.0	1.0
	2 x 2	1.70	1.94
	4 x 4	1.94	2.11
	6 x 6	2.08	2.24

\*S/k Slab stiffness (S) to composite support value (k) ratio.

1 ft=.305m

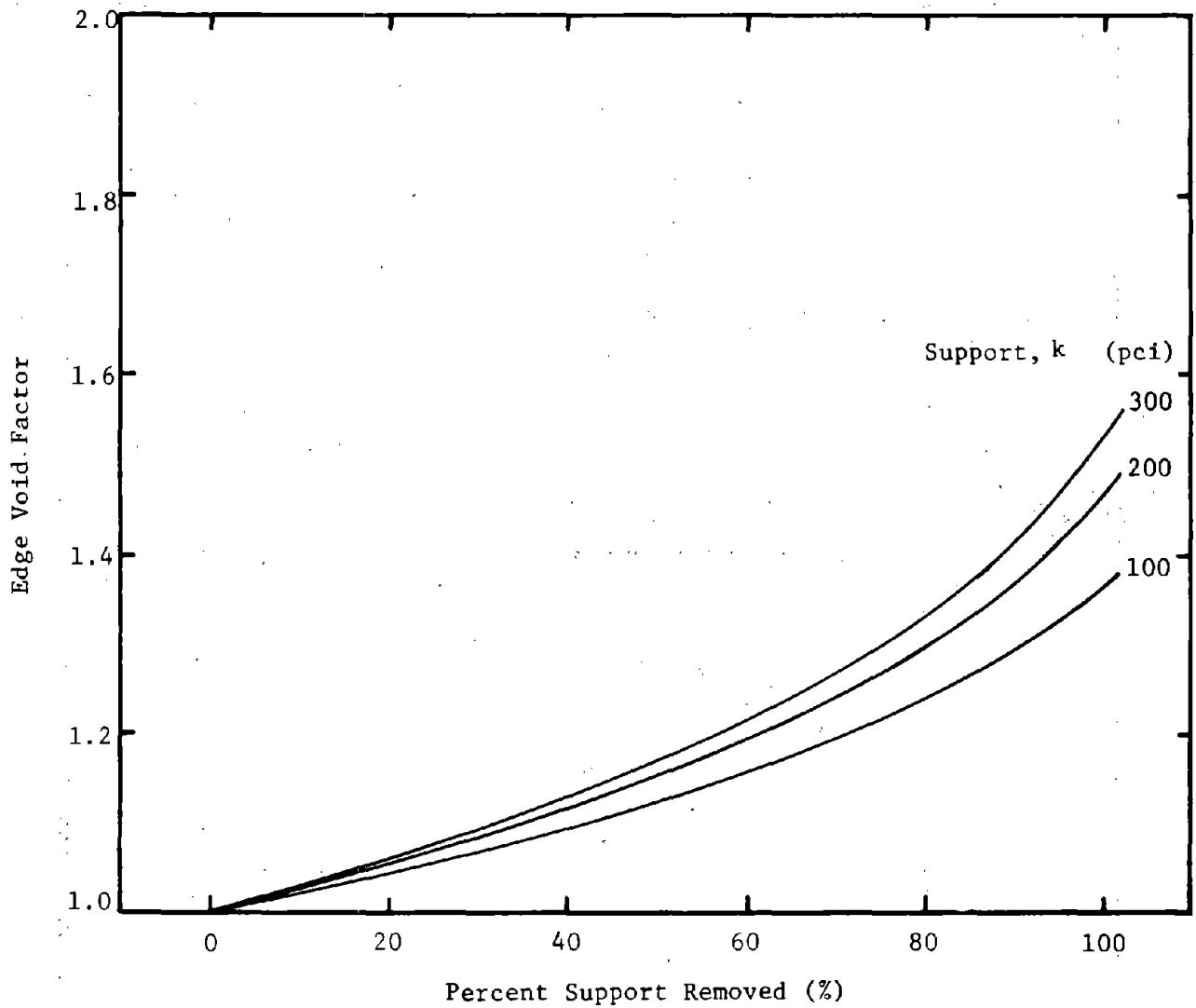


FIGURE 20. Effect of natural subgrade support and its loss on the void factor for a 5 x 6 ft. void

1 ft=.305m  
 1 pci=27.7g/cc

The results from the analysis performed in this section may be mathematically described as follows:

$$\sigma_v = C_v \sigma_L \dots \dots \dots (9)$$

or

$$\sigma_v = C_v \cdot C_L \cdot \sigma_i \dots \dots \dots (10)$$

where:

$\sigma_v$  = the critical stress in pavement corrected for void conditions, psi, (1 psi=6.9kN/m<sup>2</sup>)

$C_v$  = stress adjustment factor to account for voids beneath the pavement,

$\sigma_L, C_L, \sigma_i$  as described previously.

The value of  $C_v$  may be selected from the following guidelines, but the designer should recognize that this is a first approximation. Thus, future studies should be directed toward improving this adjustment factor.

<u>Condition</u>	<u><math>C_v</math></u>
Edge	1.1
Corner	1.5

#### Fatigue Curve Development

One of the major distress mechanisms associated with rigid pavements is the fatigue of concrete (Ref. 12). Fatigue of concrete is defined as "the process of progressive localized permanent structural change occurring in the material subjected to conditions which produce fluctuating stresses and strains at some point or points and which may culminate in cracks or complete fracture after sufficient number of fluctuations" (Ref. 17)<sup>1</sup>. Rigid pavements possess this characteristic of failing by progressive fracture and one of the major contributors to failure is the repeated application of flexural stresses. Therefore, a relationship of concrete strength, stress, and load applications was considered as a basis for the development of the fatigue relationship.

---

<sup>1</sup>Mills, R. E., and R. F. Dawson, "Fatigue of Concrete," Proceedings, Seventh Annual Meeting, Highway Research Board, Washington, D.C. 1928, pp 160-172.

## Failure Criteria

The basis for using cracking alone as a design criteria is inadequate since the formation of a crack in the pavement slab is not necessarily a functional failure. Therefore, some measure of severity of the crack must be used to determine deterioration in the field. Class 3 or Class 4 cracking, as determined at the AASHO Road Test, was chosen to represent a condition that requires an overlay. The data from the controlled field experiments at the AASHO Road Test were collected and analyzed to obtain the best information available for the prediction of fatigue distress in rigid pavements. This fatigue approach will result in a life prediction slightly greater than an initial crack approach, but it is felt to be more representative of field conditions.

## Traffic

The traffic quantity used in developing the fatigue curve was the number of 18-kip (8172kg) equivalent single axle wheel loadings which were computed using the AASHO equivalency factors for a terminal serviceability of 2.5 (Ref. 18<sup>1</sup>). The actual traffic taken from the Rigid Pavement Section Performance Records of the AASHO Road Test was the number of applications to the time when Class 3 and 4 type cracking was produced.

## Stresses

From the AASHO traffic records it was determined that the average distance from the pavement edge to the center of the outside wheel was approximately 26-32 inches (66.04-81.3cm) (Ref. 19<sup>2</sup>). Therefore, it was questioned as to whether the stresses to be used for the fatigue curve should represent an interior or edge loading condition. Slab theory was applied to obtain an indication of how the maximum principal stress varies as the load is positioned from the edge to an interior loading condition (Figure 21). By reviewing Figure 21 it can be concluded that the large difference in stresses occurs at two feet (.61m) from the pavement's edge. At 29 inches (73.7cm) there is only a 10-15 percent difference; hence an interior condition was assumed. Therefore the stresses used for developing the fatigue curve were computed by the ELSYM5 computer program for an 18-kip (8172kg) single axle load. The 18-kip (8172kg) load was used since all actual applications were converted to 18-kip (8172kg) equivalencies. These computed stresses represent a horizontal tensile stress in the direction parallel to the roadway centerline at the bottom of the concrete for the pavement structure given in Figure 22. The family of curves used to predict the stresses for various combinations of thicknesses are illustrated in Figure 22.

---

<sup>1</sup>"AASHTO Interim Guide For Design of Pavement Structures, "American Association of State, Highway and Transportation Officials, 1972.

<sup>2</sup>"The AASHO Road Test Report 3, Traffic Operation and Pavement Maintenance," Special Report 61C, Highway Research Board, Washington, D.C., 1962.

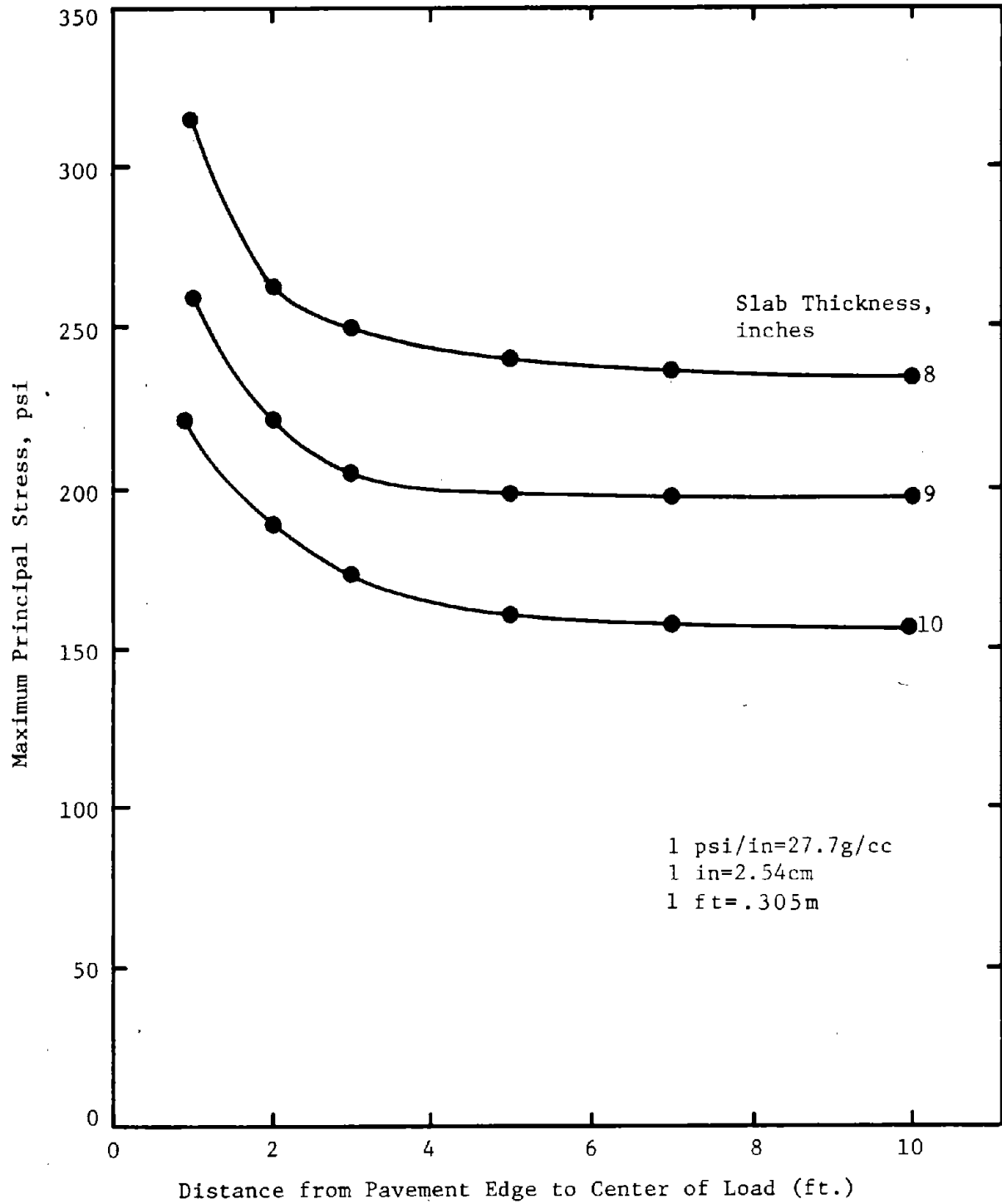


FIGURE 21. Relation of slab stress and distance from pavement edge to center of load for  $k = 100$  psi/in (Ref. 13).

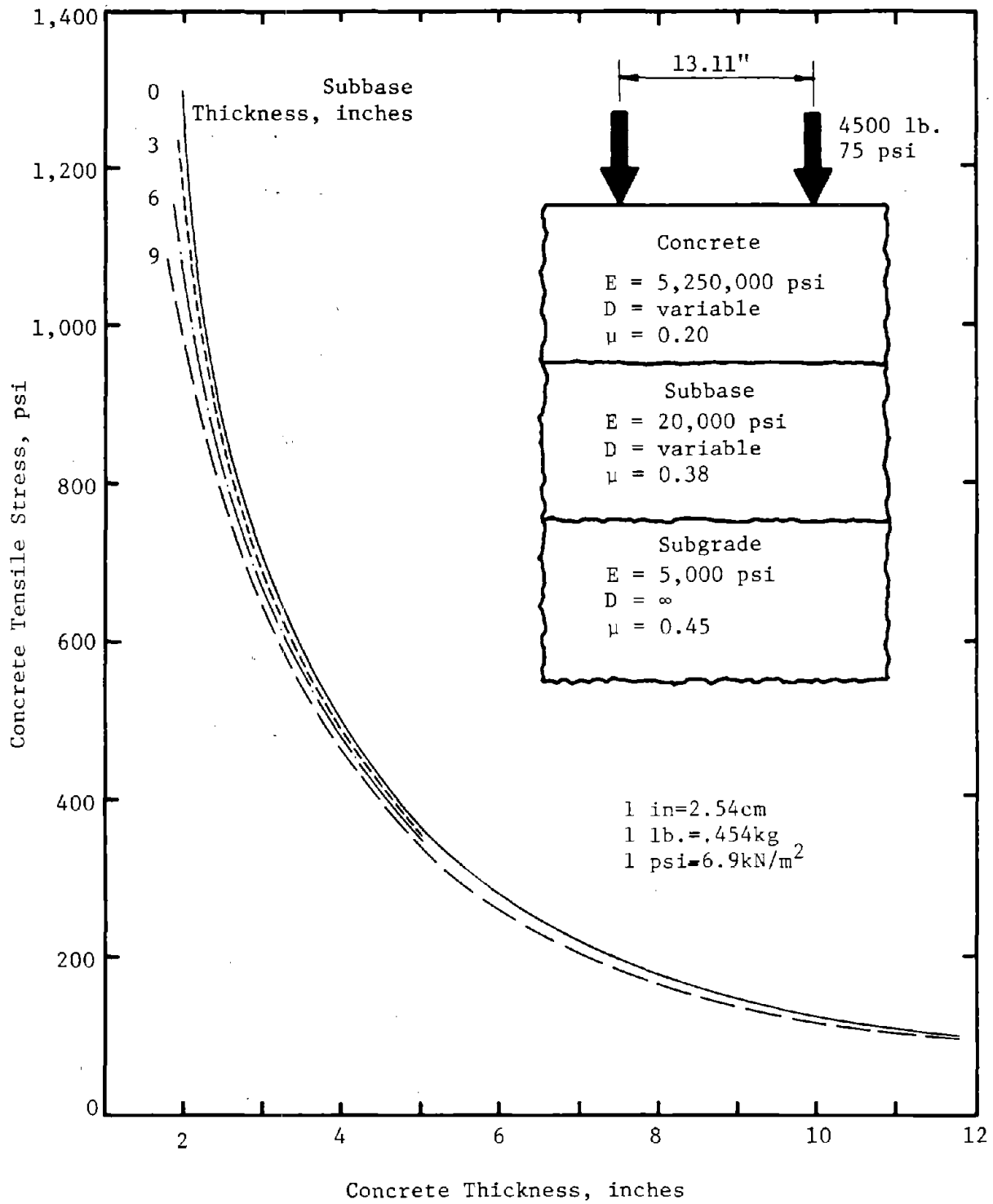


FIGURE 22. Relation of concrete tensile stresses for various combinations of layer thicknesses for an 18-kip(8172kg) single axle load

## Analyses

In generating an initial fatigue curve, only sections which exhibited Class 3 and 4 cracking were considered. Nonreinforced concrete pavement sections along with corresponding reinforced pavement sections were randomly selected for the development of the fatigue curve. A regression analysis was performed and resulted in the following equation:

$$N_{18} = 14,480 \left(\frac{f}{\sigma}\right)^{3.43} \dots \dots \dots (11)$$

There was a large variation in the data as presented in Figure 23. (The R<sup>2</sup>-value determined from the regression analysis was only 69%). Due to this large variation in data, variables that were suspected of affecting the applied stress were investigated. These are discussed in the following paragraphs.

Pumping - During the AASHO Road Test all sections experienced some pumping, except a few sections in Loop #2. To estimate the amount of material pumped, a "pumping index" was computed. This index approximated the accumulated volume of material pumped per unit length of pavement (Ref. 12). In developing the initial fatigue curve, pumping was considered since pumping causes a loss of support or creation of a void space beneath the pavement resulting in an increase in stress, which may have caused difference in performance histories of rigid pavement sections with the same design variables.

At the AASHO Road Test, there was no clear-cut evidence associating the pumping index with the occurrence of Class 3 and 4 cracking. Some sections which experienced Class 3 and 4 cracking had a much lower pumping index than those which did not. This was also the case when failure was based on the serviceability concept as reported in Reference 20<sup>1</sup>. From this investigation, it was determined that no one value of the pumping index could be related to premature Class 3 and 4 cracking.

In summary, the pumping analysis showed that as the fatigue life increased, the pumping index increased. This implies, as was found at the AASHO Road Test, that pumping was dependent upon traffic and load as observed from Figure 24. Therefore, it was concluded that, although pumping had an effect on the probability of survival of a section, it was dependent on traffic, load and thickness, and independent of Class 3 and 4 cracking. Thus, pumping effects were not considered in the development of the final fatigue curve.

---

<sup>1</sup>Yimprasert, Piti, and B. Frank McCullough, "Fatigue and Stress Analysis Concepts for Modifying the Rigid Pavement Design System," Research Report 123-16, Center For Highway Research, University of Texas at Austin, January 1973.

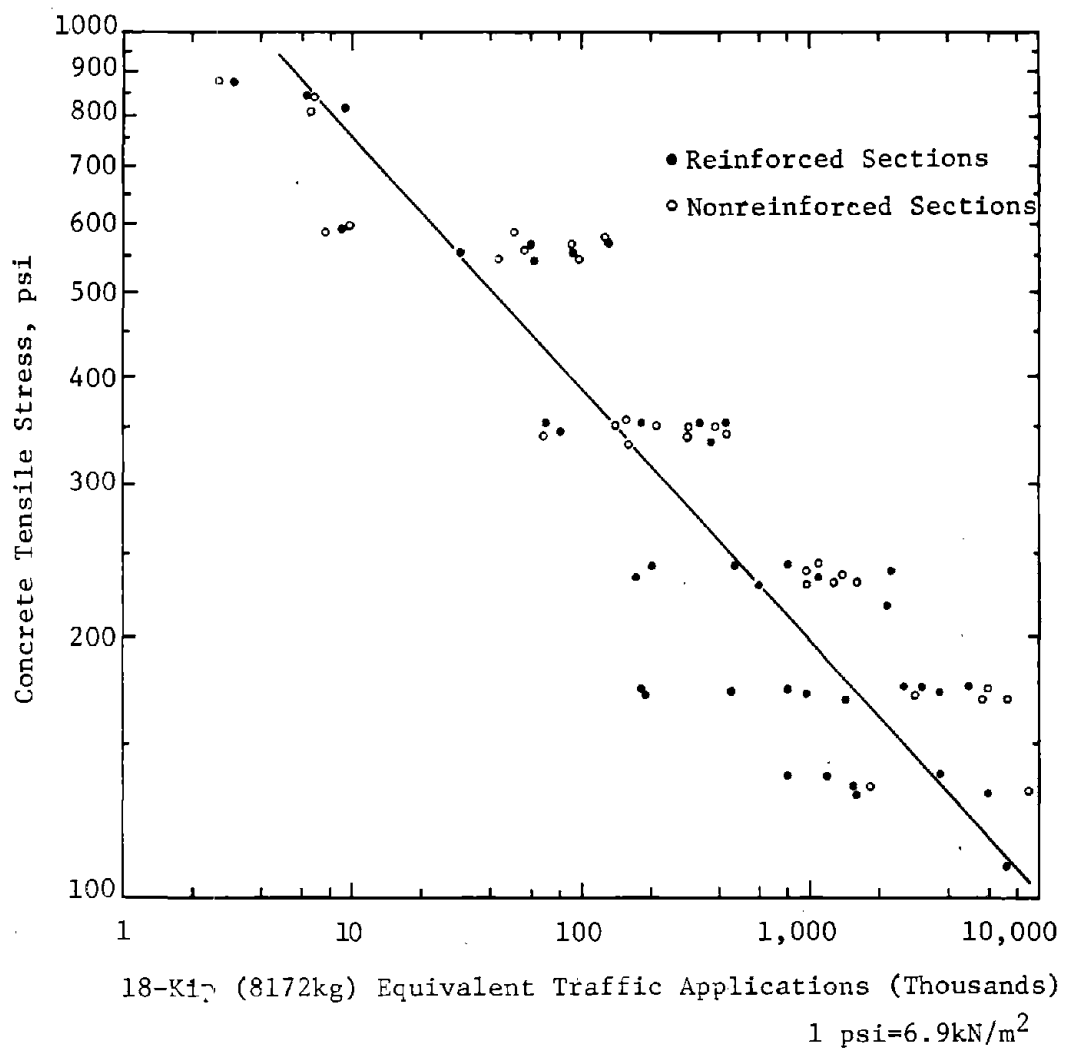


FIGURE 23. Initial fatigue curve based on randomly selected sections which contained Class 3 and 4 cracking.



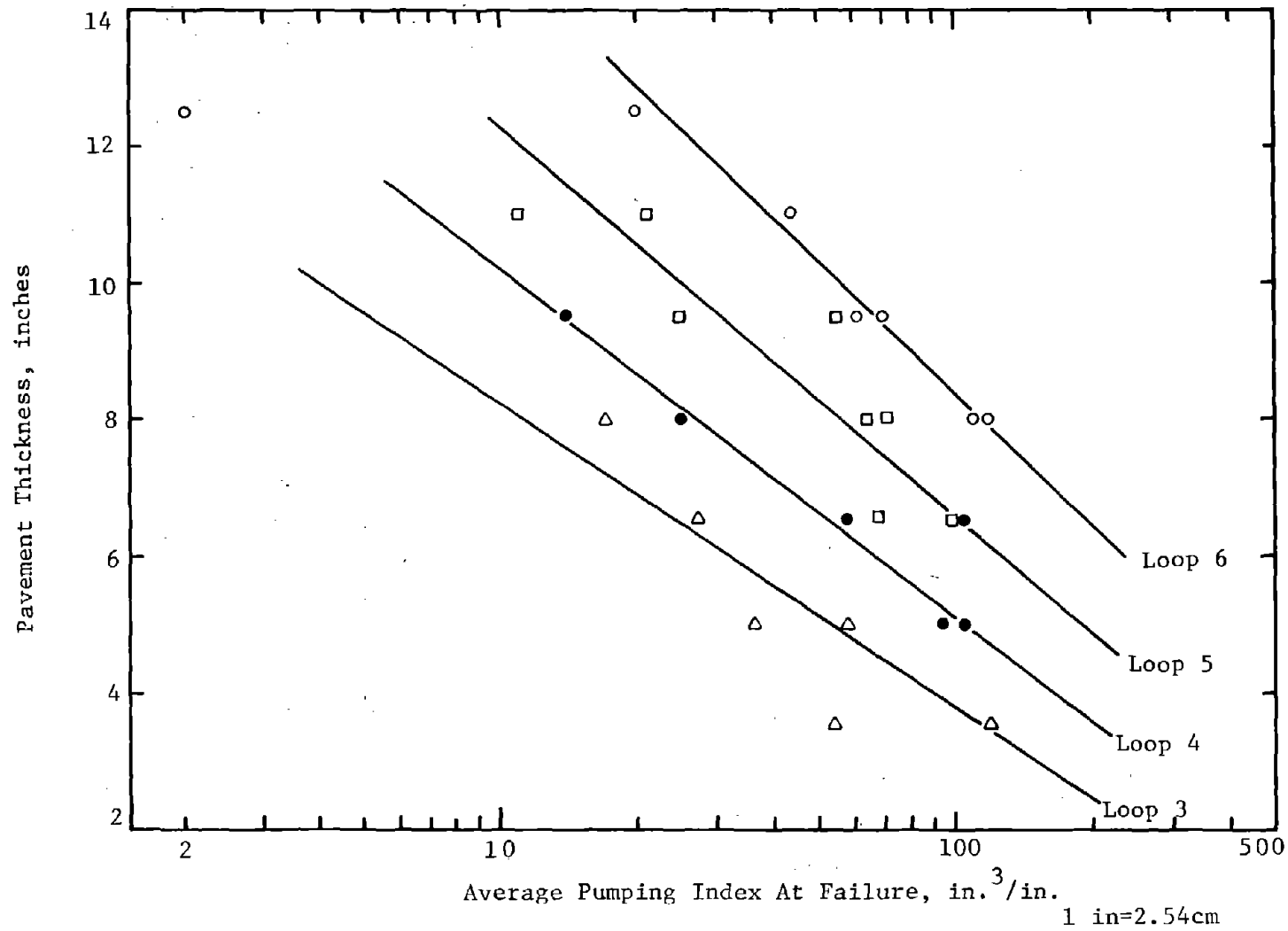


FIGURE 24. Relationship of average pumping index during the pavement serviceability life to load and pavement thickness.

Equivalency Factors - The equivalency factors, determined at the AASHO Road Test, were developed using the pavement performance or serviceability concept. This concept gives the number of equivalent load applications to a limiting level of serviceability defined as a functional failure of the pavement. Using cracking as a failure criterion, applicability of the equivalency factors was investigated. This analysis illustrated that there is some error in using equivalency factors based on serviceability to relate traffic to the mechanistic failure criterion of cracking. This is illustrated in Figure 25 where each loop has a different fatigue curve. Therefore, an attempt was made to find new equivalency factors based on a mechanistic failure criterion. This work involved a large amount of extrapolation and interpolation, which results in error, and therefore the equivalency factors previously developed at AASHO were used to develop the final curve.

Pavement Type - In the fatigue analysis, reinforced panels 40 feet (12.2m) long and non-reinforced panels 15 ft. (4.6m) long were used. An analysis was completed to determine if any differences existed in the performance of the two types of pavement. It was observed that essentially no difference existed in the lives of the pavements, although the nonreinforced sections had a greater probability of survival, as was also observed in References 20 and 21<sup>1</sup> when using the serviceability criteria. The major difference in performance occurs in the time interval between Class 1 and 2 and Class 3 and 4 type cracking (Table 5). Generally, for nonreinforced sections, Class 3 and 4 cracking occurred less than 6 months after Class 1 and 2 cracks formed, whereas the time intervals between the two types of cracking for the reinforced sections were greater than 6 months. The quicker occurrence of Class 1 and 2 cracking with reinforced pavements implies that cracking in the longer panels results from temperature and load, whereas for the shorter panels it is primarily a result of load. This demonstrates the ability of the reinforcement to hold the crack openings to a minimum value for longer slab lengths. Figure 26 shows cumulative frequency diagrams for the two pavement types. From the analyses, it was concluded that a nonreinforced 15 foot (4.6m) slab has the same fatigue relationship as the reinforced 40 foot (12.2m) slab.

Seasonal Effects - No cracks occurred in the Loop 1 pavements, which were not subjected to traffic, thus none of the cracks appearing in the traffic loops can be attributed solely to seasonal changes (Ref. 21). From reference 12, tests were made to determine the variation of properties in the subsurface layers. This variation was applied, and it was shown that the average change in the underlying layers did not significantly affect the stresses (Ref. 20). Temperature was also considered, but there was no significant increase in cracking failures during the colder months (Figure 26). Rainfall, which caused pumping, seemed to be the primary contributor to cracking.

---

<sup>1</sup>"The AASHO Road Test, Proceedings of a Conference held May 16-18, 1962, St. Louis, Mo.," Special Report 73, Highway Research Board, Washington, D.C., 1962.

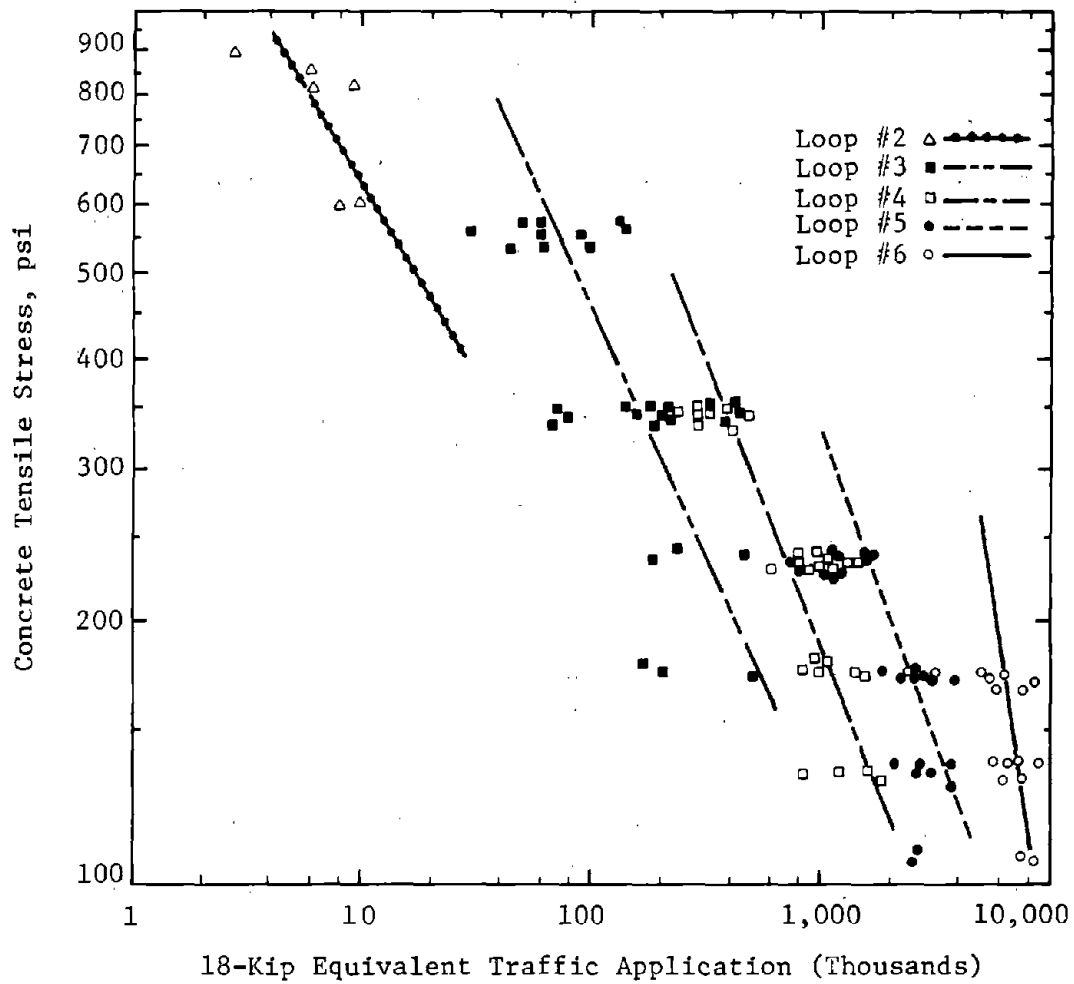


FIGURE 25. Relation of stress and load applications prior to Class 3 and 4 cracking.

1 kip=454kg  
 1 psi=6.9kN/m<sup>2</sup>

TABLE 5. Summary of the time interval between Class 1 and 2 and Class 3 and 4 cracking for each loop

Loop Number	Percent of Nonreinforced Sections		Percent of Reinforced Sections	
	< 6 Months	> 6 Months	< 6 Months	> 6 Months
2	29	71	20	80
3	93	7	40	60
4	91	9	12	88
5	92	8	20	80
6	75	25	36	64

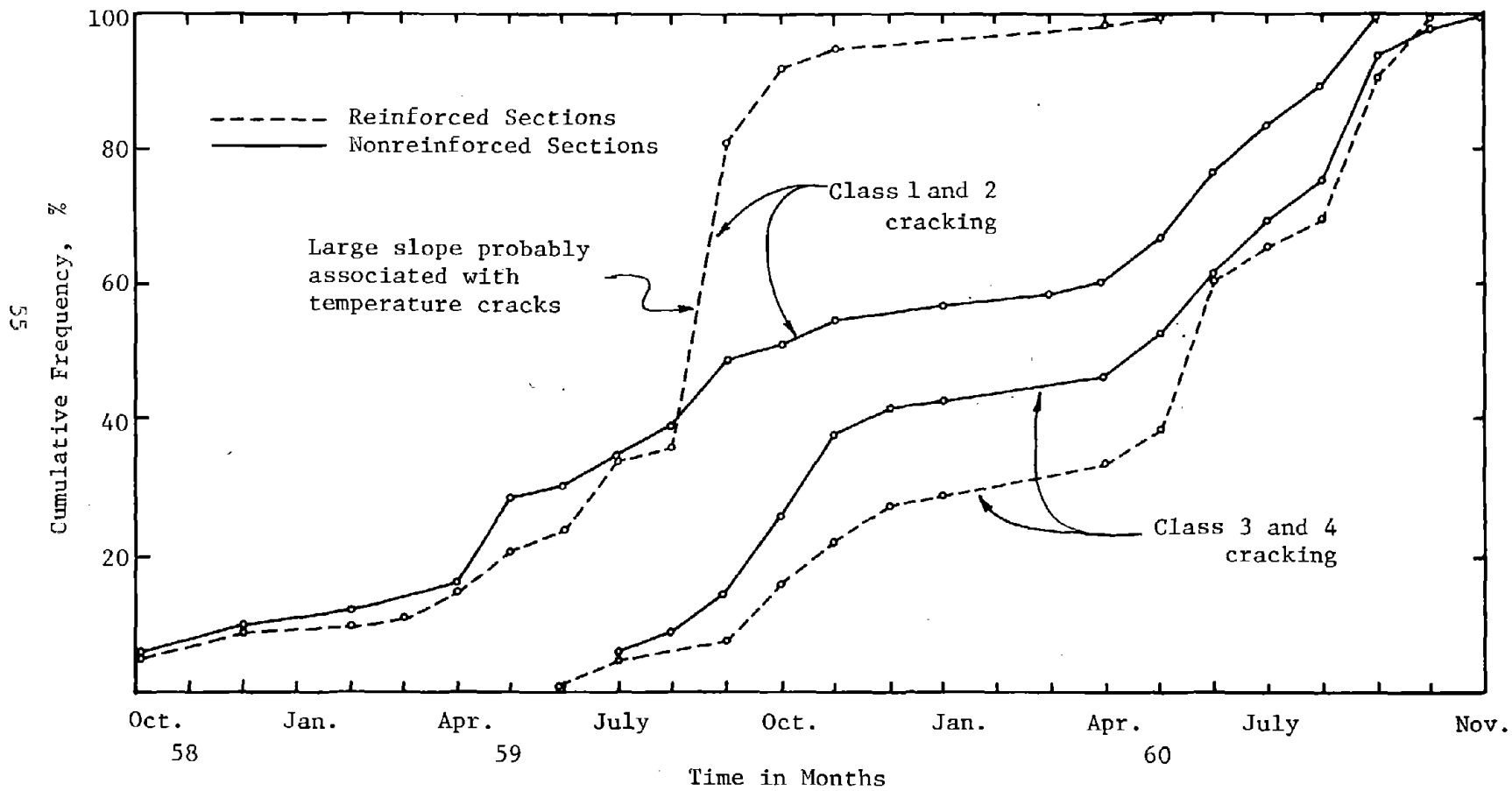


FIGURE 26. Cumulative frequency diagram for each class of cracking for each pavement type for AASHO rigid sections which failed.

### Finalized Curve

From these analyses, none of the variables investigated had a significant effect on the scatter of the initial fatigue curve data. The final fatigue curve was generated by running a regression analysis using all sections which contained Class 3 and 4 cracking, rather than the random sections chosen initially. The completed regression analysis resulted in the following equation with an  $R^2$  term of 83 percent:

$$N = 23,440 \left(\frac{f}{\sigma}\right)^{3.21} \dots \dots \dots (12)$$

The above equation is presented in Figure 27 which shows a comparison with other fatigue curves.

### Evaluation of New Materials

In recent years new materials have been studied as their effectiveness in rehabilitating an existing concrete pavement to extend its serviceable life. Discussions follow for two methods which are being studied extensively.

#### Polymer-Impregnated Concrete

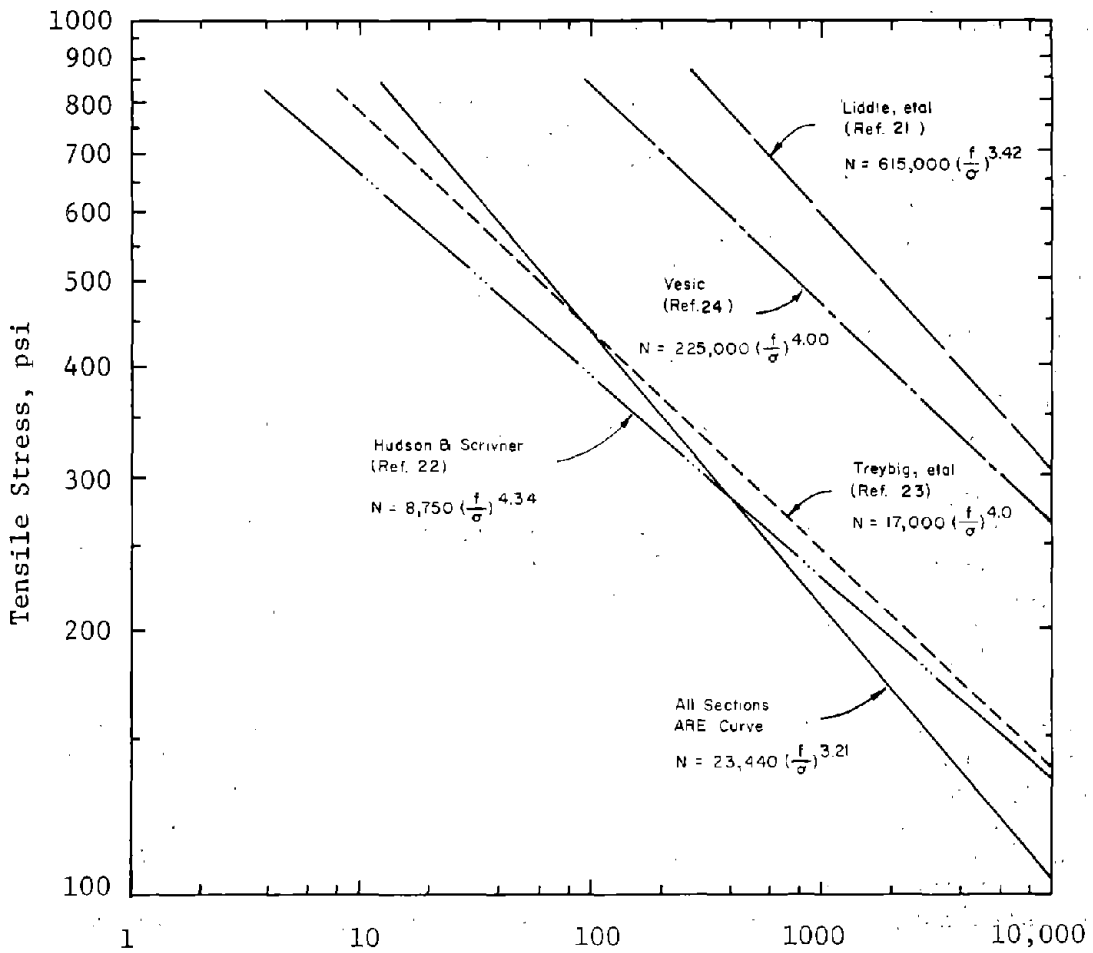
Partially or surface impregnated concrete for use in pavement rehabilitation has not been investigated very thoroughly, but has been tried with success for the repair of bridge decks. Nearly all research on the various techniques for impregnating concrete have been conducted in laboratories under ideal conditions which are not adequate for large scale use, such as highways. Most laboratory tests have been conducted on fully-impregnated samples, and the results indicate that mechanical and durability properties are generally significantly improved, but the process to achieve full impregnation is not economically applicable for field use (Ref. 25)<sup>1</sup>.

Polymer-impregnated concrete is a precast and cured hydrated cement concrete which has been impregnated with a liquid monomer of low viscosity that is subsequently polymerized (Ref. 26)<sup>2</sup>. This polymerization reaction converts the liquid monomer, which fills voids and microfractures in the concrete, into a solid plastic or polymer. This process will produce a concrete with good structural properties and resistance to freeze-thaw deterioration, water penetration, abrasion, and wear. It also has a skid resistance at least

---

<sup>1</sup> DePuy, G. W., "Highway Applications of Concrete Polymer Materials," Transportation Research Board No. 542, Transportation Research Board, 1975.

<sup>2</sup> Kubacka, L. E., J. Fontana, and M. Steinberg, "Polymer Concrete For Repairing Deteriorated Bridge Decks," Transportation Research Board No. 542, Transportation Research Board, 1975.



18-Kip Equivalent Traffic Applications (Thousands)

FIGURE 27. Comparison of newly developed fatigue curve with other curves.

1 kip=454kg  
 1 psi=6.9kN/m<sup>2</sup>

equal to that of conventional concrete. For example, tensile and compressive strengths of polymer-impregnated concrete specimens can be 4 to 5 times greater than those of control specimens (Ref. 27)<sup>1</sup>.

Polymer-impregnated concrete has been produced with a variety of monomer systems; the nature of this process largely restricts the choice of monomers to those which have double bonds and can be polymerized by a free radical mechanism. Some of the monomers which have been used are isobornyl methacrylate, isobutyl methacrylate, methyl methacrylate, and stearyl methacrylate. Some of the more important monomer characteristics which must be considered to achieve good results are viscosity, polymerization rate, evaporation rate, safety in handling, resultant polymer properties, and cost.

Polymer-impregnated concrete is formed by drying cured conventional concrete to remove excess moisture, diffusing or soaking a low viscosity monomer through the void structure at atmospheric pressure, and polymerizing the monomer to form a polymer by the most convenient and economical means available. Although polymer-impregnated concrete has been tried mainly for the repair of bridge decks (Ref. 27), another possible application of this technique would be the repair of cracked slabs. The bonding characteristics and penetration of the monomer systems indicate that cracks could be sealed and that some structural integrity can be restored to the concrete. Other techniques have also been tried to achieve the same results but at a reduced cost and time. Two preliminary experiments considered are a rubber and neoprene (resistant to methyl methacrylate) pressure-mat technique for impregnation and using sulphur as the impregnant (Ref. 28)<sup>2</sup>. The pressure-mat technique was to achieve a greater monomer penetration through higher pressure in a shorter soak period, which is important for penetration depth. The results showed promise for economizing laboratory-field techniques (Ref. 28). Sulphur, as an impregnant, could have potential application to highways due to its excellent resistance to acids and salts and the fact that it is much cheaper than methyl methacrylate. Sulphur impregnated concrete has been demonstrated to have properties similar to polymer-impregnated concrete. If no corrosion problems arise from possible side reactions with water and oxygen, sulphur-impregnated concrete could prove to be more economical and practical for large scale usage to protect and strengthen concrete overlays.

Before any conclusions or recommendations can be drawn for surface-

---

<sup>1</sup>Fowler, David W., James T. Houston, and Donald R. Paul, "Polymer-Impregnation Concrete For Highway Applications," Research Report 114-1, Center For Highway Research, University of Texas at Austin, February, 1973.

<sup>2</sup>Mehta, H. C., W. F. Chen, J. A. Manson, and J. W. Vanderhoff, "Innovations In Impregnation Techniques For Highway Concrete," Transportation Research Board No. 542, Transportation Research Board, 1975.



impregnated concrete, more research and field tests must be completed. This will determine the practical feasibility for large-scale impregnation of highways, since the structural capacity can definitely be improved. This would also determine the advantages of increased strength properties, based on fatigue, in relation to the increased construction costs.

### Fibrous Concrete

In recent years, considerable interest has been generated in using fibrous concrete as an overlay material for existing pavements. Fibrous concrete is a composite material consisting of conventional concrete containing a dispersion of small fibers composed of steel (which is the most common), fiberglass, nylon, asbestos, polypropylene, or polyethylene (Ref. 29)<sup>1</sup>. The reasons for considering fibrous concrete as potentially advantageous for pavement arise mainly from the increase in flexural strength. While flexural strength can be doubled quite easily under laboratory conditions, fiber concentrations compatible with standard mixing and placing equipment and procedures in the field increase strength by approximately 50 percent. This increase in strength can result in improved fatigue resistance. Although the fibers offer improved strength to a pavement, the rather severe environmental conditions to which a pavement is subjected may result in corrosion of the steel fibers and loss of the beneficial effects of the fibers. This results from the large surface area to volume ratio of the fibers.

Some of the places where fibrous concrete has been used include the U.S. Army tests on slabs on grade, the Tampa International Airport, various Detroit highways, a bridge deck at Winona, Minnesota, Lockbourne AFB, Ohio, and Cedar Rapids and Greene Co., Iowa (which is discussed in detail below).

In September and October 1973, three miles (4.8km) of fibrous, jointed and continuously reinforced concrete resurfacing was placed in Greene Co., Iowa. The project was sponsored by Greene County, Iowa, the Highway Research Board, and other private organizations. The test sections were placed on a 51 and 52 year old concrete pavement which carries a low traffic volume. This research project contains 41 test sections, which include 4 JCP, 4 CRCP, and 33 fibrous sections. The major variables that were considered are overlay thickness, cement content, fiber content and size, and the degrees of bonding. Table 6 lists all sections and shows the variation in the above variables. The elastic jointed CRCP sections have joints spaced at 8 feet (2.4m) intervals with a bond breaking coating applied to the longitudinal steel in the joint areas. The CRC overlays are 3 and 4 inches (7.6 and 10.2cm) thick with some bonded and others unbonded to the old slab.

---

<sup>1</sup>Parker, Frazier, Jr., "Steel Fibrous Concrete For Airport Pavement Applications," U.S. Army Engineer Waterways Experiment Station, Report No. FAA-RD-74-31, November 1974.

Table 6. Summary of Section in Greene Co., Iowa fibrous concrete research project

Section No.	Station Begin	Numbers* End	Cement (lbs./CY.)	Fiber Content, lbs./CY.**		Overlay Thickness (in.)	Bond	Joint Spacing (ft.)	Centerline Joint
				1"	2-1/2"				
1	+ 00	4 + 04	569	0	0	5	Partial	20	Yes
2	4 + 67	9 + 00	569	(Mesh)		4	Partial	30	Yes
3	9 + 00	10 + 98	569	(CRC Anchor)		4	Bonded	8	Yes
4	10 + 98	16 + 65	569	(CRC)		4	Unbond	8	Yes
5	17 + 16	24 + 00	569	(CRC)		3	Unbond	8	Yes
6	24 + 00	25 + 85	569	(CRC Anchor)		3	Bonded	8	Yes
7	26 + 58	31 + 61	600	60		3	Partial	40 FD	Yes
8	32 + 16	33 + 57	750		60	3	Partial	40	Yes
9	34 + 28	38 + 19	600	100		3	Partial	40 FD	Yes
10	38 + 75	42 + 00	750	100		3	Partial	40	Yes
11	42 + 00	45 + 60	750		100	3	Unbond	40	Yes
12	46 + 04	49 + 52	750	100		3	Bonded	40	Yes
13	50 + 05	53 + 70	600	60		3	Partial	40	No
14	54 + 45	57 + 48	500 +234 FA	100		3	Partial	40	Yes

\*Variation in beginning station numbers due to transition sections.

\*\*Dimensions refer to fiber length.

1 station=30.5m<sub>3</sub>  
 1b/cy=59327kg/m<sup>3</sup>  
 1 in=2.54cm  
 1 ft=.305m

TABLE 6. (Continued)

Section No.	Station Begin	Numbers* End	Cement (lbs./CY.)	Fiber Content, lbs./CY.**		Overlay Thickness (in.)	Bond	Joint Spacing (ft.)	Centerline Joint
				1"	2-1/2"				
15	57 + 94	61 + 64	500 +234 FA		100	3	Partial	40	Yes
16	62 + 15	65 + 72	600		60	3	Partial	40	Yes
17	66 + 35	69 + 92	750	60		3	Partial	40	Yes
18	69 + 92	74 + 01	600	160		3	Partial	40	Yes
19	74 + 01	77 + 44	600	160		3	Partial	40	Yes
20	77 + 84	81 + 44	750	160		3	Partial	40	Yes
21	82 + 10	85 + 76	750		100	3	Bonded	40	Yes
22	86 + 15	88 + 64	500 +234 FA	160		3	On Grade	40	Yes
23	88 + 64	90 + 54	750	160 (Bridge)		3	Bonded	0	No
24	90 + 54	95 + 63	600	100 (Curb)		3	Partial	40	Yes
25	95 + 85	99 + 66	750 CC		100	3	Unbond	40	No
26	100 + 43	104 + 00	750		160	2	Partial	40	Yes
27	104 + 32	107 + 46	600	100		2	Partial	40	Yes
28	107 + 83	111 + 85	750	100		2	Partial	40 FD	Yes

\* Variation in beginning station numbers due to transition sections.

\*\* Dimensions refer to fiber length.

1 station=30.5m<sub>3</sub>  
 lb/cy=59327kg/m<sup>3</sup>  
 1 in=2.54cm  
 1 ft=.305m

TABLE 6. (Continued)

Section No.	Station Begin	Numbers* End	Cement (lbs./CY.)	Fiber Content, lbs./CY.**		Overlay Thickness (in.)	Bond	Joint Spacing (ft.)	Centerline Joint
				1"	2-1/2"				
29	112 + 04	116 + 00	750	100		2	Bonded	40	Yes
30	116 + 00	119 + 50	750	160		2	Partial	40	Yes
31	120 + 00	123 + 00	600	100		2	Partial	40	No
32	123 + 14	127 + 58	750	100		2	Partial	40	No
33	127 + 99	131 + 89	600	160		2	Partial	40	Yes
34	132 + 22	136 + 00	750	160		2	Partial	40	Yes
35	136 + 65	140 + 00	750		100	2	Unbond	40	Yes
36	140 + 00	143 + 74	750		100	2	Bonded	0	Yes
37	144 + 17	147 + 21	600		60	3	Partial	40	No
38	147 + 92	151 + 84	569		(Mesh)	4	Partial	30	Yes
39	152 + 50	155 + 43	569		None)	5	Partial	20	Yes

\*Variation in beginning station numbers due to transition sections.

\*\*Dimensions refer to fiber length.

1b/cy=.59327kg/m<sup>3</sup>  
 1 in=2.54cm  
 1 ft=.305m  
 1 station = 30.5 m

Welded wire fabric was used to provide 0.45 percent longitudinal steel at mid-slab depth in the CRC sections. It was supported on continuous transverse angle irons fastened to the existing concrete at 8-foot (2.44m) intervals. These supports also served as crack initiators to form the transverse joints. An asphalt coating was applied to a 16 inch (40.6cm) length of the longitudinal wire across the joints.

The fibrous overlays are 2 and 3 inches (5.1 and 7.6cm) thick and contain variation in numerous other variables. The jointed concrete overlays are 4 inch (10.2cm) wire mesh and 5 inch (12.7cm) plain concrete sections. The joint spacings are 30 and 20 feet (9.15 and 6.1m), respectively. The machine, built by Gomaco, was equipped with a rotating drum that contained ridges which formed the grooves.

The original pavement was 18 feet (5.5m) wide although the overlay was built to 22 feet (6.71m). To obtain uniform support on each 2 foot (.61m) extension a 4 inch (10.16cm) deep lean concrete base was placed on the edge of the pavement prior to the overlay. The concrete for all test sections was controlled to have a 4 inch (10.16cm) slump and 6% air when placed. The coarse aggregate was pea gravel with a 3/8 inch (.038cm) maximum size due to the thickness of the overlay and old pavement in the unbonded sections. A cement grout was used in the bonded sections.

The term cracking per square foot is used to compare cracking in different sections of the pavement. Cracking per square foot is calculated by the following equation:

$$C_i = \frac{\sum X_j}{w \cdot \ell_i} \times 100 \text{ (ft}^2/\text{ft}^2\text{)} \text{ (1ft=.305m)} \dots \dots \dots (13)$$

where:

$C_i$  = cracking coefficient expressed as cracking per square foot in Section i, (1ft=.305m)

$X_j$  = length of crack j, either longitudinal or transverse, in feet, (1 ft=.305m)

w = width of roadway in feet, (1 ft=.305m)

$\ell_i$  = length of Section i, in feet. (1 ft=.305m)

It is cautioned that cracking per square foot or meter is only a measure of the amount of cracking in each section and does not distinguish among degrees of severity of the cracks (crack width, spalling).

An inspection of the sections after 2-1/2 years of service revealed several aspects of the performance of the fibrous concrete pavement. The 3 inch (7.6cm) sections performed significantly better than the 2 inch (5.1cm) sections as can be observed in Figure 28. This indicates that the 3 inch (7.6cm) sections have a long fatigue life, as would be expected. The cracks in the 2 inch (5.1cm) sections tended to be wider and contain more distress than in the 3 inch (7.6cm) sections regardless of the bond condition. This can be attributed to the corrosion of the fibers across the cracks. As the load induced cracks propagate up and become wider with continued load applications (fatigue) the fibers corrode and deteriorate because of environmental conditions.

The fiber content affected the pavement performance or cracking (Figure 28), whereas the length of the fibers (1 and 2-1/2 inches) (2.54 and 6.35cm) seemed to have no effect on the amount of cracking, although the 2-1/2 inch (6.35cm) fibers seemed to result in overall smaller crack width than with the 1 inch (2.54cm) fibers.

From the Greene Co. project different types of pavement (JCP, CRCP, Fibrous) can be compared for the amount, not severity, of cracking. The performance of the JCP and CRCP sections are given in Figures 29-31. Thickness had a definite effect on all type pavements, whereas bonding, after 2-1/2 years of service, did not affect the amount of cracking. The major difference in performance between types of pavements is in the type of cracking. JCP and CRCP sections contained transverse cracking, whereas the fibrous sections contained longitudinal cracking. The longitudinal cracking in the fibrous sections seemed to be associated with curling or warping of the slabs, which was not the case in the thicker JCP and CRCP slabs. By comparing Figures 28, 29, and 30 it can be observed that the 3 inch (7.62cm), 160 lb. (72.6kg) fiber content pavements had the least amount of cracking after 2-1/2 years of service.

From this project, it was demonstrated that equipment and procedures are available for the feasible production of large quantities of fibrous concrete. Fibrous concrete pavement overlays do have potential for good serviceability if thermal cracks do not develop so that no detrimental effects can reach the fibers or if joint spacing is controlled such that thermal cracks do not form.

#### Implementation

Based on various projects reviewed, the following summarizes the characteristics of the above materials for future consideration.

Polymer or Sulphur-Impregnated Concrete - This technique has primarily been used on the existing surface of bridge decks to increase strength properties and can be expensive. Once remaining life and fatigue characteristics are determined for this material, the design procedure can be applied for evaluating various designs.

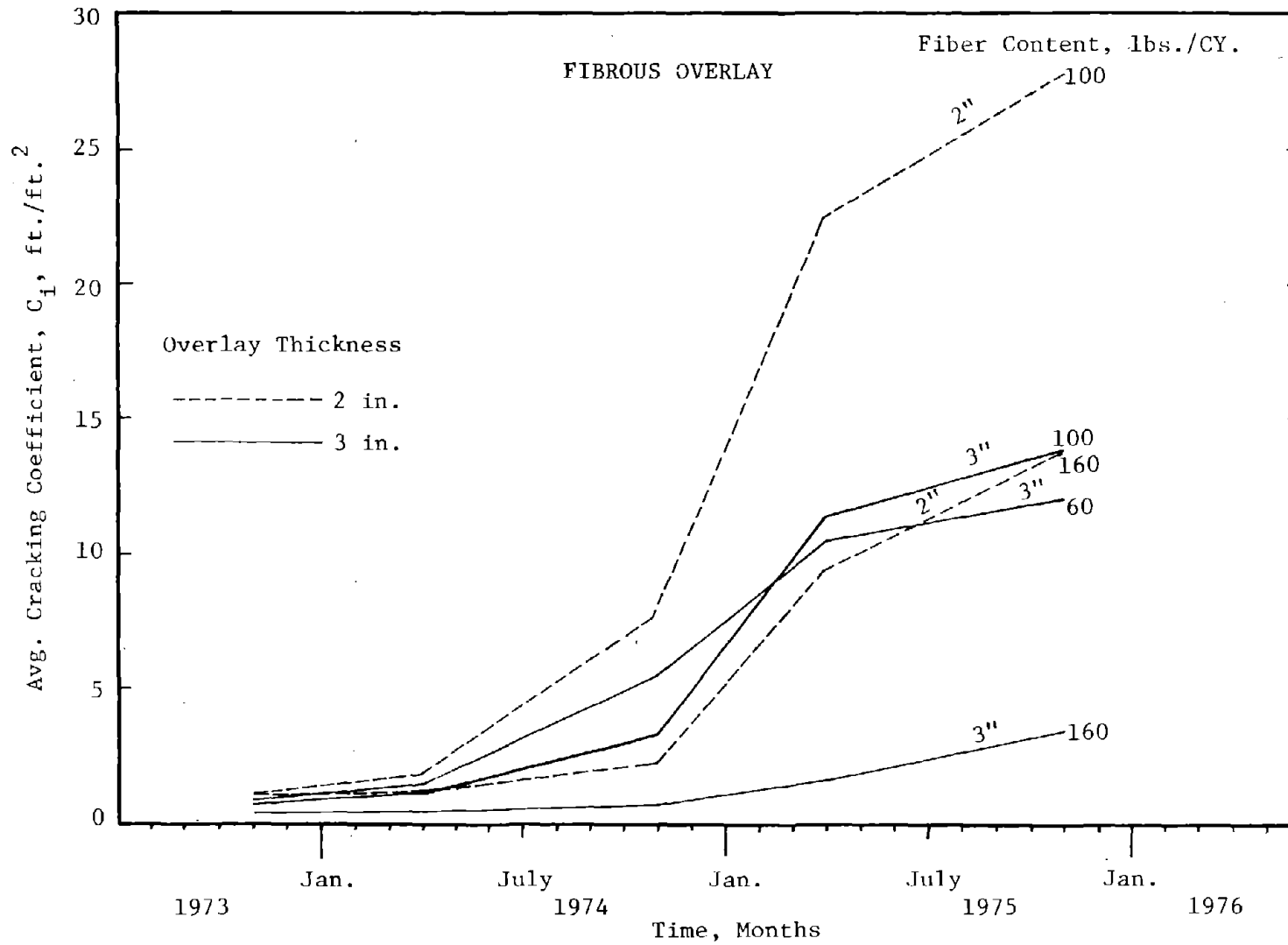


FIGURE 28. Development of cracking with time on Greene Co. fibrous overlay pavements.

1 in=2.54cm  
 1 ft=.305m  
 lbs/cy=.59327kg/m<sup>3</sup>

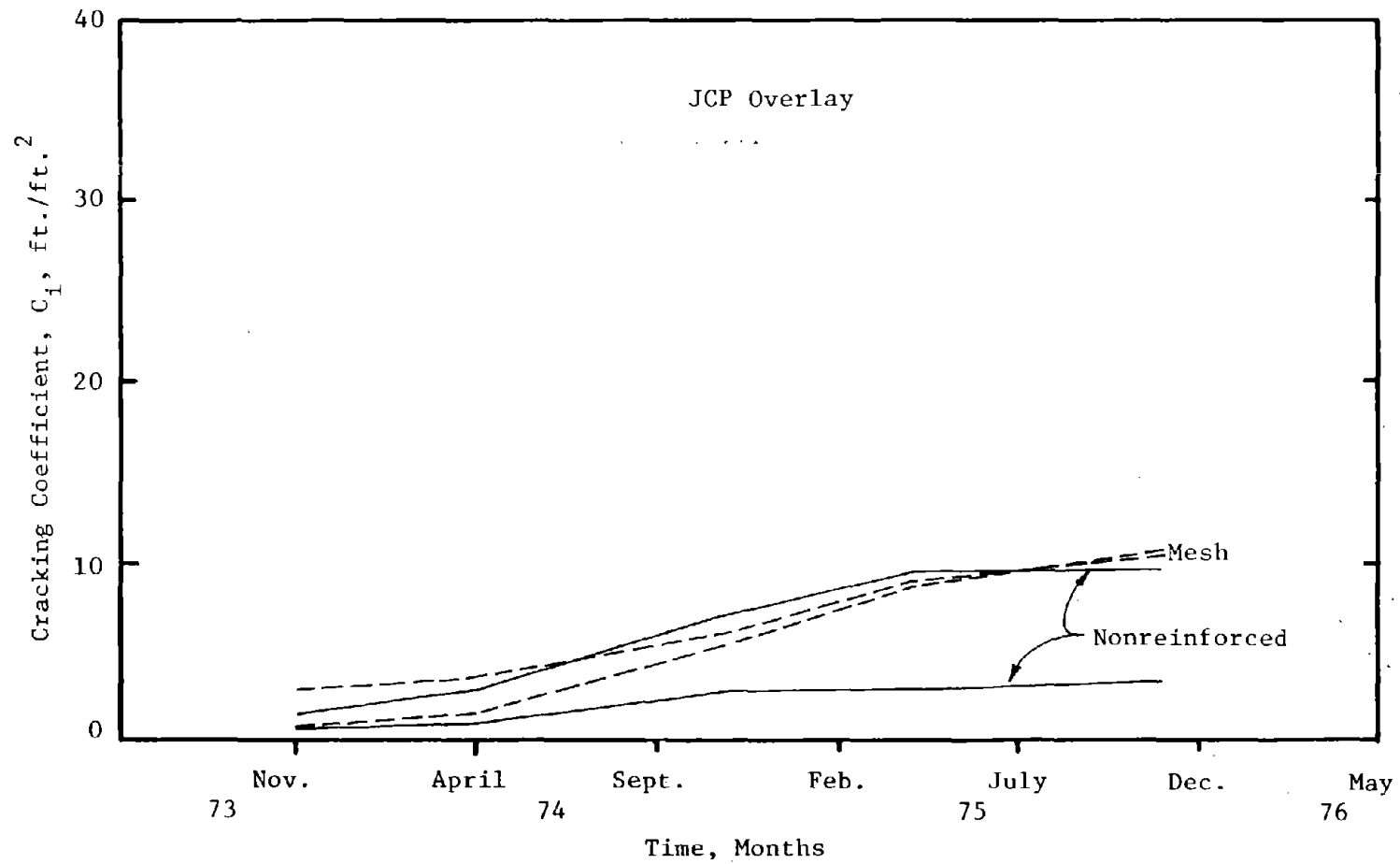


FIGURE 29. Development of cracking with time on Greene Co. jointed concrete overlay pavements.

1 ft = .305m



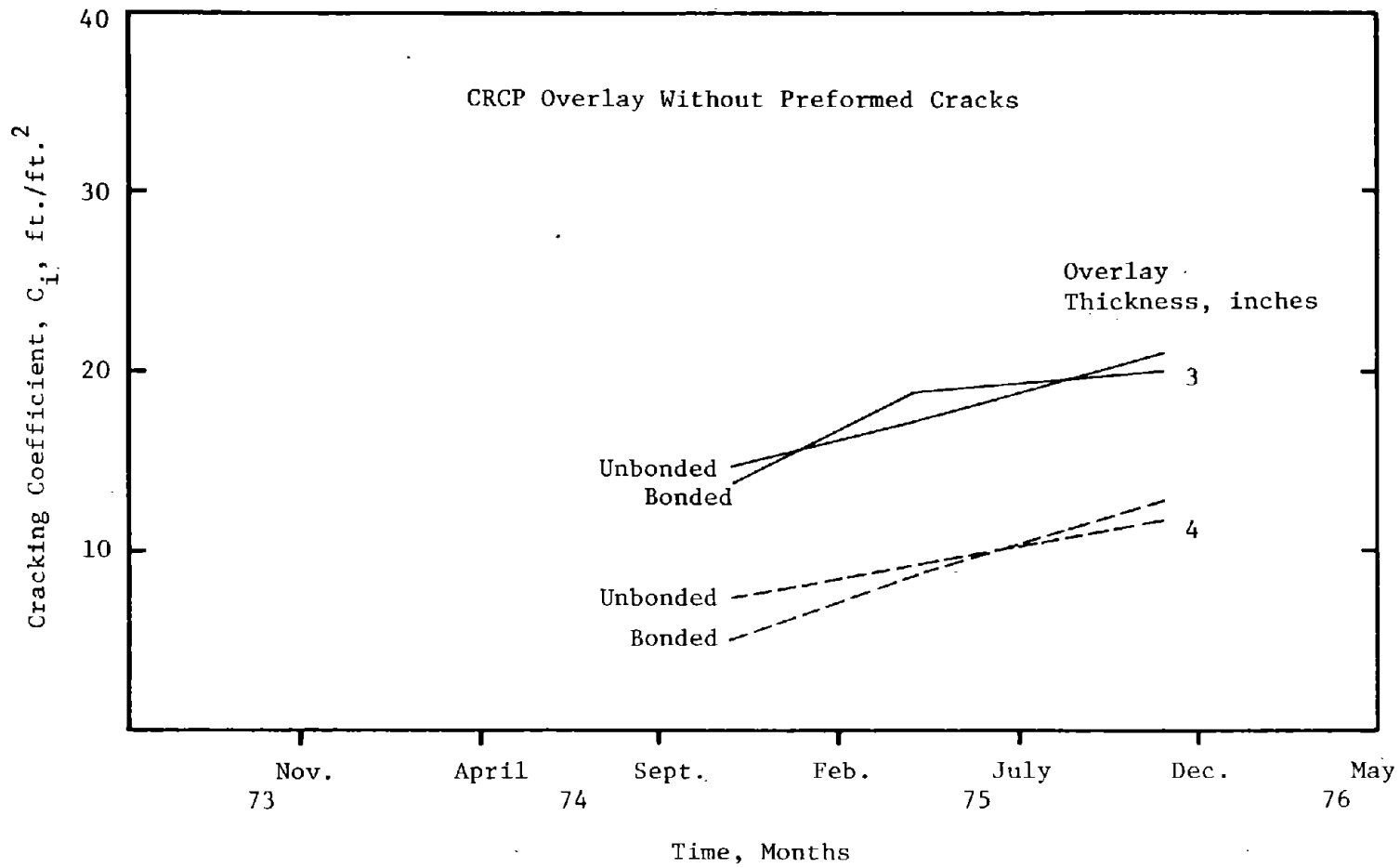


FIGURE 30. Development of cracking with time on Greene Co. CRC overlay pavement.

1 in=2.54cm  
1 ft=.305m

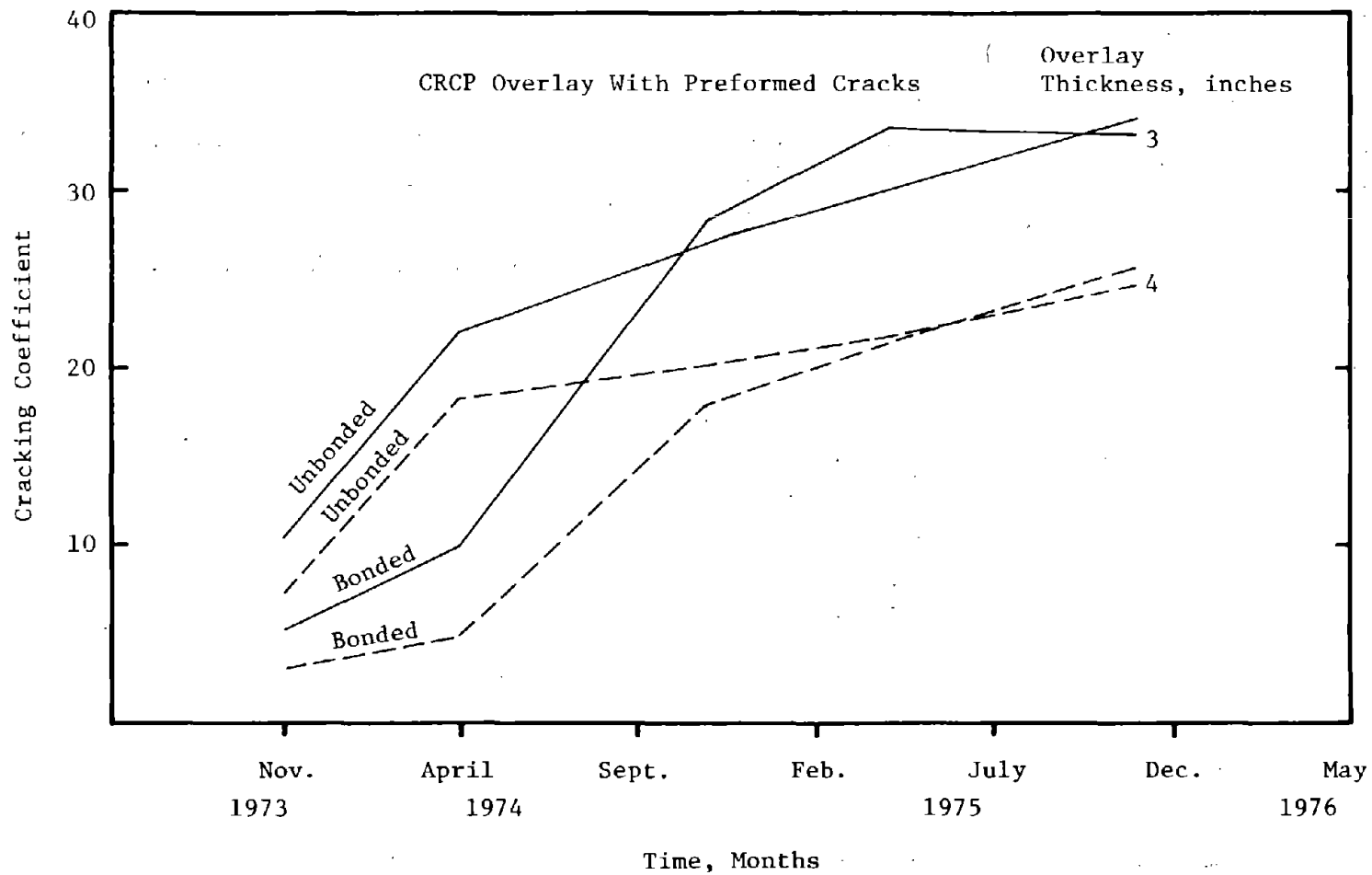


FIGURE 31. Development of cracking with time on Greene Co. CRC overlay pavement that had preformed crack initiators installed.

1 in=2.54cm

Fibrous Concrete - This material has been proven to be economically feasible and can produce reasonable performance. Testing procedures and fatigue characteristics must be established before it can be adequately compared to other conventional or new materials using the program developed.

Elastic Jointed CRCP - Elastic jointed CRCP has been adequate in previous experiments. A definite need exists to coordinate a preformed crack spacing with material properties and subbase friction to avoid intermediate cracking and future spalling.

### Summary

This chapter has presented the development of the criterion that enables a "working" design procedure to be established from the concepts presented in Chapter 2. It is advantageous to summarize the criterion development here and show how it fits into the overall overlay design procedure.

The basic principle of the design procedure is the determination of stress due to wheel loads and then relating repeated applications of this stress to the pavement life. The stress is computed using elastic layered theory and may be expressed by the following equation:

$$\sigma = f (E_i, D_i, \mu_i, P, p) \dots \dots \dots (14)$$

where:

$\sigma$  = interior stress in pavement due to an 18-kip (8172kg) single axle wheel load,

$E_i$  = modulus of elasticity of  $i^{\text{th}}$  layer in the pavement system,

$D_i$  = thickness of  $i^{\text{th}}$  layer,

$\mu_i$  = Poisson's Ratio of  $i^{\text{th}}$  layer,

$P$  = wheel load on pavement, and

$p$  = tire pressure.

The interior stress computed is then adjusted to account for the critical loading position on the pavement, i.e. edge loading for continuous pavements or corner loading for jointed pavements, and for the presence of voids beneath the existing pavement, if any. These adjustments result in the design stress which may be expressed as follows:

$$\sigma = C_v \cdot C_L \cdot \sigma_i \dots \dots \dots (15)$$

where:

- $\sigma$  = design stress,
- $C_v$  = stress adjustment due to presence of voids,
- $C_L$  = stress adjustment for edge or corner load position, and
- $\sigma_i$  = interior stress in pavement computed by elastic layered theory (Eq. 14).

The design stress is then entered into the following fatigue equation which was developed as described in this chapter:

$$N = 23,440 \left( \frac{f}{\sigma} \right)^{3.21} \dots \dots \dots (16)$$

where:

- $N$  = number of 18-kip (8172kg) axle load applications until Class 3 and 4 cracking appears,
- $f$  = flexural strength of concrete, and
- $\sigma$  = design stress (Eq. 15).

Based on this fatigue equation, the pavement overlay thickness that reduces the design stress,  $\sigma$ , to a level that will allow the desired pavement life,  $N$ , is selected as the design thickness.

For some pavement overlay systems, primarily flexible overlays on rigid pavements, reflection cracking criteria must be considered in addition to the fatigue criterion. Development of criteria to reduce reflection cracking is presented in the following chapter.

## CHAPTER 4

### REFLECTION CRACKING

Reflection cracking was recognized as one of the principal forms of distress in resurfaced pavements at the 1932 annual meeting of the Highway Research Board. This led to a great deal of experimentation of various techniques for the control of reflection cracking. Then, at a workshop on pavement rehabilitation in 1974, reflection cracking was again recognized as being a major problem (Ref. 30)<sup>1</sup>. Obviously, the problem had not been solved.

The present state-of-the-art for preventing reflection cracking in overlays over PCC pavements is to a large degree based on experience gained from trial and error methods of in-service highways, and has been of an empirical nature with no concentrated research effort. A definition of reflection cracking is contained in Highway Research Board Special Report 113 which states that it is the "cracking of a resurface or overlay above underlying cracks or joints." A more detailed description is that reflection cracks are fractures in an overlay or surface course that are a result of, and reflect, the crack or joint pattern in the underlying layer, and may be either environmental or traffic induced. Such cracking must be prevented to retain the structural integrity of the overlay, preclude water intrusion and maintain a smooth riding surface. Before any attempt can be made to prevent these cracks, the causes or failure mechanisms must be defined. Once these are defined, then a procedure can be developed so that an economical determination of material properties or treatments can be completed.

#### Failure Mechanisms

The basic mechanisms leading to the development of reflection cracking are horizontal and differential vertical movements between the original pavement and overlay (Refs. 31<sup>2</sup>, 32<sup>3</sup>, 33<sup>4</sup>, 34<sup>5</sup>). As stated by

---

<sup>1</sup>Sherman, George B., "Reflection Cracking", Pavement Rehabilitation: Proceedings of a Workshop, Report No. FHWA-RD-74-60, Federal Highway Administration, June 1974.

<sup>2</sup>"Preventing Reflection Cracks With An Asphalt Crack - Relief Layer", Construction Leaflet No. 16, The Asphalt Institute, December 1975.

<sup>3</sup>Bone, A. J., and L. W. Crump, "Current Practices and Research on Controlling Reflection Cracking," Bulletin No. 123, Highway Research Board, 1956, (pp 33-39).

<sup>4</sup>Bone, A. J., L. W. Crump and V. J. Roggeveen, "Control of Reflection Cracking in Bituminous Resurfacing Over Old Cement-Concrete Pavements." Proceedings, Highway Research Board, Vol. 33, 1954 (pp 345-354).

<sup>5</sup>Davis, M. M., "Reflection Cracks in Bituminous Resurfacing," Report No. 12 Ontario Joint Highway Research Programme, University of Toronto, July 1960.

Finn (Ref. 35)<sup>1</sup>, a well developed and generally accepted description of the mechanisms and response variables associated with reflection cracking have not been established. There have been a considerable amount of field observations and theoretical analysis of reflection cracking, but there have not been many controlled projects where sufficient data were taken to accurately determine the cause or factors associated with this type of cracking (Ref. 36)<sup>2</sup>. Also, with the limited information available, much of this is concerned with asphaltic concrete over asphaltic concrete, as for example Arizona and Colorado (Refs. 37<sup>3</sup>, 38<sup>4</sup>, 39<sup>5</sup>).

#### Horizontal Movements

It has been generally accepted that the major cause of reflection cracking is due to horizontal movements as a result of expansion and contraction of the existing slab from temperature and moisture changes. Many of these cracks are largely an expansion-shrinkage phenomenon which usually start to occur within the first year of service, and then accelerate with traffic (Refs. 30, 36, 40<sup>6</sup>). Hairline cracks have been found to develop within a few months after overlay placement, during the first cool weather experienced by the pavement and progress to a detrimental stage within a few years. Thus, the money spent to extend the pavements service life may be ineffective in terms of rehabilitation. An example

---

<sup>1</sup>Finn, F. N., K. Nair, and J. Hilliard, "Minimizing Premature Cracking of Asphalt Concrete Pavements", Prepared for 1976 Annual Meeting of the AAPT, Woodward-Clyde Consultants, February 1976.

<sup>2</sup>"Pavement Rehabilitation: Materials and Techniques, NCHRP Synthesis of Highway Practice No. 9, Highway Research Board, 1972.

<sup>3</sup>Way, George, "Prevention of Reflection Cracking in Arizona Minnetonka-East (A Case Study)", Federal Highway Administration Report No. FHWA-AZ-HPR-224, Arizona Department of Transportation-Phoenix, Arizona, May 1976.

<sup>4</sup>Kanarowski, Stanley M., "Study of Reflection Cracking in Asphaltic Concrete Overlay Pavements - Phase I" Report No. AFWL-TR-71-142, U. S. Army Engineer Construction Engineering Research Laboratory, Air Force Weapons Laboratory, Kirtland AFB, New Mexico, March 1972.

<sup>5</sup>Safford, Mark and Phil McCabe, "Reflection Cracking in Bituminous Overlays", Interim Report No. CDOH-P&R-R&SS-72-1, Colorado Division of Highways - Denver, Colorado, December 1971.

<sup>6</sup>McCullagh, Frank R., "Reflection Cracking of Bituminous Overlays on Rigid Pavements", Special Report 16, Engineering Research and Development Bureau, New York State Department of Transportation, February 1973.

of this temperature-cracking relationship is illustrated in Figure 32. Because of the bond between the overlay and concrete pavement, the tensile stresses produced from joint movements become critical in the area of the concrete joints. This development of reflection cracking due to environmental loadings are dependent upon the magnitude and rate of temperature drop, slab length, gauge length across the joint, and properties of the resurfacing material. Hence, all these factors must be included in the evaluation of the environmental effects or loadings on the overlay.

#### Differential Vertical Movements

At the workshop on Structural Design of Asphalt Concrete Pavement System in 1970, discussion Group E concluded, (Ref. 35),

"Although we can accept that volume changes in a underlying material layer can contribute to the development of reflection cracking, we are uncertain what role is played by repeated traffic loading either in a flexural way or in a relative movement way."

It has been shown and reported by McCullagh (Ref. 40) and McGhee (Ref. 41)<sup>1</sup> that in some cases reflection cracking is primarily load associated (Table 7). In most cases differential vertical deflections across joints are not obtained, thus it becomes very difficult to determine which cracks are a result of horizontal or differential vertical movements. In a study reported by Brownridge (Ref. (42)<sup>2</sup>), deflections at a joint were obtained in the same manner as the Virginia study for the 18-kip (8172kg) axle load (Ref. 41<sup>1</sup>). These values are tabulated in Table 8 for two different temperatures. As expected, the differential vertical deflections vary with season, and this should be taken into account in design. Although for this study, it was generally noted that most of the reflection cracks were caused from horizontal movements, it is suggested that some have occurred due to differential deflections as can be seen by comparing the two sets of data (Tables 7 and 8). Differential vertical movements are caused by traffic loadings which depress abutting slab ends resulting in shear-stress concentrations of the overlay material at the joints (Ref 43<sup>3</sup>, 44<sup>4</sup>). Therefore, reflection cracking caused by differential vertical

---

<sup>1</sup>McGhee, K. H., "Efforts to Reduce Reflective Cracking of Bituminous Concrete Overlays of Portland Cement Concrete Pavements", Virginia Highway & Transportation Research Council, VHTRC 76-R20, November 1975.

<sup>2</sup>Brownridge, F. C., "An Evaluation of Continuous Wire Mesh Reinforcement in Bituminous Resurfacing", AAPT Proceedings, Vol. 33, 1964.

<sup>3</sup>Tons, E., A. J. Bone, and V. J. Roggeveen "Five Year Performance of Welded Wire Fabric in Bituminous Resurfacing", Bulletin No. 290, Highway Research Board, 1961, (pp. 15-38).

<sup>4</sup>Roggeveen, V. J., and E. Tons, "Progress of Reflection Cracking in Bituminous Concrete Resurfacing", Bulletin No. 131, Highway Research Board, 1956, (pp. 31-46).

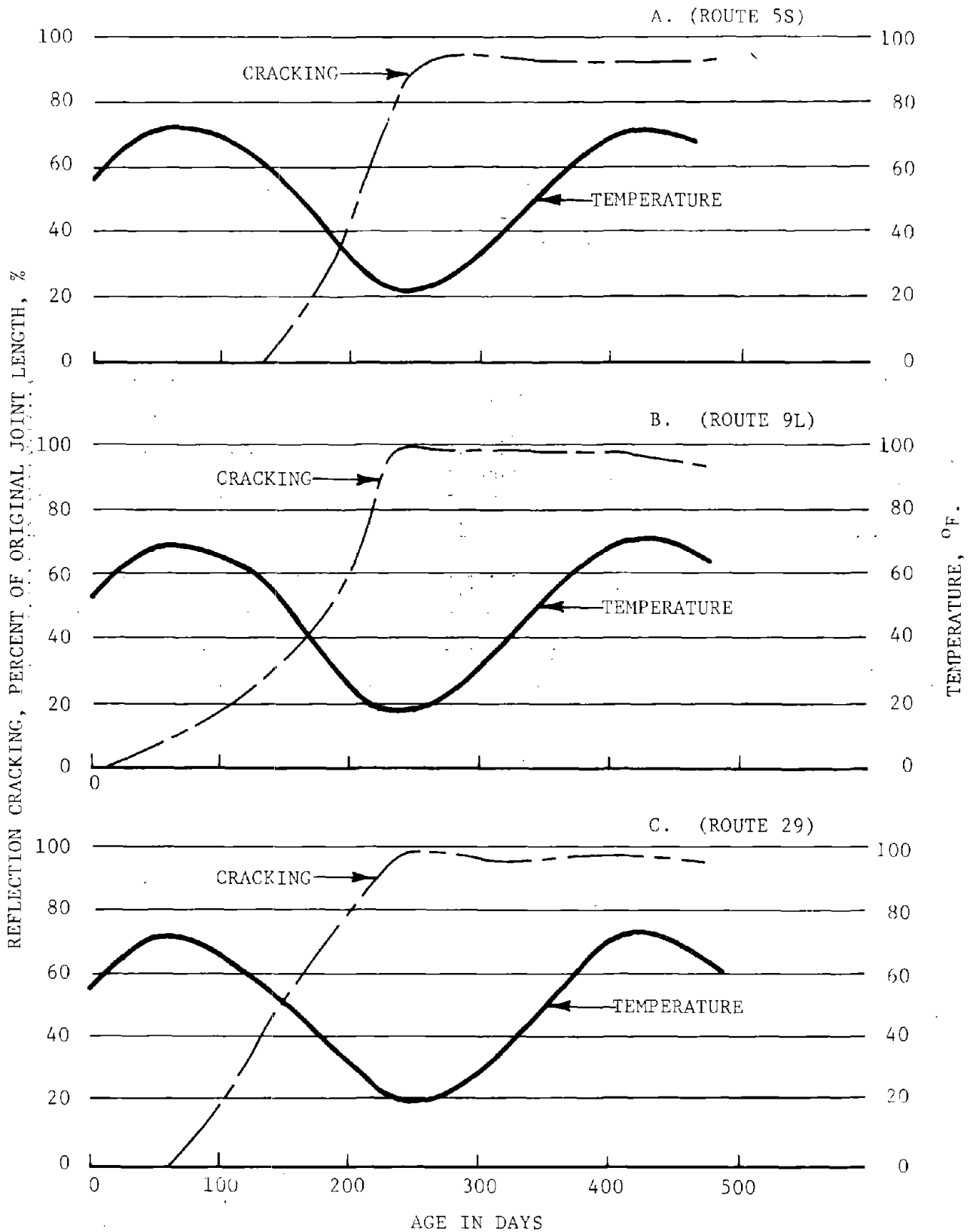


Figure 32. Development of reflection cracks caused by the expansion-shrinkage phenomenon or environmental loadings for three projects in New York State (Ref. 40).

$$^{\circ}\text{C} = .5554(^{\circ}\text{F} - 32)$$



Table 7. Effect of differential deflections on percent reflected cracks for two projects in Virginia (Ref. 41).

Differential Deflection* (in.)	Percent Joints Cracked, %			
	Route 460 Project		Route 13 Project	
	Fabric	Control	Sanded	Control
0	0	44	24	100
0.002	29	54	57	100
0.004	88	74	77	100
0.006	88	100	93	100
0.008	100	100	--	---

\*Measurements were taken with the Benkleman Beam using an 18-kip (8172kg) single axle load.

1 in = 25.4 mm

Table 8. Differential deflections across joints in PCC pavements for various temperatures.  
(Ref. 42).

Slab Corner Vertical Movements (inches)-October 23-Temp. = 78°F.

Station	Defl. W. Slab	Defl. E. Slab	Diff. Defl.	Defl. W. Slab	Defl. E. Slab	Diff. Defl.
21+32	.0116	.0112	.0004	.0116	.0112	.0004
23+70	.0094	.0060	.0034	.0104	.0090	.0014
32+70	.0062	.0116	.0054	.0098	.0070	.0028
36+80	.0080	.0082	.0002	.0080	.0082	.0002
42+20	.0052	.0126	.0074	.0122	.0088	.0034
49+88	.0062	.0122	.0060	.0104	.0080	.0024
52+88	.0060	.0156	.0096	.0156	.0102	.0054
55+92	.0050	.0148	.0098	.0120	.0082	.0038
61+88	.0106	.0130	.0024	.0120	.0126	.0006
63+70	.0098	.0110	.0012	.0116	.0102	.0014

Avg = .0034  
Std. Deviation = .00300

Slab Corner Vertical Movements (inches)-December 6-Temp. = 32°F.

Station	Defl. W. Slab	Defl. E. Slab	Diff. Defl.	Defl. W. Slab	Defl. E. Slab	Diff. Defl.
21+32	.008	.010	.0020	.006	.008	.0020
23+70	.012	.014	.0020	.010	.008	.0020
32+70	.006	.010	.0040	.008	.006	.0020
36+80	.004	.006	.0020	.004	.004	.0000
42+20	.016	.018	.0020	.012	.010	.0020
49+88	.010	.008	.0020	.008	.006	.0020
52+88	.004	.008	.0040	.006	.006	.0000
55+92	.010	.008	.0020	.010	.004	.0060
61+88	.012	.008	.0040	.012	.006	.0060
63+70	.020	.018	.0020	.012	.010	.0020

Avg. = .0025  
Std. Deviation = .00157

1 in = 25.4 mm  
1 station=30.5m  
°C=.5554 (°F-32)

deflections is a shear-fatigue phenomenon and is dependent on the magnitude of the differential deflection across the joint or crack. The factors which are important in differential deflections are magnitude of load, amount of load transfer across the joint or crack, and the differential subgrade support under the slab.

#### Summary

Reflection cracking is a nationwide problem and occurs in virtually all types of overlays. It generally starts within a year of construction, depending on the degree of horizontal joint movement and the magnitude of differential deflections. Although the problem has been defined as being caused by horizontal or differential vertical movements, it should be emphasized that the combined effect of these loadings must be considered before reflection cracking can be adequately explained. Even though field experience and some laboratory work have been conducted, solutions to the problem are only in early stages of development. (Ref. 35). No criteria can be directly applied to general situations in which procedures and techniques can be selected to prevent reflection cracking. Also current detailed information from field and laboratory studies are inconclusive due to limited time and data.

#### Preventive Methods Used

The primary objective of any overlay design is to provide a highway with adequate performance over a maximum useful life with minimum required maintenance. Asphaltic concrete overlays represent the most widely used and accepted form of roadway resurfacing due to low initial cost, ease of application and surface characteristics. Therefore, most information given on preventive methods is concerned with asphaltic concrete overlays, for which reflection cracking is more severe than for PCC overlays.

Existing methods of analysis and design of overlays do not consider the problem of reflection cracking directly. However, several techniques have been used experimentally for the control of reflection cracking. These have varied from placing a material over the crack to prevent bonding of the overlay at that point, to breaking the pavement itself into smaller pieces prior to overlaying. These treatments, none of which have become universally accepted, generally fall into one of the five classifications:

- 1) Treatments to existing PCC pavements
- 2) Stress or strain relieving interlayers,
- 3) Cushion courses,
- 4) Special overlay treatments, and
- 5) Increased overlay thickness.

Based on the factors influencing the development of reflection cracks, it is now possible to evaluate the various techniques by considering how they should perform with respect to the mechanism causing failure. In preventing these cracks, the treatment, to be of practical application, not only should eliminate reflection cracks, but should not: (1) reduce the strength, stability, or service life of the overlay or existing pavement, (2) add excessive costs, (3) delay construction progress, and (4) require special skills, techniques or equipment (Refs. 32, 33).

#### Treatments to Existing PCC Pavement

Three subdivisions of this classification are presented: (1) crack sealing and filling, (2) breaking and seating of the existing PCC pavement, and (3) subsealing the joints or cracks.

Crack Sealing and Filling. None of the attempts to fill or seal cracks have resulted in any significant reduction of reflection cracks (Ref. 30). Although, Wood (Ref. 45)<sup>1</sup> and Ludwig (Ref. 46)<sup>2</sup> have reported California and Texas to have had limited success with using a "Petroelastic" crack sealer and molten sulphur, respectively. This type of treatment alone does not prevent horizontal or differential vertical movements, hence reflection cracking in overlays over PCC pavements can not be controlled. Also, this method is normally used on asphaltic concrete pavements and not PCC pavements.

Breaking and Seating PCC Pavement. Several authors have reported on the effectiveness of breaking and seating the original PCC slab for controlling reflection cracking (Refs. 30, 32, 38, 47<sup>3</sup>, 48<sup>4</sup>, 49<sup>5</sup>). This method involves

---

<sup>1</sup>Wood, William A., "Methods of Minimizing Reflection Cracking In Bituminous Overlays," FHWA Notice N 5140.9, A paper presented at the 34th annual meeting of SASHTO - Myrtle Beach, South Carolina, January 1976.

<sup>2</sup>Ludwig, A. C., and L. N. Pena, Jr., "The Use of Sulphur to Control Reflective Cracking," Air Force Civil Engineer, Volume 10, No. 4, November 1969.

<sup>3</sup>Kipp, O. L. and C. R. Preus, "Minnesota Practices on Salvaging Old Pavements by Resurfacing," Proceedings, Highway Research Board, Vol. 30, 1950, (pp. 261-273).

<sup>4</sup>Lyon, J. W., "Heavy Pneumatic Rolling Prior to Overlay: A 10-Year Project Report," Highway Research Record No. 327, Highway Research Board, 1970.

<sup>5</sup>Korfhage, G. R., "The Effect of Pavement Breaker-Rolling on the Crack Reflectance of Bituminous Overlays," Highway Research Record No. 327, Highway Research Board, 1970, (pp. 50-63).

the use of a hydraulic hammer, pneumatic breaker, or heavy roller (50 + tonés) to break the pavement and put it in full contact with the underlying layer. It has been shown to be a reasonable and inexpensive procedure for reducing reflection cracks in pavement over weak subgrades (Ref. 30). When used over strong subgrades the existing PCC pavement will not crack as expected and therefore this treatment will be less effective in reducing reflected cracks as explained by Lyon (Ref. 50)<sup>1</sup>. Breaking the slab into smaller sections reduces localized horizontal movements and seating the slab reduces differential deflections at joints and cracks caused by voids. This method then serves to reduce reflection cracks caused by both failure mechanisms, Figure 33 (Ref. 51<sup>2</sup>, 52<sup>3</sup>, 53<sup>4</sup>, 54<sup>5</sup>). Figure 34 illustrates how the various levels of treatments can be used to decrease deflections (Table 9) and the occurrence of reflection cracks. One of the disadvantages associated with this method is cracking the pavement into smaller sections results in a loss of structural integrity, requiring larger overlay thicknesses for a given fatigue life.

---

<sup>1</sup>Lyon, James W. Jr., "Slab Breaking and Seating on Wet Subgrade with Pneumatic Roller," Highway Research Record 11, Highway Research Board, 1963.

<sup>2</sup>Smith, L. L. and W. Gartner, "Welded Wire Fabric Reinforcement for Asphaltic Concrete," Highway Research Board Bulletin No. 322, Highway Research Board, 1962.

<sup>3</sup>Velz, P. G., "Effect of Pavement Breaker Rolling on Crack Reflectance in Bituminous Overlays," Highway Research Board Bulletin No. 290, 1961, (pp. 39-52).

<sup>4</sup>Stackhouse, J. L., "Seating Old Pavements with Heavy Pneumatic-Tired Rollers Before Resurfacing." Highway Research Record 11, Highway Research Board, 1963, (pp. 99-100).

<sup>5</sup>Billingsley, N. A., "Salvaging Old Pavements by Resurfacing," Highway Research Circular 43, 1966, (pp. 1-12).

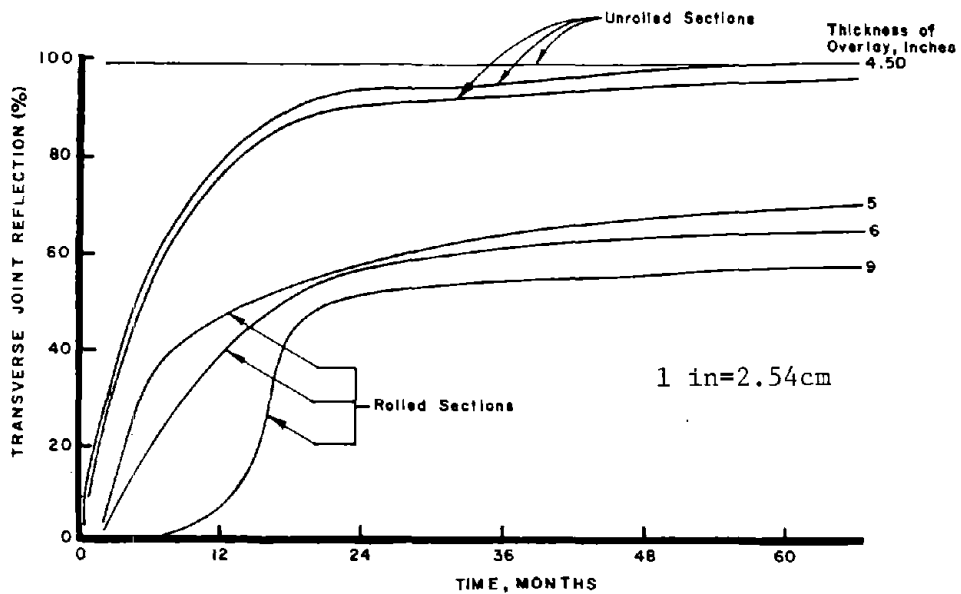


Figure 33. Effect of increased overlay thickness and pavement breaking by rolling on reflection cracking (Ref. 48).

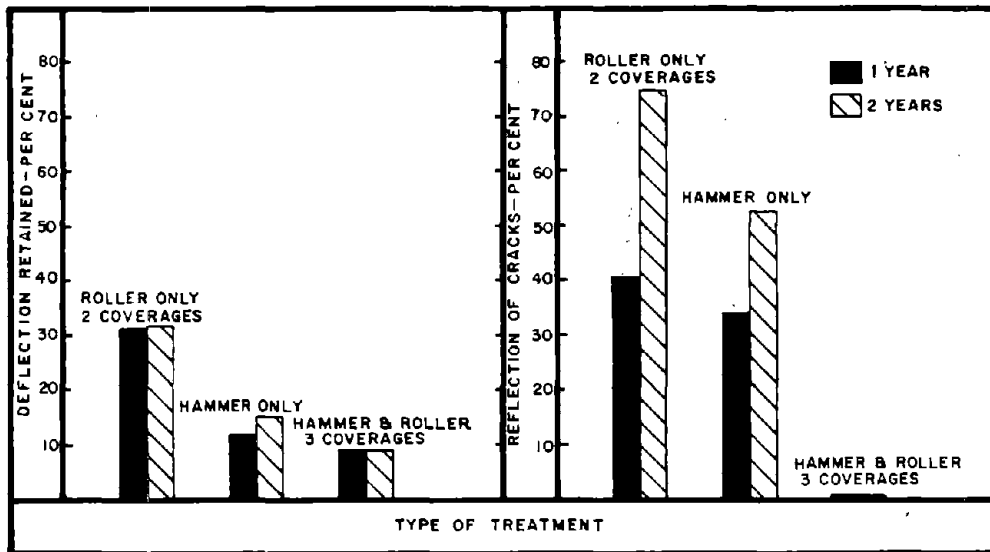


Figure 34. Changes in reflection cracking and deflections for 1 and 2 years of traffic vs. original conditions, for various optimum treatments. (Ref. 50).

Table 9. Reduction in deflection values by breaking and seating the slab (Ref.50 ).

Section	Method	Avg. Benkleman Beam Deflections (in.)					
		Before Seating		1 Yr. After Overlay		2 Yr. After Overlay	
		Max.	Min.	Max.	Min.	Max.	Min.
1	Hammer only	0.085	0.016	0.010	0.005	0.013	0.008
2	Roller only	0.122	0.018	0.014	0.008	0.019	0.008
3	Hammer and roller	0.154	0.012	0.013	0.006	0.013	0.009

1 in=2.54cm

Subsealing the Joints and Cracks. Undersealing with an asphalt or pressure grouting with a cement in the existing PCC pavement are reported in References 35, 38, 55<sup>1</sup>, 56<sup>2</sup>, 57<sup>3</sup>, 58<sup>4</sup>, 59<sup>5</sup>. This is done to re-establish support with, or increase the strength of the foundation materials to reduce differential vertical movements at joints and cracks, thereby reducing reflection cracks. Holes are drilled in the existing slab and then a subseal material is pumped under the slab to fill voids or strengthen the subgrade by the conventional approach. Washington State's pavement mud-jacking program uses a method which is similar in many ways to the conventional method, except for the procedure used to reach the bottom side of the pavement (Ref. 60)<sup>6</sup>. The slurry is injected horizontally, rather than through the top of the pavement, as in the conventional method. Driving horizontally under the slab, as opposed to vertically, can result in several advantages, such as: (1) maintaining slab integrity, (2) reducing problems associated with cracking, and (3) less interruption to traffic. This treatment should be considered as an economic alternative when large differential deflections do exist. Although the method is helpful in reducing differential deflections without breaking the slab, it can be expensive and time consuming, and is not effective against the mechanism of horizontal movements.

#### Stress or Strain Relieving Interlayers.

These treatments will be defined as layers less than one inch (1 in= 2.54cm) in thickness which offer negligible structural benefit to the pavement (Ref. 38). They include bond breakers (stone dust, sand, waxpaper, building

---

<sup>1</sup>Vicelja, J. L., "Methods to Eliminate Reflection Cracking in Asphalt Concrete Resurfacing Over Portland Cement Concrete Pavements," Proceedings, AAPT, Vol. 32, 1963.

<sup>2</sup>Perry, B. F., "Subsealing of Concrete Pavements," HRB Bulletin No. 322, Highway Research Board, 1962, (pp. 30-33).

<sup>3</sup>"Specifications for Undersealing Portland Cement Concrete Pavements with Asphalt," Specification Series No. 6, The Asphalt Institute, December 1966.

<sup>4</sup>"Mudjacking-Slabjacking-Limejacking-Subsealing," Maintenance Aid Digest, MAD 2, Federal Highway Administration, April 1971.

<sup>5</sup>Fahnestock, T. V., and R. L. Davis, "A New Approach to Subsealing," Highway Research Record No. 11, Highway Research Board, 1963.

<sup>6</sup>Slater, Don, "Washington's Shoulder Mudjacking Rescues Depressed Pavements," Rural and Urban Roads, January 1977, (pp. 38-39).



paper, etc.), fabrics and conventional tack coats. (Ref. 61<sup>1</sup>, 62<sup>2</sup>, 63<sup>3</sup>, 64<sup>4</sup>). Conceptually, the use of stress or strain relieving interlayers over joints and cracks increase the gauge length for the development of strain, decreasing the potential of reflection cracking caused by environmental loadings. There is no increase in the structural capacity of the pavement contributed by the stress relieving interlayers, hence reflection cracking due to traffic loadings (differential deflections) may not be improved. This was demonstrated by the Virginia Study (Ref. 41) where sand and non-woven fabrics were placed over joints in a jointed concrete pavement (Table 7). The degree of effectiveness of the sand and fabrics were strongly influenced by the magnitude of the differential deflections, since they have no ability to distribute shear stresses. Conventional tack coats have not been effective in preventing large cracks or joints from reflecting (Ref. 30). Another technique which is in the experimental stage, is the use of ground tread rubber, sand and residual asphalt in emulsion form which acts as a strain relieving layer (Ref. 64, 65<sup>5</sup>). It is believed that the elastic property of the rubber, when combined with the viscoelastic property of asphalt, will result in improved performance. Caution must be taken when stress or strain relieving interlayers are used in areas where acceleration and braking occur since thin overlays will tend to shove or ripple.

---

<sup>1</sup>Carey, Donald E., "Evaluation of Synthetic Fabrics for the Reduction of Reflective Cracking," Report No. 70-1B (B), Research and Development Section, Louisiana Department of Highways - Baton Rouge, Louisiana, April 1975.

<sup>2</sup>McDonald, E. B., "Reduction of Reflective Cracking by Use of Impervious Membrane," South Dakota Department of Highways - Pierre, South Dakota.

<sup>3</sup>"Reinforcing Fabric For Bituminous Seal Coat," Research Project No. 73-20 (2) Bureau of Materials, Testing and Research, Pennsylvania Department of Transportation.

<sup>4</sup>Morris, Gene and Charles McDonald, "Asphalt-Rubber Stress Absorbing Membranes and Recycled Tires," Rural and Urban Roads, August 1976.

<sup>5</sup>Galloway, B. M., "Use of Rubber Aggregate in a Stress Relieving Interlayer for Arresting Reflection Cracking of Asphalt Concrete Pavements," Proceedings, International Symposium on Use of Rubber in Asphalt Pavements, 1971.

## Cushion Courses.

These treatments will be defined as layers which are greater than one-inch in thickness (Ref. 38). Several advantages of using a cushion layer are apparent when the distress mechanisms, discussed earlier, are related to the expected behavior of the pavement when using this strategy: (1) it helps insulate the existing slab, decreasing localized horizontal movements, (2) it reduces horizontal movements transferred from the existing slab to the overlay, and (3) it absorbs some of the differential deflection at joints and cracks. This method, theoretically, should delay reflected cracks caused by both failure mechanisms. Several sources of information indicate that the use of a granular or asphalt treated cushion course, rates from poor to excellent (Ref. 30, 32, 47, 54, 66<sup>1</sup>, 67<sup>2</sup>). Figure 35 illustrates the results of a Michigan study on the effectiveness of a granular cushion course. Normally, untreated granular cushion courses, which have ranged from 4 to 6 inches (10.2 to 15.2cm) in thickness, have greatly reduced reflection cracks, but have not eliminated the cracking. An open-graded hot mix containing 25-35 percent interconnecting voids and made of crushed material, has been reported to reduce reflection cracking (Ref. 31, 68<sup>3</sup>). This layer contains unusually large size aggregates, which bridge the joints or cracks, resulting in reduced differential deflections. The large void ratio in the layer serves to absorb the horizontal movements at joints and cracks thereby decreasing reflection cracks caused by both failure mechanisms. One of the problems associated with cushion courses is the possible introduction of a water conduit or reservoir between layers. Many material properties related to reducing stress transfer between layers has the offsetting effect of increasing drainage. Thus, another set of problems may be inadvertently introduced if care is not used.

It becomes apparent that if cushion courses are used between PCC overlays and pavements, the critical stress could be significantly changed depending on the modulus and thickness of the cushion courses. Therefore, a brief sensitivity analysis was completed to determine how the stresses used in the fatigue analysis would vary. Figure 36 shows the general pavement structure used for the analysis. Elastic layered theory was used to compute the tensile stresses in the pavement at points located in Figure 36. Figures 37 and 38 illustrate that the stresses are only slightly decreased in the existing uncracked PCC pavement with in-

---

<sup>1</sup> Cople, F., and L. T. Oehler, "Michigan Investigation of Soil Aggregate Cushions and Reinforced Asphaltic Concrete for Preventing or Reducing Deflection Cracking of Resurfaced Pavements," Highway Research Record No. 239, Highway Research Board, 1968.

<sup>2</sup> Stackhouse, J. L., "Preparing Old Pavements for Resurfacing With 50-Ton Compactor," Proceedings, Highway Research Board, Vol. 38, 1959, (pp. 464-471).

<sup>3</sup> Johnson, Robert D., "Thin Overlay Bituminous Macadam for the Control of Reflex Cracking," Highway Research Record 150, Highway Research Board, Washington, D.C., 1966.

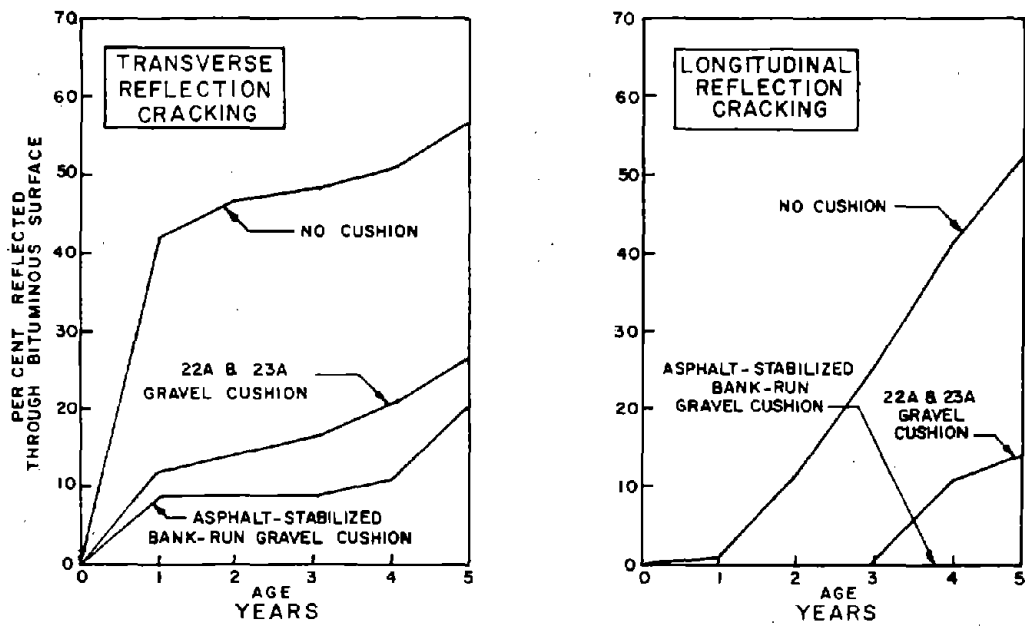


Figure 35. Transverse and longitudinal reflection cracking as influenced by an aggregate cushion course. (Ref. 66).

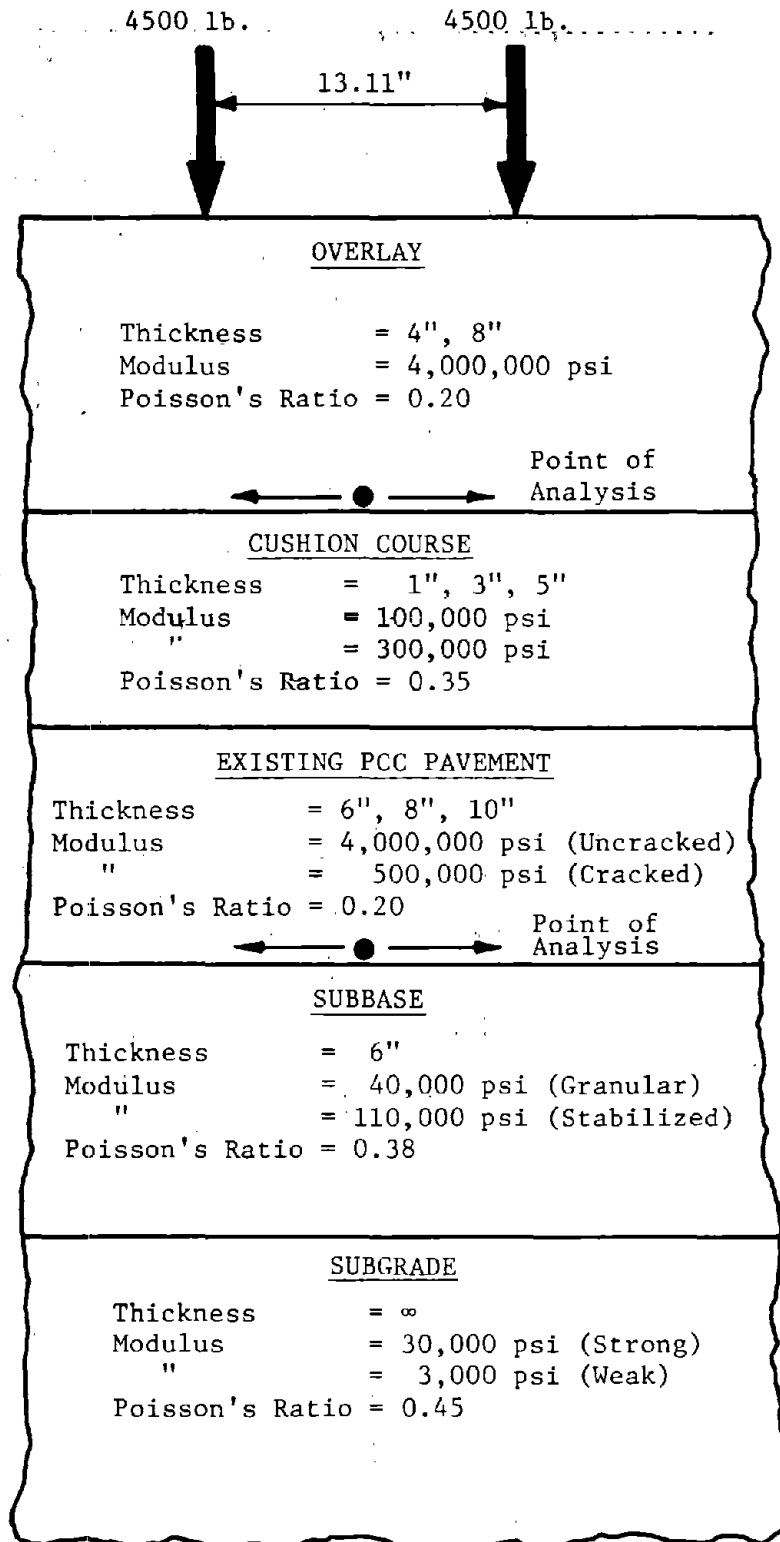


Figure 36. Pavement structure used in the brief sensitivity analysis of a cushion course.

1 psi=6.9kN/m<sup>2</sup>  
 1 in=2.54cm  
 1 lb=.454kg

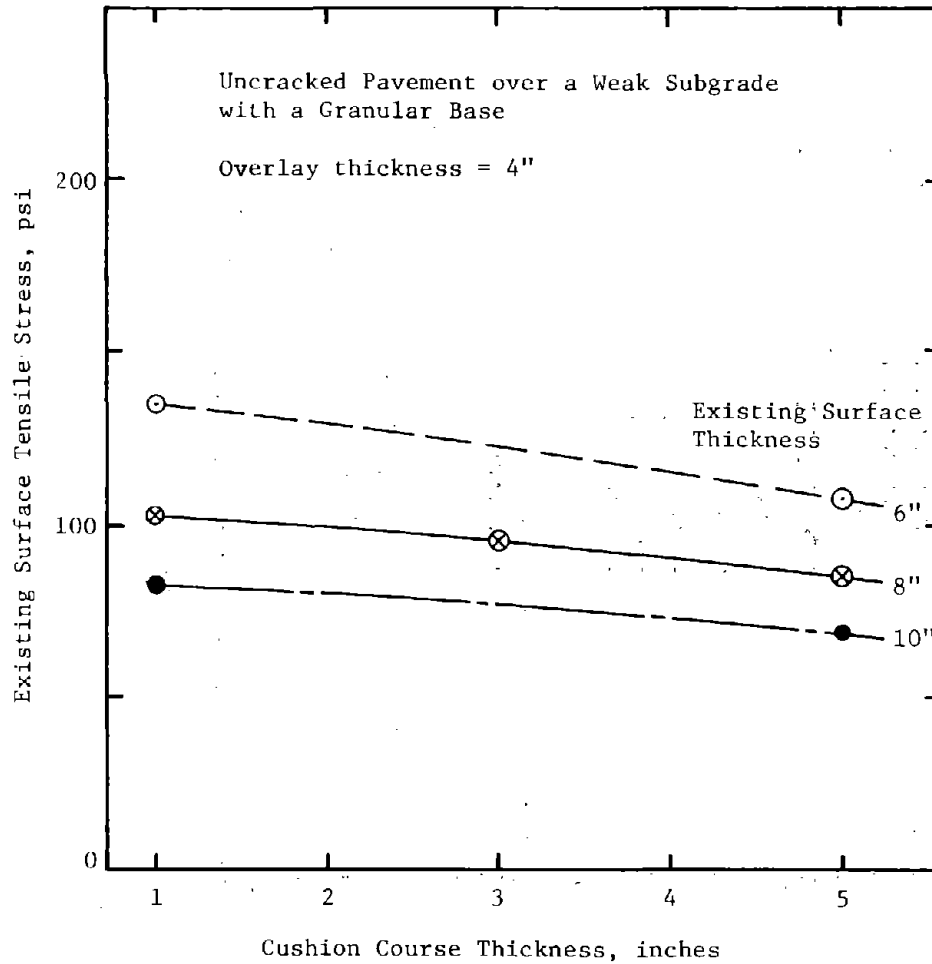


Figure 37. Relationship between cushion course thickness and stress in the existing surface for different existing surface thicknesses.

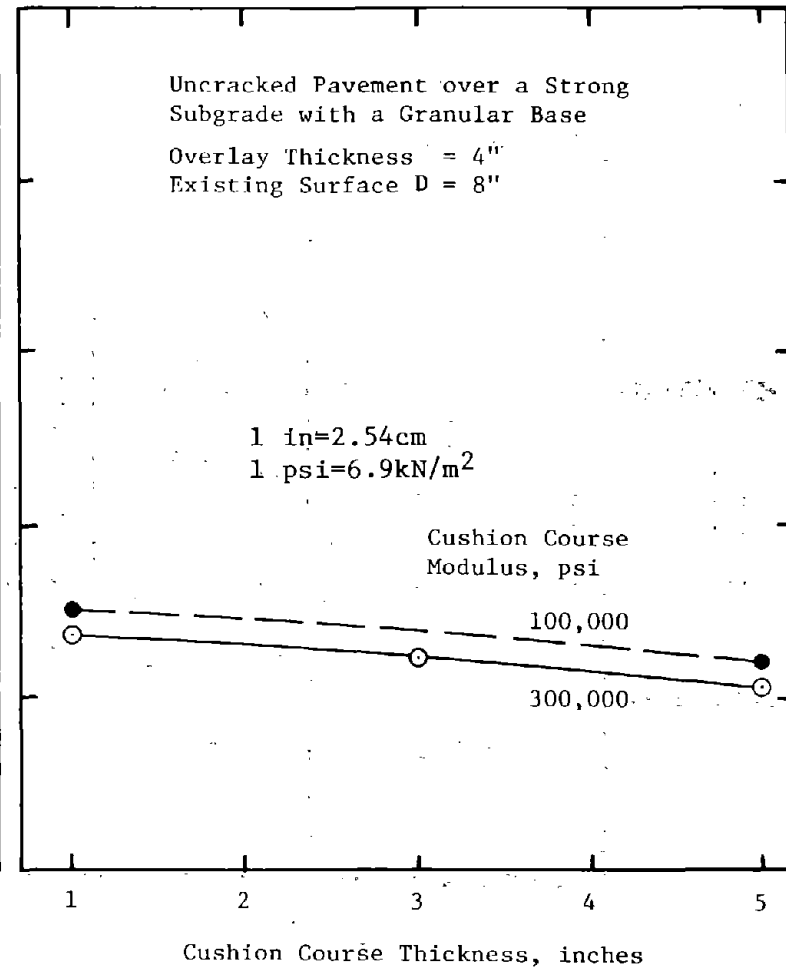


Figure 38. Relationship between cushion course thickness and existing surface stress for different moduli of the cushion course.

creasing cushion course thickness. Hence, an increase in cushion course thickness will not significantly reduce the overlay thickness required to resist fatigue. A change in the modulus of an asphaltic cushion course does not affect the stress in the existing PCC pavement to a large degree (Figure 38).

If granular cushion courses were used (moduli  $< 50,000$  psi) (or  $< 345,000 \text{ kN/m}^2$ ), then the stresses will begin to increase to the joint where the fatigue life will be affected. More overlay thickness would be required for a weaker cushion course based on fatigue. Figures 39-43 give an indication of how the cushion courses can affect the stresses in the overlay. By reviewing Figures 39-43, it is observed that the stresses in the overlay increase with an increase in thickness and a decrease in the modulus of the cushion course, for uncracked PCC pavements. Hence, it becomes necessary to check the stresses in the overlay when cushion courses are used, even for designs which are based on existing uncracked PCC pavements.

Although the sensitivity analysis did not include asphaltic concrete overlays, the strains in the AC overlay should be checked when cushion courses are used. This is to insure that the overlay thickness will be sufficient based on fatigue of uncracked PCC pavements. Several drawbacks to the use of this technique of controlling reflection cracking exist. First, supplies of high quality granular materials are becoming scarce and, therefore, expensive. Second, a thickness of six inches (15.2cm) has been determined to be necessary to control reflection cracking (Ref. 30). When an additional thickness of subsurface material is added to this, the result is often an unacceptable increase in the elevation of the roadway, especially in urban areas. Third, the thickness of the cushion required is comparable to the thicknesses required for new pavement construction; therefore, the structural capacity of the existing roadway is not being fully utilized. Finally, the development of alligator cracking in the new surface layer is not unusual, indicating a failure of the new structure.

#### Special Overlay Treatments.

Two subdivisions of this classification are presented: (1) use of steel or fabric reinforcement, and (2) special asphalt specifications, and/or use of admixtures.

Steel or Fabric Reinforcement. The purpose of the steel reinforcement is to distribute the stresses caused by movements occurring at the joints or cracks, thereby, decreasing the potential of reflection cracking caused by both failure mechanisms (Ref. 51). Steel reinforcement may be placed in narrow strips only over the joints and cracks, or continuously over the entire length of the project. Either welded wire fabric or expanded metal reinforcement may be used. Several agencies have studied the performance of reinforcement for controlling reflection cracking (Ref. 30, 32

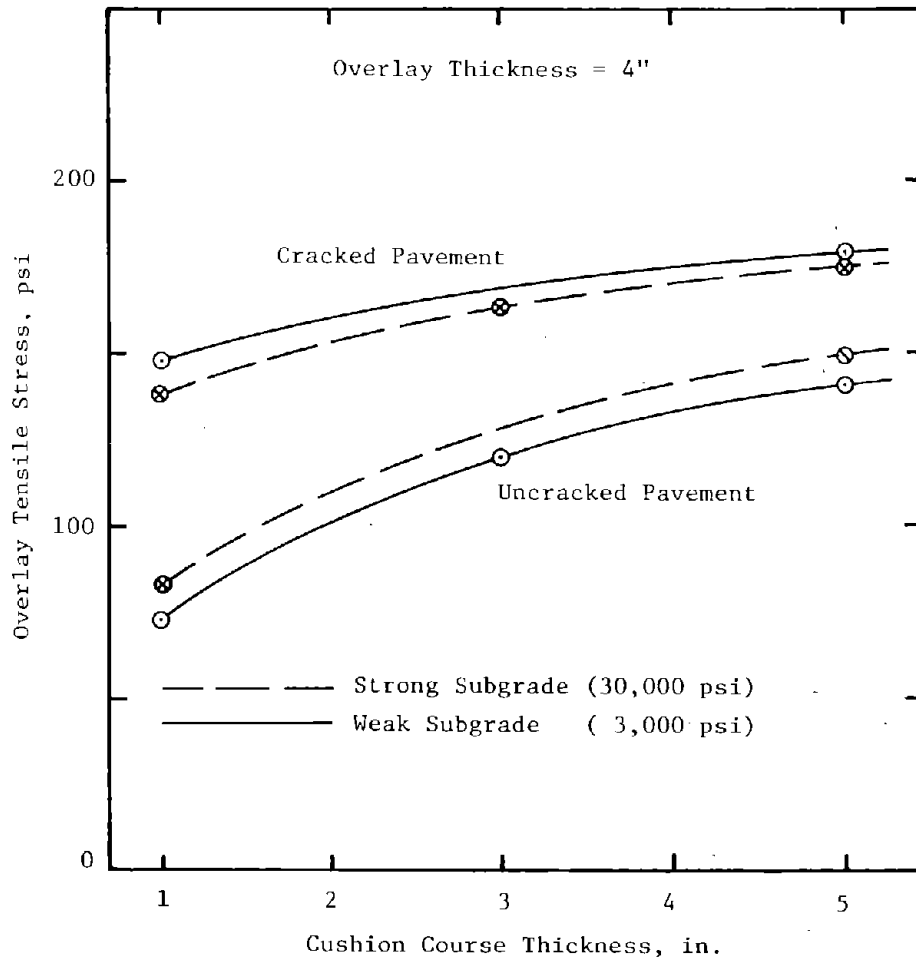


Figure 39. Relationship between cushion course thickness and overlay stress for various existing pavement conditions and type subgrades of a 4 inch overlay.

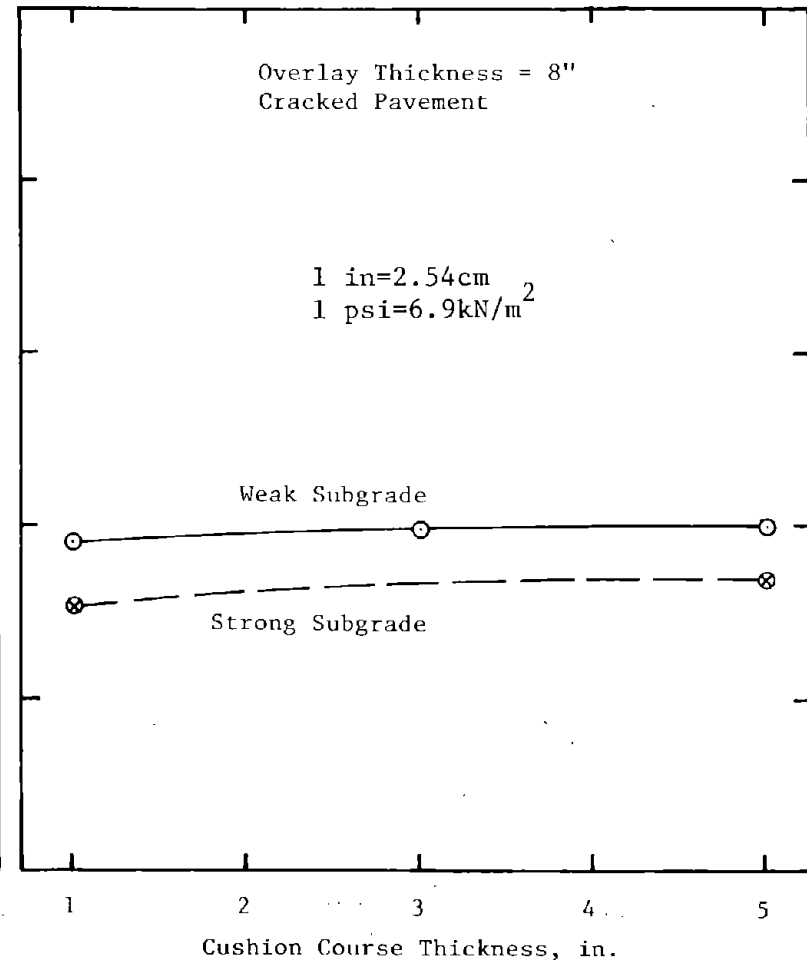


Figure 40. Relationship between overlay stress and thickness of cushion course for different subgrades of an 8 inch overlay.

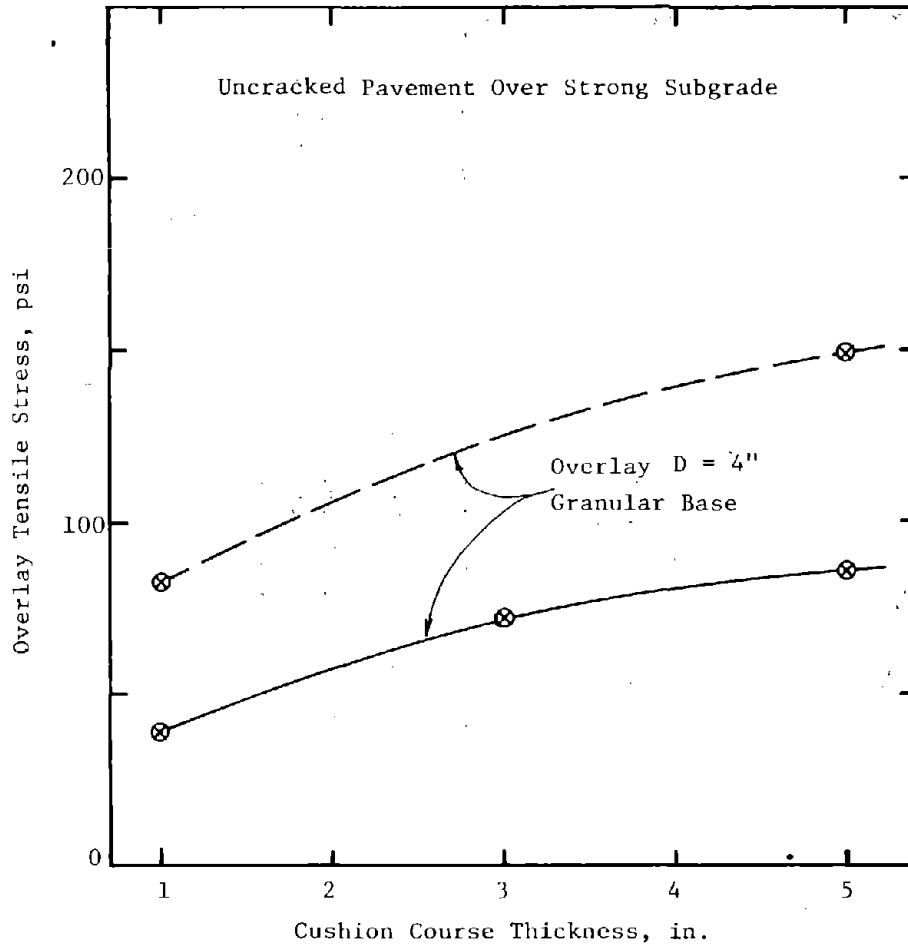


Figure 41. Relationship between overlay stress and cushion course thickness for different moduli of the cushion course for a strong subgrade.

1 in=2.54cm  
1 psi=6.9kN/m<sup>2</sup>

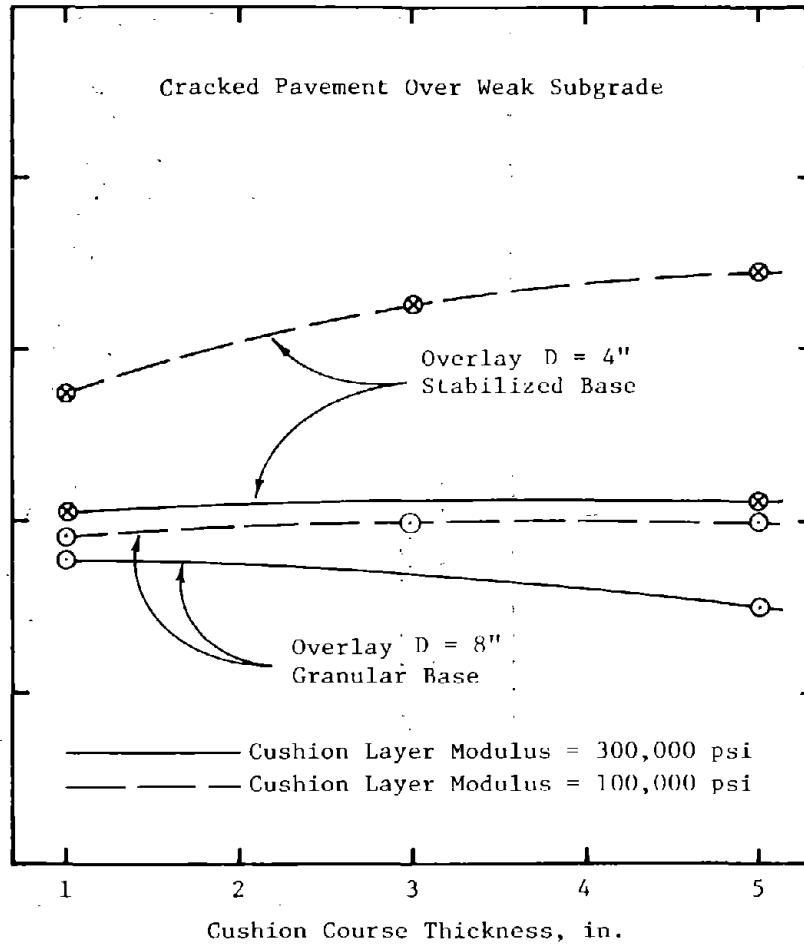


Figure 42. Relationship between overlay stress and cushion course thickness for different subbase materials and overlay thicknesses for a weak subgrade



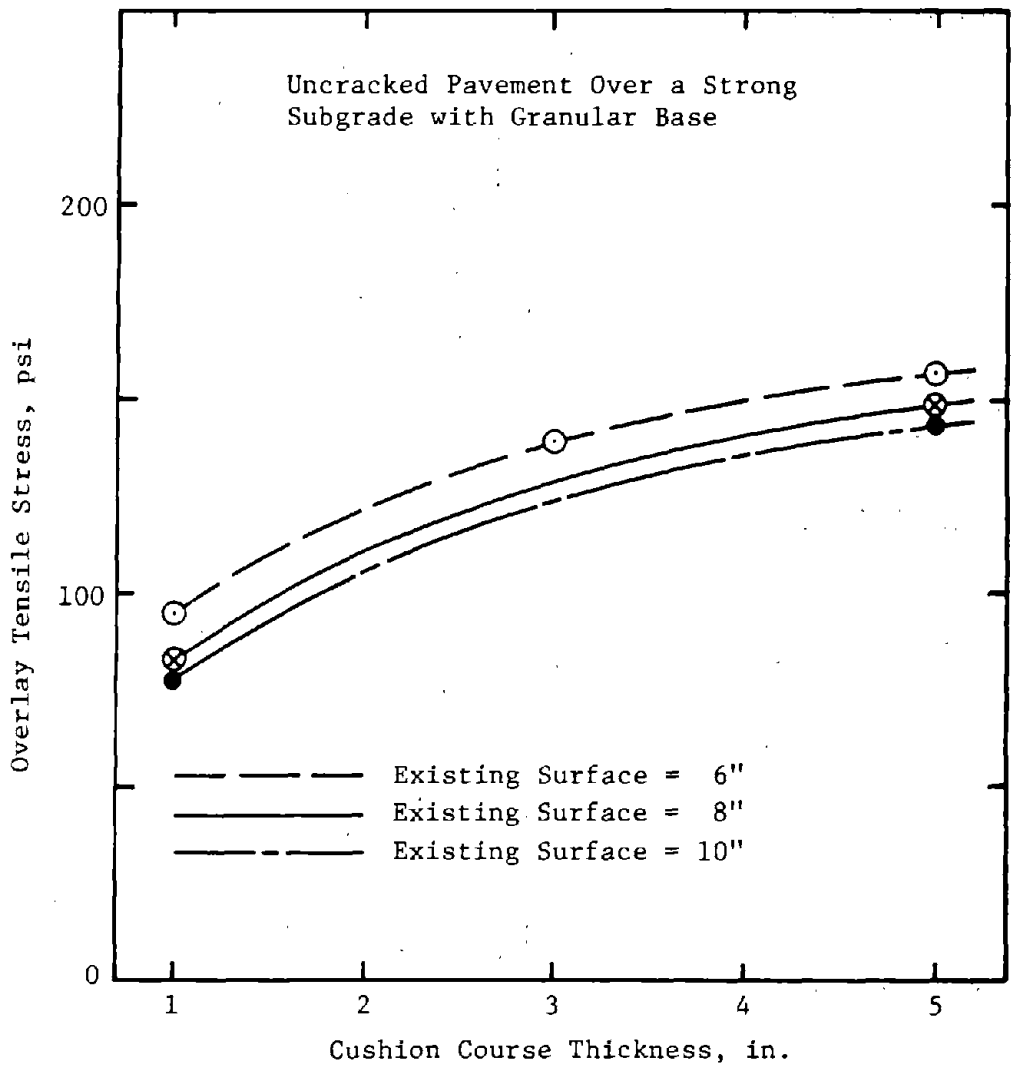


Figure 43. Relationship between cushion course thickness and overlay stress for different existing surface thicknesses.

1 in=2.54cm  
 1 psi=6.9kN/m<sup>2</sup>

33, 42, 43, 51, 55, 69<sup>1</sup>, 70<sup>2</sup>, 71<sup>3</sup>, 72<sup>4</sup>). In general, it has been found that reinforcement can be an effective measure for reducing reflection cracking (Table 10). It has also been found that because asphaltic concrete overlays have voids, water enters the structure, and causes corrosion problems in as little as four years of service (Ref. 30). Numerous publications of the Highway Research Board and the Association of Asphalt Paving Technologists have reported improved performance over limited periods of time (4-6 years).

Reinforcement not only has been successful in reducing reflected cracks, but reduces horizontal displacement at areas where braking and acceleration occur as shown in Table 11. However, due to the corrosion of the steel, there is little evidence of a significant reduction in cracking over long periods of time. Figure 44 shows the results of a Michigan study using reinforcing steel to reduce reflection cracks.

Due to the corrosion of steel, synthetic fiber fabric is presently being field tested as a reinforcement material in asphaltic concrete overlays (Ref. 37, 63, 70). Results thus far are inconclusive, but lab tests and limited field experiments indicate an increase in overlay strength (Figure 45) and performance. Some of these synthetic fibers include spun bonded nylon, nonwoven polypropylene, and polyester open weave fabrics. Field tests and observations reported by Smith from a study completed in Iowa (Ref. 73)<sup>5</sup> show fabrics can reduce reflection cracks. Although differential deflections were not measured for the Iowa study, it is hypothesized that cracking developed primarily from shearing stresses, and

---

<sup>1</sup>Zube, E., "Wire Mesh Reinforcement in Bituminous Resurfacing," Highway Research Board Bulletin 131, Highway Research Board, 1956, (pp. 1-8).

<sup>2</sup>Busching, H. W., E. H. Elliott, and N. G. Reyneveld, "A State of the Art Survey of Reinforced Asphalt Paving," Proceedings, AAPT Vol. 39, 1970, (pp. 766-798).

<sup>3</sup>"Wire Mesh Reinforcement of Bituminous Concrete Overlays," Bur. of Phys. Res., Res. Report 66-1, New York State Department of Public Works, October 1966.

<sup>4</sup>Chastain, W., Jr., and R. H. Mitchell, "Evaluation of Welded Wire Fabric in Bituminous Concrete Resurfacing," Highway Research Record No. 61, Highway Research Board, 1963.

<sup>5</sup>Smith, Richard D., "Prevention of Reflection Cracking in Asphalt Overlays with Structufors, Petromat, and Cerex," Project HR-158, Iowa Research Board, May 1977.

Table 10. Percent of reflected cracks and joints after 30 months of service for welded wire fabric reinforcement (Ref. 51).

Test Section	Crack Width, (in.)	Reflected Cracks, %	
		Non-Reinforced	Reinforced w/ Wire Fabric
I	<1/16	13	0
	1/16	64	0
	1/8	60	0
	3/16	66	-
	1/4	36	-
	5/16	100	-
	3/8	82	-
	1/2	75	0
	3/4	32	0
II	<1/16	16	0
	1/16	18	0
	1/8	29	-
	1/4	100	-
	1/2	96	9
	3/4	54	17

1 in=2.54cm

Table 11. Horizontal displacement of control points in the outer wheel path of surface course (Ref. 51).

Distance from Intersection (ft.)	Displacement, * inches			
	Tyler Street		Pearce Street	
	Non-Reinforced	Reinforced w/ Wire Fabric	Non-Reinforced	Reinforced w/ Wire Fabric
0	-.156	-.156	-.250	-.188
25	-.312	0	-.094	-.156
50	0	-.125	-.250	-.250
75	0	-.312	-.312	-.188
100	-.375	0	-.063	-.250
125	0	-.188	-.375	-.125
150	-.312	-.250	-.063	-.063
Average	-.165	-.147	-.201	-.174

\*A negative number denotes movement opposite from direction of traffic or caused by acceleration forces.

1 in=2.54cm  
1 ft=.305m

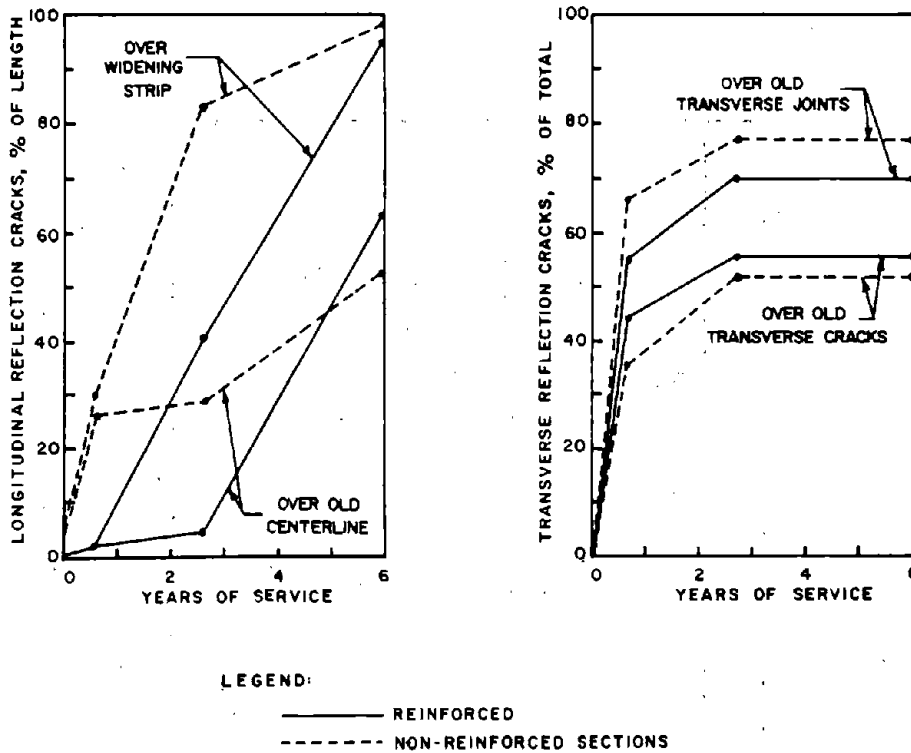


Figure 44. Average Reflection cracking for reinforced and non-reinforced sections. (Ref. 66).

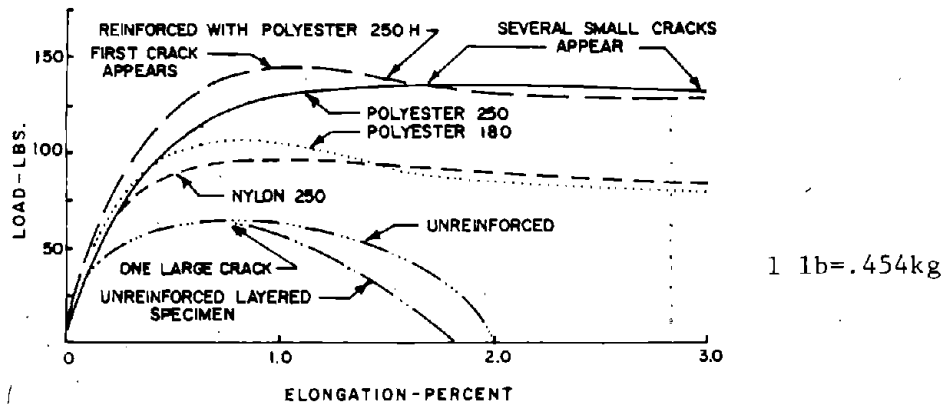


Figure 45. Load-Elongation relationship obtained from testing reinforced and non-reinforced specimens in tension. (Ref. 70).

temperature related reflection cracking has been retarded, as was the case for the Virginia study (Ref. 41). Thus, from the studies reviewed, reinforcing fabrics can reduce temperature related reflection cracks, but due to the inability of the fabric to distribute shearing stresses, reflection cracks caused by differential vertical deflections can not be controlled. A few of the synthetic fabrics, such as nonwoven polypropylene, have been used as an impervious membrane to prevent water from entering the pavement thereby reducing the severity and number of reflection cracks (Figure 46). Reinforcing fabrics will not completely eliminate the reflected cracks, but indications are that the crack widths are smaller during colder months and nearly closed during warmer months (Ref. 62), illustrating the reinforcing effect.

Special Asphalt Specifications - Recognizing that horizontal and differential vertical movements cause reflection cracking, a more flexible overlay that could withstand larger levels of stress and strain without failure could be a solution. There has been some experimentation with the use of different grades of asphalt and admixtures for controlling reflection cracking, but the results have generally not been favorable (Ref. 74)<sup>1</sup>. This is understandable since the amount of strain which must be endured, particularly in severe climates is much greater than even the softest paving mixture could be expected to endure (Refs. 32, 33). One study conducted by Roberts in Iowa (Ref. 75)<sup>2</sup>, showed that the use of softer asphalt cements allows the reflection cracks, developed during cold weather, to heal during warm periods.

There have been studies which indicate that mix strength may be increased by the use of additives (limestone, dust, asbestos fibers, etc.) when related to a strain at failure (Refs. 38, 76<sup>3</sup>, 77<sup>4</sup>, 78<sup>5</sup>, 79<sup>6</sup>).

---

<sup>1</sup>Tuckett, G. M., G. M. Jones and G. Littlefield, "The Effects of Mixture Variables on Thermally Induced Stresses in Asphalt Concrete," Proceedings, AAPT, Vol. 39, 1970, (pp. 703-744).

<sup>2</sup>Roberts, S. E., "Cracks in Asphalt Resurfacing Affected by Cracks in Rigid Bases," Proceedings, Highway Research Board, Vol. 33, 1954, (pp. 341-344).

<sup>3</sup>Wortham, G. R., and L. M. Hatch, "Asbestos Fiber as a Filler in a Plant-Mix Pavement," Research Project No. 24, Idaho Department of Highways, December 1969.

<sup>4</sup>Mellott, Dale B., "Asbestos Fibers in ID-2A Bituminous Concrete-Phase II, Research Project No. 70-12, Pennsylvania Department of Transportation, Bureau of Materials, Testing and Research, October 1975.

<sup>5</sup>Blackhurst, M. W., Foxwell, J. A., and Kietzman, J. H., "Performance of Asbestos Asphalt Pavement Surface Courses with High Asphalt Contents," Highway Research Record 24, Highway Research Board, 1963.

<sup>6</sup>Zuehlke, G. H., "Marshall and Flexural Properties of Bituminous Pavement Mixtures Containing Short Asbestos Fibers," Highway Research Record 24, Highway Research Board, 1963.

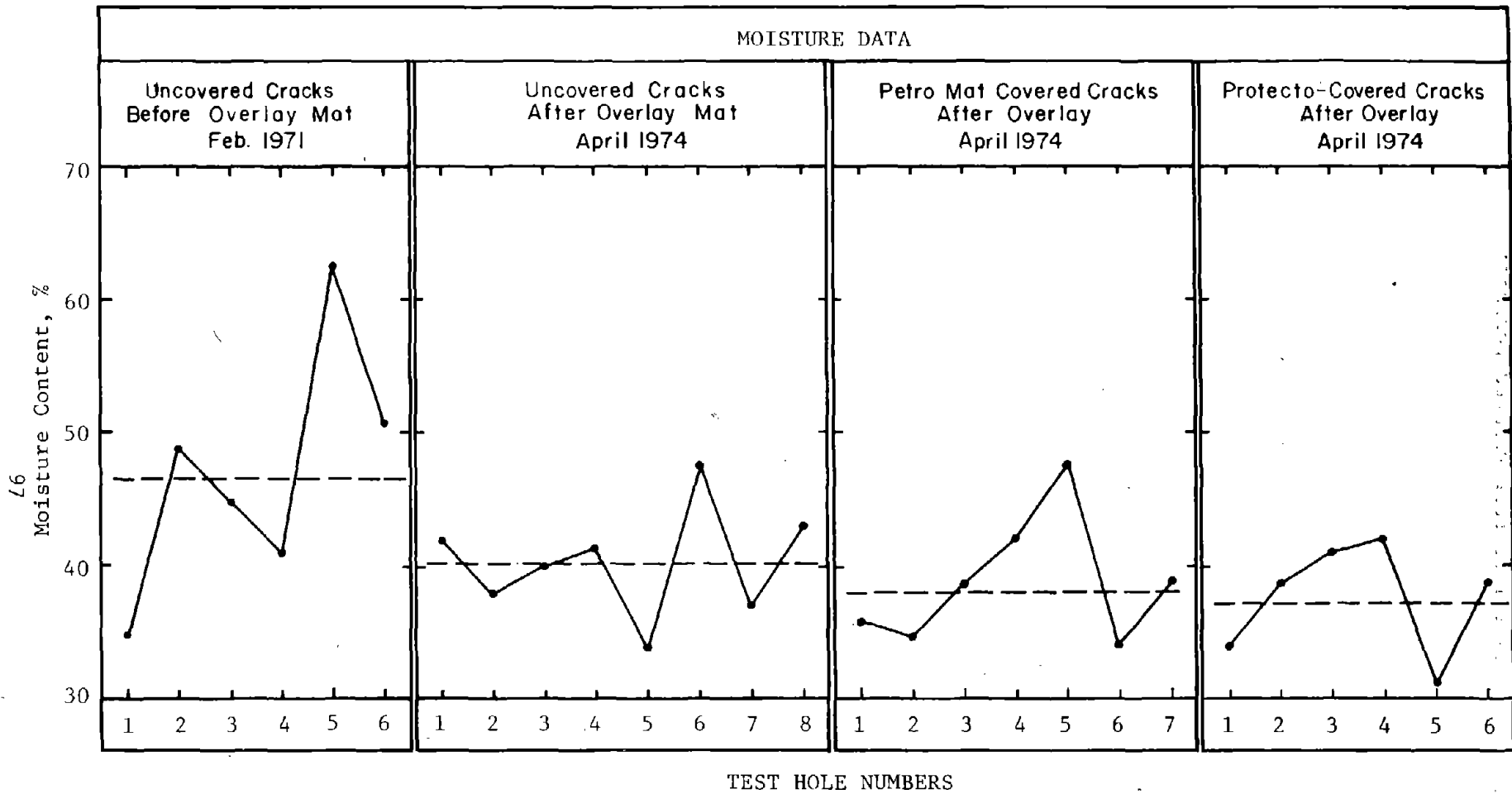


Figure 46. Effect of impervious membranes on the moisture content of underlying layers.

The use of natural rubber and neoprene in various amounts to increase the extensibility of the asphalt mix has been attempted to a limited extent (Refs. 30, 37, 44, 80<sup>1</sup>, 81<sup>2</sup>). Most of the results indicate that fillers or additives alone will not improve the performance of an overlay over a long period of time as shown in Figure 47 (Refs. 32, 36, 82<sup>3</sup>).

#### Increased Overlay Thickness

There is some evidence that reflection cracking may be reduced through the use of thicker resurfacing layers by reducing the stress per cross-sectional area and insulating the existing pavement (Refs. 32, 69). In one case, reported in Reference 30, the asphaltic concrete surfacing, which has experienced no traffic, was 4, 5 and 6 inches (10.2, 12.7, and 15.2cm) in thickness over a PCC base. The reflection cracks penetrated the 4 inch (10.2cm) thickness, only partially penetrated the 5 inch (12.7cm) thickness, and did not penetrate the 6 inch (15.2cm) thickness. The disadvantage of this is the increased cost and the fact that some roads have a limit to which the grade may be raised (Ref.32). If we examine the value of increased resurfacing thickness in light of the distress mechanisms discussed previously, it is relatively easy to understand why this strategy is economically ineffective for controlling reflection cracking (Figure 33).

The use of increased thickness does not alter the gauge length over which the stresses must act above the cracks and joints in the existing surface. The amount of movement expected at the joints is altered by the increased insulating effect of the greater thicknesses, and the increased resistance to movement at the joints provided by the greater thickness. Evidently, these two factors are not enough to prevent the development of reflection cracks. The results of several reflection cracking studies, where the overlay varied from 1-1/2 to 10 inches (3.8 to 25.4cm), all showed some degree of reflection cracking. From this evidence, it is safe to conclude that increasing the thickness of the asphalt concrete resurfacing will not eliminate reflection cracking (Refs. 10, 45, 51, 53, 69, 83<sup>4</sup>, 84<sup>5</sup>).

---

<sup>1</sup>James, J. G., "A Full Scale Road Experiment with Rubberized Asphalt on Concrete Using Expanded Metal Over the Concrete Joints," Road Research Laboratory Note 3511, 1959.

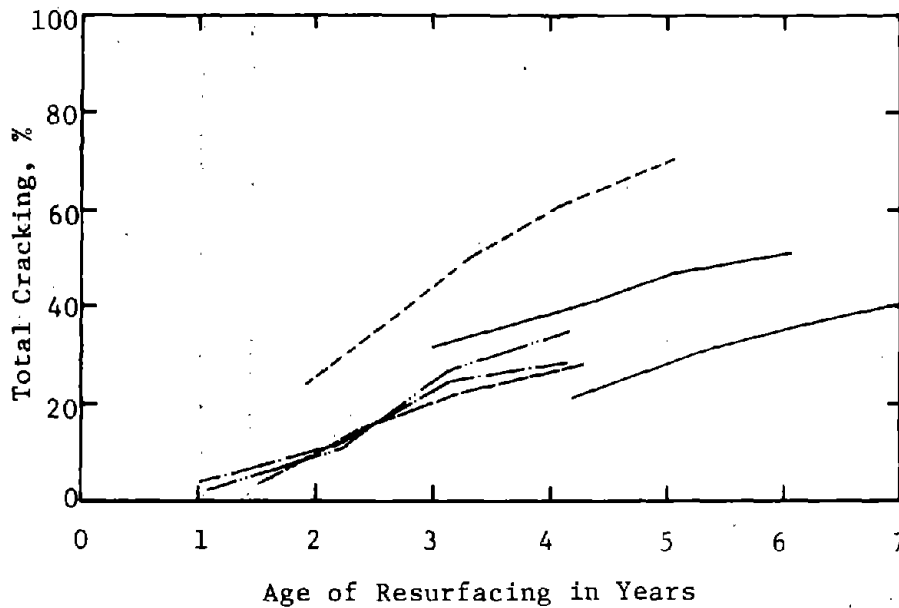
<sup>2</sup>Carroll, J. A., and D. G. Diller, "Use of Rubberized Asphalt to Control Reflection Cracking in Asphalt Concrete Overlays," Proceedings, International Symposium on Use of Rubber in Asphalt Pavements, 1971, (pp. 356-366).

<sup>3</sup>Gould, V. G., "Summarized Committee Report 1948-1960: Salvaging Old Pavements by Resurfacing," HRB Bulletin No. 290, Highway Research Board, 1961, (pp. 1-14).

<sup>4</sup>Van Breeman, William, "Discussion of Possible Designs of Composite Pavements," Highway Research Record 37, Highway Research Board, 1963.

<sup>5</sup>Housel, William S., "Design Maintenance and Performance of Resurfaced Pavements at Willow Run Airfield," Highway Research Board Bulletin 322, Highway Research Board, 1962.





LEGEND

- Type I, 2-1/2 in. thick (Massachusetts Bituminous Conc.),
- Type I, 3-1/2 in. thick (Massachusetts Bituminous Conc.),
- Type I plus Emulsified Rubber Asphalt, 2-1/2-in. thick,
- Type I plus CRS Synthetic Rubber, 2-1/2-in. thick,
- · - · - Type I plus Natural Rubber Crumbs, 2-1/2-in. thick.

1 in=2.54cm

Figure 47. Use of rubber additives to reduce the percent cracking in standard mixtures (Ref. 44).

## Summary

Reflection cracking studies to date have been of an empirical nature with no concentrated research effort. Studies to determine life expectancy of the above treatments have been neglected and adequate documented data is scarce. No one treatment is a cure for all situations; rather, the reported crack preventing methods should be integrated into an overlay design, directly tailored to the nature of distress (Ref. 37). Figure 48 shows a flow diagram which lists each type treatment that could be considered depending on the failure mechanism. Table 12 summarizes the various techniques reviewed from the literature and shows where they were used.

It should be kept in mind that careful evaluation and consideration should be given in selecting a treatment so that other distress mechanisms (rutting, disintegration, shoving, fatigue cracking, etc.) do not develop. Hence, the development of a rational analytical model which adequately explains the reflection cracking phenomenon would not only enable the prediction of service lives of overlays, but also provide a basis for evaluating and comparing the various treatments. With the development of this model, new materials and new construction procedures could be evaluated as to their effectiveness in reducing reflection cracking.

## Model Development

A well-developed and generally accepted mechanistic model that adequately explains reflection cracking phenomena has not been established. Many existing methods of analysis and design of resurfacing layers do not even consider the problem of reflection cracking directly. Some methods deal with the problem by predicting the rate at which cracks, in an underlying layer of a pavement, will reflect through a bituminous overlay (Ref. 85<sup>1</sup>, 86<sup>2</sup>). This involves the application of fracture mechanics to the problem of the initiation and growth of reflection cracks under the combined influence of repeated vehicular loadings and changes in temperature.

The hypothesis of fracture mechanics theory is that fracture initiates in the material from some pre-existing flaw which creates stress concentrations. This increase in stress at the discontinuities is usually represented by a stress-intensity factor normally determined by finite element analy-

---

<sup>1</sup>Ramsamooj, D. V., "Prediction of Reflection Cracking in Pavement Overlays" Highway Research Record No. 434, Highway Research Board, 1973.

<sup>2</sup>Luther, Michael S., Kamran Majidzadeh, and Che-Wei Chang, "Mechanistic Investigation of Reflection Cracking of Asphalt Overlays," Transportation Research Record No. 572, Transportation Research Board, 1976.

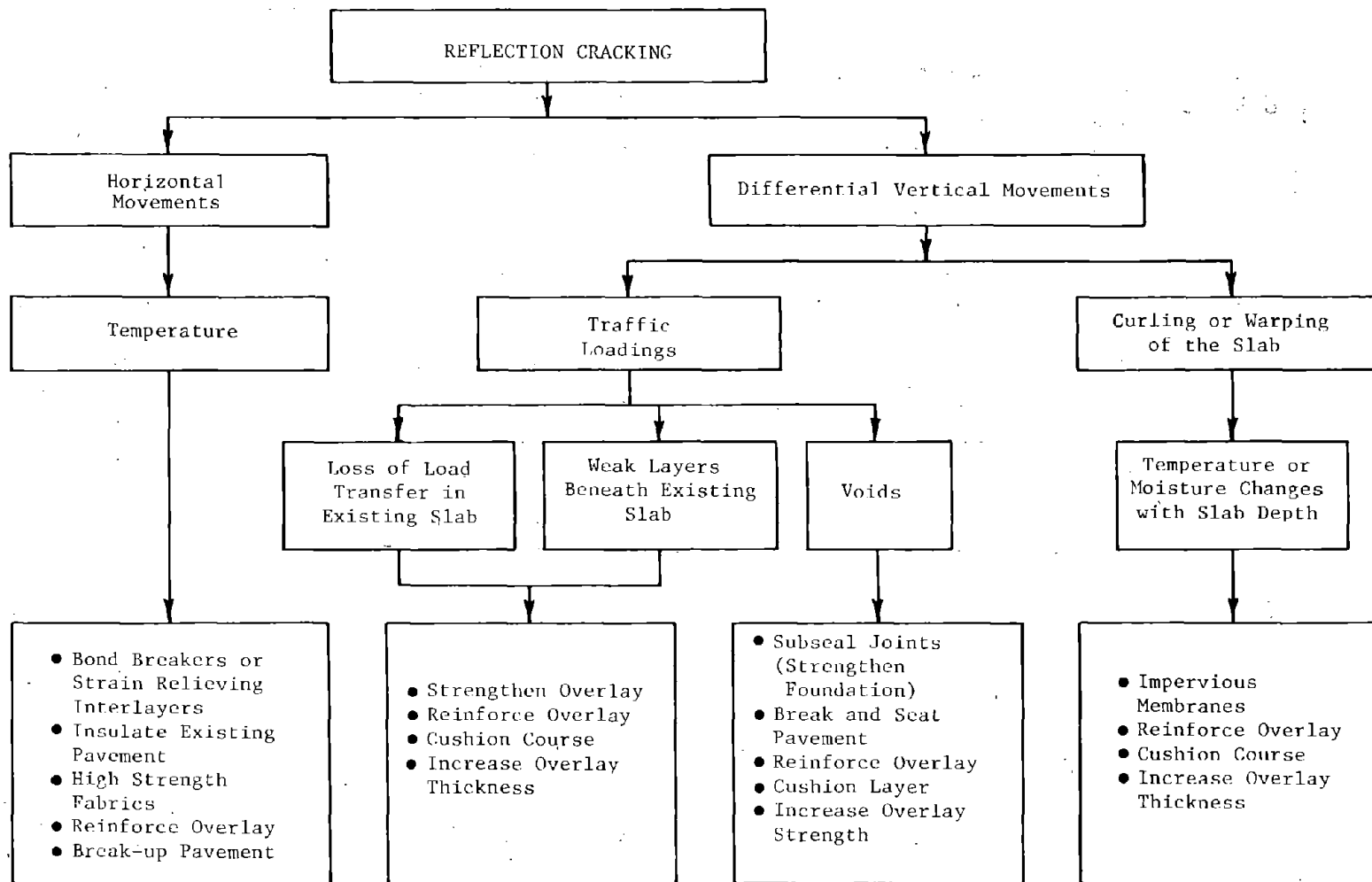


Figure 48. Flow diagram to determine a treatment which can be considered to reduce reflection cracking.

Table 12. Various locations reviewed, where a method or type of treatment has been applied.

Classification Method Location	Treatments to Existing PCC Pavements			Stress or Strain Relieving Interlayers			Cushion Courses	Special Overlay Treatments				Increase Overlay Thickness
	Crack Filling & Sealing	Breaking & Seating Pavement	Subsealing Joints /Cracks	Bond Breakers	Fabrics	Tack or Seal Coats		Reinforcement		Asphalt Specifications	Additives	
								Steel	Fabrics			
Alabama												
Arizona												
Arkansas												
California												
Colorado												
Connecticut												
Florida												
Idaho												
Illinois												
Iowa												
Kansas												
Kentucky												
Louisiana												
Massachusetts												
Michigan												
Minnesota												
Mississippi												
Missouri												
Nevada												
New Jersey												
New Mexico												
New York												
N. Carolina												
N. Dakota												

Table 12. (Continued) Various locations reviewed, where a method or type of treatment has been applied.

Classification Method Location	Treatments to Existing PCC Pavements			Stress or Strain Relieving Interlayers			Cushion Courses	Special Overlay Treatments				Increase Overlay Thickness
	Crack Filling & Sealing	Breaking & Seating Pavement	Subsealing Joints /Cracks	Bond Breakers	Fabrics	Tack or Seal Coats		Reinforcement		Asphalt Specifications	Additives	
								Steel	Fabrics			
Oklahoma				■	■		■					
Oregon			■		■							
Pennsylvania			■	■	■			■	■			■
S. Carolina				■	■	■	■	■				
S. Dakota					■		■	■				
Tennessee							■					
Texas	■	■			■	■	■	■				■
Utah							■					■
Vermont						■		■				
Virginia				■	■							
Washington			■	■			■					
Wisconsin							■	■				
Wyoming	■				■		■					■

sis. In the initial development of a basic theory to determine how the resurfacing reacts to horizontal movements imposed on it by the continuous opening and closing of joints or cracks, repeated vehicular loadings were not considered. As a result, fracture mechanics was not used. This is not to say that the number of load applications is not associated with the problem. If no thermal or shearing forces existed in the overlay, there still could be stress concentrations occurring at the joints and cracks (Refs. 85, 86) causing reflection cracks to occur. These stress concentrations are considered in the fatigue design under the discussion of load location factors.

Tensile strains caused by wheel loads can be combined with the model using strain transformation equations. By reviewing a specific element in the overlay, these strains caused by external and internal forces (Figure 49) can be mathematically related by the following equations.

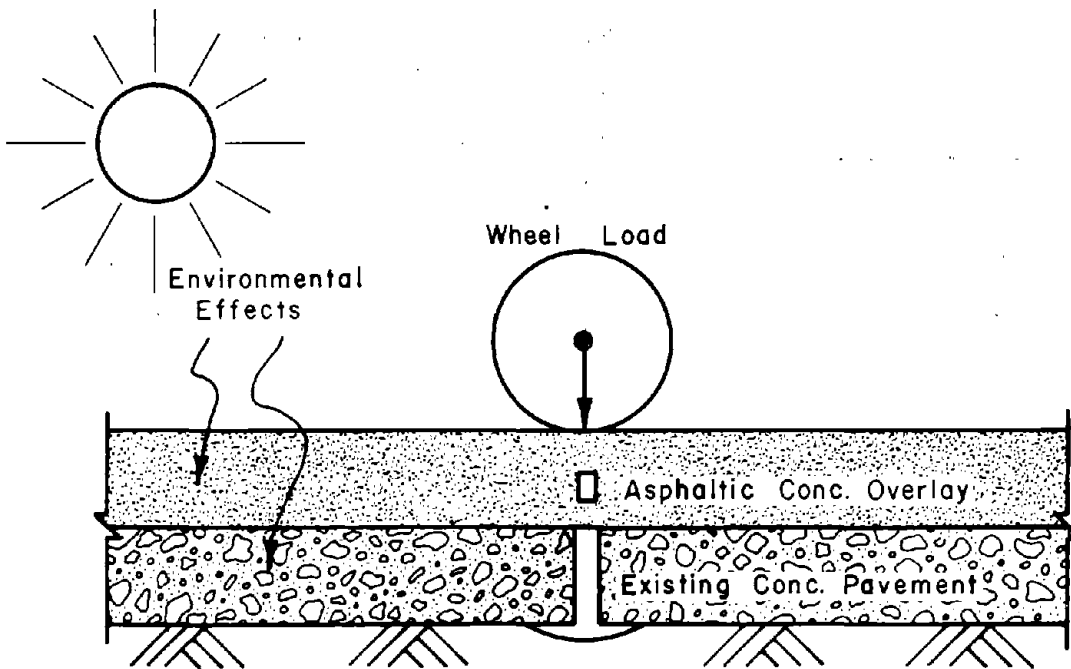
$$\epsilon_H(T_i) = f \left\{ \epsilon_{WL}(T_i) + \epsilon_o(T_i) \right\}_X \dots\dots\dots 17$$

$$\epsilon_V(T_i) = f \left\{ \epsilon_{WL}(T_i) \right\}_z \dots\dots\dots 18$$

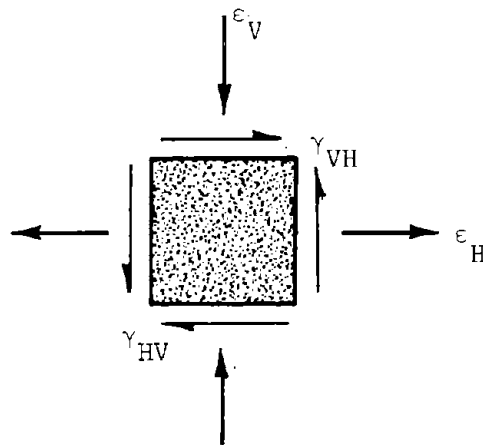
$$\gamma_{VH}(T_i) = \gamma_{HV}(T_i) = f \left\{ \gamma_{WL}(T_i) + \gamma_o(T_i) \right\} \dots\dots\dots 19$$

where:

- $\epsilon_H(T_i)$  = Total horizontal strain in the overlay, parallel to traffic flow (X), at temperature  $T_i$ , in./in. (1 in=2.54cm).
- $\epsilon_{WL}(T_i)$  = Horizontal strain in the overlay due to the applied wheel load parallel to traffic flow (X), at temperature  $T_i$ , calculated with elastic layered theory, in./in. (1 in=2.54cm).
- $\epsilon_o(T_i)$  = Horizontal tensile strain due to temperature  $T_i$  and movement of the existing concrete pavement, calculated with the model, in./in. (1 in=2.54cm).
- $\epsilon_V(T_i)$  = Total vertical strain in the overlay due to the applied wheel load, at temperature  $T_i$ , in./in. (1 in=2.54cm)
- $\gamma_{VH}(T_i)$  = Total shearing strain in the overlay at temperature  $T_i$ , in./in. (1 in=2.54cm)
- $\gamma_{WL}(T_i)$  = Shearing strain in the overlay due to the applied wheel load at temperature  $T_i$ , calculated with elastic layered theory, in./in. (1 in=2.54cm).
- $\gamma_o(T_i)$  = Shearing strain in the overlay due to the wheel load and differential deflections across a joint at temperature  $T_i$ , calculated with the model, in./in. (1 in=2.54cm).



a.) Illustration of the overall reflection cracking problem:



b.) Resulting forces acting on an element in the overlay material above a joint or crack in the existing pavement.

Figure 49. Illustrations showing the combined influence of wheel loads and environmental forces which cause reflection cracks to develop in an overlay.

The planes on which the principal strains act may be defined analytically using equation 20.

$$\tan 2\theta = \frac{\gamma_{VH}(T_i)}{\epsilon_H(T_i) - \epsilon_V(T_i)} \dots \dots \dots 20$$

As deduced from a Mohr's Circle, the analytical expression for the principal strain is:

$$\epsilon_{MAX}(T_i) = \frac{\epsilon_H(T_i) + \epsilon_V(T_i)}{2} + \left[ \left[ \frac{\epsilon_H(T_i) - \epsilon_V(T_i)}{2} \right]^2 + \left[ \frac{\gamma_{VH}(T_i)}{2} \right]^2 \right]^{1/2} \dots \dots \dots 21$$

This principal strain,  $\epsilon_{MAX}$ , is then applied in the fatigue equation to determine when Class 3 and 4 cracking will occur in the overlay. No shearing strains are associated with the principal strains. Thus, the maximum shearing strain must be checked with an allowable value, to insure the overlay has sufficient shearing strength. This maximum shearing strain can be computed by:

$$\gamma_{MAX}(T_i) = 2 \left[ \left[ \frac{\epsilon_H(T_i) - \epsilon_V(T_i)}{2} \right]^2 + \left[ \frac{\gamma_{VH}(T_i)}{2} \right]^2 \right]^{1/2} \dots \dots \dots 22$$

The above procedure would produce a generalized condition combining traffic and environmental influences, to adequately explain the reflection cracking phenomena in an overlay system. Due to temperature variations during the year, an evaluation of the wheel load effects would need to be completed for each season or temperature range. The model developed is intended as a check to resist reflected cracks resulting primarily from extreme environmental conditions and a loss of load transfer by the existing pavement. Therefore it is recommended that wheel load not be considered until the model has been physically checked with field data.

The development of this model is primarily concerned with asphaltic concrete overlays. For portland cement concrete overlays, joints should be matched or a level-up asphaltic concrete course should be used so that reflected cracks resulting from temperature movements in concrete overlays would not be a serious problem. Although this model was developed primarily for AC overlays, other materials can be analyzed by reviewing the procedure and recognizing the assumptions involved in its development.



Two different failure modes are considered in the development of the model. The first is an opening mode failure due to horizontal movements of the existing concrete pavement (Figure 50.a). It is primarily a tension failure resulting from an environmental loading condition caused by a drop in temperature. The movements of the underlying layer are transferred to the overlay causing a critical stress or strain to develop over the joint or crack. The second is a shearing mode failure resulting from inadequate load transfer across a joint or crack (Figure 50.b). Inadequate load transfer may be an initial condition, or occur due to a loss resulting from repeated load applications. It is a shearing failure resulting from an external load caused by a differential deflection across the joint. Figure 51 illustrates the overall procedure for determining if reflection cracks will result from either or both failure mechanisms based on extreme environmental conditions, and is described in the following sections.

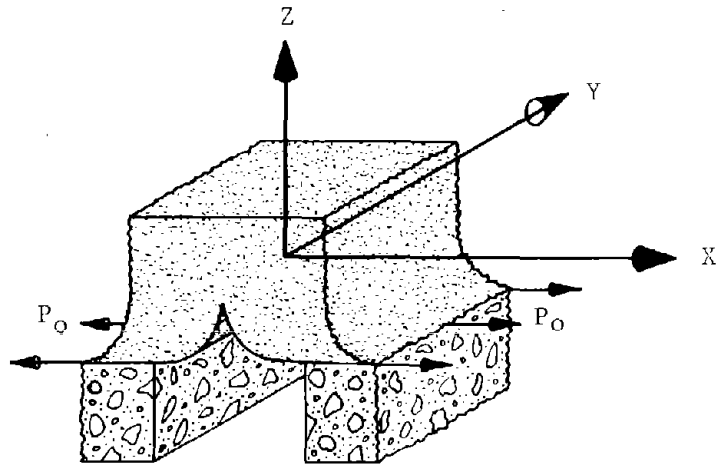
In developing the model certain limitations and assumptions were required due to unknown values and loads. Some of these are listed below:

1. Linear elasticity and all the assumptions associated with it are applicable to the problem,
2. The governing equation of static equilibrium is applicable to pavements; i.e.  $\Sigma F_x = 0$ ,  $\Sigma F_y = 0$ ,  $\Sigma F_z = 0$ ,
3. Temperature variations are uniformly distributed in the existing concrete slab,
4. Concrete movement is continuous with slab length,
5. Movement of a layer is constant through layer thickness
6. Material properties are independent of space.

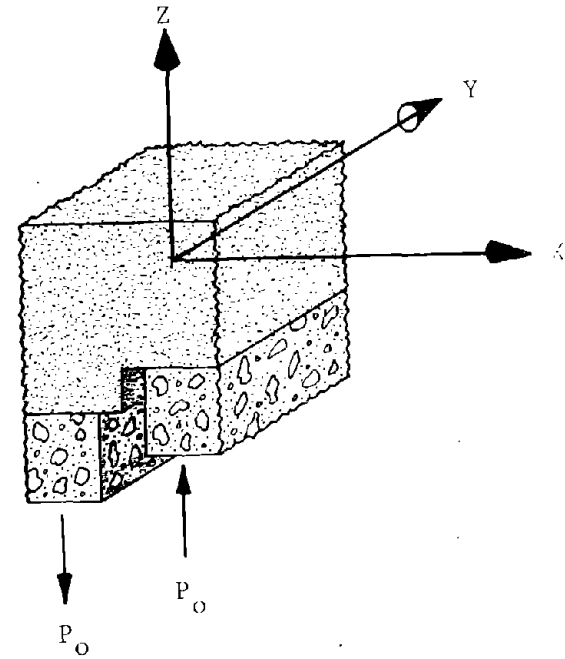
Other assumptions and boundary conditions made will be discussed in the text at specific locations. It is recommended, since this is a first development, assumptions and boundary conditions used must be verified from future field studies and corrected as necessary.

#### Horizontal Movements

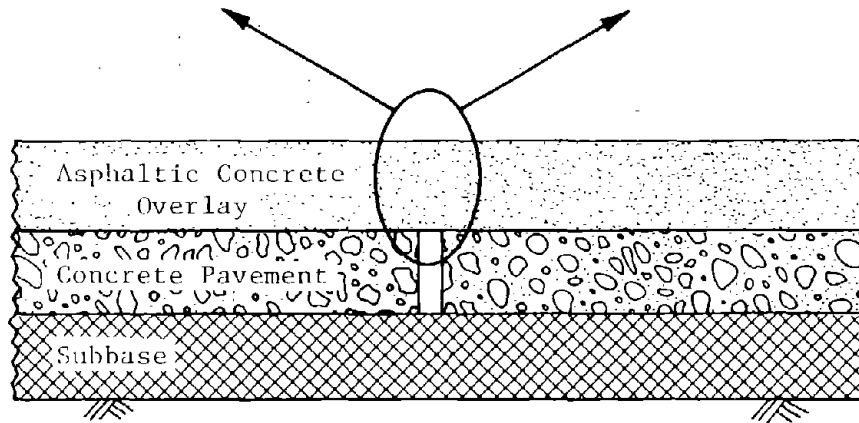
The first step in determining how the resurfacing reacts to horizontal movements of the existing concrete slab is to estimate how the slab moves and define the forces involved. This is accomplished by characterizing the existing concrete pavement through field measurements, in order to calibrate the model to actual field observations. Once this has been completed the overlay design can be evaluated for its effectiveness in reducing reflected cracks.



(a.) Opening Mode - Horizontal Movement of Underlying Layer



(b.) Shearing Mode - Differential Vertical Deflections Across a Joint or Crack



(c.) General Pavement Cross-section.

Figure 50. Different failure modes considered for the reflection cracking model.

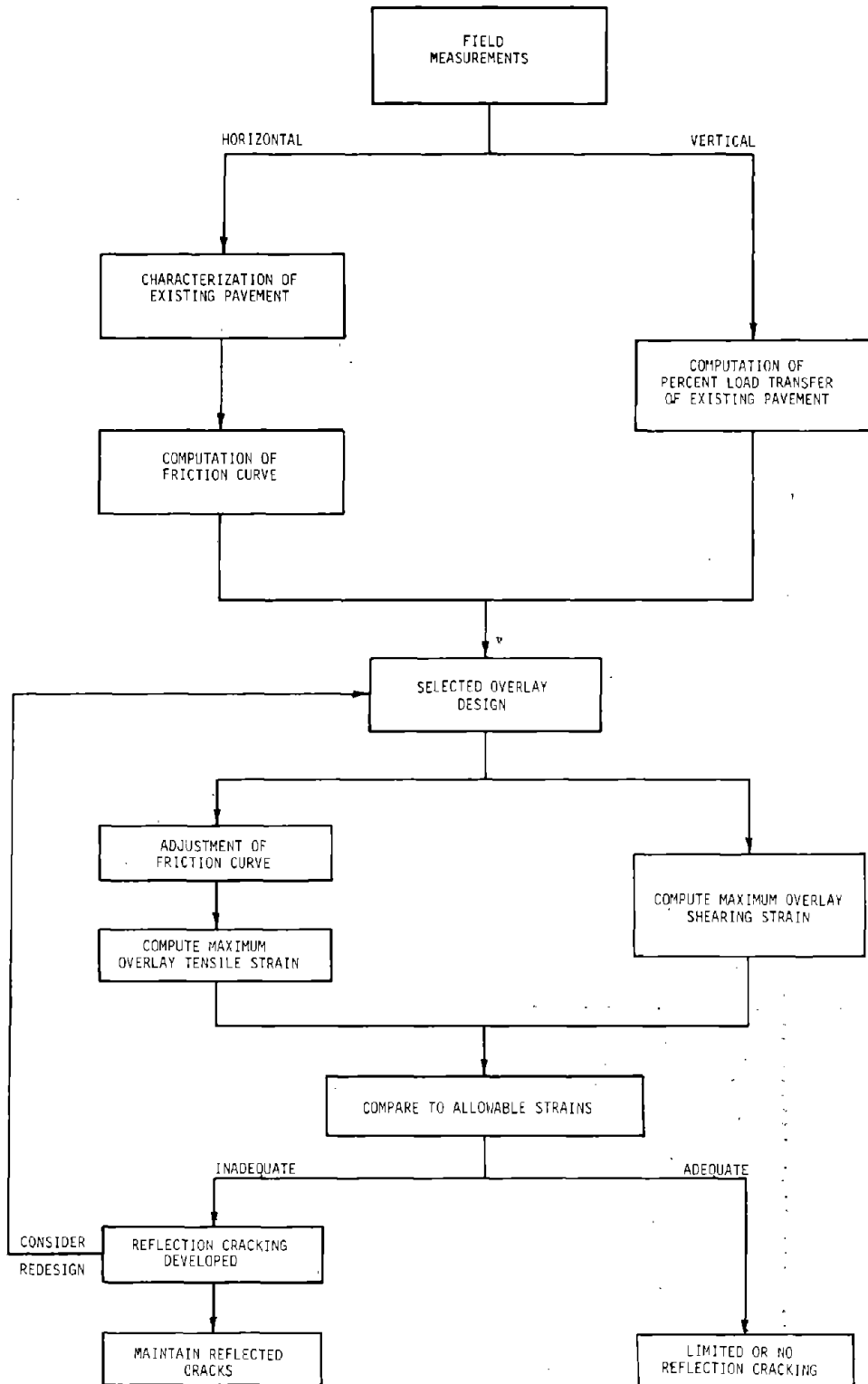


Figure 51. Flow diagram showing the overall procedure to determine if a given overlay design will eliminate reflection cracks resulting from extreme environmental conditions.

Characterization of Existing Pavement. A free concrete slab will expand and contract from its center with a change in pavement temperature (Figure 52, Ref. 87)<sup>1</sup> mathematically explained by equation 23, assuming temperature is constant through slab thickness.

$$Y_{ct} = \alpha_c \Delta T_c \ell \dots \dots \dots 23$$

where:

$Y_{ct}$  = Theoretical concrete movement at one end of the slab due to changes in temperature of the material, inches (1 in=2.54cm)

$\alpha_c$  = Thermal coefficient of concrete; can be obtained from Table 13 (Ref. 88)<sup>2</sup> when not known, in./in.°F (°C=.5554(°F-32))

$\Delta T_c$  = Change in temperature of the material, °F (°C=.5554(°F-32))

$\ell$  = One half the average crack or joint spacing, inches (1 in=2.54cm)

Frictional restraint forces exist between the slab and subbase or subgrade which oppose free slab movement, thereby causing internal forces in the concrete slab. Frictional resistance to movement is not constant but increases with movement at a decreasing rate. These frictional forces are determined and represented by force displacement curves, shown in Figure 53 (Ref. 89)<sup>3</sup>. In some current procedures which evaluate concrete pavements, this force-displacement relationship must be known (Ref. 90<sup>4</sup>, 91<sup>5</sup>). Since the relationship is dependent on material properties, moisture content

---

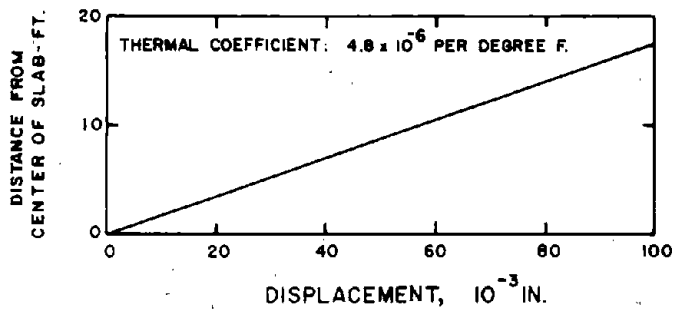
<sup>1</sup>Teller, L. W. and Earl C. Sutherland, "The Structural Design of Concrete Pavements," Bureau of Public Roads, November 1935.

<sup>2</sup>"Mass Concrete for Dams and other Massive Structures," Journal of the American Concrete Institute, Proceedings, Vol. 67, April 1970.

<sup>3</sup>Timms, A. G., "Evaluating Subgrade Friction - Reducing Mediums for Rigid Pavements," Structural Division, U.S. Bureau of Public Roads.

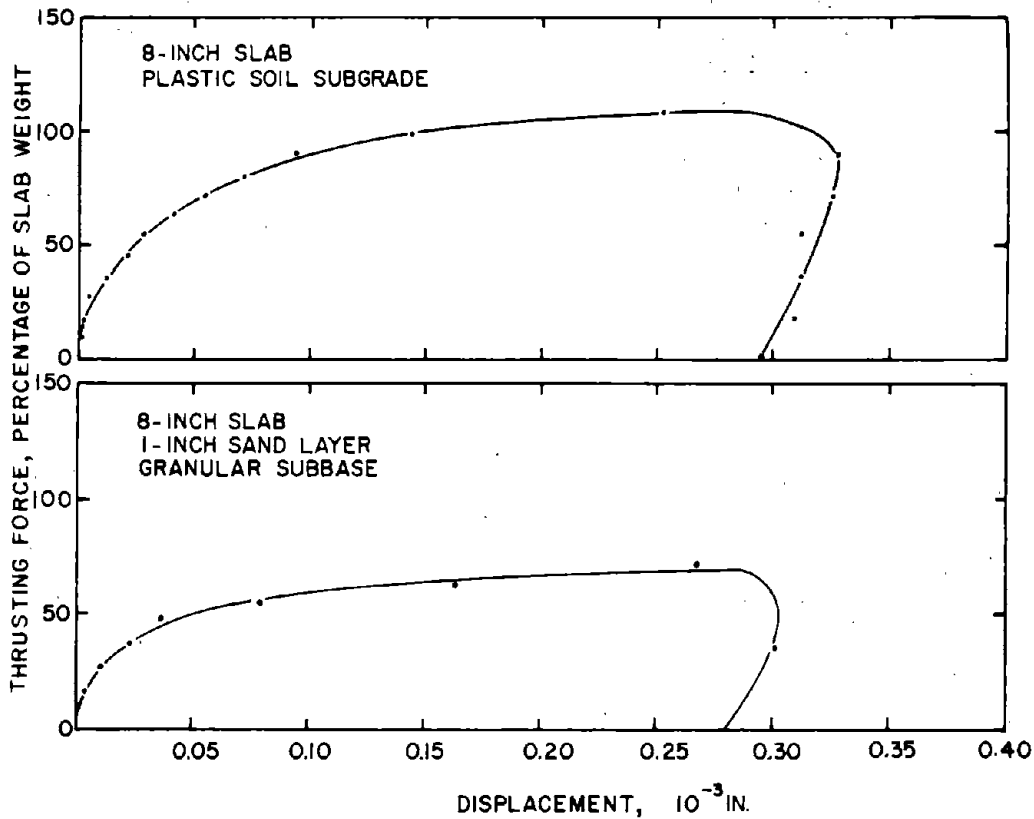
<sup>4</sup>Hudson, W. R., B. F. McCullough, Adan Abou-Ayyash, and Jack Randall, "Design of Continuously Reinforced Concrete Pavements for Highways," Research Project NCHRP 1-15, Center for Highway Research, The University of Texas at Austin, August 1974.

<sup>5</sup>Felipe Rivero-Vallejo and B. Frank McCullough, "Drying Shrinkage and Temperature Drop Stresses in Jointed Reinforced Concrete Pavements," Research Report 177-1, Center for Highway Research, The University of Texas at Austin, August 1973.



1 in=2.54cm  
 1 ft=.305m  
 $c = .5554 (^\circ\text{F}-32)$

Figure 52. Theoretical thermal displacement at various distances from the slabs center due to a temperature change of 100°F. (Ref. 87).



1 in=2.54cm

Figure 53. Typical force-displacement curves for different materials. (Ref. 89).

Table 13. Approximate thermal coefficient of concrete as a function of aggregate type (Ref. 88).

<u>Coarse Aggregate Type</u>	<u>Thermal Coefficient (10<sup>-6</sup> in./in./°F)</u>
Quartz	6.6
Sandstone	6.5
Gravel	6.0
Granite	5.3
Basalt	4.8
Limestone	3.8

1 in=2.54cm  
<sup>o</sup>c=.5554(<sup>o</sup>F-32)

(Figure 54, Ref. 92)<sup>1</sup>, number of movements (Figures 54, 55, 56), and on the roughness of the interface of the two layers, rough estimate of actual field performance can be made. Thus, this procedure estimates the force displacement curve to calibrate the pavement model. In calculating this relationship, it is assumed that the parabolic friction curve (Figure 53) can be estimated with a constant slope line (Figure 57), for simplicity, and concrete movement is continuous throughout its length, for slabs less than 150 feet (45.8m) long (Ref. 93)<sup>2</sup> as mathematically explained by equation 24. For slabs on stabilized subbases, movement may not be continuous in every case and useage of the model for this condition will result in error.

$$Y_c(x) = \alpha_c \Delta T_c \left[ X - \beta X^\beta \right] \dots \dots \dots 24$$

where:

$Y_c(x)$  = Actual concrete movement at a distance X from the slab's center due to a temperature change of  $\Delta T_c$ , inches (1 in=2.54cm),

X = Distance from slab's center to point of observation, inches (1 in=2.54cm)

$\beta$  = Restraint coefficient

.. The  $\beta$  term is a restraint coefficient that represents any force which restricts free concrete movement. It is also a function of slab length due to free end movement of the concrete slab. Therefore it must be assumed that the slab is, and will remain, in static equilibrium at any given period in order for  $\beta$  not to change with time. This value can be determined from field observations of concrete movement over some temperature change. By measuring change in slab length for some temperature differential, knowing the thermal coefficient will permit computation of the  $\beta$  value for the pavement as it exists in the field. A  $\beta$  equal to 1.0 would imply no concrete movement or a fixed system, and a  $\beta$  equal to zero means theoretical concrete movement or a frictionless system.

Equation 24 states mathematically that concrete movement is linear with a change in temperature, as illustrated in Figure 58 for a daily cycle. This restraint coefficient also applies to annual variations of pavement.

---

<sup>1</sup>Teller, L. W. and H. L. Bosley, "The Arlington Curing Experiment," Bureau of Public Roads, Vol. 10, No. 12, February 1930.

<sup>2</sup>Friberg, Bengt F., "Frictional Resistance Under Concrete Pavements and Restraint Stresses in Long Reinforced Slabs," Proceedings, Vol. 33, Highway Research Board, 1950.

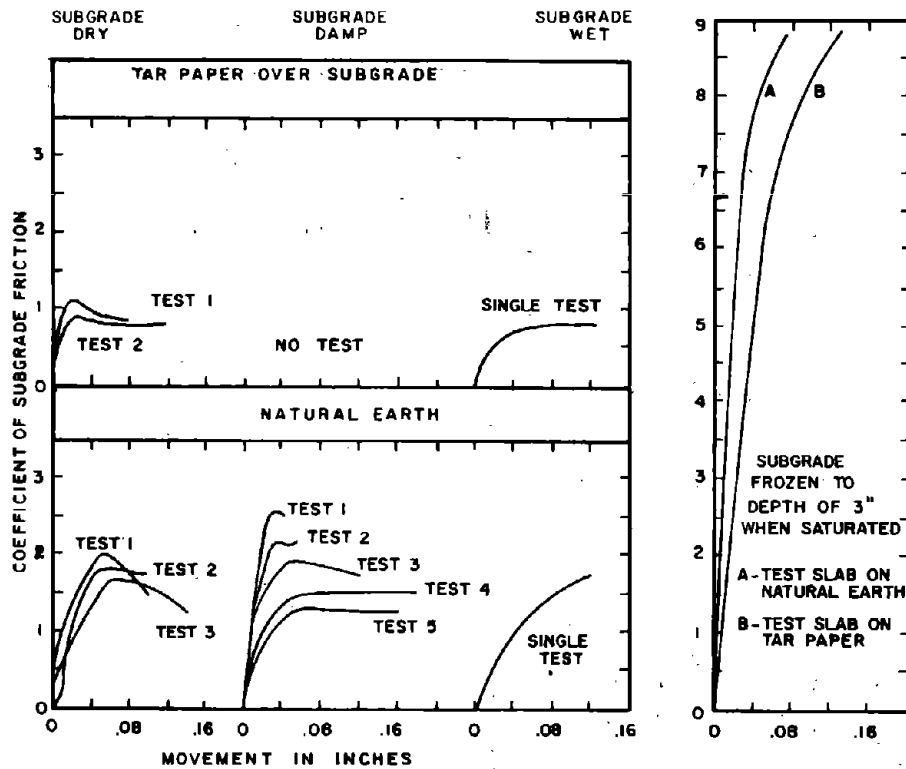


Figure 54. Force-displacement curves for various subgrade conditions. (Ref. 92)

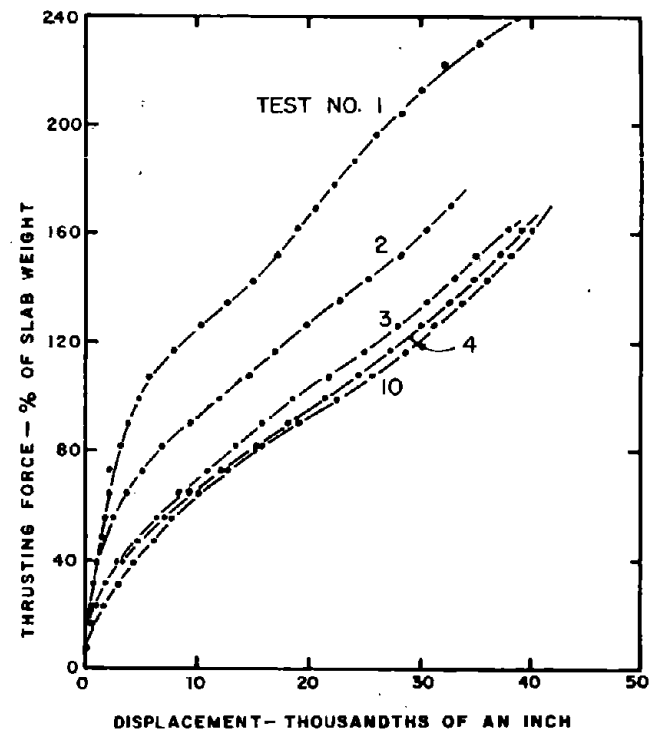
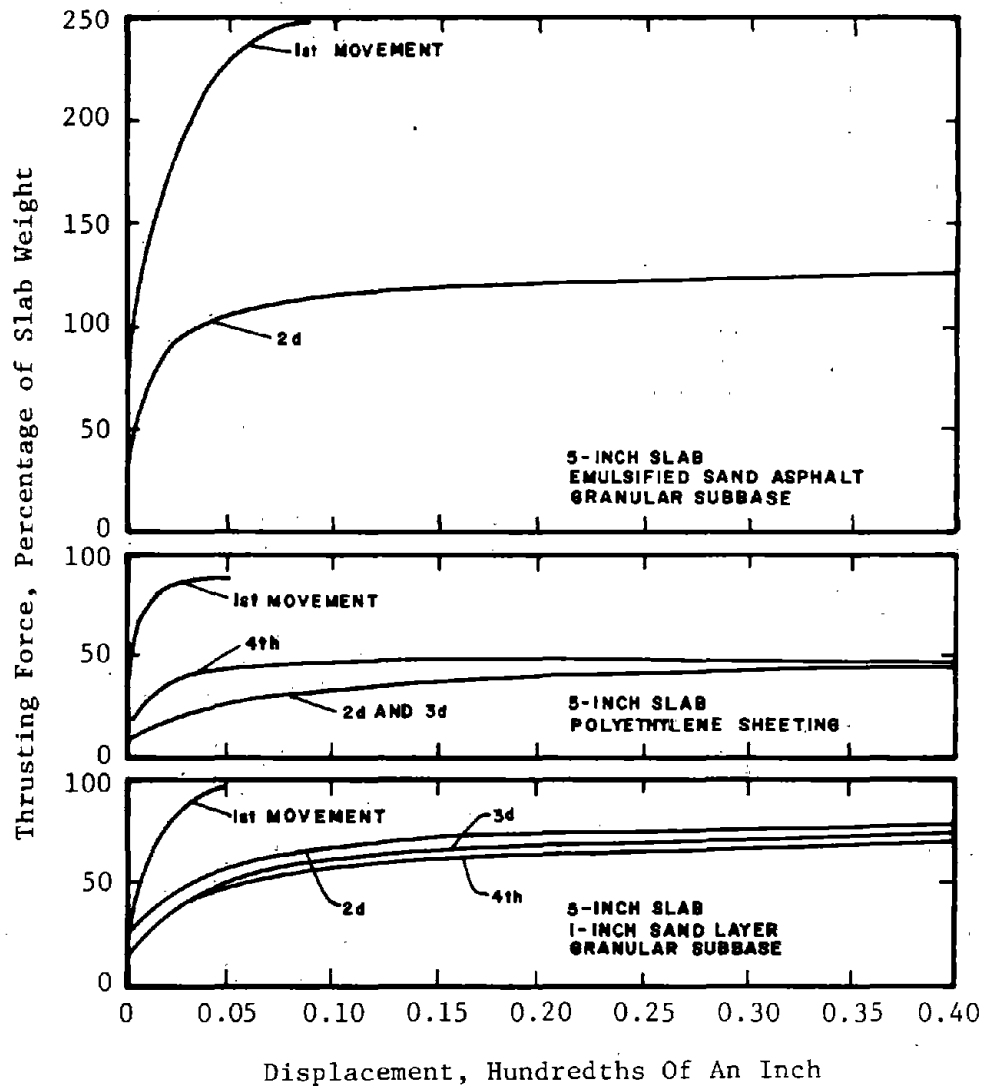


Figure 55. Force-displacement curves for repeated tests on a 6-inch concrete slab. (Ref. 87)

1 in=2.54cm





1 in=2.54cm

Figure 56. Effect of successive slab movements on the force-displacement relationship for various materials beneath the slab (Ref. 89).

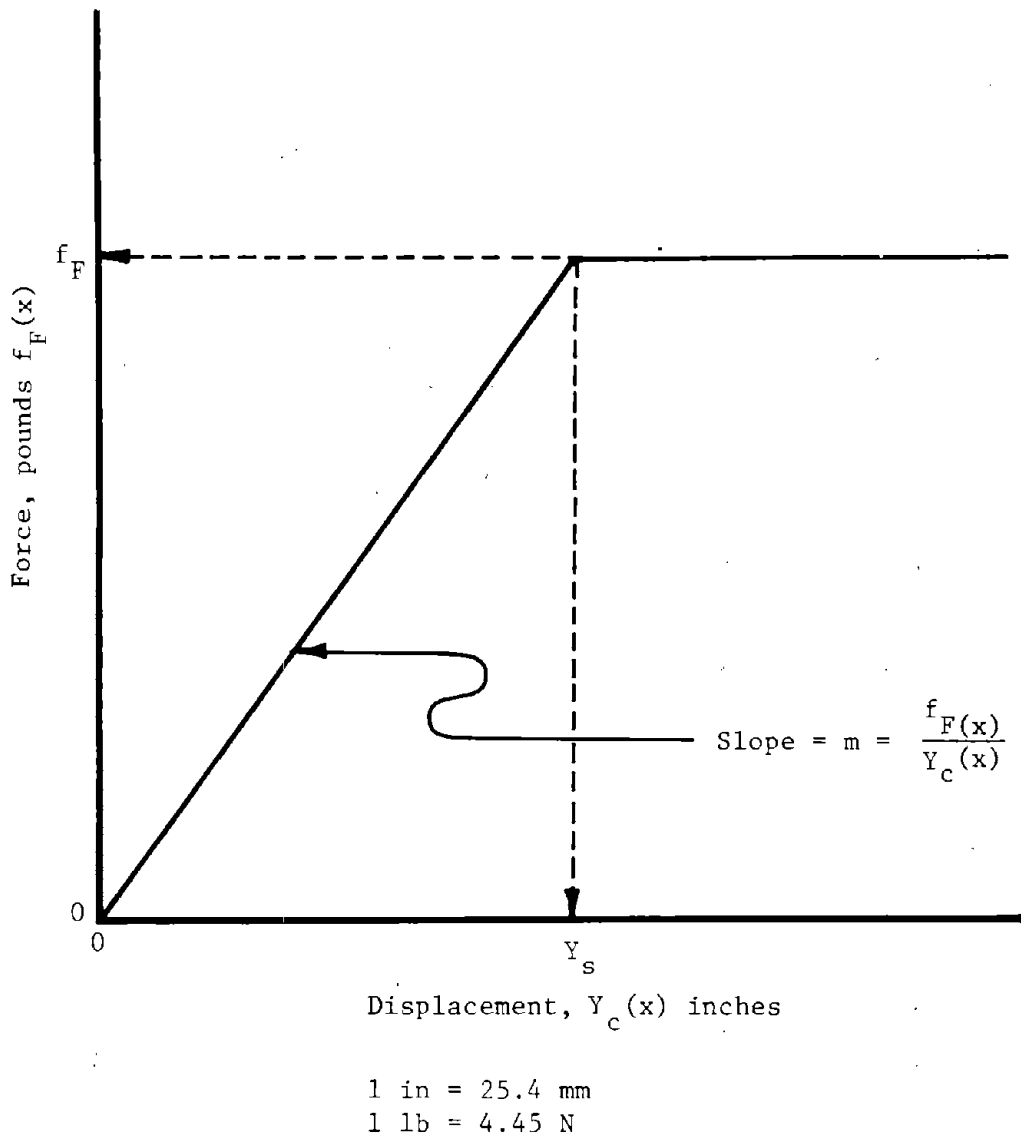


Figure 57. Theoretical force-displacement relationship between concrete slab and underlying layer assumed in the model.

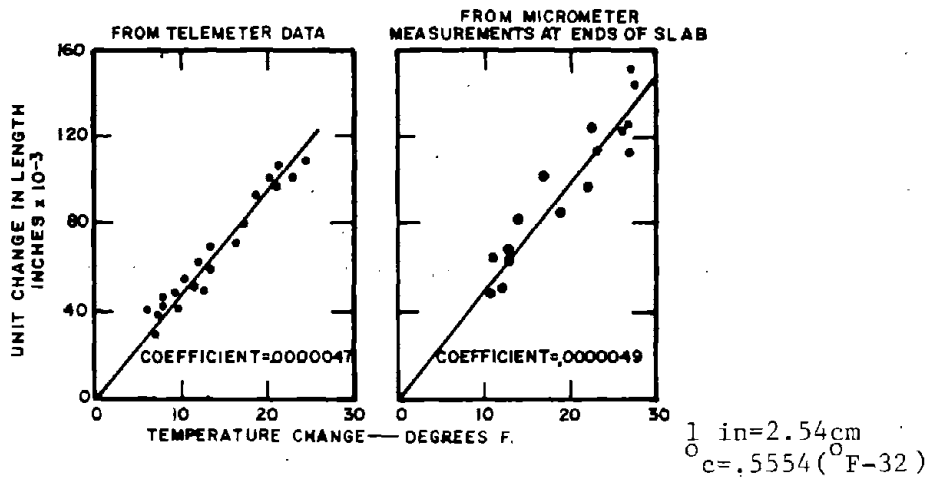


Figure 58. Relationship between temperature change and movement of a concrete pavement for a daily basis (Ref. 87).

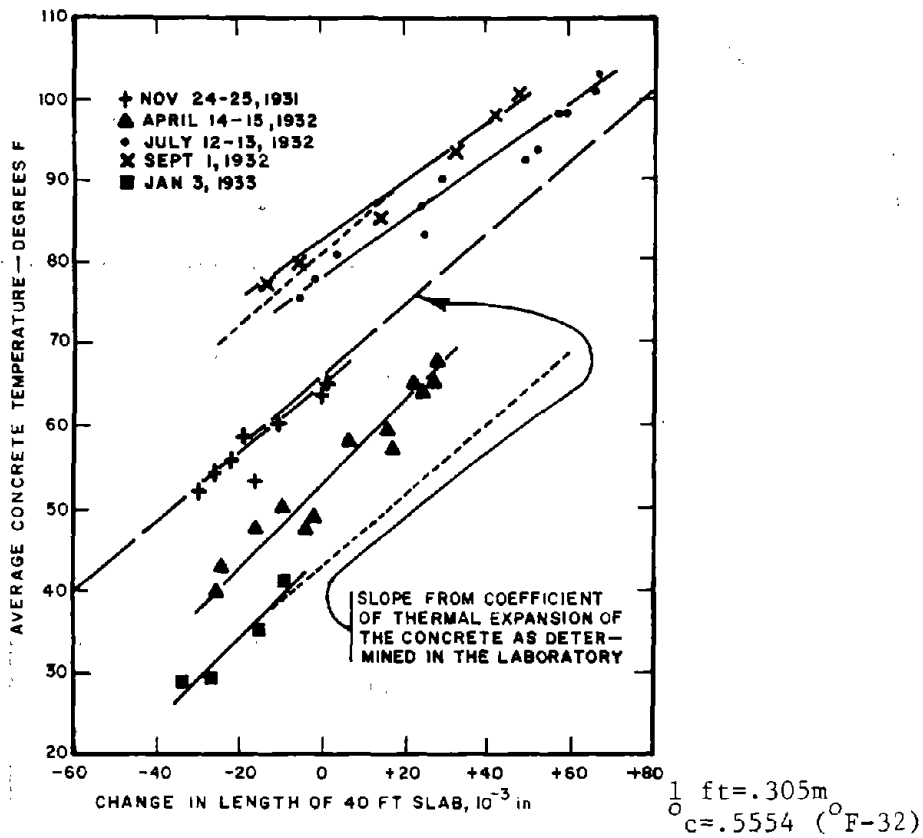


Figure 59. Relationship between average concrete temperature and change in length of a pavement slab for various periods during the year (Ref. 87).

movement, as observed in Figure 59. Annual variations of concrete movement are linear with temperature change, although this relationship may be increased or decreased depending on concrete shrinkage and if incompressibles are allowed to enter the joints (Figure 59). When incompressibles are present, caution must be taken in determining the restraint coefficient since some restrictions to movement may exist that are not considered in the force equations to be developed. Computation of the restraint coefficient characterizes the existing concrete pavement and allows the friction curve to be determined.

Computation of Friction Curve. In evaluating the forces to compute the slope of the friction curve, two different existing pavement types will be considered: (1) plain concrete pavement and (2) reinforced concrete pavement. For developing this model, a plain concrete pavement is referred to as a pavement which contains no steel or contains steel but is uncracked. A reinforced pavement contains steel and is cracked.

Plain Concrete Pavement - If no concrete movement occurs ( $\beta = 1.0$ ), the internal forces in the concrete slab are equal to the theoretical thermal forces which can be expressed by a linear deformation relationship and Hooke's Law.

$$F_c = E_c A_c \alpha_c \Delta T_c \dots\dots\dots 25$$

where:

$E_c$  = Creep modulus of concrete (If the creep modulus is not known, it is suggested that the modulus of elasticity be used; this assumes a purely elastic material), psi (1 psi=6.9kN/m<sup>2</sup>)

$A_c$  = Cross-sectional area of concrete per foot width of pavement, in.<sup>2</sup>/ft. width (1 in.<sup>2</sup>=6.45cm) (1ft=.305m)

When concrete movement does occur, this relaxes or decreases the theoretical temperature forces, resulting in equation 26 for estimating the true concrete force at mid-slab between joints or cracks, assuming continuous concrete movement and static equilibrium.

$$F_{cB} = E_c A_c \left[ \alpha_c \Delta T_c - \frac{Y_c}{l} \right] \dots\dots\dots 26$$

where:

$$Y_c = \frac{Y(T_L) - Y(T_H)}{2} \dots\dots\dots 27$$

$$\Delta T_c = T_H - T_L \dots\dots\dots 28$$

$Y(T_H)$  = Joint or crack width at the high temperature  
 $T_H$  ( $^{\circ}F$ ), inches (1 in=2.54cm) ( $C=.5554(^{\circ}F-32)$ )

$Y(T_L)$  = Joint or crack width at the low temperature  
 $T_L$  ( $^{\circ}F$ ), inches (1 in=2.54cm) ( $^{\circ}C=5.44(^{\circ}F-32)$ )

Shrinkage is not included in equation 26 because it is assumed that all shrinkage has occurred prior to the characterization of the pavement. For a plain jointed concrete pavement the force in the concrete slab must be equal and opposite to the frictional restraint forces (Figure 60) developed through concrete movement. The total friction force is a function of concrete movement and weight which can be basically expressed as:

$$F_i = \int_0^{\ell} f_F(x) dx \dots \dots \dots 29$$

Incorporating Figure 57 into equation 29 results in:

$$F_i = \int_0^A mY_c(x) dx + (f_F)(\ell-A) \dots \dots \dots 30$$

where:

- $m$  = Theoretical slope of the force-displacement curve (Figure 57),
- $A$  = Distance from slab's center to the point at which sliding occurs, assuming  $Y_c > Y_s$ , inches (1 in=2.54cm),
- $f_F = mY_s$  = Friction force at which sliding occurs (Figure 57), lb. (1 lb=.454kg),
- $Y_s$  = Concrete movement at which sliding occurs, inches (1 in=2.54cm).

The value of  $A$  can be determined if the movement at which sliding occurs,  $Y_s$ , is known and applied to equation 24.

$$Y_s = \alpha_c \Delta T_c \left[ A - \beta A^{\beta} \right] \dots \dots \dots 31$$

If  $Y_s$  is not known, Table 14 can be used as an estimate for several materials to permit calculation of  $A$ . Therefore the slope of the force-displacement curve can be determined for the conditions that exist in the field; by equating equations 26 and 30, thus characterizing and calibrating the model to the existing plain concrete pavement.

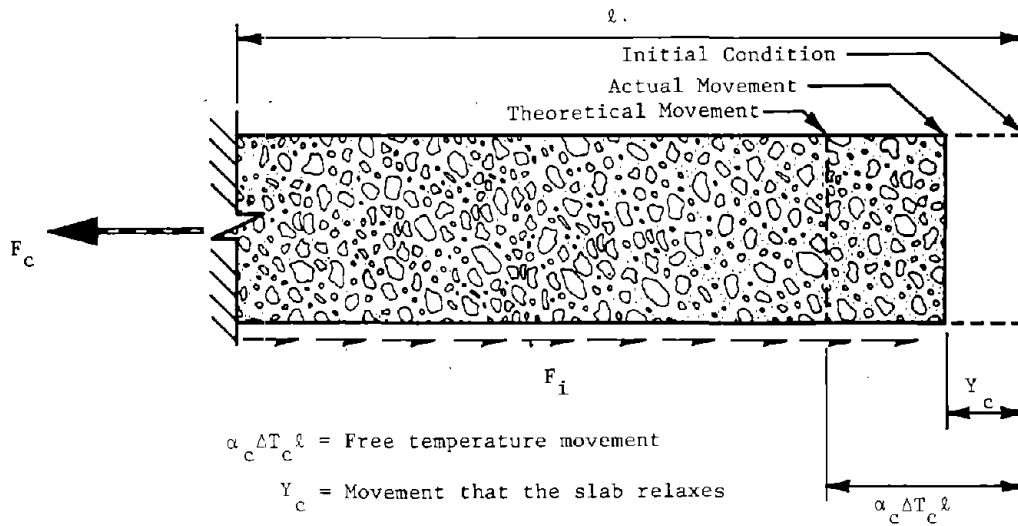


Figure 60. Free body diagram of a plain jointed concrete pavement.

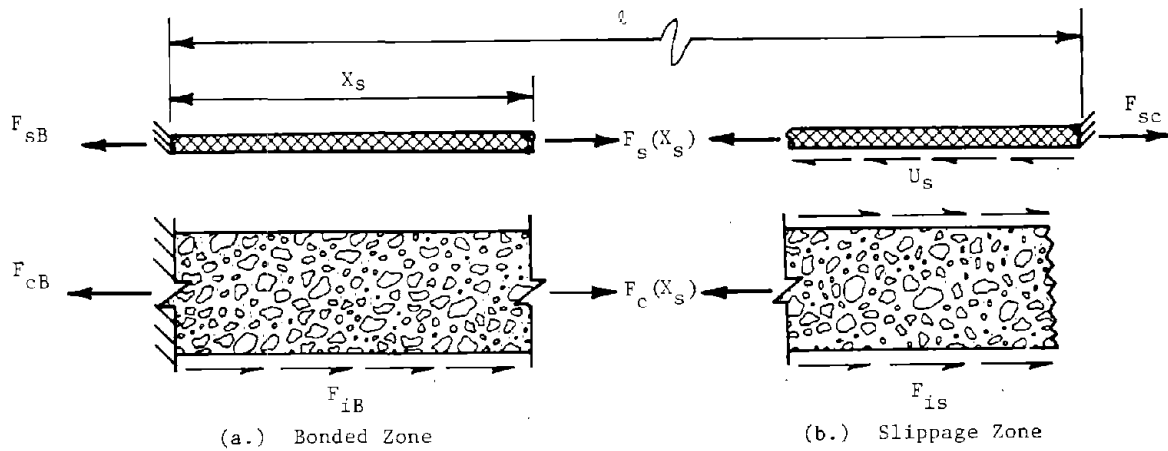


Figure 61. Free body diagram of a cracked reinforced concrete pavement.

Table 14. Movement between the concrete slab and underlying layer at which sliding or constant friction force occurs.

<u>Material</u>	<u>Movement at sliding, inches</u> *
Polyethylene Sheeting	0.02
Granular Subbase **	0.25
Sand	0.05
Sand Asphalt	0.02
Plastic Soil ***	0.05

1 in=2.54cm

\* Values were derived by reviewing as much data on friction curves as available.

\*\* Believed to be moisture dependent but no data are available to be reviewed.

\*\*\* Highly dependent on moisture as illustrated in Figure 54.

Reinforced Concrete Pavement - For a jointed reinforced concrete pavement, steel is only considered in evaluating crack measurements. When joint measurements are evaluated, no steel is input into the model, which assumes a plain concrete pavement. Hence, the following equations only apply to the cracks of a reinforced concrete pavement.

If steel is present, as for a CRC pavement, a more complicated analysis is required to determine the slope of the friction curve. There are basically two regions in a reinforced concrete pavement (Figure 61); (1) the bonded zone, and (2) the region where slippage occurs between the concrete and steel. The forces developed in the steel due to concrete length changes are in essence the net difference in the theoretical movement due to environmental conditions and the actual relief movement experienced by the concrete. Assuming the materials behave elastically, undergo the same temperature differential, and are in static equilibrium, results in a relationship between concrete and steel forces for the bonded region, where slippage does not exist.

$$F_c = F_s \frac{E_c A_c}{E_s A_s} + E_c A_c \Delta T_c (\alpha_c - \alpha_s) \dots \dots \dots 32$$

where:

- $E_s$  = Modulus of elasticity of the steel, psi (1 psi=6.9kN/m<sup>2</sup>),
- $A_s$  = Cross-sectional area of the steel per foot width of pavement, in.<sup>2</sup>/ft. width (1 in<sup>2</sup>=6.45cm)(1 ft=.305m),
- $\alpha_s$  = Thermal Coefficient of the steel, in./in./°F (°C=.5554(°F-32)).

The derivation of equation 32 is given in Appendix A. This equation does not apply to the region where slippage occurs between the concrete and steel.

Near an open crack the concrete has no stress, therefore all of the force is carried by the steel (Figure 61.b). Force in the steel is transferred to the concrete through slippage or bonding forces until the same relaxation strains or movement exist in both materials at some distance,  $X_s$ , from the slab's center. The internal steel force at the crack can be computed assuming a basic linear deformation relationship and Hooke's Law.

$$F_{sc} = E_s A_s \left[ \alpha_s \Delta T_l + \frac{Y_c(X_s)}{l-X_s} + \frac{Y(T_H)}{2(l-X_s)} \right] \dots \dots \dots 33$$



where:

$$\Delta T_1 = T_H - T_1 \dots\dots\dots 34$$

$T_1$  = Lowest temperature the pavement has experienced,  
 $^{\circ}F$  ( $^{\circ}C = .5554$ )  $^{\circ}F - 32$ ).

$\alpha_s \Delta T_1$  = Theoretical thermal strain in steel, in./in (1 in=2.54cm).

$\frac{Y_c(X_s)}{l - X_s}$  = Strain in steel produced by movement of the  
 concrete for temperature  $T_1$ ,

$\frac{Y(T_H)}{2(l - X_s)}$  = Existing strain in the steel prior to characteriza-  
 tion measurements, in./in (1 in=2.54cm).

$X_s$  = Distance from center of two adjacent cracks to the  
 point where slippage occurs between concrete and  
 steel, inches. (1 in=2.54cm).

The reason for using  $\Delta T_1$  instead of the characterization temperature change,  $\Delta T_c$ , is that  $T_1$  is one of the important factors in determining  $X_s$ . Once the bond between concrete and steel has been broken, it is assumed slippage occurs for these points, independent of smaller temperature differentials. Therefore the bonding force, after maximum slippage, is dependent on temperature through concrete movement.

The bonding force that results from slippage and the lowest temperature experienced by the pavement can be determined by:

$$U = \mu p (l - X_s) \dots\dots\dots 35$$

where:

$\mu$  = Bonding stress between the concrete and steel, psi, (1psi=6.9kN/m<sup>2</sup>),

$p$  = Perimeter of the steel per foot width of pavement,  
 in./ft. width (1 in=2.54cm)(1 ft=.305m).

The bonding stress between concrete and steel is a value that is very difficult to determine for reinforced pavements. If it is observed that no fatigue cracking has occurred and all existing cracks are a result of temperature stresses, the bonding stress can be estimated by (Ref. 94)<sup>1</sup>:

---

<sup>1</sup>Bresler, Boris, Reinforced Concrete Engineering, John Wiley & Sons, 1974.

$$\mu = \frac{f_T A_c}{\ell P} \dots \dots \dots 36$$

$f_T$  = Concrete tensile strength, psi (1psi=6.9kN/m<sup>2</sup>)

Derivation of equation 36 is given in Appendix A. If fatigue cracking is present, equation 36 is not applicable and the bonding stress must be estimated or measured. It can be estimated theoretically, using the ACI equation (Ref. 95)<sup>1</sup>.

$$\mu = \frac{9.5 (f'_c)^{1/2}}{d} \dots \dots \dots 37$$

$f'_c$  = Compressive strength of concrete, psi (1psi=6.9kN/m<sup>2</sup>)

$d$  = Diameter of a reinforcing bar, inches (1 in=2.54cm)

Therefore, the steel force at the point where slippage occurs is:

$$F_s (X_s) = F_{sc} - U \dots \dots \dots 38$$

At this point,  $X_s$ , the concrete and steel are assumed to be perfectly bonded, permitting the application of equation 32 to determine the concrete force at slippage.

$$F_c (X_s) = F_s (X_s) \frac{E_c A_c}{E_s A_s} + E_c A_c \Delta T_1 (\alpha_c - \alpha_s) \dots \dots \dots 39$$

Equating forces allows computation of the frictional restraint force in the region where slippage between concrete and steel occur (Figure 61.b), thus defining the slope of the force-displacement curve.

$$F_{is} = \int_{X_s}^A m Y_c (x) dx + f_F (\ell - A) = F_c (X_s) - U \dots \dots \dots 40$$

The concrete force at mid-slab can be determined by using the following equation.

---

<sup>1</sup>Ferguson, Phil M., Reinforced Concrete Fundamentals 3rd Edition, John Wiley & Sons, 1973.

$$F_{cB} = E_c A_c \left[ \alpha_c \Delta T_1 - \frac{Y_c}{l} \right] + F_{cB} (\Delta T = 0) \dots \dots \dots 41$$

where:

$F_{cB} (\Delta T = 0)$  = Concrete force at mid-slab prior to characterization measurements; is derived in Appendix A.

The steel force at mid-slab is computed by applying equation 32:

$$F_{sB} = F_{cB} \frac{E_s A_s}{E_c A_c} + E_s A_s \Delta T_1 (\alpha_s - \alpha_c) \dots \dots \dots 42$$

Therefore different values of  $X_s$  are selected until the forces balance, determining the slope of the force-displacement curve.

$$F_{sB} + F_{cB} = F_i + F_{sc} \dots \dots \dots 43$$

where:

$$F_i = \int_0^A m Y_c(x) dx + f_F (l-A) \dots \dots \dots 44$$

Thus characterizing a reinforced concrete pavement is an iterative procedure, and is dependent on many variables. Basic assumptions were made to simplify the determination of slippage and frictional forces that restrict concrete movement. As stated previously, in evaluating a jointed reinforced concrete pavement that is uncracked, it is assumed that a plain jointed pavement exists for the characterization. Normally the thermal coefficients of concrete and steel are very similar, which would only result in a small error by assuming that no steel exists. If the reinforced pavement is cracked, crack measurements should be treated as a reinforced concrete pavement and joint measurements treated as a plain concrete pavement. From this characterization, the specified overlay design can be evaluated for its effectiveness in reducing reflection cracks. This is accomplished in a two step process; (1) evaluating the change in the frictional restraint forces, and (2) evaluating the overlay design itself.

Adjustment of Friction Curve. When an overlay is constructed over an existing pavement the total weight or normal force of the pavement system is increased. This increase in overburden pressure can have various effects, which are material dependent, on the force-displacement curve, as explained in Appendix A. In order to account for this added overburden pressure, equation 45 was developed to determine the friction curve to be used in the overlay analysis.

$$m_o = m \left[ 1 + \frac{D_o \delta_o}{D_c \delta_c} \right] \dots \dots \dots 45$$

where:

- $m_o$  = Adjusted slope of the friction curve for the overlay analysis,
- $D_o$  = Overlay thickness, inches (1 in=2.54cm)
- $\delta_o$  = Overlay unit weight, pcf (1 pcf=16kg/m<sup>3</sup>)
- $D_c$  = Concrete thickness, inches (1 in=2.54cm)
- $\delta_c$  = Concrete Unit Weight, pcf (1 pcf=16kg/m<sup>3</sup>)

The derivation of equation 45 is given in Appendix A. As explained there, it applies only to non-plastic soils or subbases. For plastic soils it is recommended that the friction curve from the characterization process be used until more information can be obtained.

Overlay Evaluation. In evaluating how the overlay will perform only two conditions will be considered: (1) unbonded, and (2) bonded to the existing concrete pavement.

Unbonded Overlay - An unbonded overlay will be described as an overlay which is separated from the existing concrete pavement by some material which will not transfer movement or forces to the overlay. Such a material of this type could be a sand layer, an unbound granular cushion course or a low friction material. Therefore the only horizontal tensile strains in the overlay are temperature related, and are computed using the theoretical relationship:

$$\epsilon_o = \alpha_o \Delta T_o \dots \dots \dots 46$$

where:

- $\epsilon_o$  = Thermal coefficient of the overlay material, in./in./°F (°C=.5554(°F-32)).
- $\Delta T_o$  = Design temperature change of the overlay material that is expected to occur over the design period, °F (°C=.5554(°F-32)).

The temperature of any pavement varies with depth or thickness. This design temperature change of the overlay material,  $\Delta T_o$ , should represent an average value throughout the overlay thickness. It is computed by subtracting the lowest temperature expected to occur in the design period,  $T_o$ , from a base temperature,  $T_o'$ .

$$\Delta T_o = T_o' - T_o \dots\dots\dots 47$$

The base temperature is material dependent and represents the temperature at which no thermal stresses exist in the overlay. This will vary for different conditions and therefore will be referred to as the ring and ball temperature for asphaltic concrete overlays.

Bonded Overlay - An overlay of this type, transfers movement and forces from the existing surface to the overlay. For this model the resurfacing is assumed to be well bonded to the underlying concrete. This observation was verified at several locations given by Bone, et.al., in Reference 33, due to the action of traffic, roughness of existing pavement, adhesiveness of the asphalt, and in some cases, the presence of a prime coat. Therefore movement of the concrete pavement must be absorbed by the overlay material directly above the joint or crack. This type of overlay can be fully bonded over the entire slab length or the bond may be broken for some specified distance across the joint. For this bonded condition the restraint coefficient, previously determined, is increased for two reasons, (1) increase in frictional restraint forces, and (2) bonding between the overlay and existing concrete pavement. From the previous section on Adjustment of Friction Curve, if the slope of the friction curve is not increased then the restraint coefficient,  $\beta$ , determined from the characterization is equal to the restraint coefficient,  $\beta_u$ , for the unbonded portion of the overlay,  $\beta_u$ . If the slope of the friction curve is increased (equation 45), the restraint value for the unbonded portion must be determined. This is completed by assuming a totally unbonded overlay. Movement of the existing concrete pavement for the unbonded overlay can be described as:

$$Y_c(x) = \alpha_c \Delta T \left[ x - \beta_u x^{\beta_u} \right] \dots\dots\dots 48$$

where:

$\Delta T$  = The design temperature change for the existing concrete pavement, expected to occur over the design period,  $^{\circ}F. (^{\circ}C = .5554(^{\circ}F - 32))$ .

The design temperature change of the existing concrete pavement is determined by subtracting the minimum temperature expected to occur,  $T_c$ , from a base temperature of the concrete pavement,  $T_c'$ .

$$\Delta T = T_c' - T_c \dots\dots\dots 49$$

When an asphaltic overlay is used which can have temperatures of  $300^{\circ}F.$  ( $148.8^{\circ}C$ ) at placement, heat will be transferred to the existing pavement, causing it to expand. This initial movement is absorbed by the overlay before it cures. As the overlay cools or cures it becomes stiffer and more resistant to movement, causing thermal strains to develop. Therefore the base temperature will represent the temperature after overlay place-

ment, assuming all initial expansion and contraction of the existing pavement occurs before the overlay has cured. The minimum temperature expected to occur for the concrete slab is found by using Figure 62 (Ref. 96)<sup>1</sup>, which only pertains to asphaltic concrete overlays. It is assumed that the temperature at the bottom of the overlay (Figure 62) will be equivalent to the temperature of the concrete slab.

The restraint value,  $\beta_u$ , can be determined by using the same equations developed in the characterization. Knowing the slope of the friction curve,  $m_o$ , various values of  $\beta_u$ , are selected until the forces balance. Once the restraint coefficient has been determined for the unbonded portion, the restraint value must be determined for the bonded section  $\beta_B$ . This is accomplished by breaking the pavement into two parts and evaluating the resulting forces existing in each section (Figure 63). Movement of the existing pavement for the bonded overlay condition is expressed as:

$$Y_{cB}(x) = \alpha_c \Delta T \left[ x - \beta_B x \right] \begin{matrix} X_B \\ 0 \end{matrix} \dots \dots \dots 50$$

and

$$Y_{cu}(x) = Y_{cB}(X_B) + \alpha_c \Delta T \left[ x - \beta_u x \right] \begin{matrix} X_{BB} \\ 0 \end{matrix} \dots \dots \dots 51$$

where:

$Y_{cB}(x)$  = Concrete movement where the overlay and existing pavement are bonded (Figure 63.a) at a distance  $x$  from the slab's center, inches (1 in=2.54cm).

$Y_{cu}(x)$  = Concrete movement where the overlay and existing pavement are unbonded (Figure 63.b) at a distance  $X_B + x$  from the slab's center, inches (1 in=2.54cm).

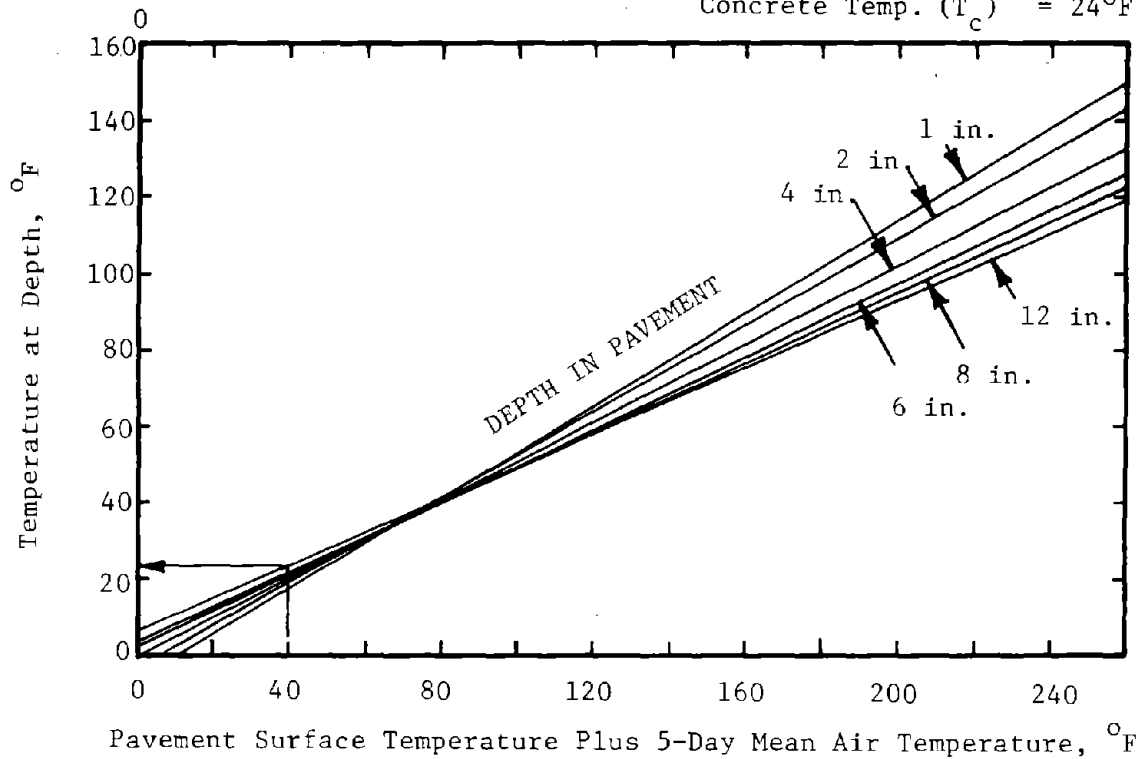
$X_B$  = Distance from slab's center to the edge of the bond breaker, inches (1 in=2.54cm).

$X_{BB}$  = Width of bond breaker on one side of the joint, inches (1 in=2.54cm).

---

<sup>1</sup>Asphalt Overlays and Pavement Rehabilitation, Manual Series #17, The Asphalt Institute, November 1969.

EXAMPLE: 5-Day Mean Air Temp.\* = 30°F  
 Min. Surface Temp. = 10°F  
 40°F  
 Overlay Thickness(D<sub>o</sub>) = 12"  
 Concrete Temp. (T<sub>c</sub>) = 24°F



\*Note: The 5 day mean air temperature can be represented by the lowest average weekly temperature obtained from historical records.

$$^{\circ}\text{C} = .5554(^{\circ}\text{F} - 32)$$

$$1 \text{ in} = 2.54 \text{ cm}$$

Figure 62. Predicting pavement temperatures at the bottom of an asphalt overlay (Ref. 96).

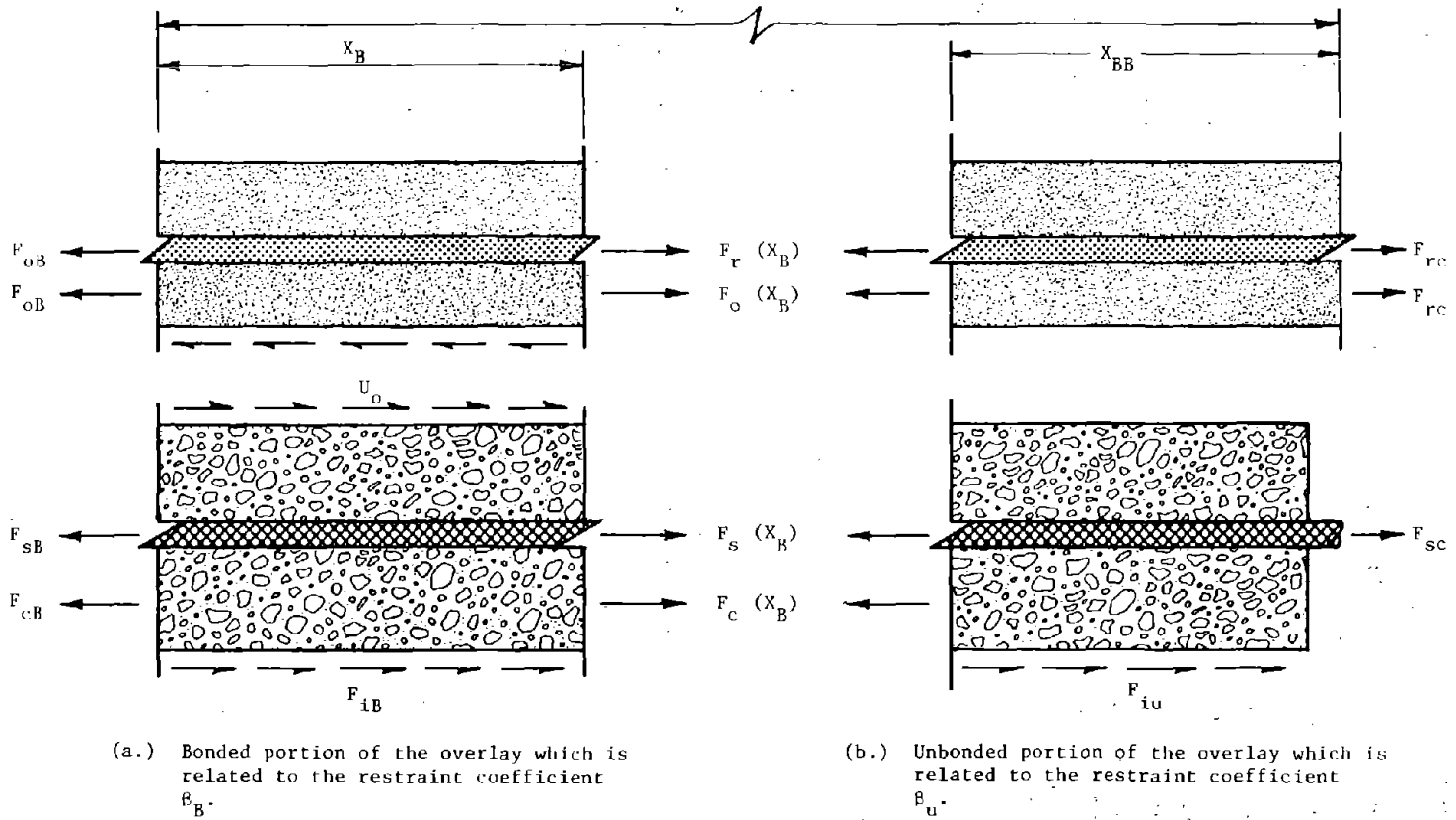


Figure 63. Free body diagram illustrating the forces used in evaluating a bonded overlay for reflection cracking potential.



For various materials and different asphaltic concrete mix designs, the force transferred from the existing pavement to the overlay is related to concrete movement in the form of a force-displacement curve, as between the concrete slab and subbase, or is in the form of bonding forces caused by slippage as between the concrete and steel. No data are available to adequately define a relationship to explain the force transfer between the two materials. Therefore two purely theoretical conditions were used to estimate this relationship. The first assumes, in the section where concrete and overlay are bonded, concrete equals movement of the overlay, and is constant with pavement thickness. Asphaltic concrete is a visco-elastic material that approaches an elastic state at low temperatures. The critical conditions occur at these low temperatures, hence the above assumption was believed to be reasonable. The second uses an average bonding stress between overlay and existing surface, in the section where existing pavement and overlay are bonded, to compute the force transferred between the two layers.

$$U_o = 12 \mu_o X_o \dots \dots \dots 52$$

where:

- $U_o$  = Force transferred between overlay and existing pavement layers, lb./ft. width (1 lb=.454kg)(1 ft=.305m)
- $\mu_o$  = Average bonding stress between the overlay and existing pavement psi; theoretical values for asphaltic concrete overlays are given in Table 15 (1 psi=6.9kN/m<sup>2</sup>).
- $X_o$  = Distance over which slippage occurs between overlay and existing surface in the bonded overlay, inches (1 in=2.54cm).

Table 15 lists values of bonding stress which were estimated using engineering judgment and physical characteristics of existing concrete pavements. These values and the theoretical relationship (equation 52) should be verified from future field studies.

The following relationship can be used to relate forces in the concrete and overlay layers where movement of both layers are equal.

$$F_{oB} = F_{cB} \frac{E_o A_o}{E_c A_c} + E_o A_o \Delta T_o (\alpha_o - \alpha_c) \dots \dots \dots 53$$

where:

- $F_{oB}$  = Force in the overlay material between two adjacent joints or cracks in the existing pavement, lb./ft. width (1 lb=.454kg) (1 ft=.305m),
- $A_o$  = The cross-sectional area of overlay material per foot width of pavement, in.<sup>2</sup>/ft. width (1 in<sup>2</sup>=6.45m) (1 ft=.305m),

Table 15: Theoretical average bonding stress between the existing concrete pavement and asphaltic concrete overlay

Condition of Existing Surface	Average Bonding Stress, psi*
1. Smooth: polished surface; no exposed coarse aggregate.	50
2. Rough: Same as for a smooth surface but some of as-constructed texture remains; small amount of coarse aggregate exposed.	500
3. Very Rough: Worn surface with exposed coarse aggregate; contains aggregate popout; contains surface texture.	1200
4. Jagged: Grooves present; numerous aggregate popouts; coarse aggregate highly exposed.	Very large, Assumed infinite

(1 psi=6.9kN/m<sup>2</sup>)

\* Bonding stresses are theoretical values, which should be verified from future field studies.

$E_o$  = Creep modulus of the overlay material, psi (1 psi=6.9kN/m<sup>2</sup>)

The creep modulus is used due to the long term loading condition and should be determined for various temperatures and each mix design considered. In most cases test values will not exist, therefore Figures 64-66 (Ref. 97<sup>1</sup> and 98<sup>2</sup>) can be used to obtain an estimate. The penetration index (Figure 64), loading time, and temperature difference are used in Figure 65 to determine the stiffness of the bitumen. A loading time of 20,000 seconds has normally been used, although the designer may select a 12 hour loading time due to daily temperature cycles. The temperature difference represents the difference between the Ring and Ball test temperature and the minimum temperature expected to occur,  $T_o$ , for the overlay material. Figure 66 is used to estimate the stiffness of the asphaltic concrete mix,  $E_o$ , given the stiffness of the bitumen.

Equation 26 cannot be applied to determine the concrete force due to the difference in restraint forces of the bonded and unbonded sections. The concrete force at mid-slab can be computed by:

$$F_{cB} = E_c A_c \left[ \alpha_c \Delta T - \frac{Y_c(X_B)}{X_B} \right] \dots \dots \dots 54$$

where:

$Y_c(X_B)$  = Concrete movement at the edge of the bond breaker where the two layers are unbonded, inches.

The frictional force generated by slab movement is:

$$F_i = \int_0^{X_B} m_o Y_{cB}(x) dx + \int_{X_B}^l m_o Y_{cu}(x) dx \dots \dots \dots 55$$

For a reinforced pavement the forces in the steel are computed using:

$$F_{sc} = E_s A_s \left[ \alpha_s \Delta T + \frac{Y_c(X_s)}{l-X_s} + \frac{0.5 Y(T'_c)}{l-X_s} \right] \dots \dots \dots 56$$

---

<sup>1</sup>McLeod, N. W., "Influence of Hardness of Asphalt Cement on Low-Temperature Transverse Pavement Cracking," Proceedings, Canadian Good Roads Association, 1970.

<sup>2</sup>Heukelom, W. and A.J.G. Klomp, "Road Design Dynamic Loading," Proceedings Association Asphalt Paving Technologists, Vol. 33, 1964.

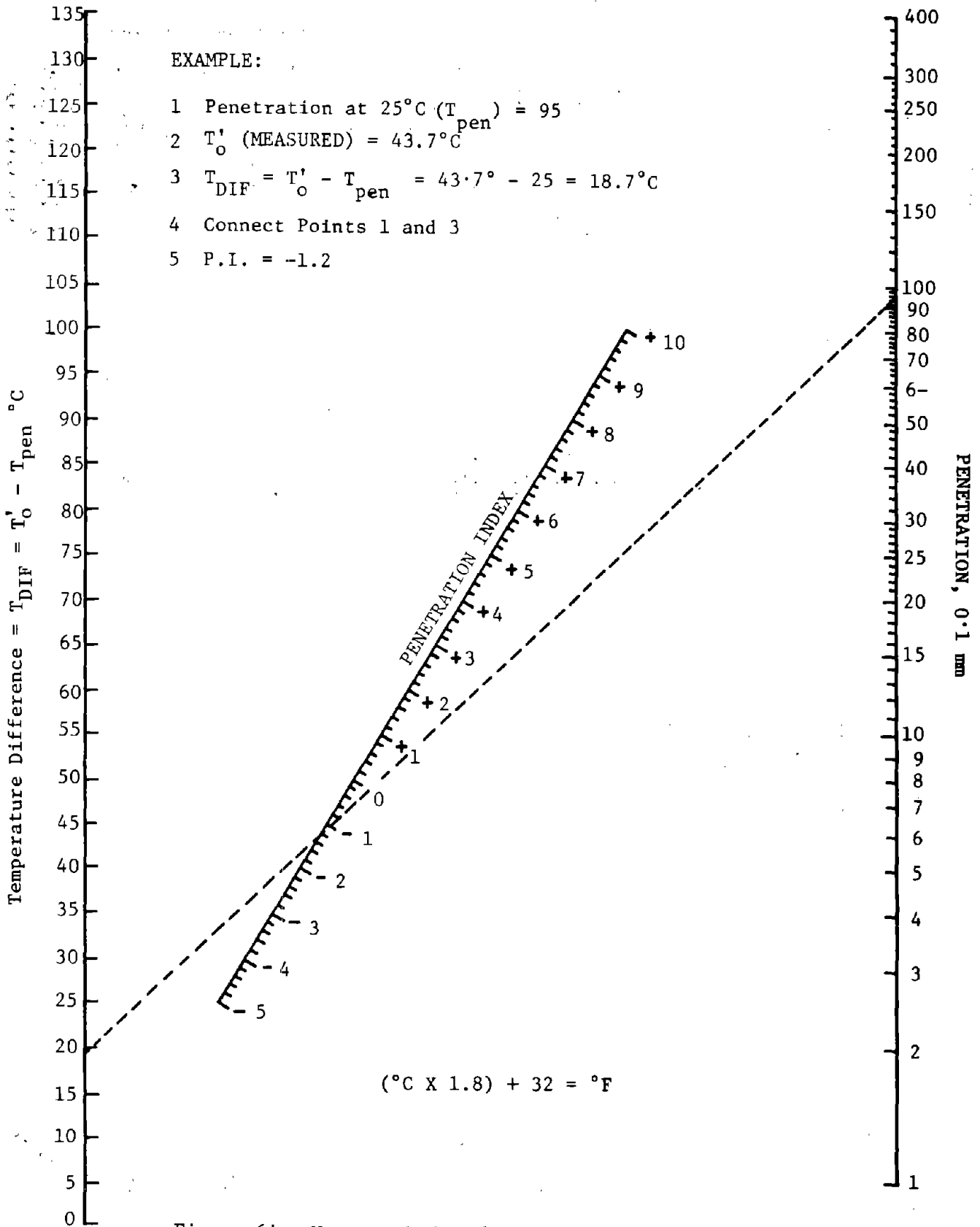
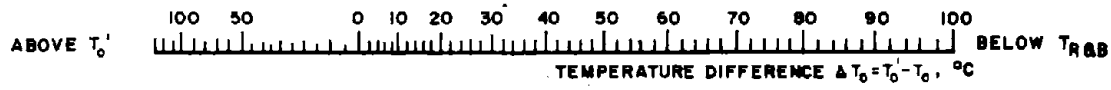
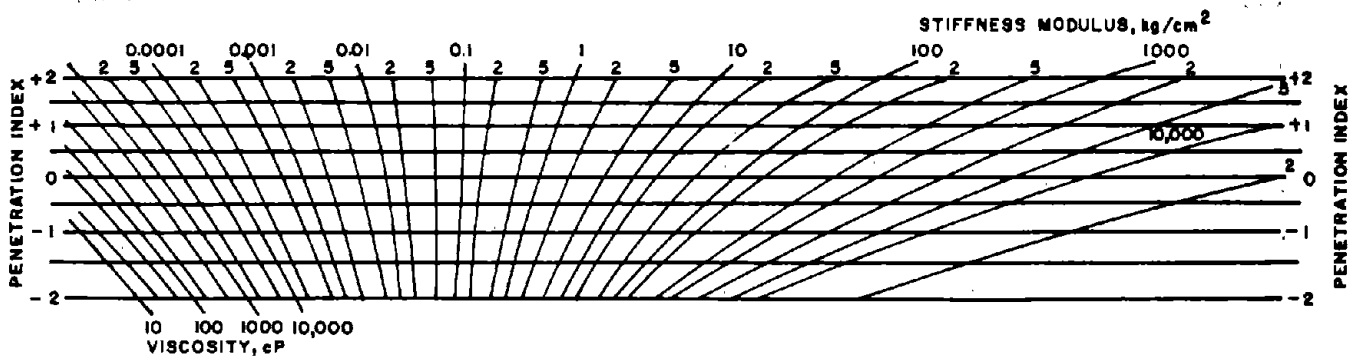


Figure 64. Nomograph for determining Pfeiffer and Van Doormaal's Penetration Index (Ref.97).



$\text{Kg/cm}^2 \times 14.2234 = \text{psi}$   
 $^{\circ}\text{C} = .5554(^{\circ}\text{F} - 32)$

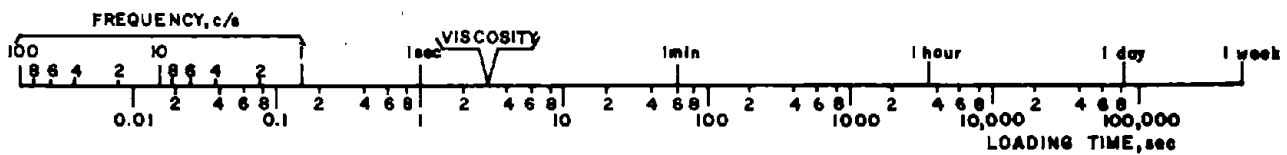


Figure 65. Nomograph for predicting the stiffness modulus of asphaltic bitumens (Ref. 98).

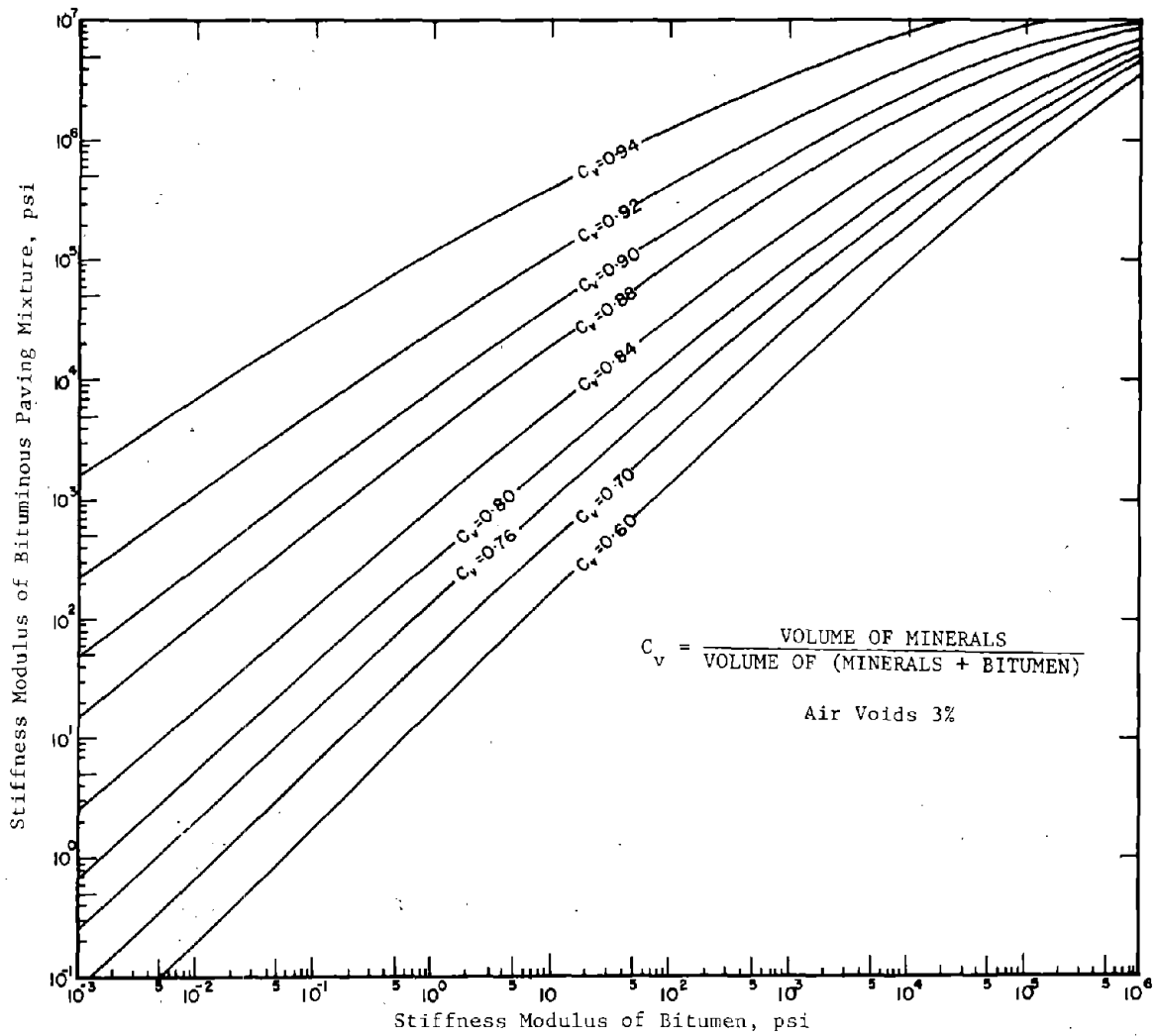


Figure 66. Relationships between moduli of stiffness of asphalt cements and of paving mixtures containing the same asphalt cements (Based on Hukelom and Klomp). (Ref. 98).

1 psi=6.9kN/m<sup>2</sup>

$$F_{sB} = F_{cB} \frac{E_s A_s}{E_c A_c} + E_s A_s \Delta T (\alpha_s - \alpha_c) \dots 57$$

where:

$$Y(T'_c) = Y(T_H) + 2\alpha_c (T_H - T'_c) \left[ \lambda - \beta \lambda^\beta \right] \dots 58$$

$Y(T'_c)$  = Crack width for the base or reference temperature of the existing concrete pavement during overlay placement, inches (1 in=2.54cm).

The force in the overlay at a joint or crack can be determined by:

$$F_{oc} = E_o A_o \left[ \alpha_o \Delta T_o + \frac{Y_c(X_B)}{X_o + X_{BB}} \right] \dots 59$$

If reinforcement exists in the overlay, it is assumed that the overlay material and reinforcement are totally bonded prior to development of cracks. Hence equation 53 can be used to define a relationship between the forces in the overlay and overlay reinforcement ( $F_{rc}$ ,  $F_{rb}$ ). Various values of  $\beta_B$  are selected until the forces balance (Figure 63), determining the horizontal tensile strain in the overlay above the joint or crack.

$$\epsilon_{oc} = \frac{F_{oc}}{A_o E_o} \dots 60$$

This horizontal tensile strain can be computed for various temperatures and compared to an allowable tensile strain to determine if temperature reflected cracks will occur. Using this technique, reflection cracking due to environmental effects and concrete movement can be predicted to provide a basic analytical approach to predict the performance of an overlay system.

#### Differential Vertical Movements

Discontinuities in a pavement structure cause abrupt changes in the deflection basin. If there is a loss of load transfer at a discontinuity, the deflection magnitudes will vary by the amount of load that is not transferred from one slab to another. This results in differential vertical deflections at joints and cracks, described as:

$$w_d = w_L - w_u \dots 61$$

where:

$w_d$  = Differential vertical deflection between two adjoining slabs, inches (1 in=2.54cm)

$w_L$  = Deflection measured at the joint on the loaded slab, inches (1 in=2.54cm)

$w_u$  = Deflection measured at the joint on the unloaded slab, inches (1 in=2.54cm)

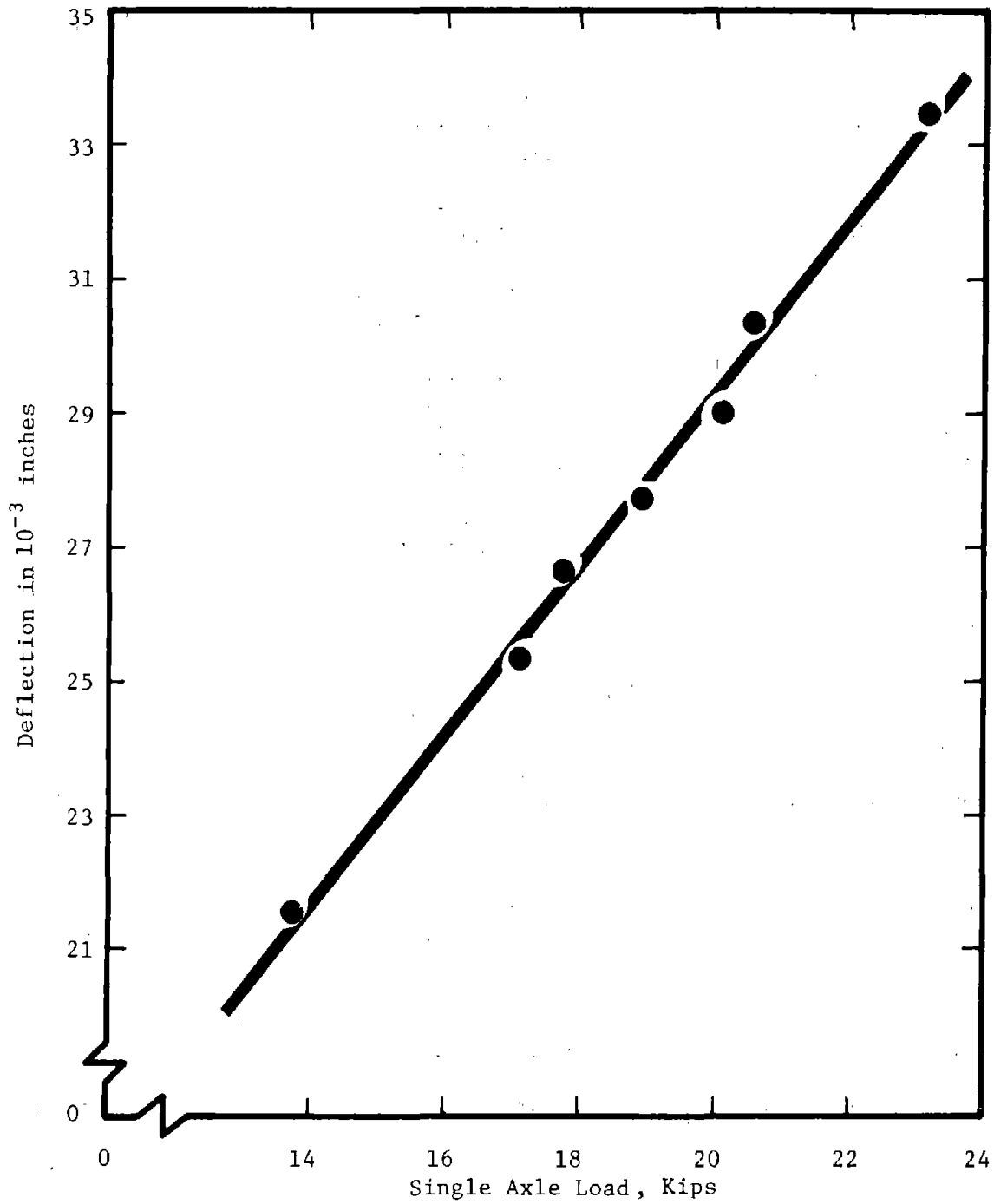
Differential vertical movements are shown to be related to reflection cracking in Table 7. These failures are caused by a shear distortion rather than a tensile or flexural distortion because the force is applied at a discontinuity (joint or crack). Field measurements of deflection magnitudes and differential deflections between loaded and unloaded slabs are obtained to predict the load an overlay must carry in shear to resist cracking. The differential deflections can be measured using a Dynaflect, Benkleman Beam (Ref. 41), or a differential deflection device that uses a dial gage to measure relative movements between two adjacent slabs (Ref. 40).

For the cases where there are no differential vertical movements, i.e. full load transfer, the shear deformation across the joint or crack is zero. No reflection cracks will occur for this condition. When differential movements do exist, there is load the overlay must carry in pure shear. For the evaluation of these shearing forces, it must be assumed that load and deflection at joints have a linear relationship (Figure 67, Ref. 99)<sup>1</sup>. This may not be the case for small loads or loads of different configurations. Therefore, caution must be taken in defining the percent load transfer across the joint for a design load that is based on a smaller characterization load, e.g. a Dynaflect. As illustrated by Figure 68, deflection increases as crack width increases, which implies there is less load transfer for wider cracks. This can be explained by reviewing Figure 69. Joints, which use keyways or aggregate interlock as a means of load transfer, require a certain amount of deflection to take place in order for load to be transferred from one slab to another. Therefore, when using a small load, as the Dynaflect, there may be an over estimate of the actual shearing force, produced by the design load, the overlay must withstand. Joint widths vary during the year as temperature varies, due to thermal movements of the concrete pavement (Figure 59). Therefore the percent load transfer can also be temperature dependent, and must be considered in design. The load transfer of a joint is estimated by:

---

<sup>1</sup>McCullough, B.F., and Harvey J. Treybig, "Determining the Relationship of Variables in Deflection of Continuously Reinforced Concrete Pavement," Departmental Research Report Number 46-4, Texas Highway Department, Aug. 1965.





1 kip=454kg  
 1 in=2.54cm

Figure 67. Example of deflection versus a single axle load (Ref. 99).

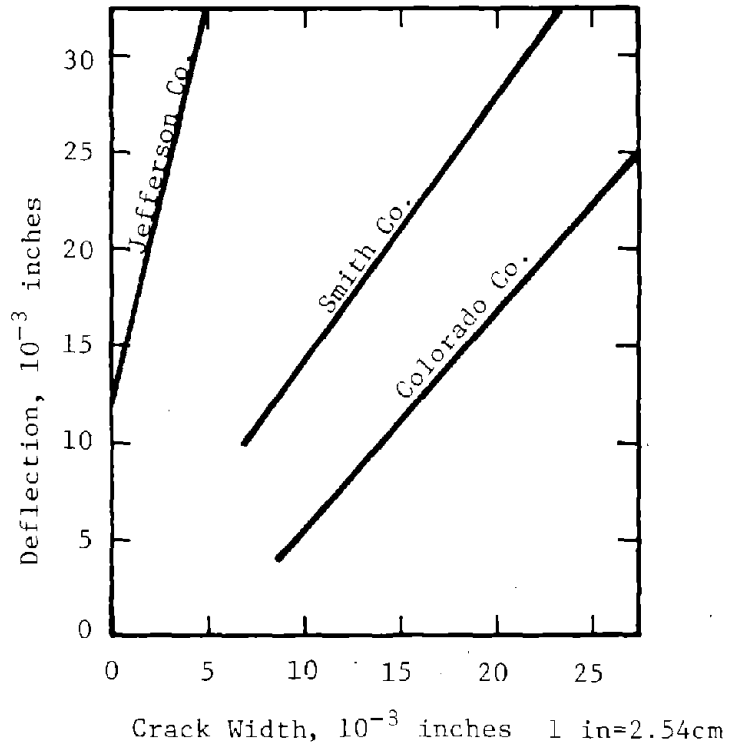
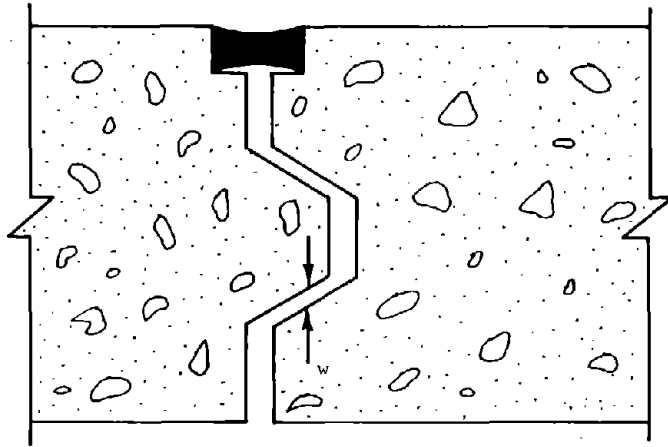
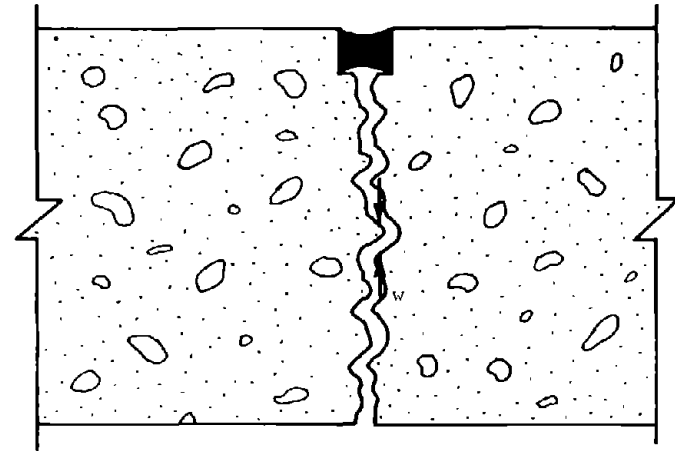


Figure 68. Comparison of regression lines (Deflection versus crack width) for three projects in Texas (Ref. 99).

$w$  = Deflection that must occur in order to transfer load from one slab to another.



(a.) Keyway used as the load transfer.



(b.) Aggregate interlock used as load transfer.

Figure 69. Vertical movements at a joint or crack are dependent on temperature

$$L_T = 1 - \frac{W_d}{W_1} \dots \dots \dots 62$$

Therefore the maximum shear force in the overlay due to a loss of load transfer is:

$$P_o = L_D (1 - L_T) \dots \dots \dots 63$$

where:

$L_D$  = The design load, lb.(1 lb=.454kg).

$P_o$  = Shear force in the overlay, lb.(1 lb=.454kg).

This maximum shear will occur under the load or where the maximum deflection occurs, and will vary transversely along with the joint according to the deflection basin. The deflection basin is dependent on many properties; existing pavement stiffness, underlying support layers, material properties, presence of voids, etc. Therefore, it becomes very difficult to accurately predict the shearing force distribution with pavement width unless the deflection basin is measured. For existing rigid pavements it is assumed that constant shearing forces exist over the width of the applied load, recognizing the effect of the deflection basin. The maximum shearing stress in the overlay can then be determined.

$$T_o = \frac{P_o}{D'_o W} \dots \dots \dots 64$$

where:

$W$  = The total width over which the load is applied, inches (1 in=2.54cm)

$T_o$  = Shearing stress in the overlay, psi (1 psi=6.9kN/m<sup>2</sup>)

$D'_o$  = Effective overlay thickness, inches (1 in=2.54cm)

$D_o$  is the thickness of the overlay itself. When reinforcement exists in the overlay or when a level-up or intermediate layer exists, the total effective overlay thickness  $D'_o$ , can be determined using:

$$D'_o = D_o + \sum_{i=1}^n D_i \frac{E'_i}{E_o} \dots \dots \dots 65$$

where:

$E'_o$  = Dynamic modulus of the overlay material, psi (1 psi=6.9kN/m<sup>2</sup>)

$E'_i$  = Dynamic modulus of layer i, psi (1 psi=6.9kN/m<sup>2</sup>)

$D_i$  = Thickness of layer i, (when reinforcement is used areas should be used) inches (1 in=2.54cm),

n = Number of layers

For pavements which contain good load spreadability, the shearing stress computed using equation 64 will be a conservative estimate. The shearing strain can be computed using:

$$\gamma_o = \frac{T_o}{G_o} \dots \dots \dots 66$$

where:

$\gamma_o$  = Shearing strain in the overlay, in./in.(1 in=2.54cm).

$G_o$  = Shearing modulus of the overlay material, psi (1 psi=6.9kN/m<sup>2</sup>)

The shearing modulus is assumed to be related to the dynamic modulus by:

$$G_o = \frac{E_o}{2(1+\mu_o)} \dots \dots \dots 67$$

where:

$\mu_o$  = Poisson's Ratio of the overlay material

Therefore substituting equation 67 into equation 66 results in a relationship for the shearing strain of the overlay material.

$$\gamma_o = \frac{2T_o(1+\mu_o)}{E_o} \dots \dots \dots 68$$

Very little data exist on the influence these localized shearing strains have on reflective cracking. It is suggested that they can be very detrimental and should be considered in design. Therefore, an analytical procedure to estimate the magnitude of shearing forces was developed. Through this procedure data can be used to adequately determine the importance of this shearing mode failure, from a loss of load transfer, in causing reflective cracks to develop.

## Summary

This model provides a rational procedure for evaluating an overlay's capability to withstand reflection cracks resulting from extreme environmental conditions. It evaluates two basic failure modes (tensile and shear strains) to determine if an overlay design will resist the stress/strain concentrations occurring at joints and cracks. The model was developed so that it could be combined with the fatigue concepts used in determining the overlays thickness. As a result fracture mechanics was not used in the evaluation, as the procedure developed by Chang, et al in Ref. 100<sup>1</sup>. These fatigue concepts may be combined with the model, after the procedure has been physically checked, by using the strain transformation equations. This then will enable the overall procedure to adequately predict the service life of an overlay system. Although a model has been presented, in many cases there may be economic or physical restraints that prevent the construction of an adequate overlay design to eliminate reflection cracks. For these conditions consideration should be made to maintain these cracks that are inevitably going to occur with time.

## Maintaining Reflection Cracks

In past years many miles of old PCC pavements have been resurfaced with asphaltic concrete. This type overlay initially provides an excellent riding surface, while adding little load-carrying capacity to the existing concrete pavement. Unfortunately, many of these pavements have been deteriorating due to the presence of reflected cracks. Once the overlay is fractured general erosion occurs which severely affects performance and requires further and costly maintenance. Therefore techniques for corrective measures for maintaining and treating these cracks, which already exist, must be found to extend the service life of the pavement with as low a cost as possible. Also if for any given overlay design a means of preventing reflection cracks can not be found, then an efficient means of treating these cracks must be developed so that the service life of the overlay can be maintenance free for as long as possible. To properly treat and correct these reflected cracks that have occurred in asphaltic concrete overlays, the process of deterioration must be identified.

## Deterioration of Overlay

Initially reflected cracks, whether caused by horizontal or differential vertical movements, are unobtrusive. As the pavement experiences more traffic applications and lower temperatures, the cracks widen,

---

<sup>1</sup>Chang, Hang-Sun, Robert L. Lytton, and Samuel H. Carpenter, Prediction of Thermal Reflection Cracking in West Texas," Research Report No. 18-3, Texas Transportation Institute, Texas A&M University, December 1975.

permitting water and foreign material to enter the pavement system. When this happens, raveling occurs at the crack faces and on its underside. Raveling of asphaltic concrete pavements is the progressive separation of aggregate particles from the pavement. Usually the fine aggregate comes off first and leaves small pock marks at the cracks edge (Ref. 33).

As the erosion continues, larger particles are broken free by traffic and the crack edges become rough and jagged. Once raveling reaches a severe enough condition, edge or "crack" deterioration occurs. Edge or "crack" deterioration is defined as pieces of the overlay which have been loosened and removed by traffic at the crack faces (Ref. 40). When reflected cracks reach this condition, they not only produce an unsightly highway, but frequently are sufficiently wide and rough to cause thumping under traffic (Ref. 33). Their maintenance presents a special and difficult problem.

#### Corrective Measures

Before the reflected cracks reach a stage where raveling becomes severe or edge deterioration occurs, corrective measures must be taken. Three different methods have been tried to control the erosion that occurs at reflected cracks: (1) sealing the cracks, (2) sawing and sealing joints, and (3) use of the heater-scarification process. The mechanism causing reflected cracks will determine if the overlay can be properly maintained to retain its initial performance. Regardless of the cause, these cracks should always be sealed to prevent water and foreign material from entering the pavement system resulting in further damage.

Sealing Cracks. From a previous study conducted by Tons and Roggeveen on sealants (Ref. 101)<sup>1</sup>, it was observed that out of 26 sealing compounds only four were adequate for successfully sealing 1/4 inch (.64cm) cracks and no sealants were adequate for 1/8 inch (.32cm) cracks. Therefore, simply sealing the cracks will help retard the progress of deterioration but it does not offer a long term solution (Refs. 38, 101, 102<sup>2</sup>). Crack sealants for asphaltic concrete pavements are given in a manual by the Asphalt Institute (Ref. 103)<sup>3</sup>, although opinions vary as to the value of sealing cracks. Overfilling of the cracks should be avoided since it will produce

---

<sup>1</sup>Tons, Egon and Vincent J. Roggeveen, "Field Testing of Materials for Sealing Cracks and Joints in Bituminous Concrete Resurfacings," HRB Bulletin No. 166, Highway Research Board, 1957.

<sup>2</sup>Clary, A. G., "Sealing Cracks in Bituminous Pavements," A paper presented at the AASHO 55th Annual Meeting in Philadelphia, October 1969.

<sup>3</sup>"Asphalt in Pavement Maintenance," Manual Series 16, The Asphalt Institute, December 1967.

pavement roughness and an unsightly appearance (Refs. 36, 38), but a slight overlap of the sealer should be permitted along the cracks edge. This will help prevent adhesion failures (Ref. 101). Also, the surface of the sealant should be sprinkled with a light sand, cement, or limestone to prevent traffic pickup (Refs. 38, 103).

Sawing and Sealing Joints. In searching for methods to extend the maintenance-free life of the asphaltic concrete overlay, there have been studies to determine if sawing and sealing joints would be sufficiently efficient to justify the added cost (Ref. 32, 38, 104<sup>1</sup>, 105<sup>2</sup>). It was reported by Wilson in Ref. 105 that crack control joints are anticipated to provide 5 to 10 years of maintenance free service, which could begin to justify the extra cost. This method can be used for cracks which already exist, or if reflection cracking is predicted for an overlay design, joints can be sawed in the overlay matching joints or cracks in the existing PCC pavement. Cracks which are 1/8 inch (.32cm) or greater, should be routed to a minimum width of between 3/8 to 1/2 inch (.92 to 1.27cm) and sealed (Ref. 36). Where reflection cracking has not occurred, but is inevitable, 1/4 inch (.63cm) grooves should be sawed in the asphaltic concrete overlay and then sealed. Theory and tests indicate that an approximately square sealant reservoir should be required to give the best performance (Ref. 36,105). It is very important that joints in the asphaltic concrete overlay be sawed directly over the existing joints in the PCC pavement, otherwise otherwise other distress mechanisms will develop resulting in early failure of the joint.

Heater-Scarification Process. If the edge or "crack" deterioration has advanced to a condition where large aggregate particles are being broken-up and removed by traffic, then a process known as heater-scarification may be warranted if an additional overlay cannot be placed for some reason. This process which has been used in various experimental projects (Refs. 37, 39), opens up the top of the asphaltic concrete overlay allowing some additive to penetrate and rejuvenate the overlay. The remolded portion destroys the old crack pattern in the overlay, but will not prevent the joints or cracks in the original PCC pavement from re-reflecting. Therefore once the cracks reflect to the surface sealing or sawing and sealing joints must be accomplished so that the edge deterioration will be significantly reduced resulting in a longer service life.

---

<sup>1</sup>Tons, Egon, "Reflection Crack Sealing," Research Report 26, Joint Highway Research Project, Massachusetts Institute of Technology, June 1958.

<sup>2</sup>Wilson, J. D., "Crack Control Joints in Bituminous Overlays on Rigid Pavements," HRB Bulletin 322, Highway Research Board, 1962.



## Differential Vertical Movements

The deterioration at reflection cracks resulting from differential vertical movements will be difficult to control economically. Since these cracks are caused by a loss of load transfer of the underlying layers, it becomes apparent that simply sealing cracks or joints cannot be a long term solution. This stems from the effect of an impact loading on the adjacent face of the crack, which loosens or crushes the aggregate (Figure 70). As the differential vertical deflections become larger, the greater the impact force; hence for large differential deflections all of the methods discussed above will offer only short term solutions.

## Horizontal Movements

The deterioration at cracks resulting from horizontal movements will be much easier to control. Since these cracks are caused by only horizontal movements of the underlying slab, there are no impact loadings on the edge of the crack. It then becomes economically feasible to seal cracks and joints which have not reached the edge deterioration stage. For cracks which have severe deterioration, the heater-scarification process could be used to remold the overlay.

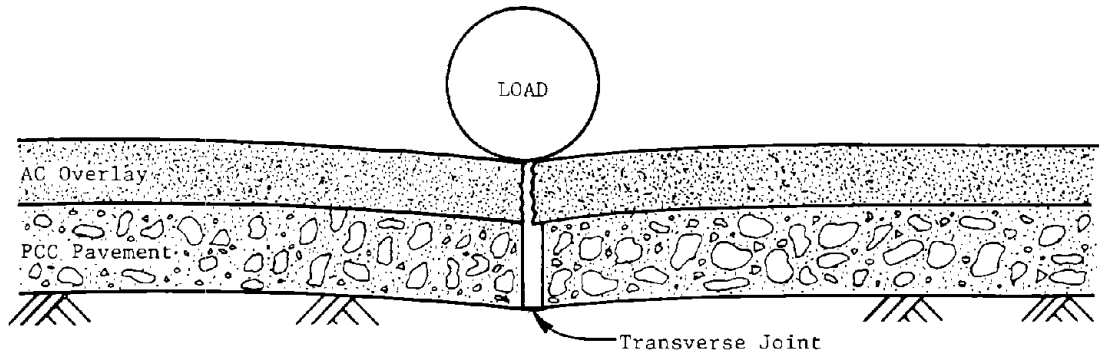
Therefore, cracks resulting from horizontal movements or small differential deflections can be treated to extend the service life of a pavement. There is no information available which could separate small and large differential deflections. Until the information can be obtained, it is left to the designer to decide if reflected cracks, resulting from differential vertical movements, can be economically treated to extend the overlay's service life.

## Guidelines for Data Collection and Analysis

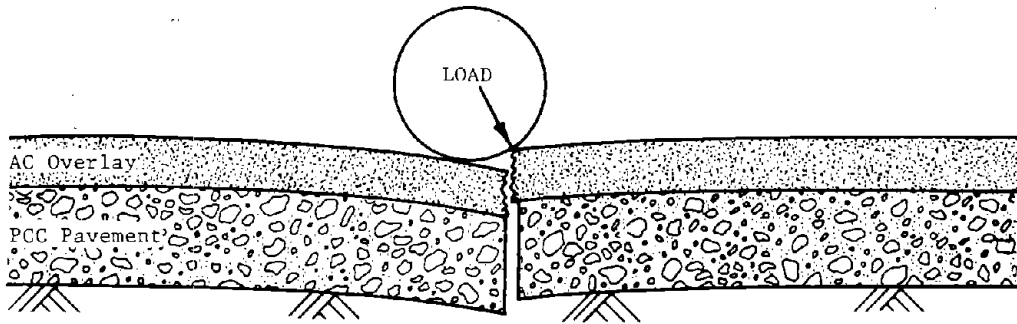
Equally important to the development of a theoretical reflection cracking model is the collection and evaluation of field observations. In order to achieve a sound basis for design, certain physical measurements are required to calibrate the model to an in-field condition. These include crack and/or joint movement, crack and/or joint spacing, and differential vertical deflection. The following will present criteria for collecting and analyzing this data to determine the characterization inputs for the model.

### Crack and/or Joint Spacing

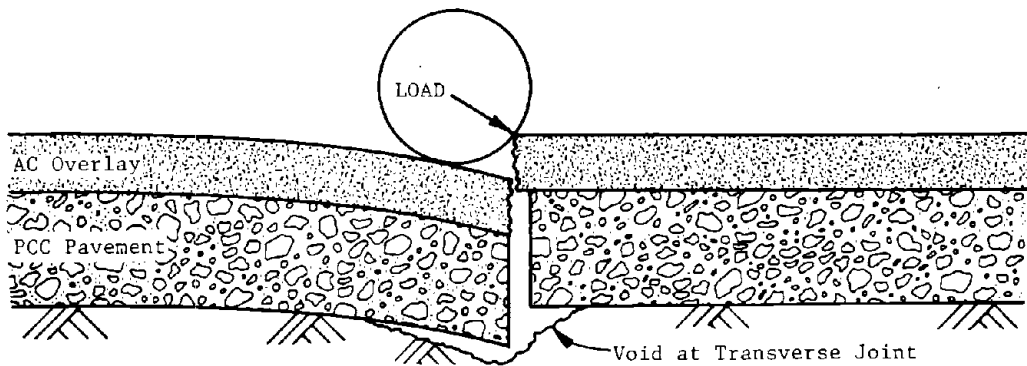
Crack spacing is determined by simply measuring the distance of the transverse cracks in the pavement from a known reference point. A rola-tape or measuring wheel and recorder can be used to record these distances. This will permit the development of a cumulative frequency distribution, as shown in Figure 71. In documenting the amount of cracking present



(a.) Full-Load Transfer at Joint  
No Impact Loading



(b.) Partial-Load Transfer at Joint  
Partial Impact Loading



(c.) No-Load Transfer at Joint  
Full Impact Loading

Figure 70. Illustrations showing an impact loading condition which may cause deterioration of the overlay at reflection cracks.

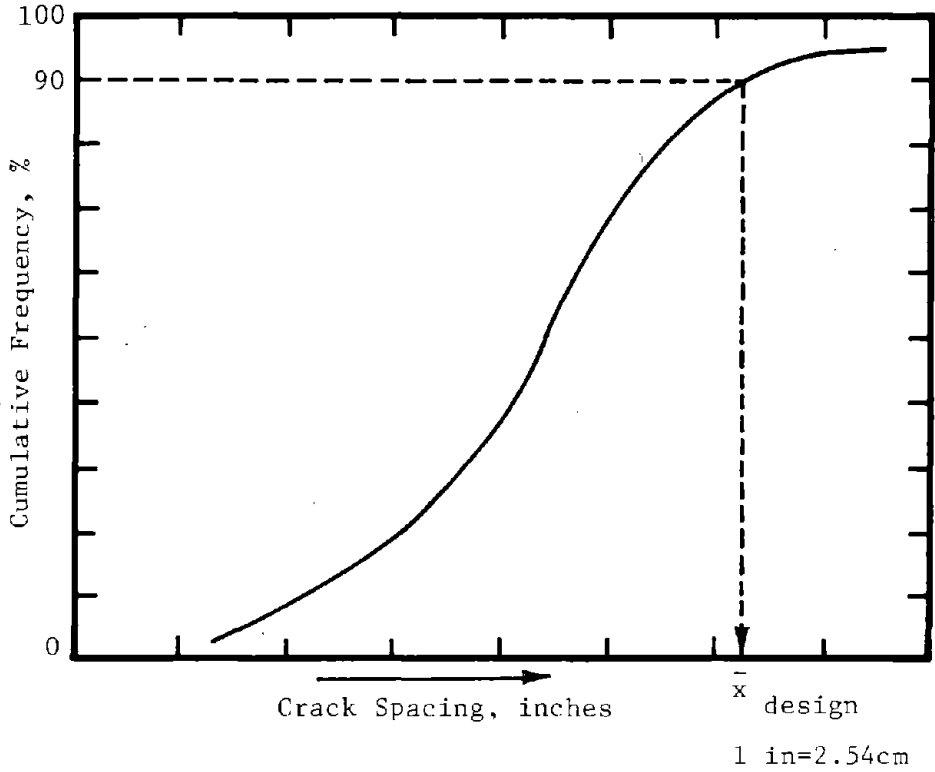


Figure 71. Cumulative frequency diagram of crack spacing for a concrete pavement.

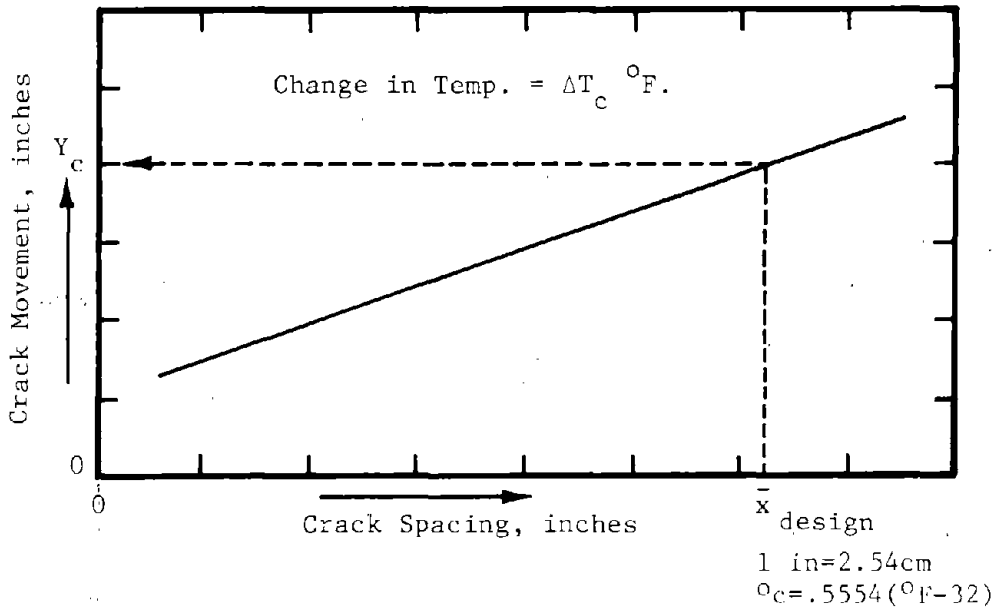


Figure 72. Relationship between crack spacing and concrete movement at a crack for a temperature change and specific location or pavement.

for reinforced pavements, joints are not to be counted as cracks, but are to be analyzed separately. For plain jointed concrete pavements, joints and only cracks which extend through the entire slab thickness are to be used in developing Figure 71. Crack spacings can be determined for various design levels. Joint spacing normally does not vary along the roadway. When used, it becomes a fixed input variable independent of design level.

#### Crack and/or Joint Movement

Movement of the slab is determined by measuring crack or joint widths for different air temperatures. Since slab movement is dependent on temperature change, it is recommended to obtain these widths over the same temperature differential as closely as possible. This will enable the user to complete the data analysis for one temperature change, and reduce the amount of error associated with different temperature differentials. Measurement of these widths can be achieved using a microscope with a graduated eyepiece capable of measuring to 0.001 inch (.0025cm). In an attempt to reduce the amount of error in reading, the microscope should be focused some distance below the concrete surface. Joints and cracks to be measured should be marked so the measurement can be taken at the same location for other temperatures. At least three readings should be taken at each location for a specific temperature and the average value recorded. Table 16 shows an example form on which the necessary data can be recorded. By recording average crack spacing with crack movement, Figure 72 may be developed. Hence, for a specific crack spacing or design level (Figure 71), the crack movement can be selected. When only joint widths are obtained, Figure 73 must be developed. This will permit the selection of a joint movement for some design level based on the joint spacing that exists in the field.

#### Differential Vertical Deflection

Load transfer is determined by measuring vertical displacement at discontinuities in the existing pavement. These measurements can be obtained using a Benkleman Beam, Dynaflect, or a differential deflection device, described in Reference 40, that uses a dial gage to measure relative movements between two adjacent slabs. Table 17 gives an example form for collecting the necessary field data. This will permit the development of the relationship illustrated in Figure 74 to determine the load transfer for various design levels.

When using the Benkleman Beam as the measuring device, the load is placed on one side of the joint and the deflection recorded. The load is then moved across the joint and the rebound or differential deflection recorded. Measurements should be taken at the edge or corner of the pavement so the measuring device will not be in the deflection basin.

Dynaflect measurements should be taken in the wheel path. Two sensors are to be placed as closely together as possible and spaced an equal distance from the pavement joint. This is done to minimize deflection differences due to the effects of the deflection basin. In this manner deflections on the loaded and unloaded slab can be obtained, and the difference represents the differential deflection.



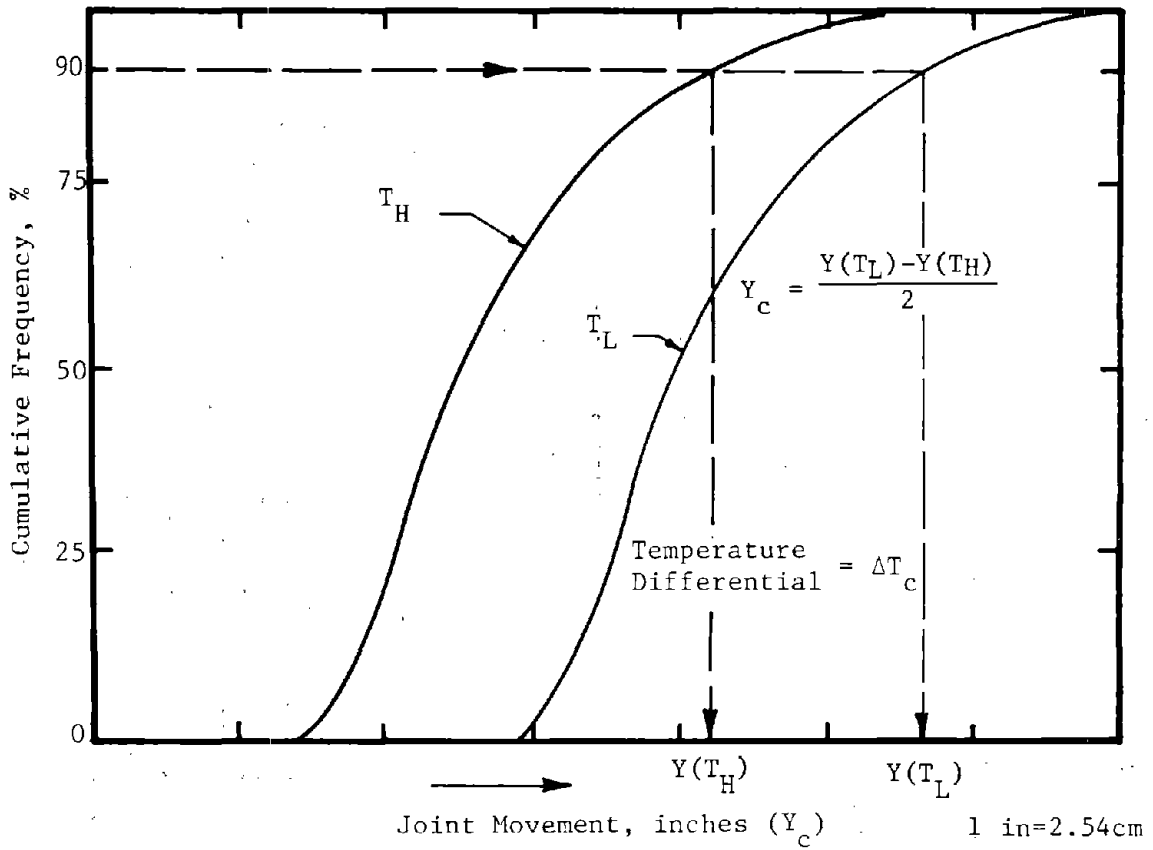


Figure 73. Illustration showing how the design joint movement, based on the characterization temperature change, can be obtained for an uncracked pavement.



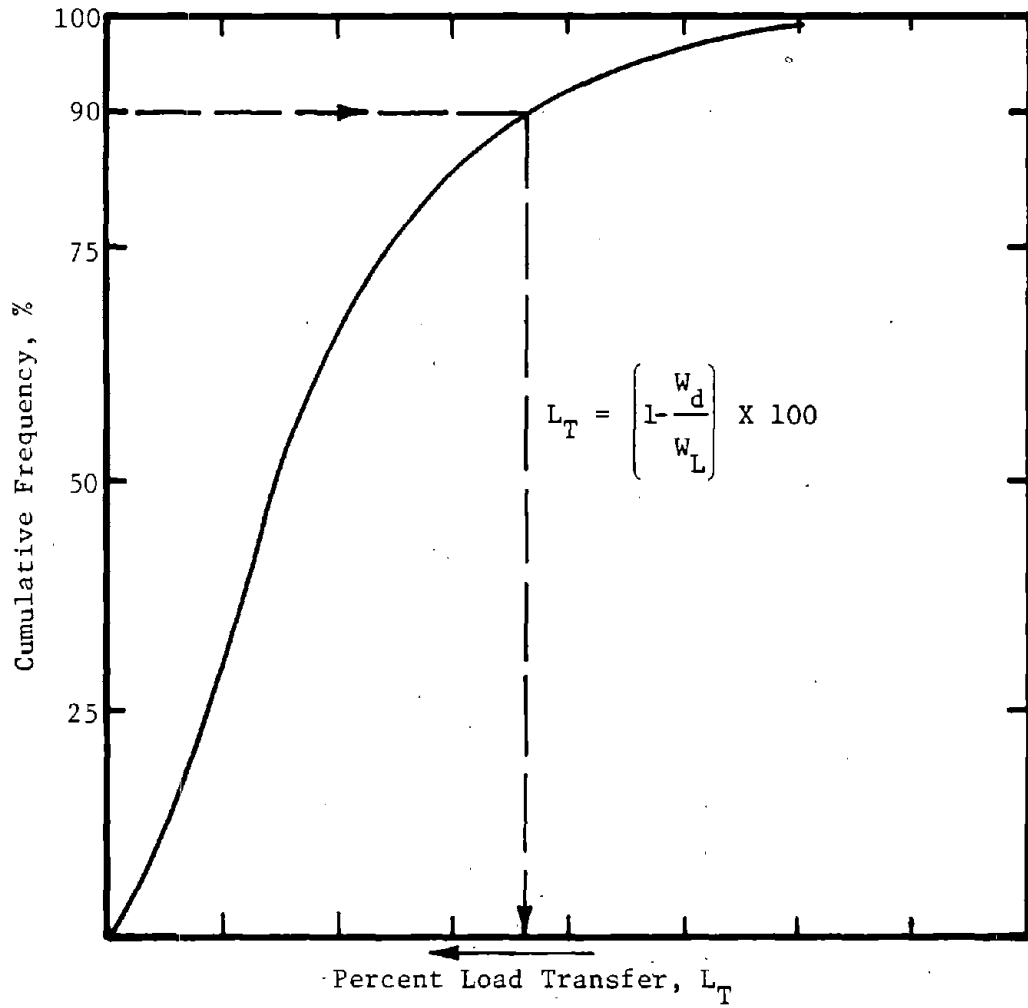


Figure 74. Illustration showing how the design differential deflection or load transfer can be obtained for some design level for an existing concrete pavement.



The differential deflection device measures directly the relative deflection between two adjacent slabs. Therefore, it can not be used alone in defining load transfer. It can be used with other deflection measuring devices to obtain the information necessary for the required inputs.

#### Treatment and Material Selection

As reviewed in the literature, no one treatment or material property will eliminate reflection cracking in all cases. The material requirements and treatment to reduce the distress mechanism of reflection cracking are project and environment dependent. The developed model can be used to predict which strain, tensile or shear, will be the dominate factor in the development of these cracks for a specific design condition. Material properties and treatment can then be selected or specified for each design based on the mechanism predicted to cause the cracks to occur. Some of the treatments which can be used are listed in Figure 48. The overlay material can then be designed to eliminate or reduce reflection cracking resulting from one of the failure mechanisms.

#### Summary

This chapter provides a procedure for evaluating an overlay's ability to resist reflection cracks. It present a model for determining the cause and lists various techniques which can reduce the severity of reflected cracks.

In developing this procedure, a literature review was completed to determine causes and treatments. It was found that two mechanisms, tensile and shear distortions, were the major cause of reflected cracks. Tensile distortions were a result of horizontal movements of the existing concrete pavement and shear distortions resulted from a loss in load transfer of the existing pavement. From this, a model was developed to determine if reflection cracks would be caused by either or both failure mechanisms. Various techniques were reviewed, but no one treatment had been successful in eliminating the cracks for all conditions.

The model is general and uses invariant material properties of the pavement system, and actual field conditions which the pavement has experienced. Field measurements are taken to calibrate the model to the actual pavement. From this it predicts critical tensile and shear strains in a selected overlay design to determine corrective measures that may be applied based on economic and field conditions. The development of this basic theory was completed to combine environmental and traffic loadings or evaluate extreme environmental conditions for predicting reflection cracks. This will determine if these cracks can be controlled economically or if physical restraints exist which will not permit the construction of an adequate overlay. For this condition, consideration was given for maintaining these cracks based on the primary cause of failure.

## CHAPTER 5

### VERIFICATION OF DESIGN CONCEPTS

This chapter presents verification of concepts developed for the overlay design procedure. As for any new procedure, data and performance records do not exist for complete verification of every concept, therefore, this chapter discusses only verification of some component parts.

In addition to the discussion of the deflection concepts, results of an overlay design using the procedure are presented. A comparison is made for the cost of constructing this overlay versus the cost of constructing an overlay based on conventional design concepts.

Also presented is a check of an overlay that was actually constructed to determine if reflection cracking should be expected. This design check is based on the reflection cracking criteria discussed in Chapter 4. With actual field measurements, based on the above condition, material values of the overlay (modulus, bond breaker, temperature, etc.) were investigated to illustrate usage of the model. This demonstrates how various overlay design values can be determined to prevent reflection cracking caused by both failure mechanisms.

#### Verification of Deflection Concepts

Two different projects were used to make comparisons between predicted and measured field data. This was done to substantiate the submodels used in the overlay design procedure. These field comparisons included data taken on a CRCP overlay at Palmdale AFB in California and an asphalt concrete overlay of a CRCP pavement on IH-45 in Walker Co. Texas.

#### Palmdale Air Force Base

Runway 7-25 consisted of a jointed concrete pavement, 12 to 14 inches (3.05 to 35.6cm) in thickness, placed directly on the subgrade. In 1969 an overlay was completed which consisted of a level-up course of asphaltic concrete and various thicknesses of a CRCP overlay. Dynaflect deflection measurements were taken in 1968 by MR and D on the existing pavement and are presented in Table 18 (Reference 106)<sup>1</sup> for the five design sections. Dynaflect measurements were taken in 1972 by Austin Research Engineers Inc after the

---

<sup>1</sup>Treybig, Harvey J., B. Frank McCullough and W. Ronald Hudson, "Continuously Reinforced Concrete Airfield Pavement - Volume I, Tests on Existing Pavement and Synthesis of Design Methods", Report No. FAA-RD-73-33-1, Prepared for Air Force Weapons Laboratory, U.S. Army Engineer Waterways Experiment Station and Federal Aviation Administration, May 1974.

Table 18. Dynaflect deflections on Runway 7-25 at Palmdale AFB (Ref. 106)

SECTION	DEFLECTIONS BEFORE OVERLAY*				DEFLECTIONS AFTER OVERLAY*			
	Between Joints		At Joints		Between Cracks		At Cracks	
	Mean 10 <sup>-3</sup> in.	Standard Deviation 10 <sup>-3</sup> in.	Mean 10 <sup>-3</sup> in.	Standard Deviation 10 <sup>-3</sup> in.	Mean 10 <sup>-3</sup> in.	Standard Deviation 10 <sup>-3</sup> in.	Mean 10 <sup>-3</sup> in.	Standard Deviation 10 <sup>-3</sup> in.
A	.390	.0251	.668	.199	.191	.0300	.220	.0418
B	.403	.0329	.689	.152	.146	.0160	.160	.0160
C	.30	0	.648	.142	.142	.0015	.149	.0114
D	.371	.0242	.495	.112	.161	.0080	.165	.0084
E	.288	.0126	.383	.091	.160	.0149	.159	.0130

\* Sensor #1

1 in=2.54cm

overlay had been completed and had experienced some aircraft traffic. These values are also presented in Table 18. Moduli tests and thickness determinations of each layer were conducted and the average values are listed in Table 19. Therefore, with the laboratory moduli values and the before-overlay deflections, the existing JCP runway was characterized. Elastic layer theory was used to calculate deflections for various subgrade moduli for each of the sections analyzed. These are graphically illustrated in Figures 75 and 76. The in-place subgrade modulus is determined by entering Figures 75 and 76 with the interior deflection (Table 18) and projecting to the subgrade modulus scale. The resulting values are listed below.

Section Number	Average Subgrade Modulus, psi	
A	21,000	
B	24,000	
C	41,000	
D	26,000	
E	40,000	1 psi=6.9kN/m <sup>2</sup>

Then by using the overlay material properties for each section (Table 19) and the resulting subgrade modulus values listed above, deflections at the surface of the overlay can be predicted. Stress sensitivity of the subgrade is not considered in this case, since the same load was used for before-overlay and after-overlay measurements. Figures 77 and 78 show the relationship between subgrade modulus and the predicted deflection on the overlay for the design sections. By entering with the calculated subgrade modulus, the average after-overlay deflection values can be predicted for each design section. The comparison between predicted and measured deflection values are illustrated in Figure 79, and all information is summarized in Table 20.

#### Walker County

The Walker County project consisted of an 8" (20.3cm) CRC pavement, along IH-45, placed over a 6 inch (15.2cm) flexible base and 6 inch (15.2 cm) lime-stabilized subgrade. The general cross section is given in Figure 80 (Reference 10) and the details of the experimental asphalt overlay are shown in Figure 81. Dynaflect deflections were taken at various times of the year before and after overlay placement. These values are presented in Table 21, along with the standard deviation for each time period. In order to characterize the pavement, elastic layer theory was used to calculate deflections for various subgrade moduli values for the conditions in the field. Laboratory flexural tests were conducted on the concrete; hence, the following equation was used to calculate a concrete modulus:

Table 19. Material properties for each section tested on Runway 7-25 at Palmdale AFB (Ref. 106).

Section	Layer	Modulus $10^3$ psi	Poisson's Ratio*	Mean Thickness, (Inches)
A	CRCP Overlay	3,716	0.20	12.7
	Asphalt Concrete	58	0.30	1.0
	JCP Concrete	2,500	0.20	14.0
B	CRCP Overlay	4,339	0.20	13.6
	Asphalt Concrete	58	0.30	2.1
	JCP Concrete	2,570	0.20	12.2
C	CRCP Overlay	3,996	0.20	11.7
	Asphalt Concrete	58	0.30	1.0
	JCP Concrete	2,253	0.20	11.7
D	CRCP Overlay	3,621	0.20	9.6
	Asphalt Concrete	58	0.30	1.8
	JCP Concrete	2,974	0.20	11.8
E	CRCP Overlay	3,491	0.20	8.5
	Asphalt Concrete	58	0.30	2.0
	JCP Concrete	1,968	0.20	13.4

\*Poisson's Ratio was not tested but assumed to be values tabulated.

1 in=2.54cm  
1 psi=6.9 kN/m<sup>2</sup>



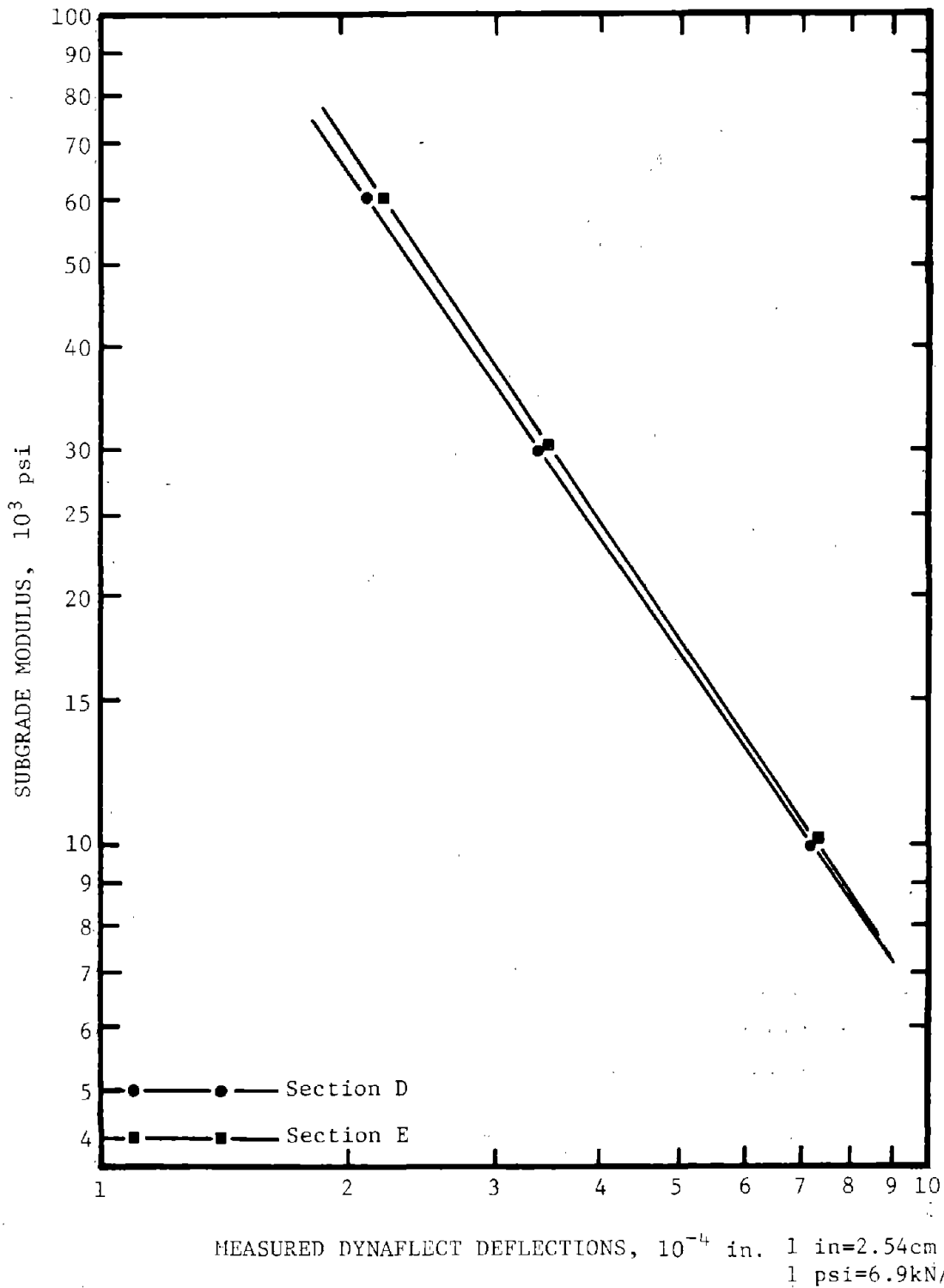
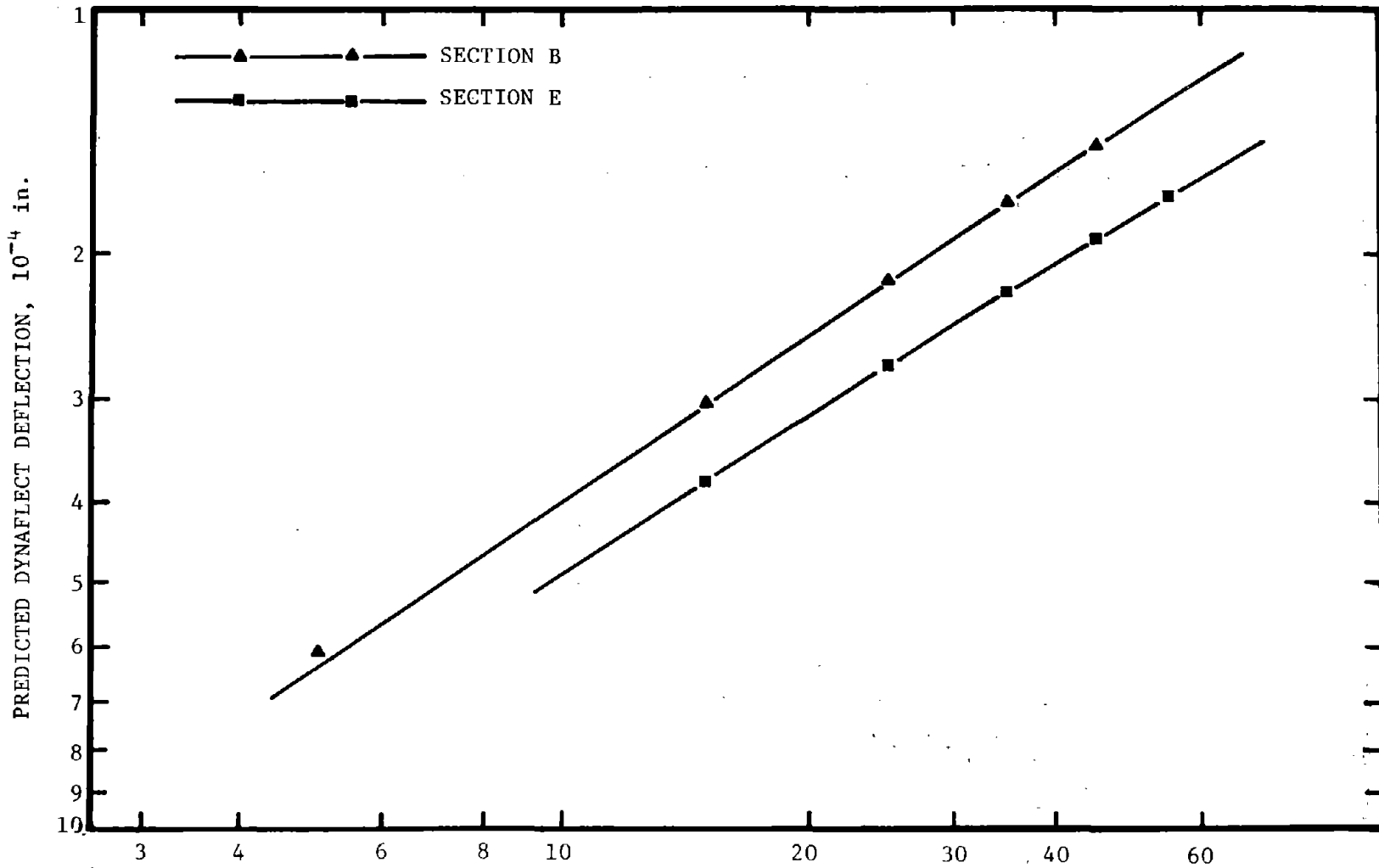


Figure 76. Computed relationship between subgrade elastic modulus and Dynaflect deflections before overlay, using elastic layer theory for Runway 7-25 at Palmdale AFB.







SUBGRADE MODULUS OF ELASTICITY,  $10^3$  psi      1 in=2.54cm  
 1 psi=6.9kN/m<sup>2</sup>

Figure 78. Computed relationship between subgrade modulus and Dynaflect deflection after overlay, for Runway 7-25 at Palmdale AFB.

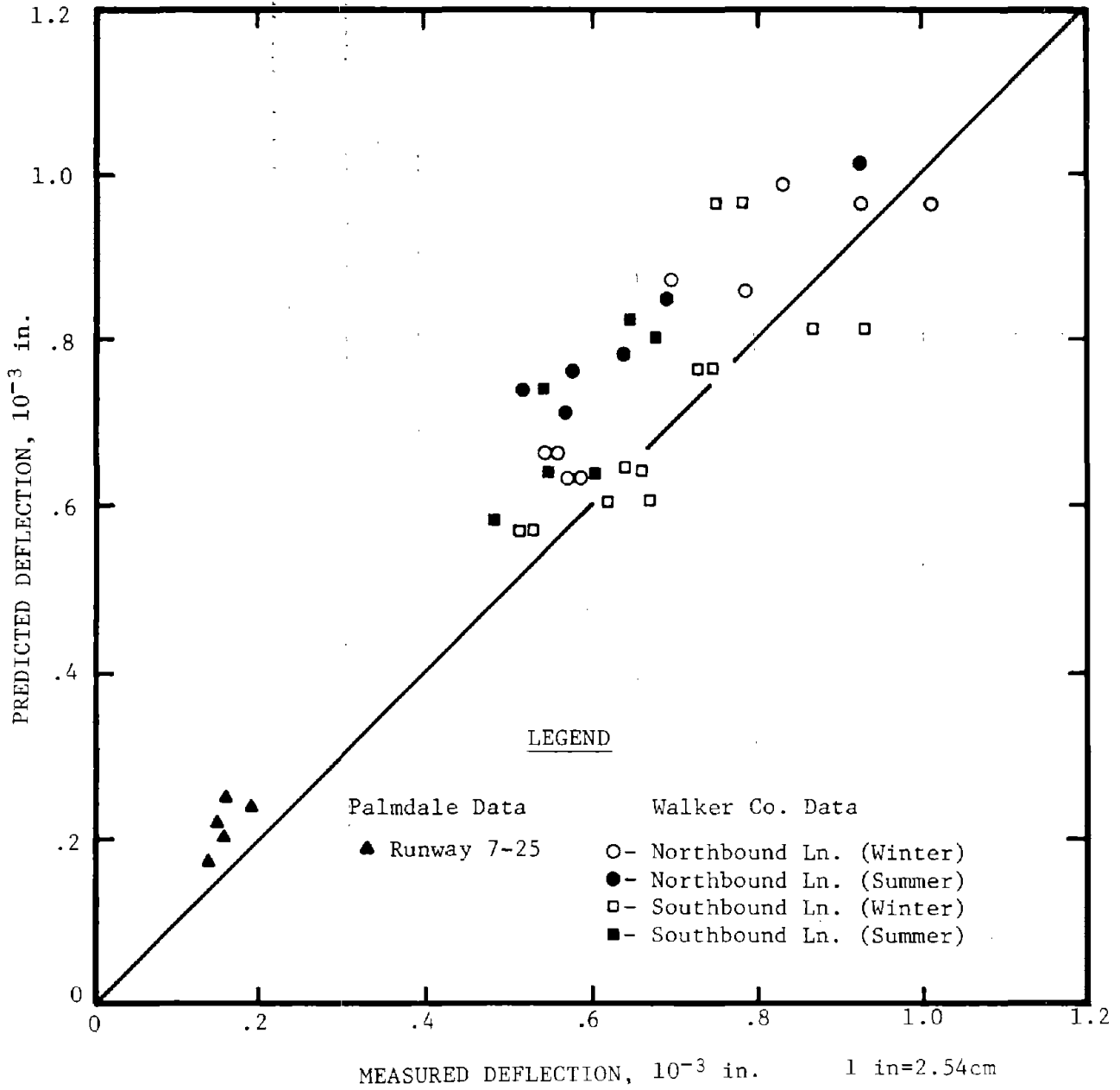


Figure 79. Comparison of predicted and measured Dynaflect deflections after overlay for the two projects considered.

Table 20. Predicted and measured deflections after overlay for Runway 7-25 at Palmdale AFB.

Section Number	Dynalect Deflection Before Overlay 10 <sup>-4</sup> inches	Predicted Subgrade Modulus psi	Predicted Dynalect Deflection 10 <sup>-4</sup> inches	Measured Dynalect Deflection 10 <sup>-4</sup> inches	Percent Difference (%)
A	3.90 ± .360	21,000 ± 3,000	2.38 ± .25	1.91 ± .30	+ 24.6
B	4.03 ± .33	24,000 ± 3,000	2.20 ± .18	1.46 ± .16	+ 50.7
C	3.00 ± ---	41,000 ± ---	1.68 ± ---	1.42 ± .02	+ 18.3
D	3.71 ± .24	26,000 ± 2,500	2.53 ± .15	1.61 ± .08	+ 57.1
E	2.88 ± .13	40,000 ± 2,500	2.05 ± .09	1.60 ± .15	+ 28.1

1 in=2.54cm  
1 psi=6.9kN/m<sup>2</sup>

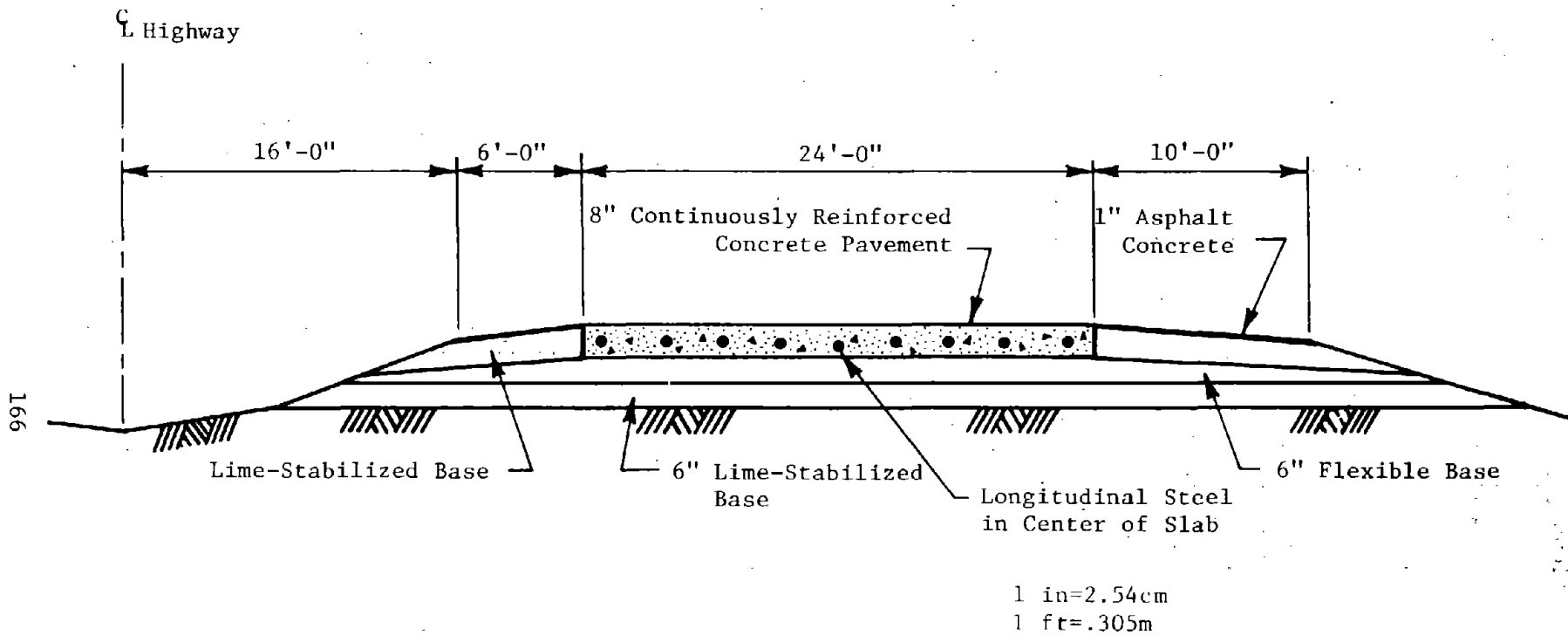
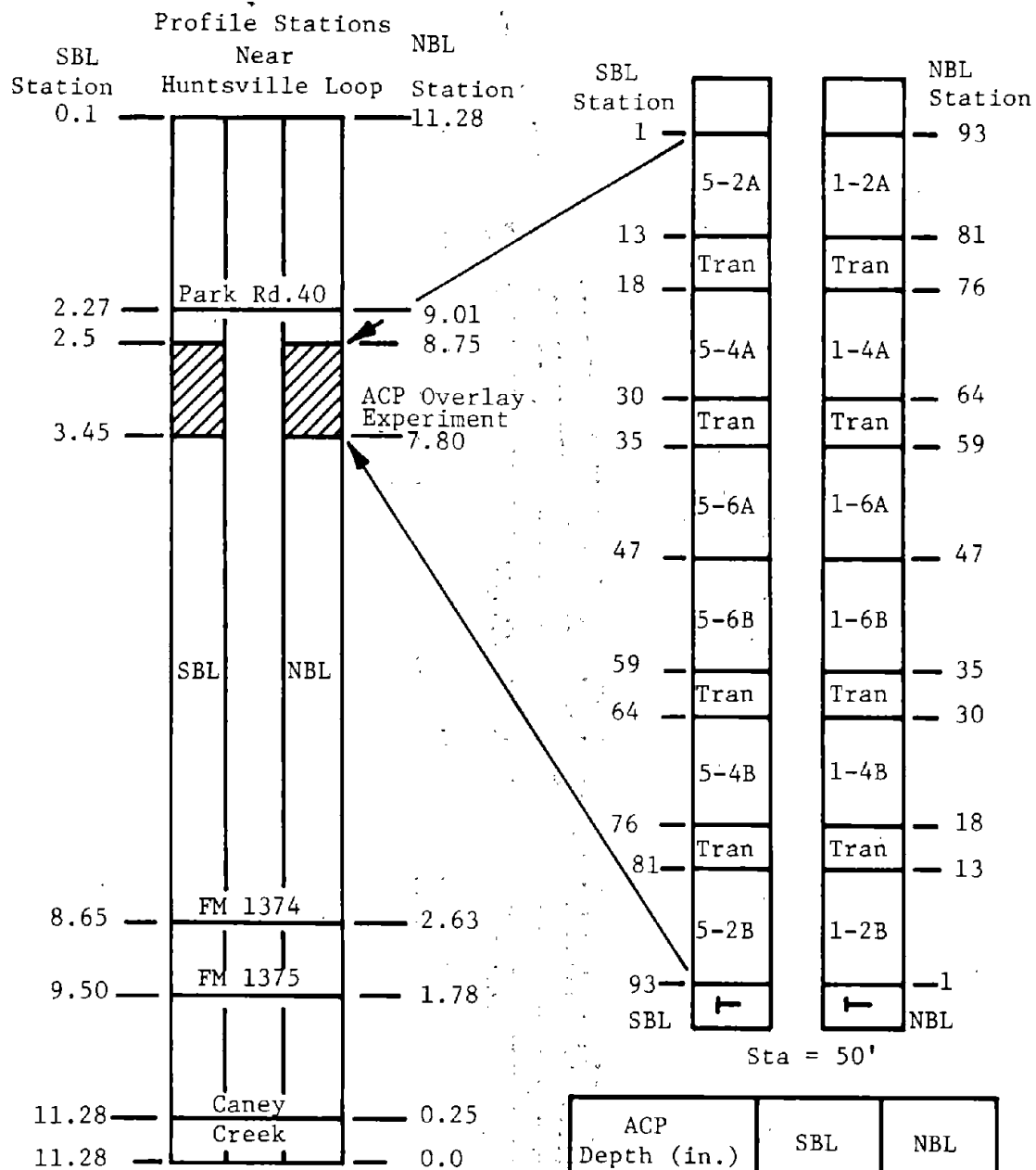


Figure 80. Typical half-section for Walker County Project on IH-45 (Ref. 107)



ACP Depth (in.)	SBL	NBL
2	5-2A	1-2A
	5-2B	1-2B
4	5-4A	1-4A
	5-4B	1-4B
6	5-6A	1-6A
	5-6B	1-6B

Figure 81. Details of the 1969 experimental asphalt concrete overlay for the Walker Co. Project (Ref. 10).

Table 21. Dynaflect deflections, before and after overlay for the Walker Co. Project (Ref. 10).

DATE	NORTHBOUND LANE					
	AVERAGE	STANDARD 2B DEVIATION	AVERAGE	STANDARD 4B DEVIATION	AVERAGE	STANDARD 6B DEVIATION
BEFORE						
6/67	.964	.172	.762	.139	.826	.176
9/67	1.079	.226	.767	.144	.856	.327
11/67	.968	.171	.756	.119	.843	.230
1/68	1.107	.247	.797	.145	.915	.402
AFTER						
2/68	.926	.369	.593	.089	.563	.148
8/68	.924	.407	.567	.093	.518	.156
1/69	1.013	.435	.585	.090	.556	.152
	2A		4A		6A	
BEFORE						
6/67	.775	.143	.379	.137	.835	.218
9/67	.835	.133	.899	.112	.875	.215
11/67	.935	.313	1.098	.166	1.102	.376
1/68	.921	.184	1.195	.212	1.151	.372
AFTER						
2/68	.786	.102	.833	.132	.695	.150
8/68	.640	.124	.688	.106	.581	.124

DATE	SOUTHBOUND LANE					
	AVERAGE	STANDARD 2B DEVIATION	AVERAGE	STANDARD 4B DEVIATION	AVERAGE	STANDARD 6B DEVIATION
BEFORE						
9/67	.820	.076	.686	.099	.668	.160
11/67	1.003	.103	.862	.115	.818	.178
1/68	.763	.074	.628	.075	.737	.138
AFTER						
2/68	.871	.115	.671	.187	.532	.121
8/68	.680	.092	.556	.161	.482	.123
1/69	.927	.158	.622	.126	.513	.112
	2A		4A		6A	
BEFORE						
9/67	.658	.066	.876	.134	.835	.089
11/67	.835	.089	1.158	.246	.916	.226
1/68	.814	.089	1.102	.215	.797	.180
AFTER						
2/68	.734	.068	.753	.090	.662	.142
8/68	.599	.046	.650	.056	.542	.114
1/69	.738	.056	.784	.095	.658	.157

$$E_c = 33(\gamma^{1.5})(f_c')^{1/2} \dots \dots \dots 69$$

where:

$E_c$  = Concrete modulus, psi (1 psi=6.9kN/m<sup>2</sup>)

$$f_c' = \frac{4000 f_r}{1000 - f_r} \dots \dots \dots 70$$

$f_r$  = Concrete flexural strength, psi (1 psi=6.9kN/m<sup>2</sup>)

$\gamma$  = Unit weight of concrete, pcf (1 pcf=16kg/m<sup>3</sup>)

The thickness of each layer was obtained from core samples. Material properties of the subbase and lime-stabilized subgrade were taken from Reference 10. Material properties used in the analysis for each layer are summarized in Figure 82. With these material properties and elastic layer theory, deflections were calculated for various subgrade moduli, as illustrated in Figure 83 to characterize the pavement. Entering Figure 83 with a specific deflection, the corresponding subgrade modulus can be found. The resulting subgrade modulus values are presented in Table 22. It was decided, after reviewing the initial measurements, that measurements made in June and September should be combined and November and January measurements should be combined. These results are presented in Table 23. Modulus tests were run on the asphaltic concrete material to obtain the temperature-stiffness relationship of the mix as shown in Figure 84. Since exact temperatures were not available during deflection testing after overlay, an average daily temperature by month was used for the analysis. (Figure 85) By taking the average daily temperature in Figure 85 and entering Figure 84, the resulting asphaltic concrete modulus can be obtained for each time during testing. The resulting moduli values to be used to predict deflections for each time period are listed below:

January	49°F	1,300,000 psi	
August	82°F	200,000 psi	$c^0 = .5554(^{\circ}F - 32)$
February	49°F	1,300,000 psi	1 psi=6.9kN/m <sup>2</sup>

To determine the subgrade modulus for after-overlay measurements, stress sensitivity was not considered, since the characterization load was the same as the load used to measure after-overlay deflections. Hence, the same subgrade moduli values tabulated in Table 23 are used with elastic layer theory to predict after-overlay deflections. These predicted and measured deflection values are tabulated in Table 24 and presented in Figure 79.

#### Discussion of Errors

By reviewing Figure 79 it is observed that the predicted deflections are, in most cases, higher than the measured deflections. Two explanations are given as to what might be the cause: (1) effect of confining

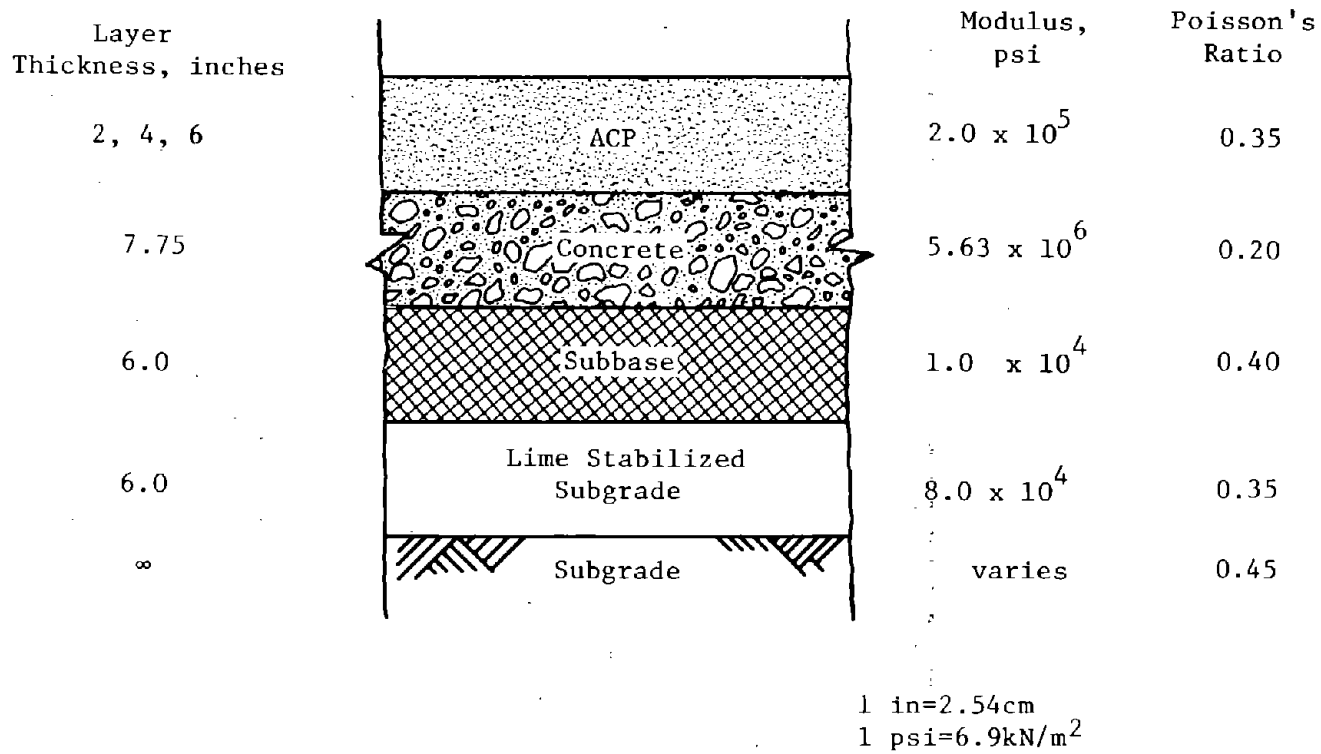


Figure 82. Material properties of each layer of the pavement structure for the Walker County Analysis.



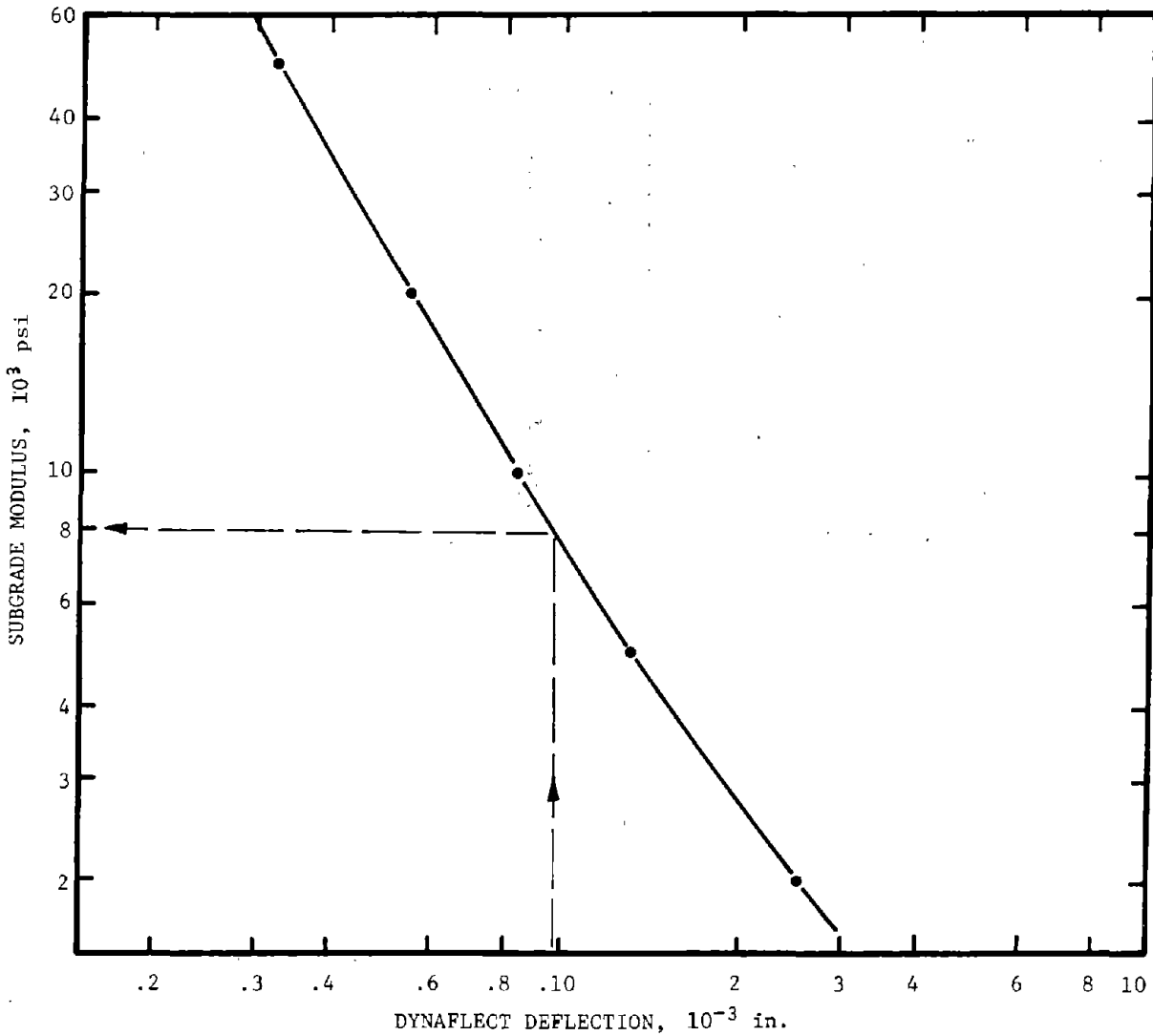


Figure 83. Computed relationship between subgrade modulus and Dynaflect deflection before overlay, for the CRC pavement in Walker County, Texas.

1 in=2.54cm  
 1 psi=6.9kN/m<sup>2</sup>

Table 22. Subgrade moduli determined from Dynaflect deflections for before-overlay measurements for the Walker Co. Project.

NORTHBOUND LANE					
Avg. Temp. °F	Date	Section 2	Section 4	Section 6	
80	6/67	8,000 psi	11,700 psi	10,300 psi	B
77	9/67	6,700	11,500	9,700	
62	11/67	7,900	11,900	9,900	
49	1/68	6,400	10,800	8,600	
80	6/67	11,400	38,000	10,000	A
77	9/67	10,000	8,900	9,300	
62	11/67	8,400	6,500	6,400	
49	1/68	8,600	5,700	6,000	
SOUTHBOUND LANE					
77	9/67	10,400 psi	13,900 psi	14,500 psi	B
62	11/67	7,500	9,600	10,500	
49	1/68	11,700	16,000	12,400	
77	9/67	15,000	9,300	10,000	A
62	11/67	10,000	6,000	8,500	
49	1/68	10,500	6,400	10,800	

°C = .5554(°F-32)  
 1 psi = 6.9 kN/m<sup>2</sup>

Table 23. Subgrade moduli determination for each section from Dynaflect deflections for before-overlay measurements, Walker Co., Project.

Lane	Section Number	Average Seasonal Deflection, $10^{-3}$ in.		Seasonal Subgrade Modulus, $10^3$ psi	
		Summer	Winter	Summer	Winter
Northbound	2B	1.022	1.038	7.2	7.1
	4B	.765	.777	11.5	11.4
	6B	.841	.879	10.0	9.2
	6A	.805	.928	9.7	6.2
	4A	.899	1.147	8.9	6.0
	2A	.855	1.127	10.7	8.5
Southbound	2B	.820	.883	10.4	9.2
	4B	.686	.745	13.8	12.2
	6B	.668	.778	14.5	11.3
	6A	.658	.825	10.1	9.6
	4A	.876	1.130	9.3	6.2
	2A	.835	.857	15.1	10.2

1 in=2.54cm  
1 psi=6.9kN/m<sup>2</sup>

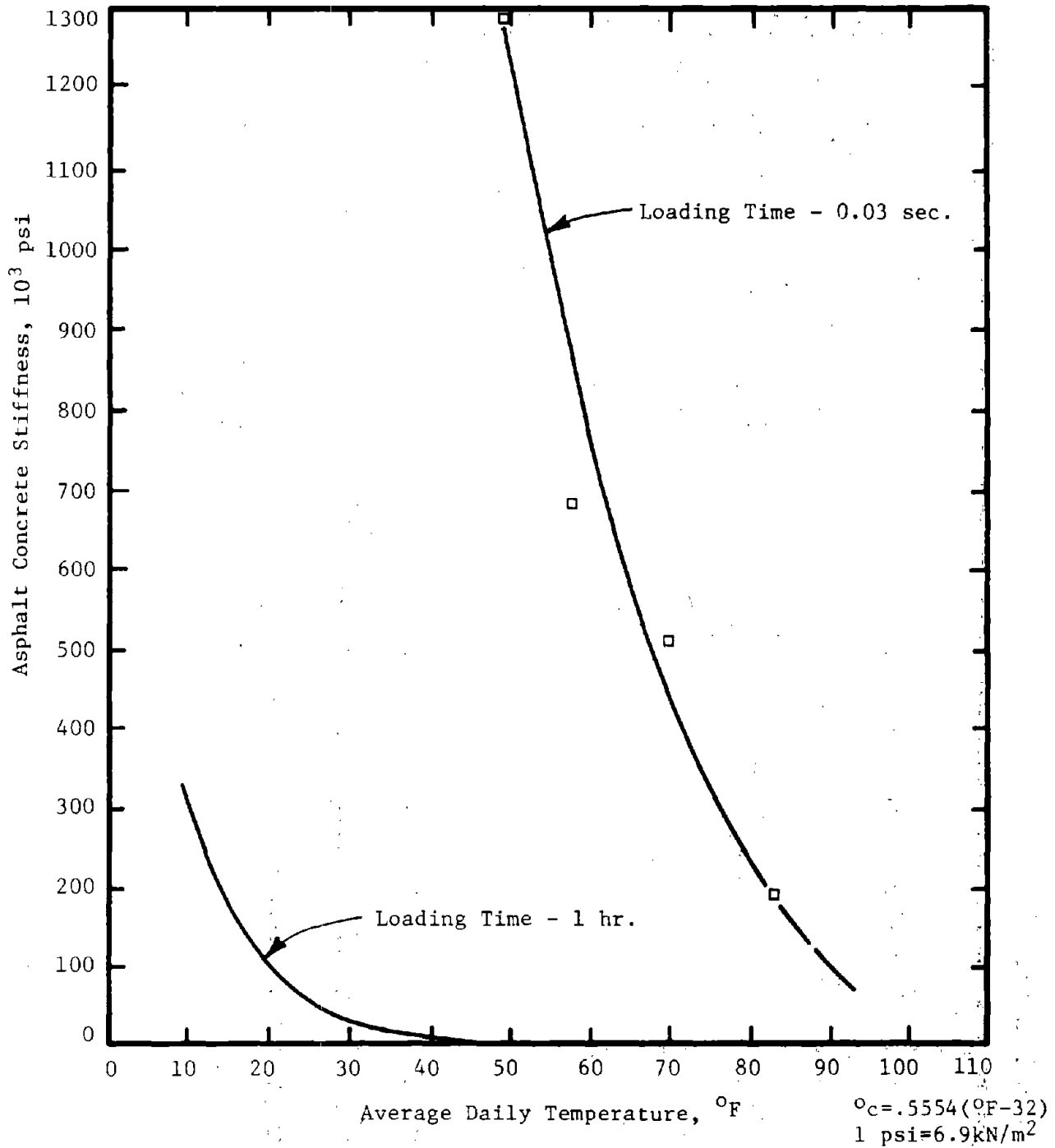


Figure 84. Asphalt concrete stiffness as a function of temperature and loading time, for the mix used at the Walker Co. Project. (Ref. 10).

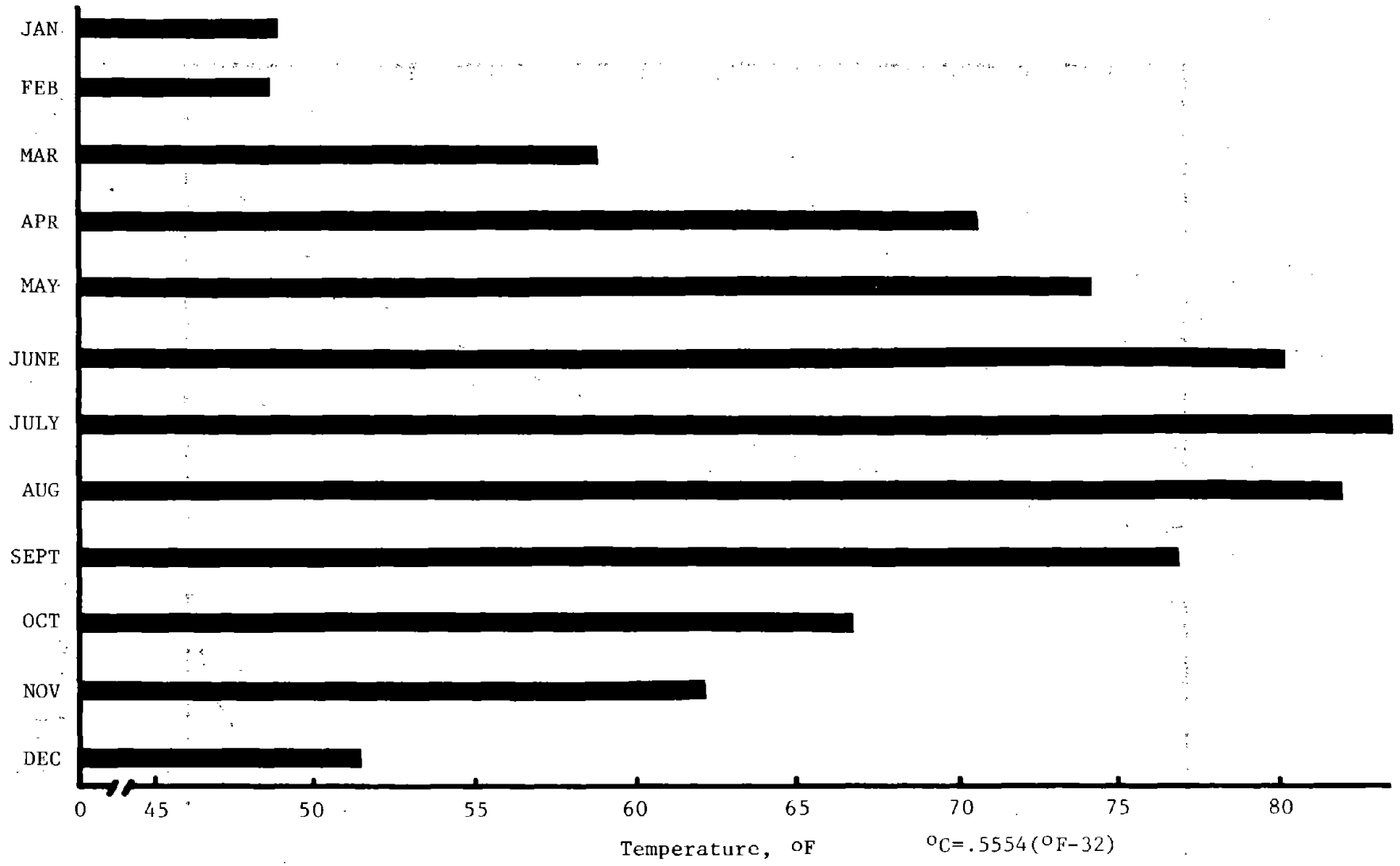


Figure 85. Average daily temperature by month for Walker County. (Ref. 10)

Table 24. Predicted and measured deflection for each section of the Walker Co. project.

NORTHBOUND

Season	Section Number	Deflection, 10 <sup>-3</sup> in.		Percent Difference
		Predicted	Measured	
Winter	2B	.962	.926	3.7
			1.013	-5.3
	4B	.633	.585	7.6
			.593	6.3
	6B	.657	.556	15.4
			.563	14.3
	6A	.872	.695	20.3
	4A	.981	.833	15.1
	2A	.854	.786	8.0
Summer	2B	1.010	.924	8.5
	4B	.716	.567	20.8
	6B	.745	.518	30.5
	6A	.760	.581	23.6
	4A	.846	.688	15.8
	2A	.781	.640	18.1

Table 24. Predicted and measured deflection for each section of the Walker Co. project. (Continued)

Season	Section Number	Deflection, $10^{-3}$ in.		Percent Difference
		Predicted	Measured	
Winter	2B	.811	.871	- 7.4
			.927	-14.3
	4B	.605	.671	-10.9
			.622	- 2.8
	6B	.570	.532	6.7
			.513	10.0
	6A	.638	.662	- 3.8
			.658	- 3.1
	4A	.958	.753	21.4
			.784	18.2
	2A	.758	.734	3.2
			.738	2.6
Summer	2B	.795	.680	14.5
			.556	12.7
	4B	.637	.556	12.7
	6B	.584	.482	17.5
	6A	.740	.542	26.8
	4A	.822	.650	20.9
	2A	.629	.599	4.8

1 in=2.54cm

pressure on subgrade modulus, and (2) a reduction of the existing surface modulus due to the presence of cracks.

Confining Pressure. In both analyses there was no consideration given to the confining pressure effect on the resulting subgrade modulus values. As shown in Figure 86 (Reference 107)<sup>1</sup>, the confining pressures can have a definite effect on the subgrade modulus derived from laboratory testing. Consider an example at Palmdale only one confining pressure was used to obtain the relationship between resilient modulus and deviator stress (Figure 87). Reviewing Figure 86, it is shown that the slope of the laboratory curve can change with changing confining pressure. The addition of an overlay to the existing pavement increases the overburden pressure, resulting in increased moduli values as shown by elastic layer theory in Figure 88. The analysis curve presented in Figure 88 is representative of the existing pavement and not the overlay. Considering the overlay, the analysis curve could have an increased slope resulting in a greater subgrade modulus for the same load; hence reducing the predicted deflection.

Existing Surface Modulus. In both cases, the laboratory modulus of the existing concrete pavement was used to characterize the pavement without regard to cracks or percent reinforcement. The laboratory modulus is always greater than an effective in-field modulus, due to the presence of cracks. If the reduced modulus of the concrete were considered, the subgrade modulus would have to be increased for the calculated and measured deflection before overlay to be equal. This increased subgrade modulus would then serve to decrease the predicted deflections after overlay. By calculating the average yearly deflection for the sections which contained 0.5% and 0.6% steel, it is observed that the reinforcement may be affecting the resulting deflection. The average yearly deflection for the 0.5% and 0.6% steel were  $0.924 \times 10^{-3}$  and  $0.832 \times 10^{-3}$  inches (.0023 and .0021cm) respectively. Since these measurements came from the same location the difference in average deflections is not solely explained by the subgrade. Rather, the higher percent reinforcement probably has a higher effective in-field concrete modulus resulting in reduced deflections. The increased effective modulus may be attributed to the effects of 20 percent more steel and/or increased load transfer. Therefore, some measure of this in-field surface modulus should be estimated when using elastic layer theory, which assumes an interior condition. No data are available to determine the shape of the deflection basin for estimating an effective concrete modulus; hence, this was not considered.

In summary, when considering the above, it should be expected that the predicted deflections are higher than measured deflections. Therefore, it may be desirable to run at least two different confining pressures

---

<sup>1</sup>"Repair East Runway Randolph Air Force Base," Report No. AF-2 Prepared for Department of the Air Force Headquarters 12th Flying Training Wing (ATC) - Randolph Air Force Base, Texas; Austin Research Engineers Inc, November 1976.



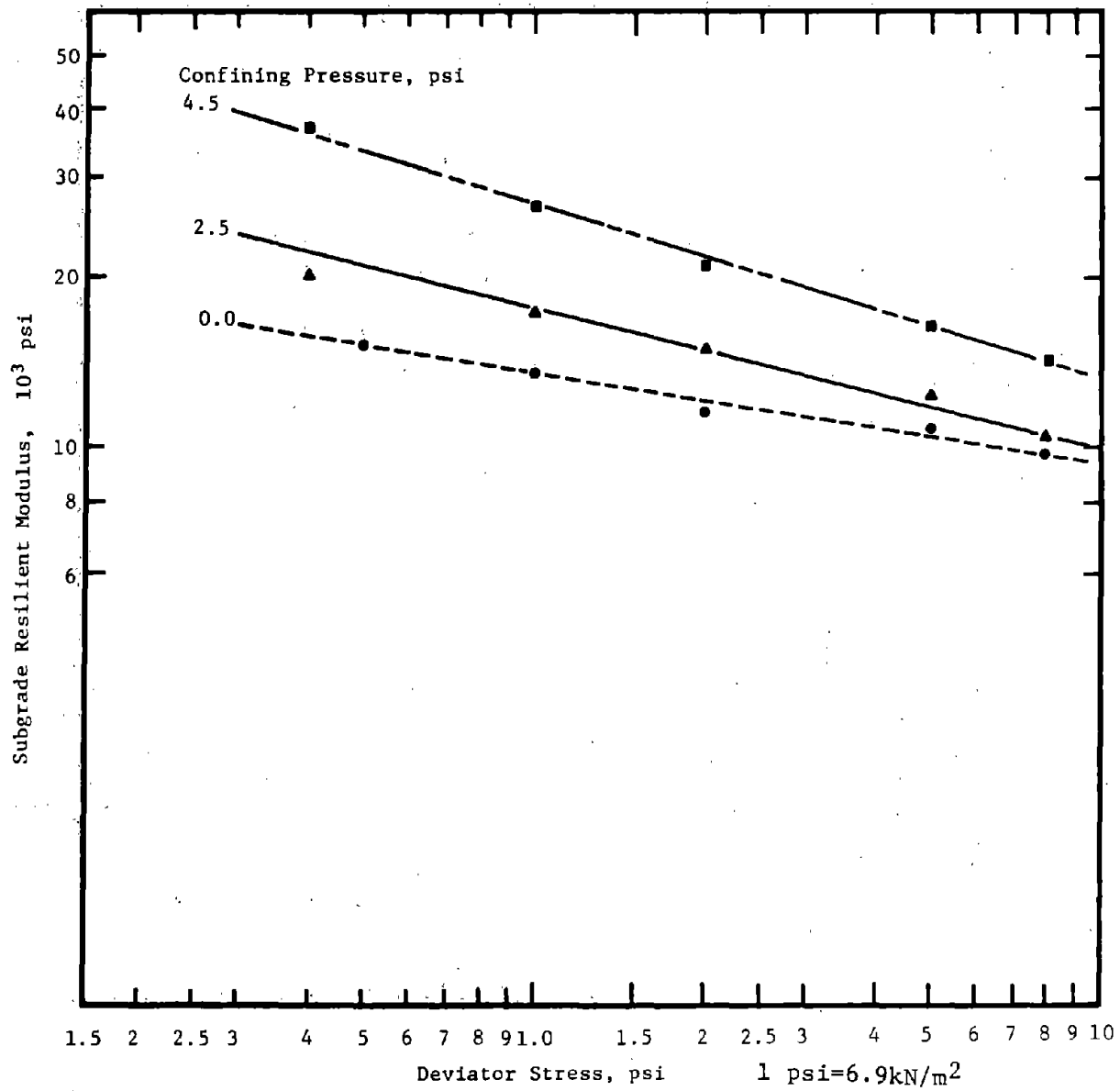


Figure 86. Effect of confining pressure on the resulting subgrade modulus (Ref. 107).

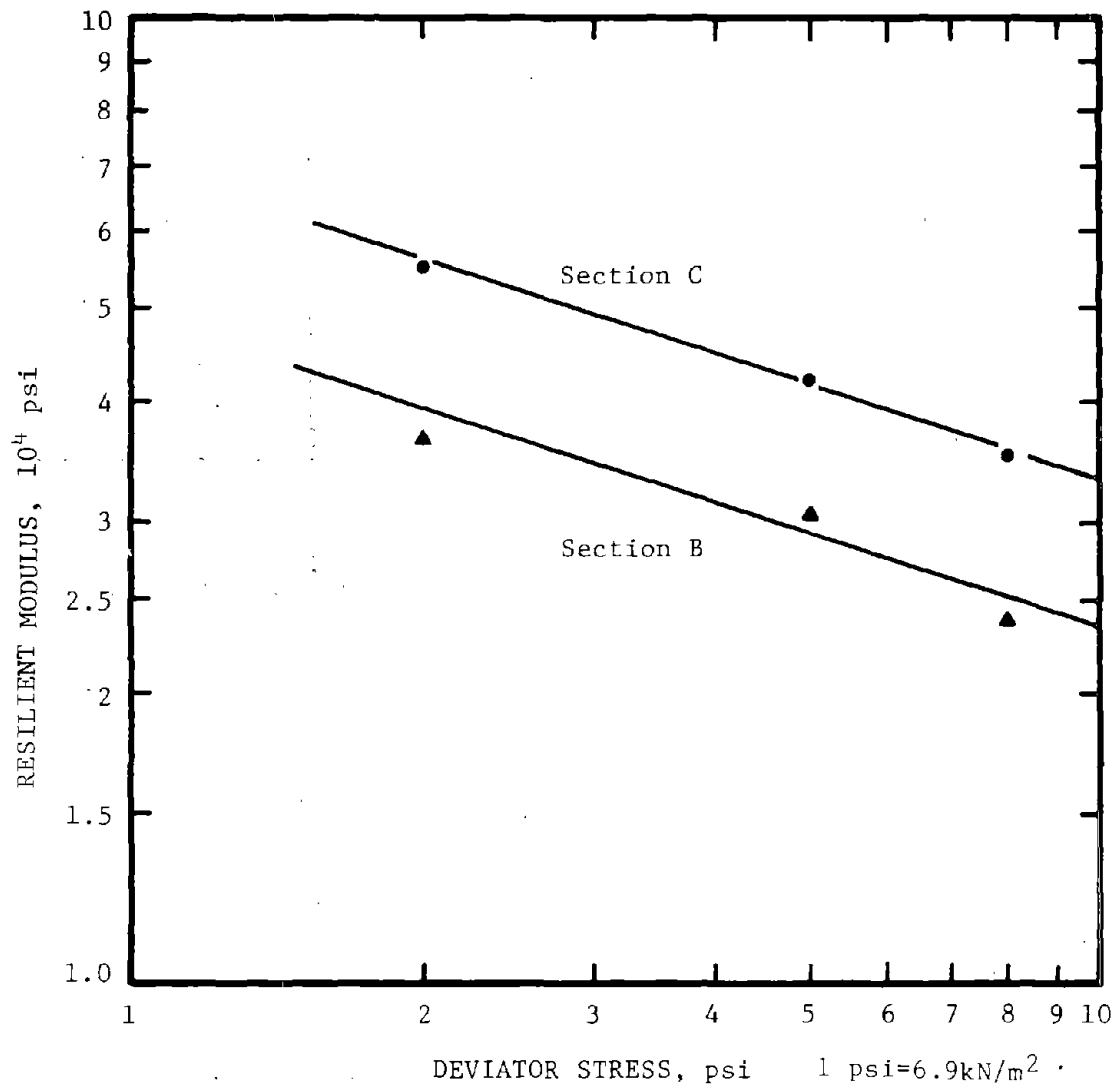


Figure 87: Relationship between deviator stress and resilient modulus for two sections on Runway 7-25 at Palmdale AFB.

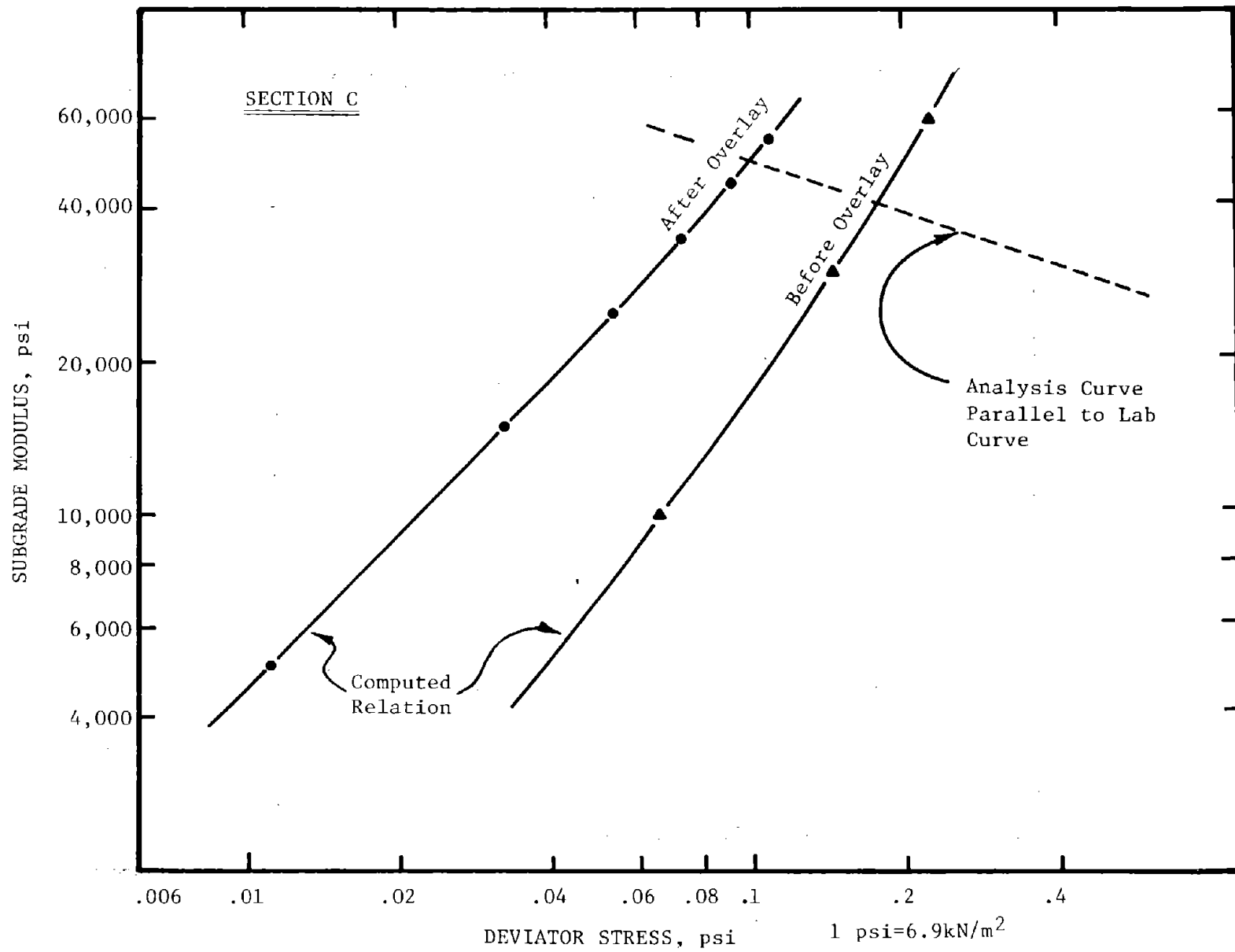


Figure 88. Relationship between deviator stress and subgrade modulus for before and after overlay conditions for Section C on Runway 7-25 at Palmdale AFB.

to obtain a more correct relationship between resilient modulus and deviator stress of the subgrade. The deflection basin of the existing surface should also be considered to account for cracks and other discontinuities in the existing pavement instead of the more uniform properties in a laboratory sample.

#### Illustrative Overlay Design Problem

This section presents the results of an overlay design using the newly developed procedure, in conjunction with a cost comparison with conventional design methods (Ref. 108)<sup>1</sup>.

The objective of this section is to compare the cost of overlaying an old pavement by two different design methods which will be referred to as "variable thickness" and "minimum conditions". The minimum condition approach based on conventional concepts, uses only one overlay thickness for the entire road. The variable thickness approach recognizes the variability of design factors along the overlay project by applying statistical knowledge, dividing the road into several small test sections and designing for the thicknesses.

Figure 89 shows the location and layout of Interstate 45 approximately 11 miles\* in length in Walker County, Texas, for which the overlay cost comparison was made. This highway serves as the main artery between the metropolitan areas of Houston and Dallas; hence, the roadway has a high percentage of trucks. During the harvest season, the roadway experiences a seasonal inflow of heavily loaded trucks from the high plains areas of Texas and Oklahoma toward Houston (Ref. 109)<sup>2</sup>.

Figure 80 is a typical half section for the pavement which consists of a uniform 8-inch\*\* slab, 24 feet\*\*\* wide. A crushed sandstone material with an open gradation was used for the subbase layer. The top 6 inches of the natural sand clay material was treated with three percent lime by weight to form a stabilized layer, to serve as a moisture barrier and to minimize moisture variations in the lower clay strata.

Input data required for this study were taken from Reference 109 by B. F. McCullough and C. L. Monismith. The newly developed computerized overlay design procedure was used to design the overlay thicknesses. Cost information was supplied by the Texas Highway Department.

---

<sup>1</sup>Srinarawat, Maitree, "Estimate the Cost Savings That May be Derived from Using a Variable Overlay Thickness Along a Project in Lieu of Designing for Minimum Conditions," Term Paper, Civil Engineering Department, University of Texas, May 1977.

<sup>2</sup>McCullough, B. F., and C. L. Monismith, "Application of a Pavement Design Overlay System," Special Report No. 1, Center for Highway Research, The University of Texas at Austin, October 1969.

\*1 mile = 1.61 km, \*\*1 inch = 25.4 mm, \*\*\*1 ft = 0.305 m

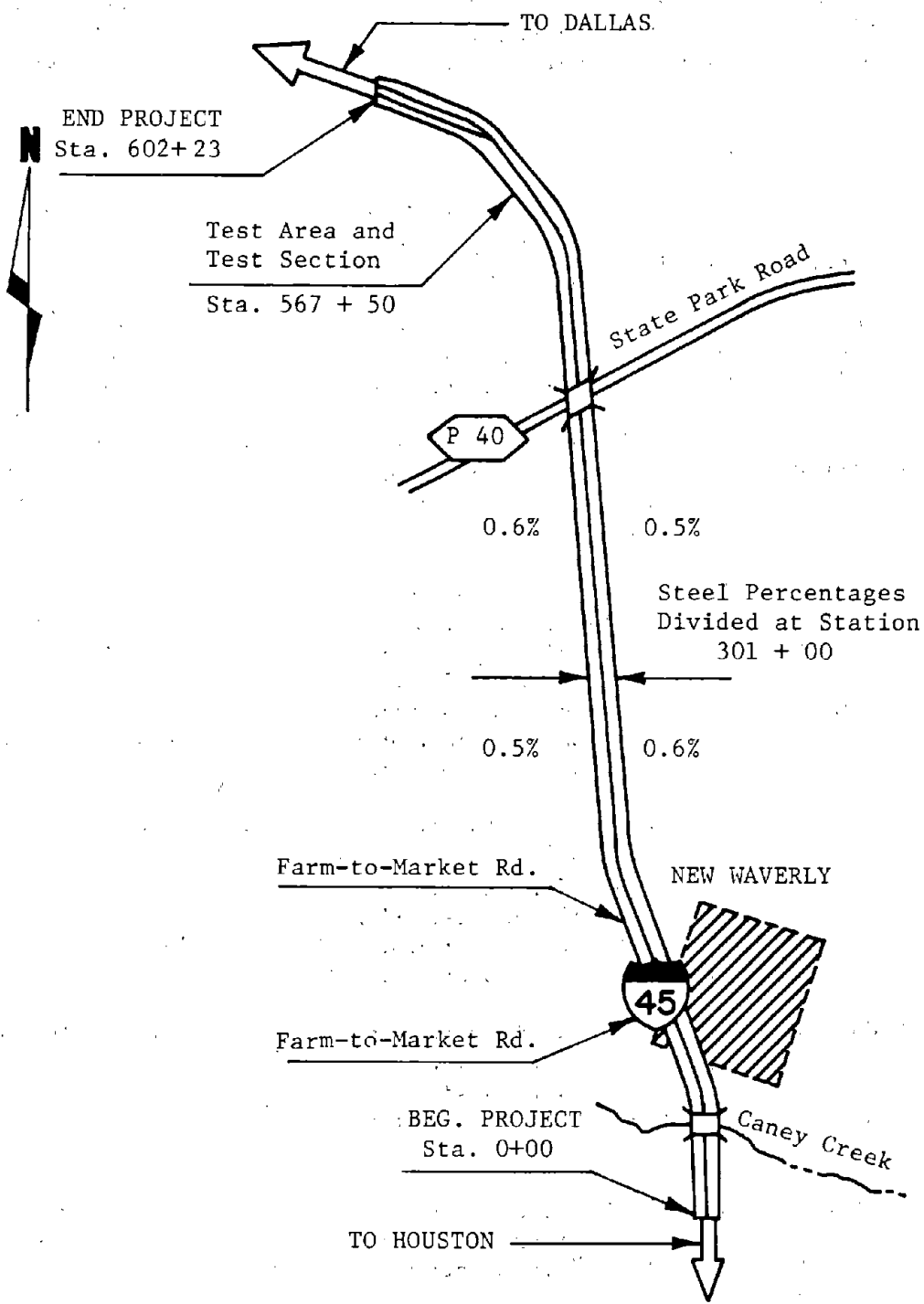


Figure 89. Location and layout of Walker County Project.  
(Ref. 10)

A deflection profile as determined by the Dynaflect was plotted (Figure 90), and these data were used along with project soil conditions to divide the roadway into 14 different sections (Table 25). The estimated means and standard deviations of the deflections were computed (Table 26). The Student t-value between adjacent test sections was then determined. A significance level of 10 percent was selected as the criterion for judging the difference between adjacent sections. Results are given in Table 27 (Ref. 109).

The design deflection was determined for each test section. The 95 percent confidence level was used to calculate the design deflection for each section. Computed values of the design deflection are given in Table 28. These values were input and executed with the overlay design computer program to find overlay thicknesses for each section for the "variable thickness" approach.

For the "minimum condition" design, the design deflection values were rearranged in descending order. Percent of the values equal to or greater than were computed. The 95 percentile value was determined (Table 29), and this 95 percentile deflection value was used as the representative of all the deflections to find one overlay thickness for the entire road section.

#### Traffic Variable

Total applications for past and predicted traffic which is composed of six single axle load groups and seven tandem axle load groups are given in Table 30. AASHO equivalency factors were used to convert mixed traffic to equivalent 18-kip (8172kg) axle load applications as shown in Table 31. In the year 1969, the roadway experienced an average daily traffic of 10,070 with 23.2 percent of these being trucks. Since statistics of the directional distribution of traffic were not available, an estimated method was used. Figure 91 is a plot of average distress along the roadway for both the southbound lane and the northbound lane. In general, the amount of distress is linearly correlated to the directional distribution factor. The total distressed area can be calculated by computing the areas under the SBL curve and the NBL curve and adding them together. The SBL distressed area is 70 percent of the total distressed area, while the NBL distressed area is equal to 30 percent of the total distressed area. Thus, directional distribution for the southbound lane equal to 70 and the northbound lane equal to 30 percent can be used. The 60 percent southbound and 40 percent northbound were used in Reference 109. The directional distribution of 65 and 35, mean of the two mentioned before, were used in this study.

#### Material Testing and Properties

An extensive amount of material sampling and testing was conducted (Ref. 109). Table 32 shows concrete density, thickness, tensile strength, and flexural strength. The concrete elastic constant, i.e., modulus of

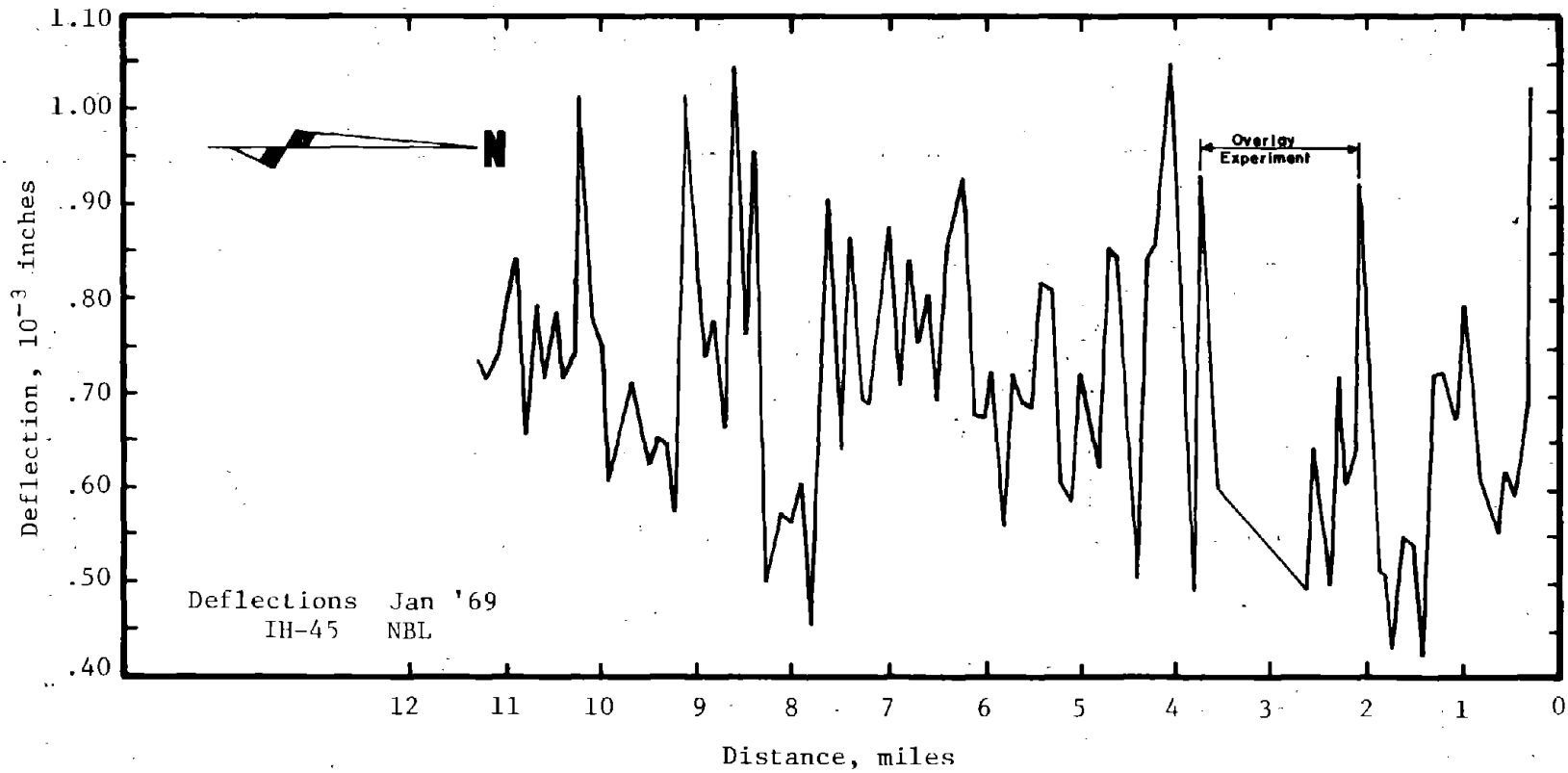


Figure 90. Deflection profile for the northbound roadway. (Ref. 109)

1 mile=1.61 km  
1 in=2.54cm

Table 25. Limits of test sections used in analysis  
for Walker County Project. (Ref. 109)

Test Section No.	Station Numbers for		Length (miles)
	NB	SB	
1	0- 14.5	99.5-114.0	1.45
2	14.5- 22.5	91.5- 99.5	.80
3	22.5- 30.5	83.5- 91.5	.80
4	30.5- 36.5	77.5- 83.5	.60
5	36.5- 43.5	70.5- 77.5	.70
6	43.5- 52.5	61.5- 70.5	.90
7	52.5- 66.5	47.5- 61.5	1.40
8	66.5- 74.5	39.5- 47.5	.80
9	74.5- 78.5	35.5- 39.5	.40
10	Overlay	Overlay	.70
11	94.5-100.5	13.5- 19.5	.60
12	100.5-107.5	6.5- 13.5	.70
13	107.5-110.5	3.5- 6.5	.30
14	110.5-114.0	0- 3.5	.35

Note:

NB - Northbound Roadway                    1 mile=1.61km  
 SB - Southbound Roadway                   1 station=30.5m

Station numbers are in 0.1 mile units



Table 26. Mean and Standard Deviation of Deflections  
for Test Sections. (Ref. 109)

Test Section	NB and SB		NB		SB	
	Mean (in.)	Standard Deviation (in.)	Mean (in.)	Standard Deviation (in.)	Mean (in.)	Standard Deviation (in.)
1	0.7553	0.1029	0.7753	0.0832	0.7453	0.1212
2	0.6893	0.0624	0.6475	0.0412	0.7312	0.0519
3	0.7850	0.1637	0.8725	0.1808	0.6975	0.0854
4	0.6050	0.1300	0.5450	0.0548	0.6650	0.1600
5	0.7730	0.0927	0.7700	0.0990	0.7766	0.0943
6	0.8672	0.1385	0.8188	0.0840	0.9155	0.1542
7	0.7514	0.1174	0.6850	0.0762	0.8230	0.1144
8	0.9218	0.1992	0.8162	0.1766	1.0275	0.1688
9	0.7012	0.1280	0.6725	0.1868	0.7300	0.0346
10	0.6946	0.1949	0.6450	0.1462	0.7533	0.2406
11	0.5969	0.1307	0.4933	0.0547	0.5857	0.1086
12	0.7307	0.1220	0.6828	0.0707	0.7785	0.1483
13	0.6566	0.1039	0.5866	0.0346	0.7266	0.1048
14	0.7925	0.1723	0.8500	0.2404	0.7350	0.1345

1 in=2.54cm

Note:

Deflection and standard deviations  
are in  $10^{-3}$  inches.

Table 27. Significance Study for Combined Data From the Two Roadways\* (Ref. 109).

Test	n	t	a	Significance
First Iteration:				
1 vs 2	34	3.003	1.692	Diff.
2 vs 3	32	3.041	1.695	Diff.
3 vs 4	28	3.024	1.701	Diff.
4 vs 5	25	3.647	1.708	Diff.
5 vs 6	31	2.061	1.696	Diff.
6 vs 7	45	2.945	1.680	Diff.
7 vs 8	43	3.455	1.682	Diff.
8 vs 9	24	2.729	1.711	Diff.
9 vs 10				Same
10 vs 11	26	2.081	1.706	Diff.
11 vs 12	27	0.389	1.703	Same
12 vs 13	20	1.232	1.725	Same
13 vs 14	10	1.387	1.812	Same
Second Iteration for Combining Like Sections and Recomparing:				
8 vs 9	35	3.604	1.930	Diff.
9 - 10 vs 11 - 14	58	0.445	1.671	Same
Third Iteration for Combining Like Sections and Recomparing:				
8 vs 9 - 14	66	2.210	1.664	Diff.

\*Note:

All significance tests performed at  $\alpha = 5$  percent.

Table 28. Design Deflection Values for 95 Percent Confidence Level Variable Thickness Approach.

<u>Test Section</u>	<u>Design Deflection in inches x 10<sup>-3</sup></u>
1	0.9373
2	0.7920
3	1.0543
4	0.8188
5	0.9254
6	1.0950
7	0.9445
8	1.2495
9	0.9118
10	1.0152
11	0.8119
12	0.9314
13	0.8275
14	<u>1.0759</u>

$$D_{\text{design}} = \bar{D}_{\text{section}} + 1.65 \sigma_{\text{section}}$$

$$\bar{D}_{\text{design}} = 0.9565 \times 10^{-3}$$

1 in=2.54cm

Table 29. Computation of Design Deflection, Minimum Condition

<u>Design Deflection</u> <u>10<sup>-3</sup> in.</u>	<u>Number equal to or</u> <u>Smaller Than</u>	<u>Percent</u>	
1.2495	14	100	95th Percentile = 1.142
1.095	13	92.8	
1.076	12	85.7	
1.054	11	78.6	
1.015	10	71.4	
.9445	9	64.3	
.937	8	57.1	
.931	7	50	
.925	6	42.9	
.912	5	35.7	
.828	4	28.6	
.819	3	21.4	
.812	2	14.3	
.792	1	7.1	

1 in=2.54cm

Table 30. Load Variables - Magnitude and Repetitions  
for Past and Predicted Traffic

Grouping, Kips <sup>1</sup>	Average Wheel Load, Kips	Total Applications	
		1961 - 1969 Past	1969 - 1981 Predicted
2 - 6 (SA)	2.61	841,090	2,380,100
7 - 11 (SA)	4.50	3,269,000	9,290,000
12 - 16 (SA)	6.76	696,000	1,971,000
17 - 18 (SA)	8.69	110,600	313,000
19 - 20 (SA)	9.59	39,800	112,600
21 - 22 (SA)	10.72	14,550	41,200
4 - 13 (TA)	2.66	1,443,340	4,086,630
14 - 25 (TA)	4.48	1,384,600	3,928,000
26 - 32 (TA)	7.17	1,639,000	4,639,000
33 - 36 (TA)	8.44	183,500	518,900
37 - 40 (TA)	9.60	40,740	115,300
41 - 44 (TA)	10.63	20,370	57,090
50 (TA)	12.50	1,940	5,490

<sup>1</sup> SA - Single Axle  
TA - Tandem Axle

1 kip=454kg

Table 31. 18-kip equivalent axle load applications.

Grouping (Kips)	Equivalence Factors	Total Applications			
		1961-1969 (Past)		1969-1981 (Predicted)	
		No. of Axles (10 <sup>3</sup> )	Equivalent 18-Kip Axle Applications (10 <sup>3</sup> )	No. of Axles (10 <sup>3</sup> )	Equivalent 18-Kip Axle Applications (10 <sup>3</sup> )
2- 6(SA)	.002	841	1.68	2,380.1	4.76
7-11(SA)	.055	3,269	179.80	9,290.0	510.95
12-16(SA)	0.35	696	243.6	1,971.0	689.85
17-18(SA)	0.85	110.6	94.01	313.0	266.05
19-20(SA)	1.41	39.8	56.12	112.6	158.77
21-22(SA)	2.10	14.55	30.56	41.2	86.52
TANDEM AXLE					
4-13(TA)	0.01	1,443.34	14.13	4,086.63	40.87
14-25(TA)	0.19	1,384.6	263.07	3,928.0	746.32
26-32(TA)	0.99	1,639.0	1622.6	4,639.0	4592.6
33-36(TA)	1.99	183.5	365.2	518.9	1032.6
37-40(TA)	3.07	40.74	125.07	115.3	353.97
41-44(TA)	4.52	20.37	92.07	57.09	258.05
50(TA)	8.0	1.94	15.52	5.49	43.92
		<b>Σ</b> 3103.73		<b>Σ</b> 8,785.23	

1 kip=454kg

1. 35% of Traffic travel due North (to Dallas)  
65% of Traffic travel due South (to Houston)

2. 100% of Traffic travel over the design lane

Total past application = .65 x 3103.73 = 2017.425

Total predicted application = .65 x 8785.23 = 5710.40

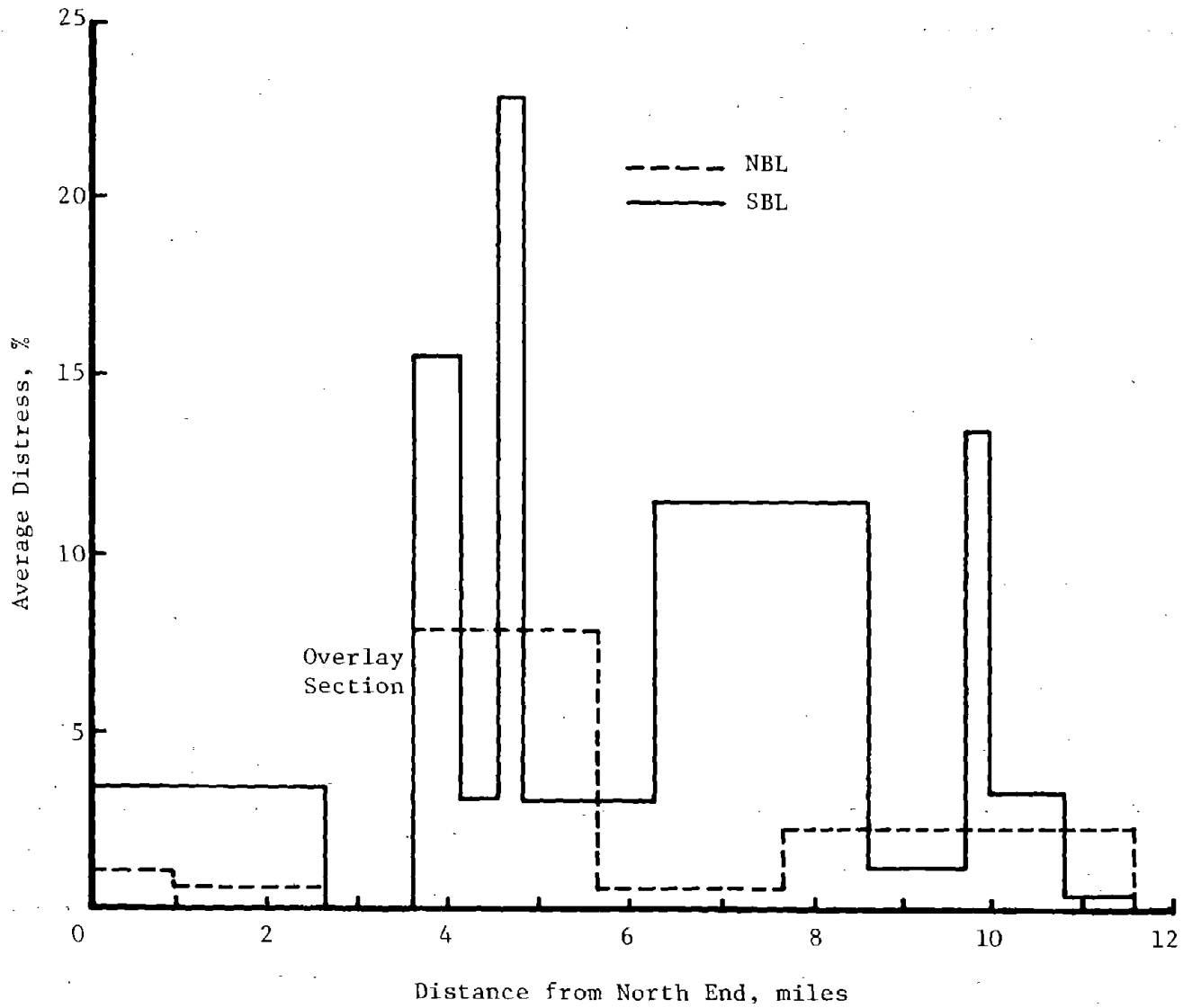


Figure 91. Plot of average distress for significantly different areas of performance - Walker County.

1 mile=1.61km

TABLE 32. TEST DATA ON CORES TAKEN FROM IH 45 IN WALKER COUNTY

Sample No. <sup>1</sup>	Density by Absolute Vol. lb/ft <sup>3</sup>	Density by Comparative Volume	Measured Thickness, in.	Splitting Tensile, psi	Flexural psi	Condition <sup>2</sup>
1 - T	146.3	140.0		535	886	C
1A - B	145.0	134.0		567	918	G
1XX - T	144.8	122.5		289	468	G
1X - B	145.0	117.5	7.750	327	529	G
2 - T	142.5	136.2		417	675	C
2A - B	141.7	126.6	7.625	395	640	C
3 - T	142.6	136.8		423	685	C
3A - B	140.3	128.1	8.125	429	695	C
4 - T	140.9	132.7		458	742	C
4A - B	140.8	128.2	8.125	263	426	C
5 - T	140.8	135.2		443	717	C
5A - B	138.8	125.9	7.750	326	528	C
6 - T	140.6	134.2		412	667	G
6A - B	142.8	127.3	8.000	458	742	G
7 - T	142.2	136.4		576	933	C
7A - B	137.3	120.0	8.125	214	346	C
8 - T	140.3	131.1		509	824	G
8A - B	140.3	125.9	8.000	358	580	G
9 - T	142.4	134.5		445	721	C
9A - B	141.6	126.9	7.750	356	576	C
10 - T	142.3	136.1		465	753	G
10A - B	141.7	134.3	7.875	387	627	G
11 - T	144.2	138.0		451	730	C
11A - B	141.8	118.3	8.250	265	429	C
12 - T	142.5	136.3		416	674	G
12A - B	142.5	129.6	8.250	409	662	G
13 - T	142.3	135.9		409	662	C
13A - B	143.6	130.4	8.000	564	913	C
14 - T	143.0	137.6		472	764	G
14 - B	143.5	125.0	8.125	323	523	G
15 - T	141.4	135.4		490	794	C
15A - B	140.8	128.0	8.000	496	803	C
16 - T	141.1	134.8		592	959	G
16A - B	144.2	132.3	8.125	447	724	G
17 - T	135.9	127.8		373	604	C
17A - B	137.9	114.8	7.875	345	559	C
18 - T	138.8	132.6		396	641	C
18A - B	141.7	121.5	8.500	354	573	G
19 - T	138.9	132.4		497	805	C
19A - B	137.9	105.8	8.000	164	265	C
20 - T	139.4	134.6		420	680	G

<sup>1</sup>T - Top half of the core  
 B - Bottom of the core

<sup>2</sup>G - Pavement in good condition.

C - Pavement cracks showing signs of deterioration

1 lb=.454kg

1 ft=.305m

1 in=2.54cm

1 psi=6.9kN/m<sup>2</sup>

(Continued)



TABLE 32 (Continued)

20A - B	140.0	122.2	7.750	309	500	C
21 - T	144.6	137.0		552	894	C
21A - B	140.1	122.0	8.250	303	491	C
22 - T	142.0	136.7		472	764	C
22 - B	140.6	116.0	8.125	286	463	G
23 - T	144.7	139.2		577	934	C
23A - B	141.1	126.0	8.375	363	588	C
24 - T	141.0	134.5		510	826	G
24 - B	140.5	128.1	8.125	384	622	G
25 - T	143.1	136.6		441	714	C
25 - B	140.9	124.2	8.000	216	350	C
26 - T	142.7	138.3		470	771	C
26 - B	145.3	127.7	7.875	607	983	G
27 - T	145.5	141.2		609	986	C
27 - B	142.4	124.7	7.750	421	682	C
28 - T	146.4	140.6		536	863	G
28 - B	145.6	117.6	7.750	416	674	G
29 - T	142.5	134.1		528	855	C
29 - B	140.0	119.3	8.625	426	690	C
30 - T	145.4	138.3		599	970	G
30 - B	141.8	123.5	7.750	392	635	G
31A - T	143.6	138.5		487	789	C
31A - B	141.9	127.0	7.625	383	620	C
32 - T	141.8	135.4		554	897	G
32 - B	140.9	130.0	8.125	413	669	G
33 - T	143.7	137.9		488	790	C
33 - B	143.1	111.4	7.875	327	530	C
34 - T	140.1	133.2		532	844	G
34 - B	141.1	119.3	7.625	327	530	G
35 - T	147.4	137.2		496	803	C
35 - B	141.4	127.3	7.875	356	576	C
36 - T	142.4	136.6		474	767	G
36 - B	144.4	127.0	8.500	602	975	G
37 - T	140.1	135.8		463	750	C
37 - B	140.8	129.9	7.875	434	703	C
37A - T	144.8	137.0		481	941	C
37A - B	142.3	124.4	8.000	377	610	C
38 - T	143.6	136.8		466	755	G
38 - B	146.5	133.8	8.000	502	813	G

elasticity, and Poisson's ratio, were obtained from a report cited in Reference 109. The subgrade modulus also was determined at several deviator stresses. Figure 92 shows the material properties and geometry of the pavement structure for this analysis.

With all the information mentioned previously, the overlay design computer program was used to design the overlay thicknesses. In order to make the cost comparison study, 58 problems were solved by the program; 28 problems for CRCP overlay for a "variable thickness", 28 problems for JCP overlay for a "variable thickness" approach, one problem for CRCP overlay by "minimum condition" and one JCP overlay for "minimum condition" approach. Figures 93 and 94 show the overlay thicknesses for the southbound and northbound lane with CRCP and JCP, respectively. The overlay thicknesses for the southbound lane are greater than for the northbound lane. This is caused by the 65 to 35 traffic split as mentioned previously. Tables 34 and 35 give the CRCP and JCP overlay cost, respectively. Figure 95 illustrates the cost-comparison by bar charts. The cost for CRCP overlay by "minimum condition" method is \$3,314,425 and by "variable thickness" method is \$3,220,416, a difference of \$94,009. The cost for the JCP overlay by "minimum condition" method is \$4,038,582 and by "variable thickness" method is \$3,942,537; a difference of \$96,045. A summary of the cost comparison is given in Table 33.

The cost comparisons were made using portland cement concrete pavement, therefore the difference in thickness between good and poor sections is not as great as would be the case for asphalt concrete pavement. Thus, the cost differential may be substantially greater for asphalt concrete pavement.

Table 33  
Summary of Results

Overlay Type	Design Alternatives	Total Cost, \$	Saving Cost, \$	Saving Cost (%)
CRCP	Min-Condition	3,314,425	94,009	2.9
	Var-Thickness	3,220,416		
JCP	Min-Condition	4,038,582	94,045	2.4
	Var-Thickness	3,942,537		

Thickness		E	$\mu$
To be determined	CRCP or JCP	$5 \times 10^6$	0.2
1.5"	Bond Breaker	$1.5 \times 10^5$	0.35
7 "	CRCP	$5 \times 10^6$	0.2
6.0"	Subbase	$1.0 \times 10^4$	} $4.5 \times 10^4$ 0.35
6.0"	Lime Stabilized Subgrade	$8 \times 10^4$	
$\alpha$		3300 2900 2400	0.45

1 in=2.54cm

Figure 92. Material properties and geometry of the pavement structure for the Walker County Analysis.

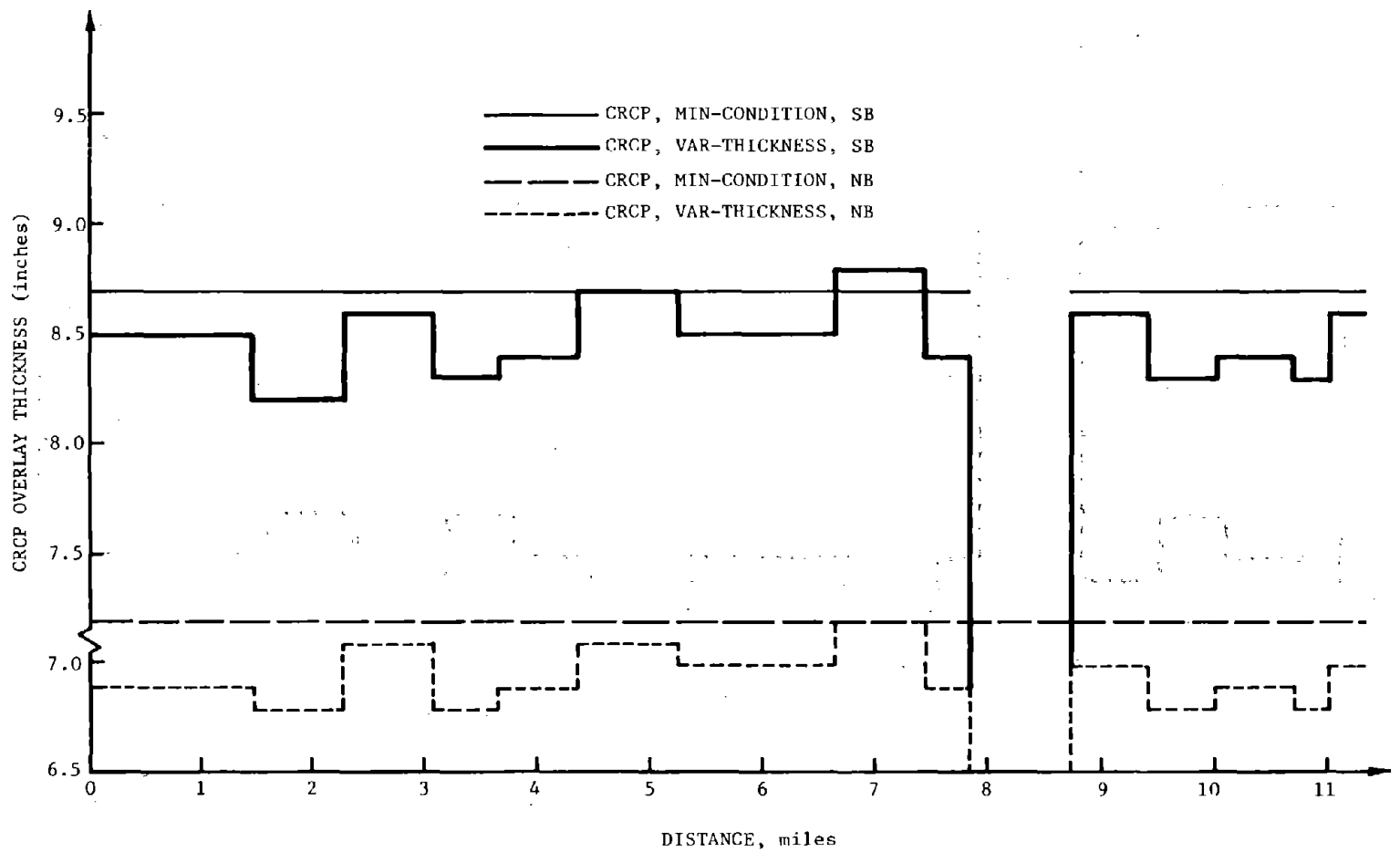


Figure 93. CRCP overlay thickness required along project.

1 mile=1.61km  
 1 in=2.54cm

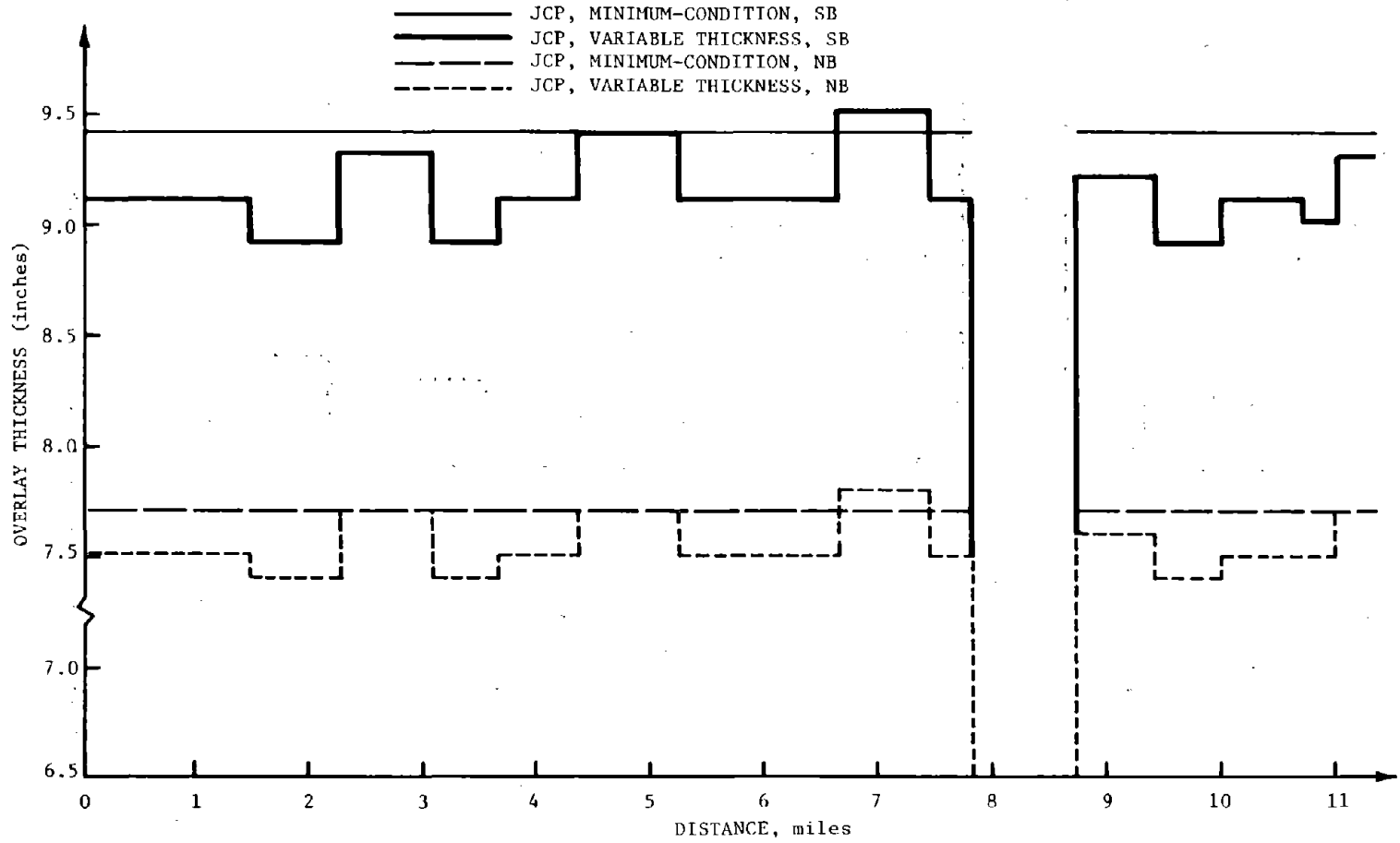


Figure 94. JCP overlay thickness required along project. 1 in=2.54cm  
1 mile=1.61km

Table 34. CRCP Overlay Cost

Test Section No.	Length Miles	Overlay Thickness (in.)		COST (Dollars)	
		NB	SB	NB	SB
1	1.45	6.9	8.5	198,627	244,685
2	0.80	6.8	8.2	107,999	130,234
3	0.80	7.1	8.6	112,764	136,587
4	0.60	6.8	8.3	80,999	98,867
5	0.70	6.9	8.4	95,889	116,734
6	0.90	7.1	8.7	126,859	155,447
7	1.40	7.0	8.5	194,557	236,248
8	0.80	7.2	8.8	114,352	139,763
9	0.40	6.9	8.4	54,794	66,705
10	0.70	7.0	8.6	97,279	119,514
11	0.60	6.8	8.3	80,999	98,867
12	0.70	6.9	8.4	95,889	116,734
13	0.30	6.8	8.3	40,500	49,433
14	0.35	7.1	8.6	49,334	59,757
Σ				1,450,841	1,769,575

Total Cost = 3,220,416

1 in=2.54cm  
1 mile=1.61km

Table 35 JCP Overlay Cost

Test Section No.	Length Miles	Overlay Thickness (in.)		COST (Dollars)	
		NB	SB	NB	SB
1	1.45	7.5	9.1	244,609	296,792
2	0.80	7.4	8.9	133,157	160,149
3	0.80	7.7	9.3	138,556	167,346
4	0.60	7.4	8.9	99,868	120,112
5	0.70	7.5	9.1	118,087	143,279
6	0.90	7.7	9.4	155,875	190,289
7	1.40	7.5	9.1	236,174	286,558
8	0.80	7.8	9.5	140,355	170,945
9	0.40	7.5	9.1	67,478	81,874
10	0.70	7.6	9.2	119,662	114,854
11	0.00	7.4	8.9	99,868	120,112
12	0.70	7.5	9.1	118,087	143,279
13	0.30	7.5	9.0	50,609	60,731
14	0.35	7.7	9.3	60,618	73,214
				Σ 1,783,003.	2,159,534

Total Cost = 3,942,537

1 in=2.54cm  
1 mile=161km

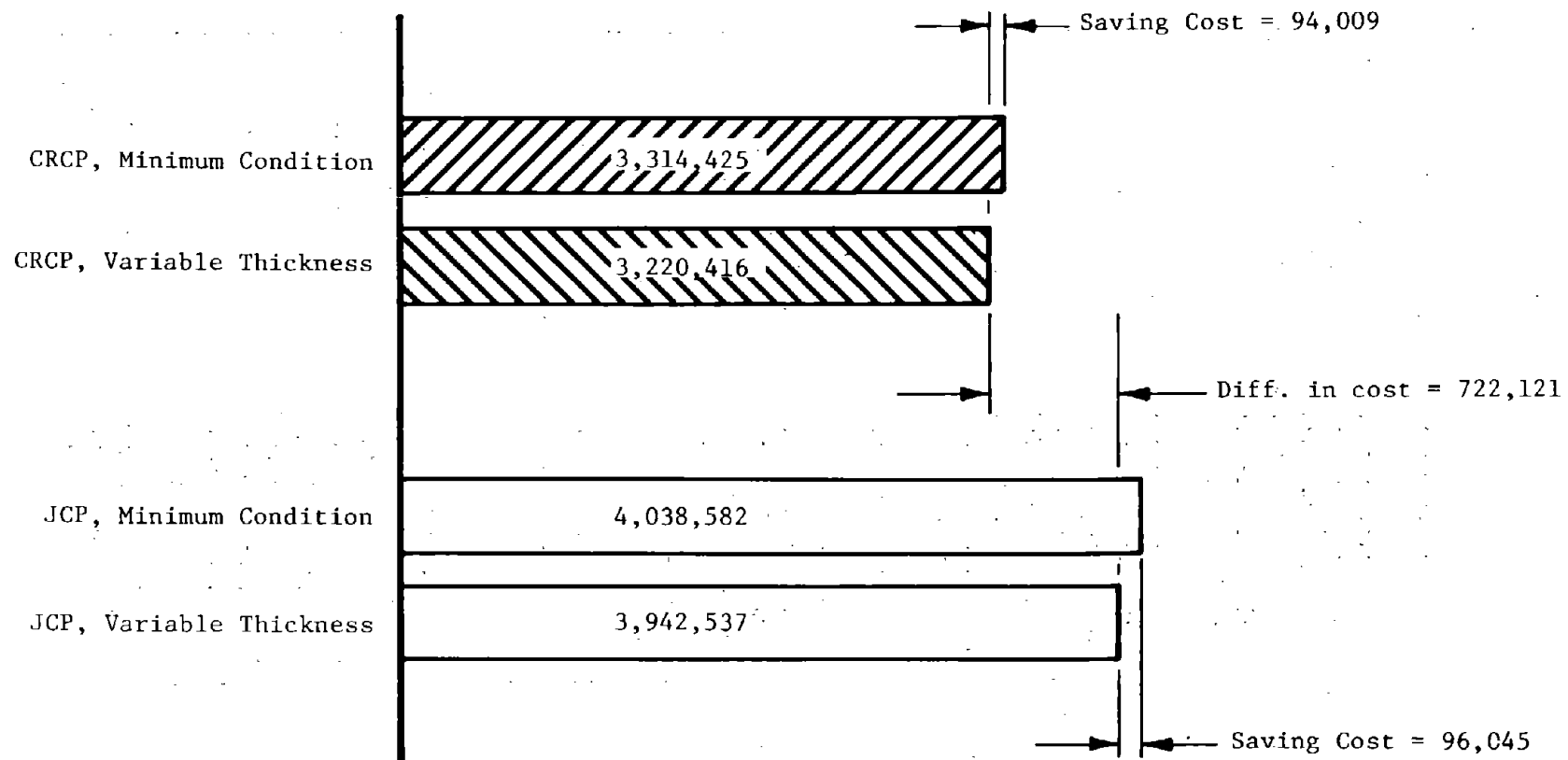


Figure 95. Comparison of total overlay cost for considering pavement type and design approach for Walker County Project, both lanes.



## Conclusions

From this study the following conclusions can be drawn:

1. The overlay cost by "variable thickness" and "minimum condition" method are about the same, the difference being about 3 percent. The difference in cost can be different from the value shown depending on the definition of minimum condition, i.e., if the weakest soil strength over the project were used, the cost difference could have been higher.
2. One important fact that the designer should keep in mind is that the "variable thickness" method recognizes the variability of the design factors along the roadway. Therefore the overlay thicknesses will conform to the structural needs, while the "minimum condition" uses one thickness for the entire eleven mile project which can result in over design in some sections and under design in other sections. Thus, the under designed sections will be the problem areas for the near future.

### Application of Reflection Cracking Model

Actual field projects were reviewed in an attempt to verify the procedure with real data. From this review, it was found that not enough data existed for any one project to predict field performance with any confidence. Therefore, only one of the projects reviewed, located in Walker County, Texas, will be discussed and described in this section. Also, selected variables used by the model which the user can control will be discussed in this section as to their effectiveness in reducing reflected cracks caused by both failure mechanisms. The results provide the user with an insight on how to determine the material property specification to produce the better performance.

#### Design Check - Walker Co.

The asphalt concrete overlay that was actually constructed on the section of IH-45 in Walker County, Texas, discussed in the previous section, was checked against the reflection cracking criteria presented in Chapter 4. The Walker County pavements consisted of an 8 inch (20.3cm) CRC pavement, previously discussed, and an 11-inch (27.9cm) plain jointed concrete pavement, both of which were overlayed at the same time and under the same conditions. The asphaltic concrete overlay exhibited reflection cracks on both concrete pavements, hence both were considered for evaluating the reflection cracking model.

No measurements exist to determine the percent load transfer for either pavement. Horizontal characterization measurements exist for the CRC pavement, but are not available for the jointed pavement. Therefore,

it was decided to calculate the subbase friction curve using the CRC pavement measurements and apply it to the jointed pavement because both have the same underlying layers.

In calculating the friction curve, all measurements and material properties were taken from References 10 and 110<sup>1</sup>. Measurements were taken at an early age when shrinkage was still occurring. Therefore, some error will exist in this calculation since the program assumes no shrinkage of the existing slab. The slope of the friction curve was computed to be 66,000 lb.(or 29,964kg)/in./ft. width of pavement.

The bonding stress between the concrete and overlay was not given or measured. Therefore, the surface condition of both pavements must be known to estimate this value. From field observations and photos, shown in Ref. 10, it was decided that the surface condition of the CRC pavement was rough containing some aggregate popouts. A bonding stress of 1,200 psi (8,280kN/m<sup>2</sup>) was selected to represent this condition for both pavements.

Thickness of the overlay varied for both pavements; 2-6 inches (5.1-15.2cm) for the CRC pavement and 4-16 inches (10.2-40.6cm) for the jointed pavement. The reflection cracking program was used to predict the tensile strains in the overlay material for each thickness (Figure 96).

In predicting tensile strains for the CRC pavement, an early crack spacing 16 feet (4.9m), had to be used because slab movement was not reported for the smaller crack spacings.

From field observations, reflection cracking was found to exist in all thicknesses for both existing pavement types. As observed in Figure 96, the tensile strain equals the allowable strain ( $1.7 \times 10^{-3}$  in./in.) ( $4.3 \times 10^{-3}$  cm/cm), at approximately 10 inches (25.4cm) for the jointed and CRC pavement. These results indicate that reflected cracks will develop for these thicknesses based on extreme environmental conditions. The results for both pavement types are very similar because they were characterized using the same friction curve, and horizontal measurements only existed for large crack spacings (16.6 feet) (5.06m) in the CRC pavement. Therefore, it would be expected that the overlay thickness-tensile strain relationship be similar for both existing pavement types. No measurements exist for smaller crack spacings, hence the percent of reflected cracks expected cannot be predicted for the CRC pavement. Reflected cracks formed for all thicknesses on the jointed pavement, therefore differential deflections must exist at joints, developing shearing strains which, when combined with tensile strains, exceed the allowable overlay strain resulting in reflected cracks.

---

<sup>1</sup>Shelby, M.D. and B. F. McCullough, "Determining and Evaluating the Stresses of an In-Service Continuously Reinforced Concrete Pavement," Report Number 62-1, Texas Highway Department, 1962.

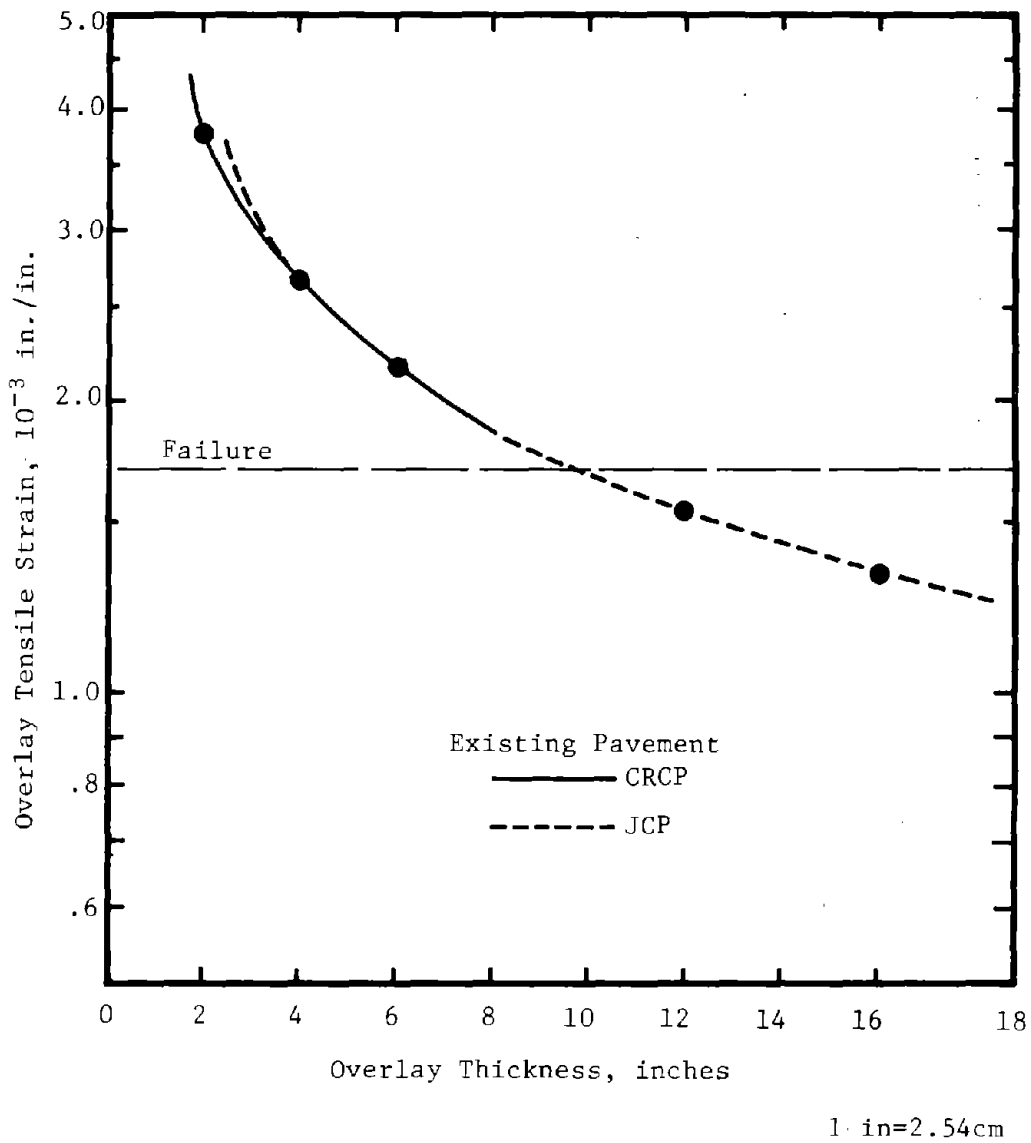


Figure 96. Tensile strain in the overlay material computed with Reflection Cracking model for the Walker Co. project based on extreme environmental conditions.

## Material Selection

The pavement structure and characterization input used for this analysis are the same as for the jointed concrete pavement described in the Walker County analysis. Various overlay material values are investigated to demonstrate usage of the model and illustrate how different materials can be used to reduce the severity of reflection cracks. For each design condition, the model can be applied in two ways: (1) Determine the tensile and shear strain for some specific design value (bond breaker width, modulus, thickness, etc.), or (2) determine at what design value the allowable overlay strain is exceeded. In this way, the user can determine if other techniques to reduce reflection cracking should be evaluated.

Temperature Differentials. The design temperature differential of the overlay is uncontrollable by the designer, but is dependent on the base temperature of the design mix. For this example a base temperature of 80°F. (26.7°C) was selected. Figure 97 illustrates the effect of temperature on the overlay tensile strain, computed by the model. As shown, reflection cracking resulting from tensile strain is very dependent on temperature, depending on the restraint coefficient, as was observed to be the case in Figure 32.

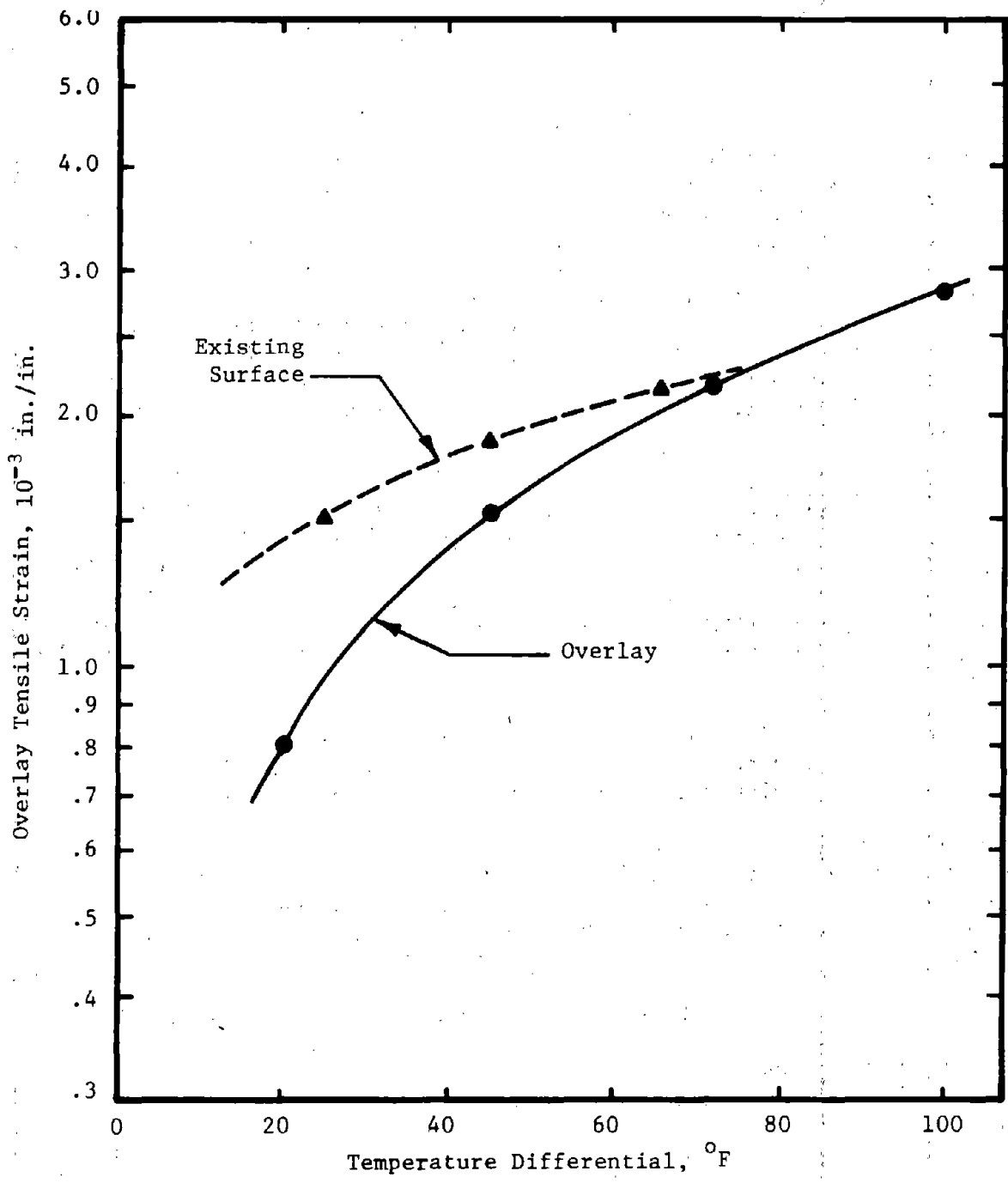
The insulating effect of the existing concrete slab is also shown in Figure 97. It is observed that reducing the temperature differential of the existing slab reduces the resulting overlay tensile strain.

For asphaltic concrete overlays shear strain is indirectly dependent on the temperature differential from the materials modulus-temperature relationship. Since only one parameter was changed for each comparison and load transfer versus crack width is not known, shear strain is predicted to be independent of temperature change.

Bond Breaker. The effects of using a bond breaker are graphically illustrated in Figure 98. As shown, the tensile strain is reduced because concrete movement is applied over a longer gage length. Shear strains are predicted to be independent of bond breaker width.

Overlay Modulus. Two different moduli are used by the model; creep and dynamic. The creep modulus pertains to horizontal thermal loadings, illustrated in Figure 99. As shown, the stiffer the overlay the smaller the tensile strain. The dynamic modulus is used in the calculation of the shearing strains, illustrated in Figure 99. As shown, the shearing strain decreases with a stronger overlay. It is recommended that this be checked from field or laboratory tests.

Overlay Reinforcement. Reinforcement is normally placed in a pavement not to stop cracking, but to control crack width. As shown in Figure 100, the reinforcement has only a very small effect on tensile strain, which



$\alpha_c = .5554 (^{\circ}\text{F}^{-1})$   
 1 in = 2.54 cm

Figure 97. Graphical illustration of the computed relationship between temperature differential of each layer and overlay tensile strain for the example considered.

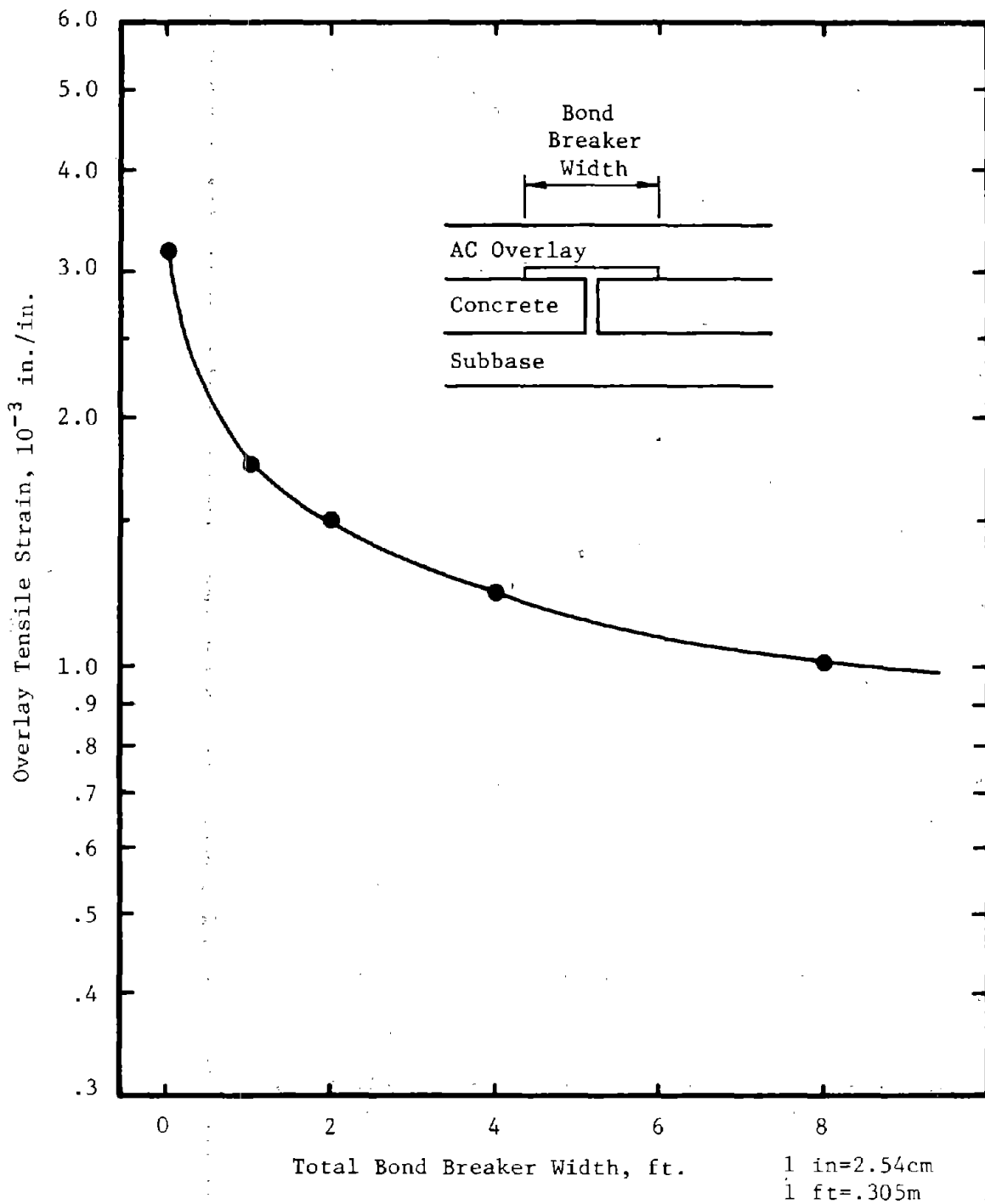


Figure 98. Graphical illustration of the computed relationship between bond breaker width and overlay tensile strain for the example considered.

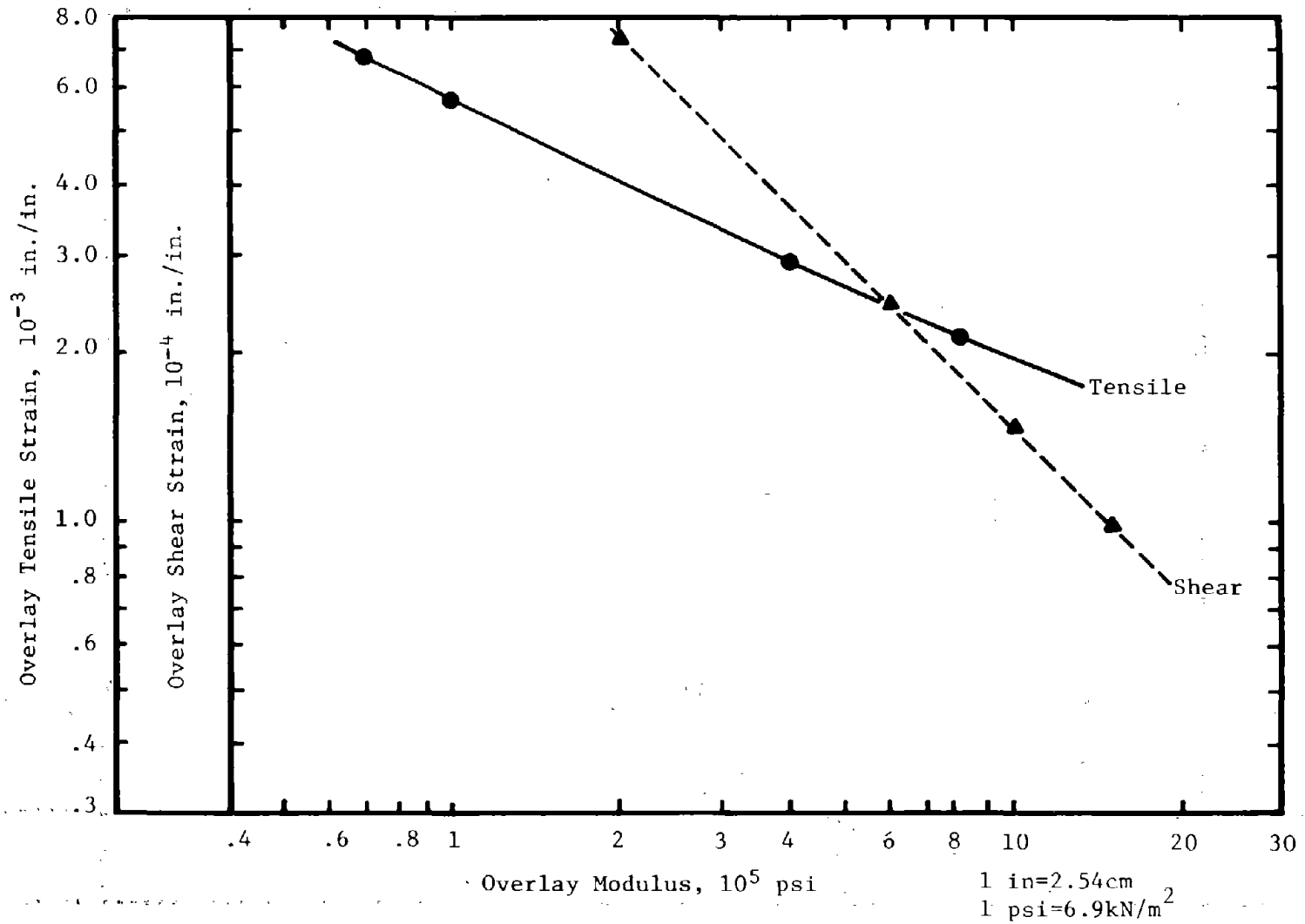


Figure 99. Graphical illustration of the computed relationship between the overlay modulus and overlay tensile and shear strain for the example considered.

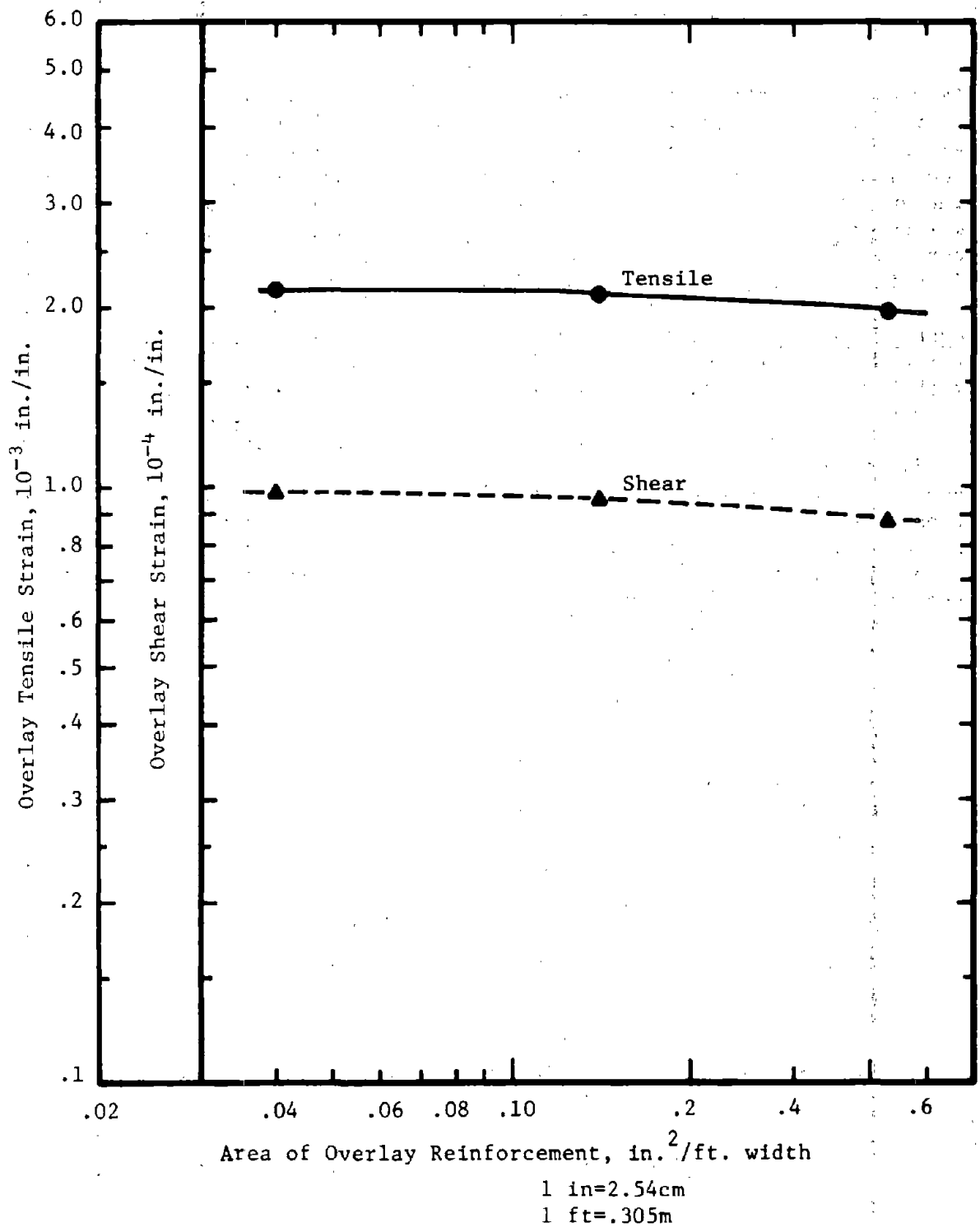
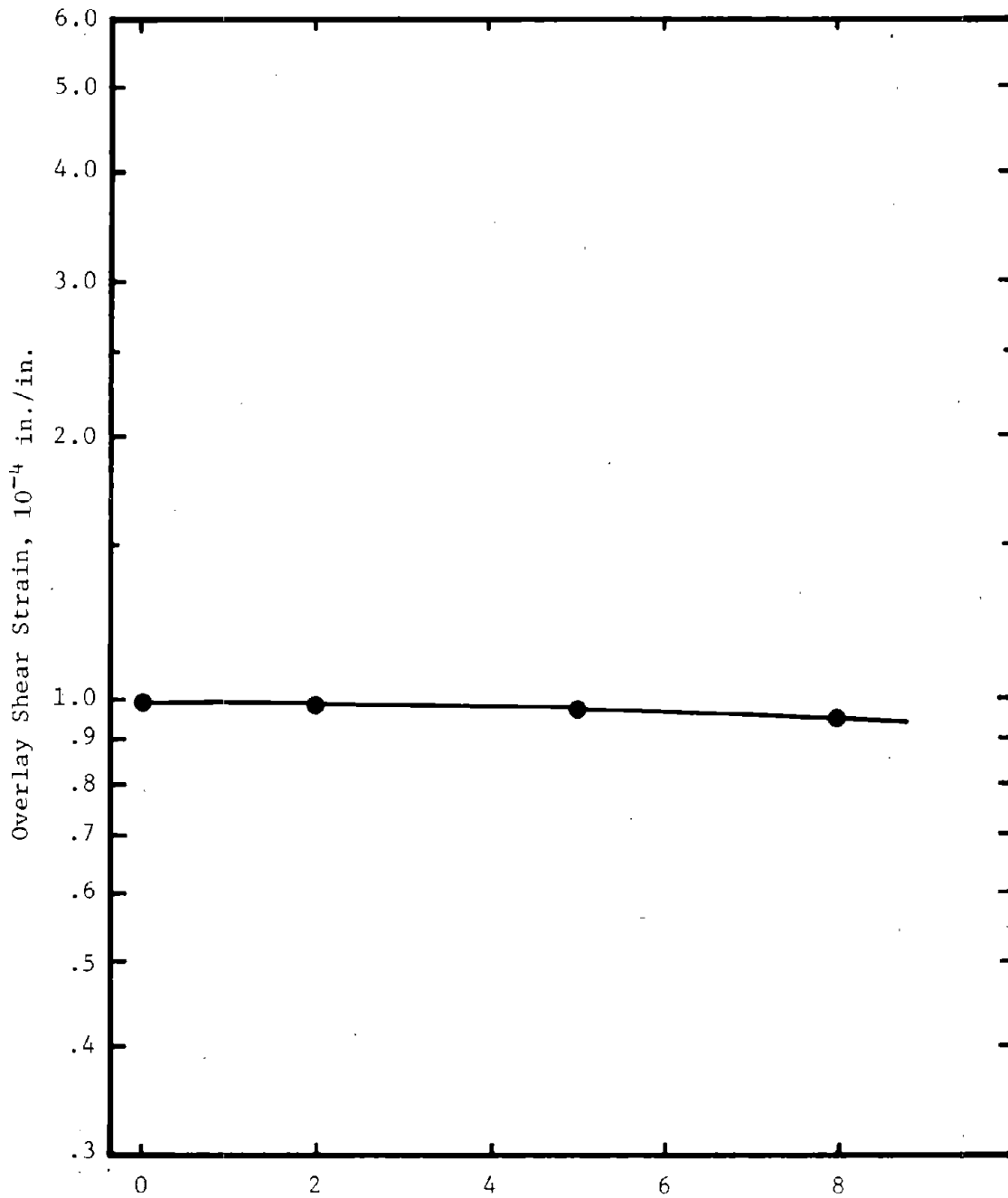


Figure 100. Graphical illustration of the computed relationship between reinforcement and overlay tensile and shear strains for the example considered.



is shown to be the case in Figure 45 between reinforced and nonreinforced sections. The shearing strain also decreases with an increase in the amount of overlay reinforcement. Although reinforcement is listed as a technique to reduce reflection cracking, it is predicted not to decrease the amount of cracking, but the severity of cracking. This could explain why corrosion has occurred within a short period of time in asphaltic concrete overlays. This observation should be checked as more information is obtained from field tests.

Cushion Course. A granular type cushion course is assumed to eliminate reflection cracks resulting from horizontal movements of the existing slab because it is assumed that no forces are transferred between the overlay and existing surface; unbonded overlay. The shearing strain is reduced by increasing the thickness of the cushion course as illustrated in Figure 101. A decrease in reflection cracking was observed to be the case in Figure 36 when a granular cushion course was used. The reflection cracking occurring for the no cushion condition (Figure 36) is probably associated with both failure mechanisms. Therefore some reflection cracking would be predicted to occur with a cushion course, where the shear strains exceed the allowable.



Thickness of Granular Cushion Course, in.  
 1 in=2.54cm

Figure 101. Graphical illustration of the computed relationship between thickness of a granular cushion course and overlay shearing strain for the example considered.

## CHAPTER 6

### SUMMARY, CONCLUSIONS AND RECOMMENDATIONS

The preceding chapters of this report have presented the concepts for a universal overlay design procedure for both flexible and rigid pavements, and the development of "working design" criteria for overlays of rigid pavements. The procedure is in a first generation and is subject to revision based on the outcome of actual use by designers over a period of time. The procedure and the resulting computer program have been developed in component parts and thus can be easily changed or expanded without major alterations to the basic concepts.

#### Summary

The design criteria developed in this project make very significant additions to and changes in the current state-of-the-art for overlay design of rigid pavements. The design procedure developed from the new criteria, which is presented in a user manual and reported under separate cover (Ref. 8), enables the design of asphaltic concrete, jointed PCC, and continuous PCC overlays for either jointed or continuous PCC pavements. There are two major design concepts included in the procedure: 1) design against fatigue cracking due to repeated wheel loads, and 2) design to reduce or minimize reflection cracking.

Elastic layered theory is the basic computational model for the fatigue analysis. It computes stresses and strains within the pavement system which are then input to a fatigue relation between stress or strain magnitude and repeated wheel load applications prior to cracking. The pavement overlay thickness that reduces the design stress or strain to a level that will allow the desired pavement life, is selected as the overlay design thickness.

Reflection cracking is analyzed through the use of a newly-developed mechanistic model which describes reflection cracking as a function of strength and creep properties of the existing materials, thicknesses of the pavement layers, volume changes due to temperature, friction forces between layers, and the width of stress relief layers. The overlay thickness as well as any other type of treatment necessary to reduce or minimize reflection cracking is selected based on these factors.

#### Conclusions

The newly developed criteria and resulting design procedure (Ref. 8), includes several concepts not previously used together before in overlay design. The use of these concepts adds a new positive dimension to the area of overlay design.

Perhaps the most basic of these new concepts is the use of elastic layered theory. It has not been previously used as part of a complete "working design procedure", even though it has become widely accepted as a very sound method of analyzing the state of stress and strain within a pavement system.

Another positive concept is the characterization of the existing pavement based on its actual structural capacity. This is accomplished by the use of nondestructive testing to determine the response of the pavement to load, in both the interior and at joints. Field measurements for the reflection cracking design and laboratory tests of existing pavement materials are also included in this phase of the procedure. A generally new type of testing is recommended for materials characterization. This is the use of repeated loading which places the material sample in conditions more similar to actual highway loading than some of the current and previously used empirical testing methods.

The design procedure includes all possible types of overlays on all types of existing rigid pavements. The fatigue analysis makes stress adjustments according to the type of existing pavement-overlay combination, joint condition as described by a ratio of measured interior to corner deflections, and the presence of voids beneath the existing pavement. Thus, the new criteria developed attempt to describe a very refined state of stress for use in the fatigue life determination.

The reflection cracking study was initially intended to be characterization and model development, but it was carried a step further and an algorithm was developed for use with experimental results to give an implementable design procedure. The confidence in the reflection cracking design is not yet as great as that in the fatigue design, but will be increased as improvements are made. Some more specific conclusions drawn from this project are as follows:

1. The design procedure was developed to provide a conceptual framework for future development. Attempts were made to use the best available techniques and theories with full recognition that a universal design procedure must be derived by iterative steps of improvement.

2. The overlay design computer program was developed in modular form. Thus component parts can be modified and improved as future research development warrants.

3. The limited verification of component models gives confidence to the overall model; e.g. the comparison of predicted and measured deflections was reasonably good.

4. Some new developments applied in the computer program are as follows:

- a. Stress to distress model based on fatigue cracking,
- b. Effect of the presence of voids on stress in pavement,
- c. Reflection cracking,
- d. Changing relation between stress and strain in the subgrade due to applied loadings, i.e. stress sensitive subgrade conditions, and
- e. Evaluation of joint load transfer and use in design

#### Recommendations

During the latter stages of the criteria development, ideas were formulated for improving certain areas of the design procedure. However, they were generally outside the scope of what could be accomplished in the first generation procedure. Some of these recommendations for improvement and implementation of the procedure are as follows:

1. Since the procedure is based on a summation of damage with time, it would be desirable and practical to conceptually modify it to permit seasonal variations to be included in the analysis. This would make the procedure more useful universally.
2. It would be desirable to have an improvement in the establishment of edge, corner, or interior loading conditions. In urban areas where curbs are used, the loading pattern is different from rural highways, i.e. there are no free corners, and there appears to be better performance with all other conditions being equal.
3. Stresses due to wheel loads and stresses due to temperature have been considered as individual components, but it would be an improvement to superimpose these stresses as new models are developed.
4. Substantial work could be directed toward future quantification of the void factors. The numbers used in the procedure are based on preliminary computer analyses and further research needs to be conducted in the field to establish void sizes that actually affect stress in the pavement.
5. The rutting model used for overlay design of flexible pavements considers the state of stress or strain in all layers of the pavement system. However, the fatigue and reflection cracking models deal with the stress or strain in only the existing surface or the overlay. It would be desirable to look at the contribution of other layers to fatigue and reflection cracking.

6. The reflection cracking model could be further verified and improved if more good field data were available.
7. Future effort needs to be directed toward the establishment of fatigue curves for new materials such as fibrous concrete and polymer concrete. With fatigue curves available it would then be relatively easy to include them as alternatives in the overlay analysis, since the basic design procedure framework permits their inclusion.

Recommendations for implementation of the design procedure are as follows:

1. An immediate implementation on a limited basis in the four environmental regions - hot and dry, cold and dry, hot and wet, cold and wet - would give an immediate guideline as to any modifications required for environmental factors. The implementation on a limited basis could be done in a state in each region. It would require working closely with state personnel in designing specific projects.
2. Design checks should be made on overlay projects that have been in service for several years and that have had before-overlay deflection measurements taken. These checks would give added confidence to the method.
3. Resilient modulus tests on a series of soils should be conducted, since the slope of the  $M_R$  vs. deviator stress relation can have an influence on the results. If it is possible that the soil mechanical properties could be correlated with the slope, then the laboratory testing could be reduced to a minimal effort.
4. The size and shapes of voids beneath concrete pavements have a major effect on stress and strain, and therefore also on performance. Studies of in-service pavements should be made to obtain practical information as to void sizes in the field and their possible correlation with soil types.

APPENDIX A

DERIVATION OF SELECTED REFLECTION CRACKING EQUATIONS

The following presents the derivation of selected equations used in the development of the reflection cracking model. Each will be derived using the same assumptions listed in the section on Model Development in Chapter 4.

Relationship Between Concrete and Steel Forces (Equation 32).

There are basically two regions in a reinforced concrete pavement; (1) the bonded zone and (2) the region where slippage occurs between the concrete and steel. It should be noted that the derivation of equation 32 is only applicable in the bonded region. Slippage between the concrete and steel can be defined by the following relationship.

$$G(x) = Y_c(x) - Y_s(x) = \int \epsilon_{cR}(x)dx - \int \epsilon_{sR}(x)dx \dots \dots \dots 71$$

where:

$\epsilon_{cR}$  = Relaxation strain of the concrete, in./in.(1 in=2.54cm)

$\epsilon_{sR}$  = Relaxation strain of the steel, in./in.(1 in=2.54cm)

$Y_s(x)$  = Movement of the steel at a distance x from the slab's center, inches.(1 in=2.54cm)

In the bonded region, movement of the concrete and steel are equal, therefore slippage does not occur. This implies that the relaxation strain of the two materials are equal.

$$Y_c(x) = \int_0^{X_s} \epsilon_{cR}(x)dx = \int_0^{X_s} \epsilon_{sR}(x)dx \dots \dots \dots 72$$

The actual strain in each material is computed by subtracting the relaxation strain from the theoretical thermal strain ( $\alpha_s \Delta T_s$ ) for the bonded portion of the slab.

$$\epsilon_c(x) = \alpha_c \Delta T_c - \epsilon_{cR}(x) \dots \dots \dots 73$$

$$\epsilon_s(x) = \alpha_s \Delta T_s - \epsilon_{sR}(x) \dots \dots \dots 74$$

where:

$\Delta T_s$  = Temperature difference of the steel and is assumed to be equal to  $\Delta T_c$ , °F

$\epsilon_c(x)$  = Actual strain in the concrete at a distance x from the slab's center, in./in.(1 in=2.54cm)

$\epsilon_s(x)$  = Actual strain in the steel at a distance x from the slab's center, in./in.(1 in=2.54cm)

Setting the relaxation strain for both materials equal (equations 73 and 74);

$$\alpha_s \Delta T_s - \epsilon_s = \alpha_c \Delta T_c - \epsilon_c \dots\dots\dots 75$$

Assuming both materials undergo the same temperature differential, and substituting an equivalent force for the existing strain of both materials results in the following relationship.

$$\alpha_s \Delta T_c - \frac{F_s}{E_s A_s} = \alpha_c \Delta T_c - \frac{F_c}{E_c A_c} \dots\dots\dots 76$$

Rearranging terms, results in equation 32 (Chapter 4):

$$F_c = F_s \frac{E_c A_c}{E_s A_s} + E_c A_c \Delta T_c (\alpha_c - \alpha_s)$$

The above equation is only applicable where the concrete and steel are bonded, assuming the materials behave elastically, undergo the same temperature differential and are in static equilibrium.

Concrete Force Prior to Characterization (Equation 41).

If the temperature change was zero, no thermal forces or concrete movement, forces still exist in the steel due to variables such as shrinkage. Therefore prior to characterization movements, the force in the steel at the crack can be computed by the following equation assuming static equilibrium.

$$F_{sc} (\Delta T_c = 0) = E_s A_s \frac{Y(T_H)}{2(l-X_s)} \dots\dots\dots 77$$

Assuming no thermal movements, the forces at the crack must be equal and opposite to the forces between the cracks.

$$\left[ F_{cB} + F_{sB} = F_{sc} \right] (\Delta T_c = 0) \dots\dots\dots 78$$



Frictional forces are not considered, since concrete movement is assumed to be zero prior to characterization. A relationship between concrete and steel, prior to characterization measurements, can be derived by substituting equation 32 into equation 78.

$$F_{cB}(\Delta T_c = 0) = \frac{F_{sc}(\Delta T_c = 0)}{1 + \frac{E_s A_s}{E_c A_c}} \dots \dots \dots 79$$

Bonding Stress Between Concrete and Steel (Equation 36).

Consider a section of reinforced concrete in which the steel reinforcement and concrete are subjected to varying stresses caused by temperature differentials.

where:  $\Delta \sigma_c A_c = \Delta \sigma_s A_s = \mu \pi d (\Delta x) \dots \dots \dots 80$

$\Delta \sigma_c$  = Change in concrete stress over the distance of  $\Delta x$ , psi (1 psi=6.9kN/m<sup>2</sup>)

$\Delta \sigma_s$  = Change in steel stress over the distance of  $\Delta x$ , psi (1 psi=6.9kN/m<sup>2</sup>)

$\mu$  = Bond stress uniformly distributed on the length  $\Delta x$ , psi (1 psi=6.9kN/m<sup>2</sup>)

$d$  = Diameter of a reinforcing bar per ft. width of pavement, in. <sup>2</sup>/ft. width (1 in=2.54cm) (1 ft=.305m).

As  $\Delta x$  approaches an infinitely small length the local bond stress  $\mu(x)$  becomes:

$$d\sigma_s A_s = \mu(x) \pi d dx \dots \dots \dots 81$$

A number of approximations have been proposed, based on experimental studies. Some of the simple expressions are listed below (Ref. 94):

$$\mu(x) = \bar{\mu} \dots \dots \dots 82$$

$$\mu(x) = 2\mu_m \frac{x}{2\ell} \dots \dots \dots 83$$

$$\mu(x) = \mu_m \sin \left( \frac{2\pi x}{2\ell} \right) \dots \dots \dots 84$$

where:

$\bar{\mu}$  = The average bond stress, psi(1 psi=6.9kN/m<sup>2</sup>)

$\mu_m$  = The maximum bond stress at the free end of the crack, psi (1 psi=6.9kN/m<sup>2</sup>)

The above equations describe the distribution of bond stress between adjacent cracks. Equation 82 was selected, for simplicity, to apply to the condition being evaluated. Tensile stress in concrete are maximum ( $\sigma_{CB}$ ) at  $x = 0$ , and zero at the cracks,  $x = \ell$ . Therefore, the following equilibrium condition must be satisfied:

$$\sigma_{CB} A_c = \pi d \int_0^{\ell} \mu(x) dx \dots\dots\dots 85$$

Substituting equation 82 and integrating results in:

$$\sigma_{CB} A_c = \pi d \bar{\mu} \ell \dots\dots\dots 86$$

This corresponds to an ultimate condition, maximum temperature change. If the concrete stress reaches its tensile strength and cracking is a result of temperature differentials or movement, then the average bonding stress can be determined by the following equation which is a slightly different form of equation 36.

$$\bar{\mu} = \frac{f_t A_c}{\ell \pi d}$$

Equation 36 is not totally applicable for the pavement condition being evaluated for the following reasons.

1. Bonding stress does not occur in the bonded region, where slippage does not occur.
2. Bonding forces are related to the frictional restraint forces, which were not considered in the development, through concrete movement.

Although application of equation 36 will result in some error, it is presented because bonding stresses which develop in pavements have not been adequately investigated.

Friction Curve Adjustment (Equation 45).

When an overlay is constructed over an existing pavement the total weight or normal force of the pavement system is increased. This can have various affects on the force-displacement curve as shown in Figures 102-107. Figures 102-105, which represent non-plastic materials, show the force required to move the slab is approximately increased proportionately with thickness or weight; mathematically explained by:

$$f_{F2} = f_{F1} \left[ 1 + \frac{D_2 - D_1}{D_1} \right] \dots\dots\dots 87$$

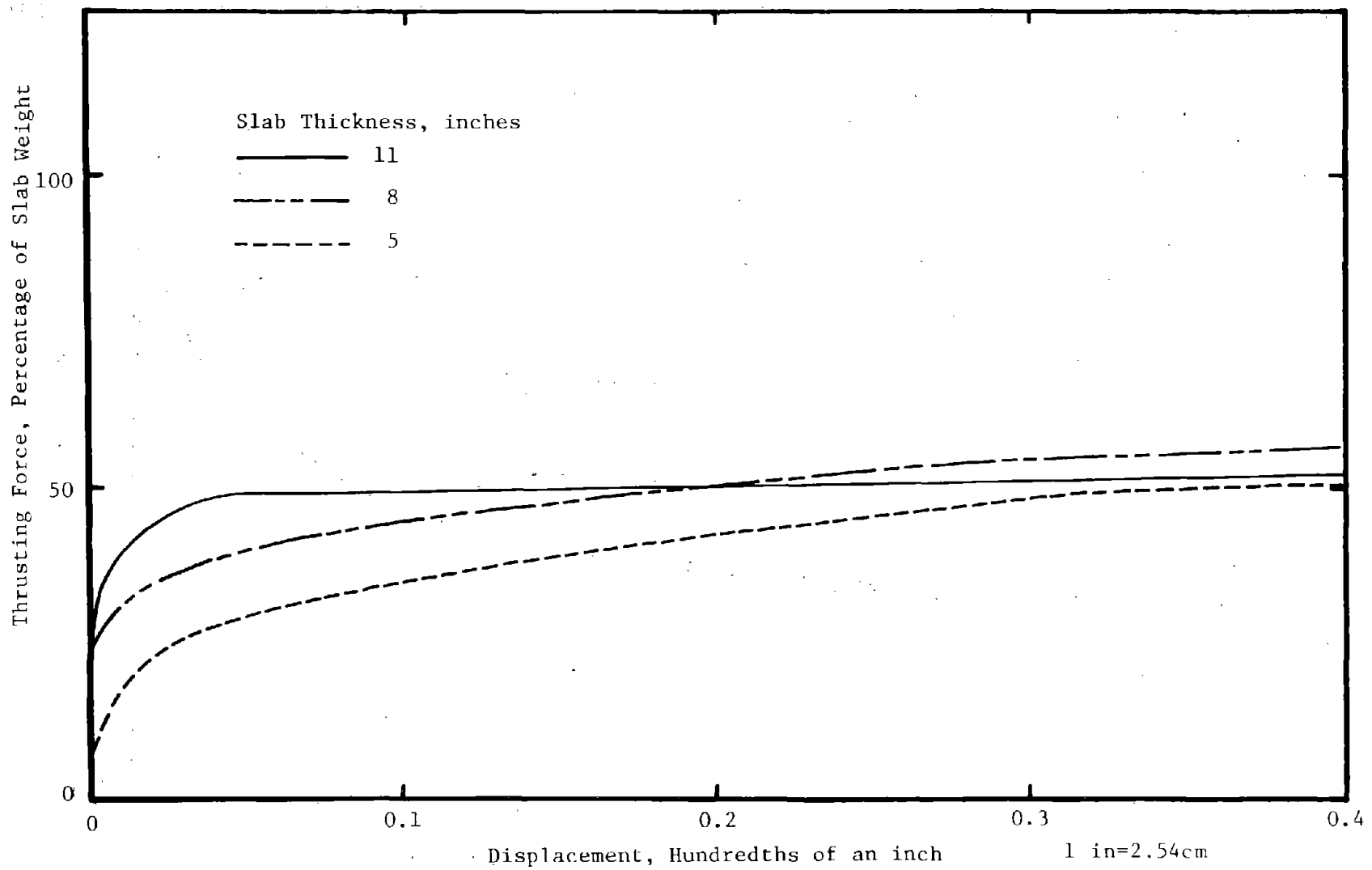


Figure 102. Force-displacement curves for concrete slabs on granular subbase with a sheet asphalt and a double layer of polyethylene sheeting (Ref. 89).

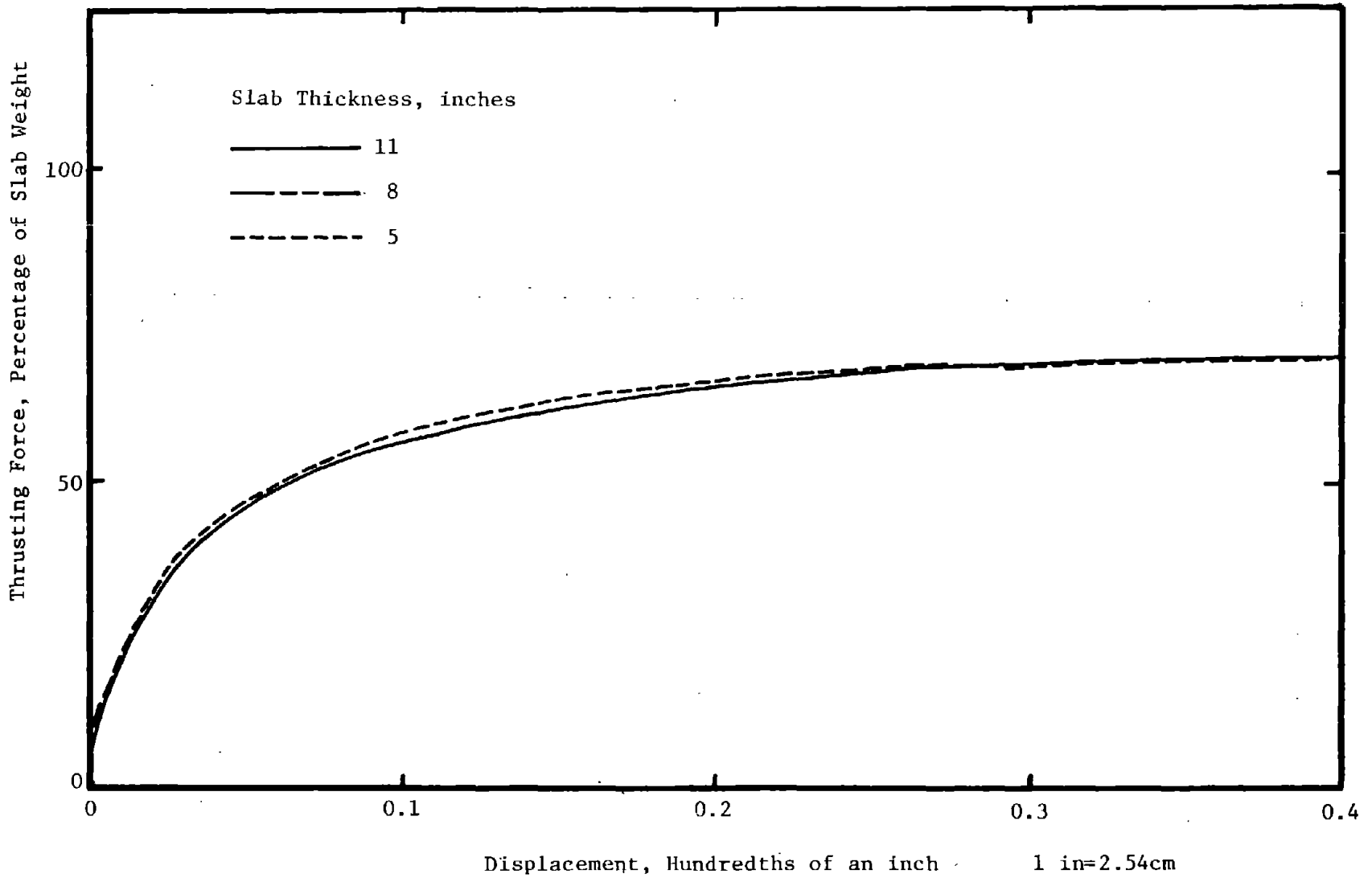


Figure 103. Force-displacement curves for concrete slabs on granular subbase plus one inch sand layer. (Ref. 89).

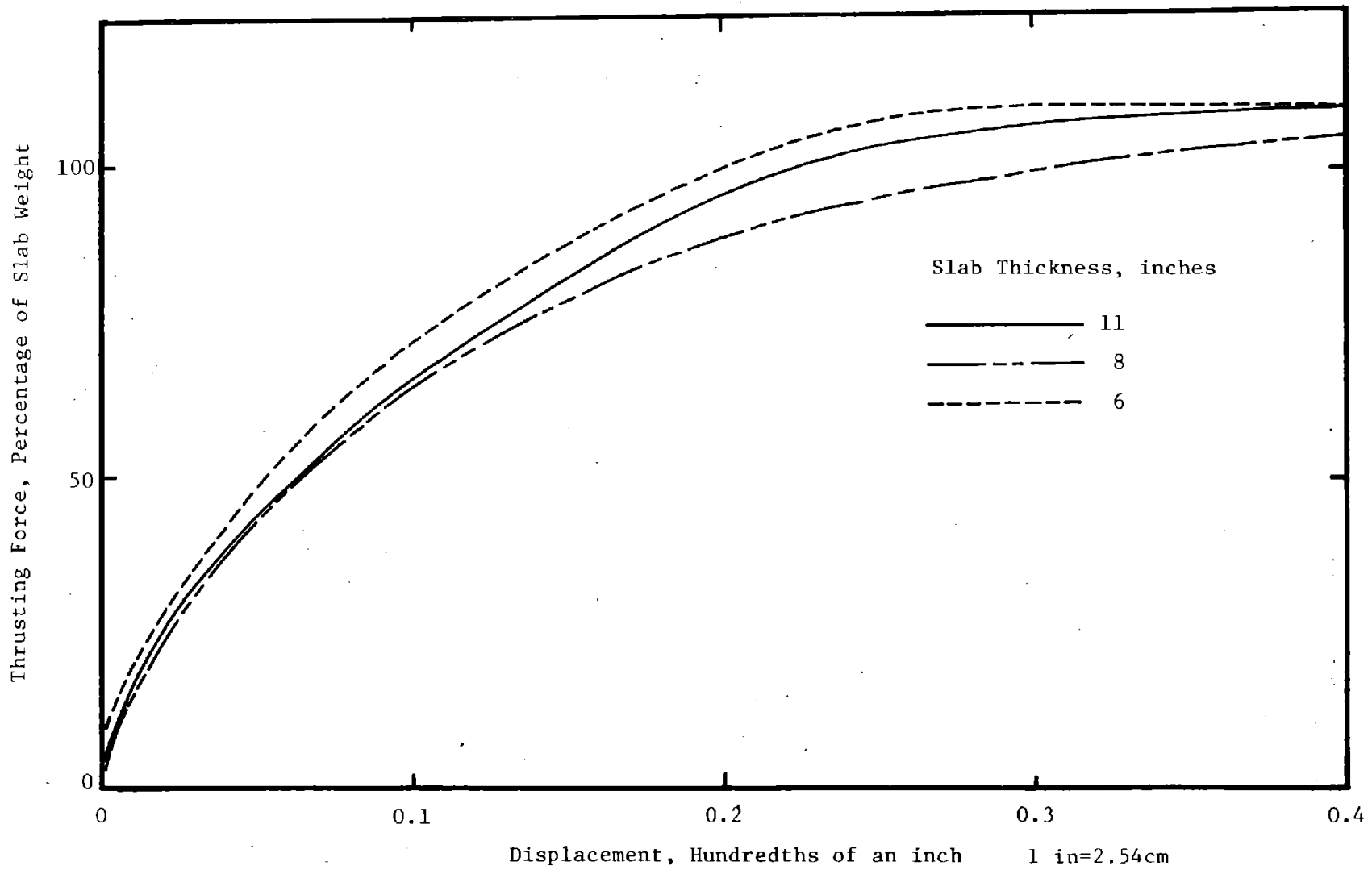


Figure 104. Force-displacement curves for concrete slabs on washed sand and gravel subbase (Ref. 89).

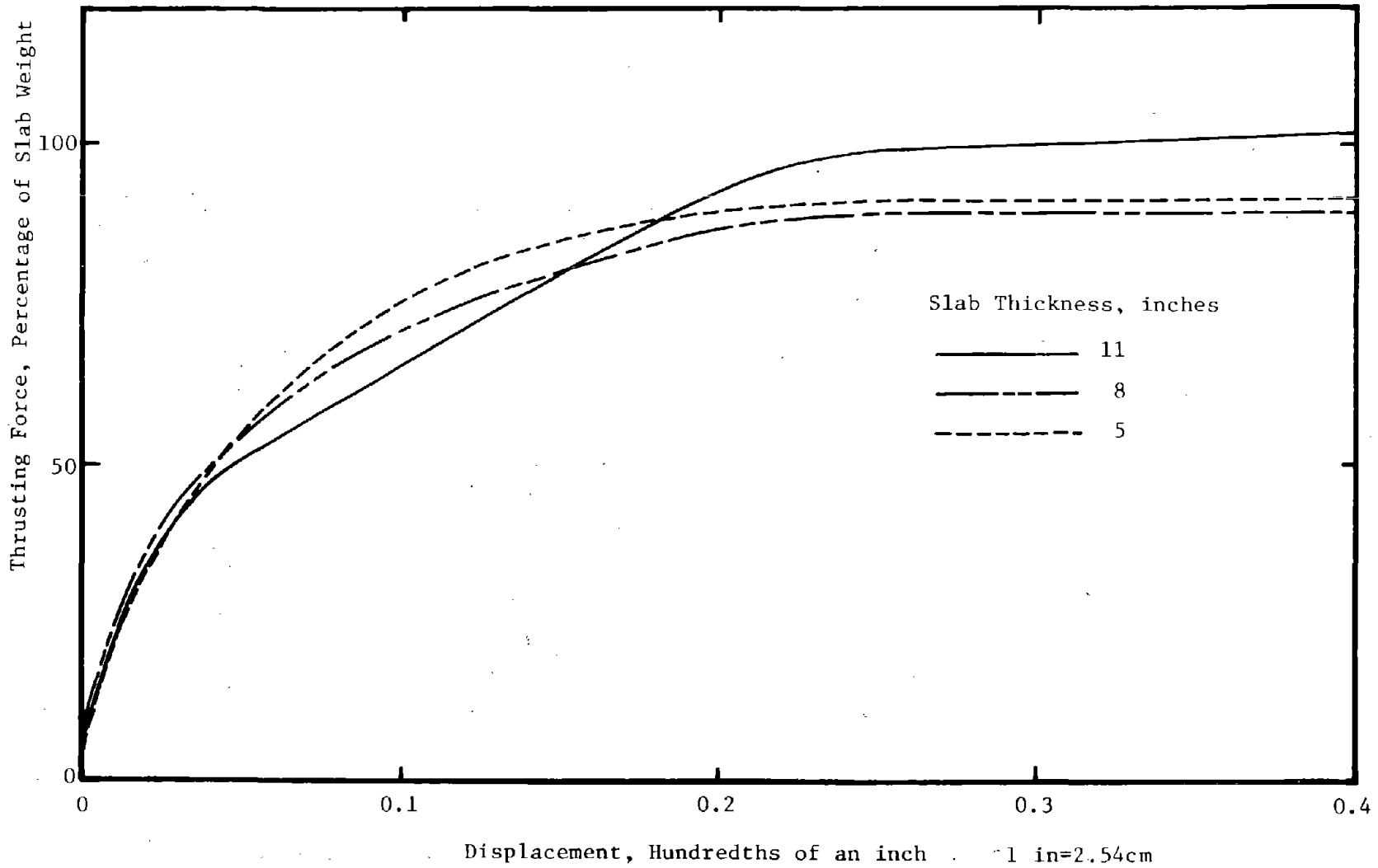


Figure 105. Force-displacement curves for concrete slabs on a granular subbase (Ref. 89).

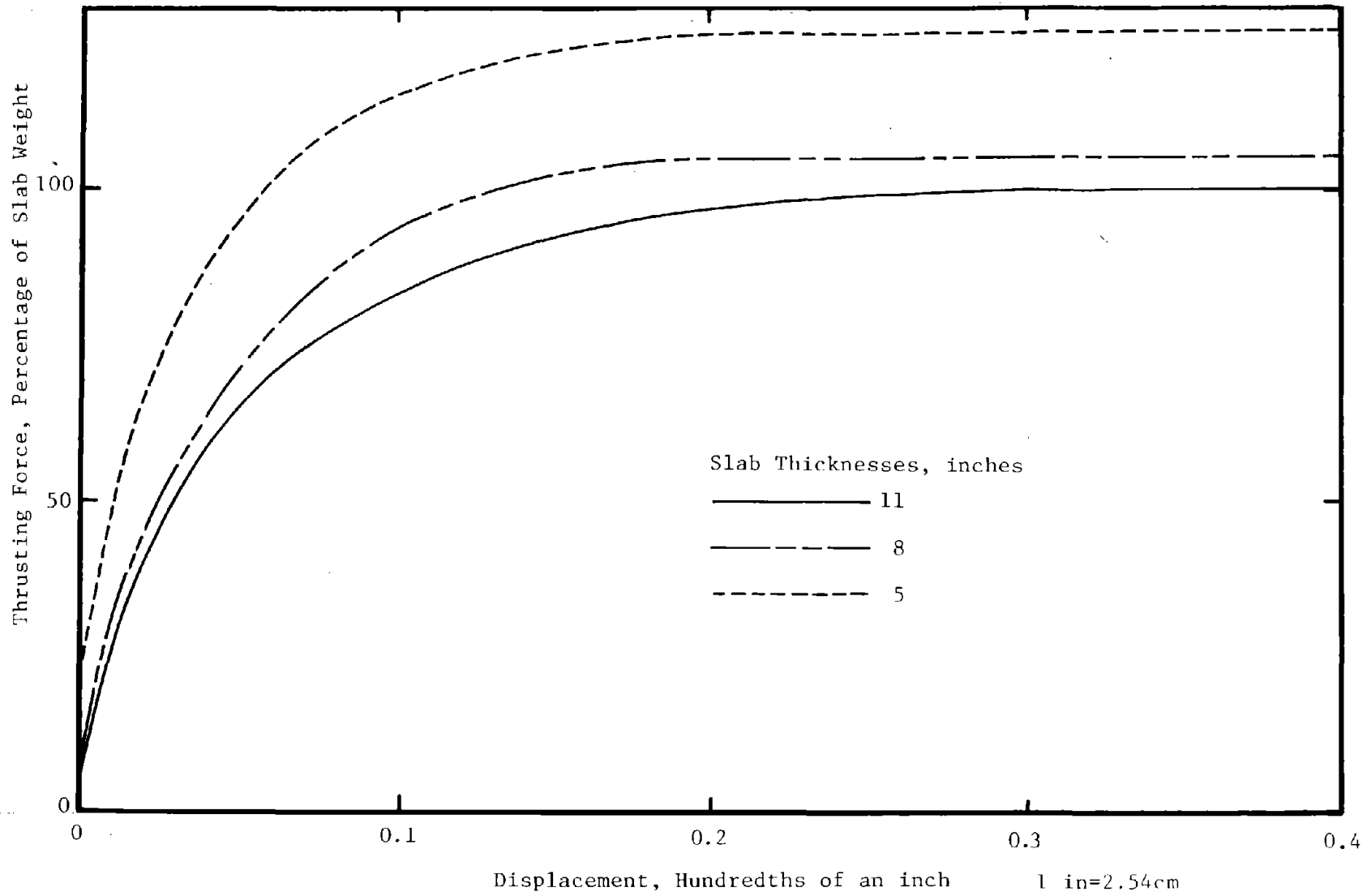


Figure 106. Force-displacement curves for concrete slabs on plastic soil (Ref.89 ).

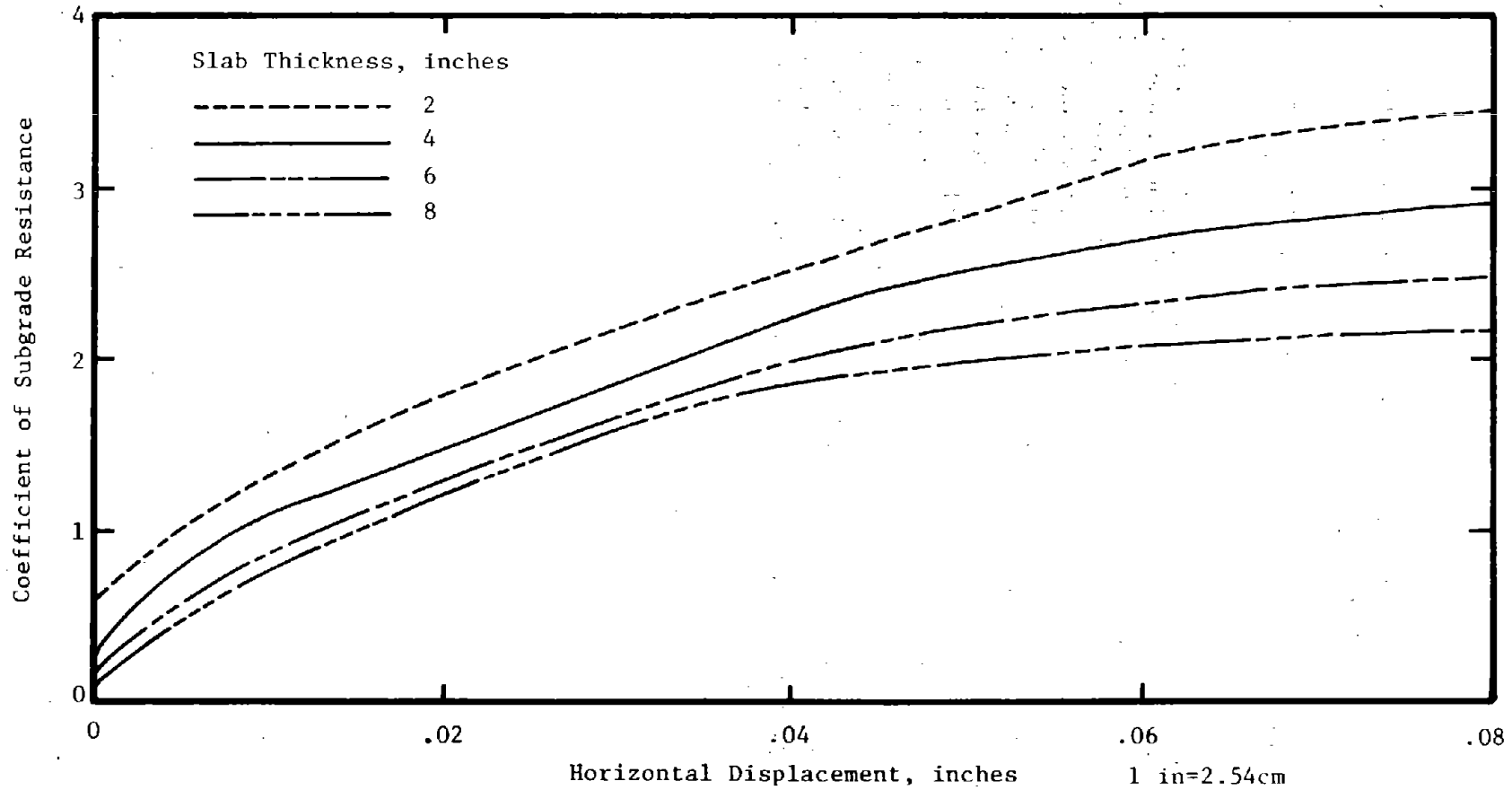


Figure 107. Force-displacement curves for concrete slabs on a silt loam soil (Ref. 111)



where:

$f_{F1}$  = Frictional restraint force at sliding for a slab  
thickness of  $D_1$ ,

$f_{F2}$  = Frictional restraint force at sliding for a slab  
thickness of  $D_2$ .

Figures 106-107 (Ref. 111)<sup>1</sup> (plastic materials) show no increase in the frictional resistance for slabs of different thickness, and therefore implies these weight effects are probably material dependent. This can be partially explained by examining Figure 108. The subgrade is found to participate in concrete movement to some degree, at various depths. The added weight of an overlay may be dissipated in the plastic material as shown by the subgrade movement curve. As the weight increases the subgrade movement at the interface also increases, thereby not having a linear increase in restraint forces with slab weight. This represents only a small amount of data to draw any conclusions and until more information can be obtained concerning friction curves, the slope, from the characterization process should be used in the overlay analysis for a conservative estimate or for plastic soils. If it is decided by the designer to consider the increase in pavement weight, equation 45 may be used for only non-plastic soils, to determine the slope of the friction curve for the overlay analysis.

$$m_o = m \left[ 1 + \frac{D_o \delta_o}{D_c \delta_c} \right]$$

---

<sup>1</sup>Kelley, E. F., "Application of the Results of Research to the Structural Design of Concrete Pavements," Public Roads, August 1939.

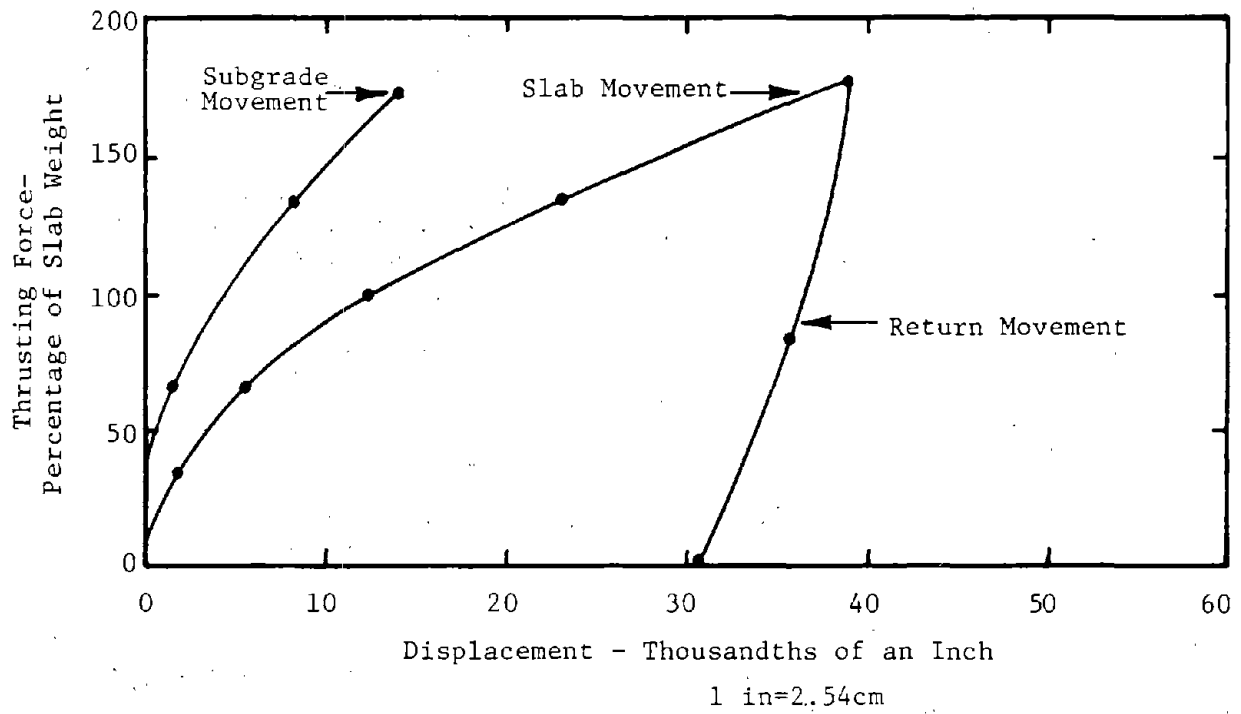


Figure 108. Relative movements of the concrete pavement and subgrade for a 6-inch (15.2cm) slab (Ref. 87).

## REFERENCES

1. "Pavement Rehabilitation Design Procedures" RFP-237, Federal Highway Administration, Washington, D.C., March 12, 1974.
2. "Pavement Rehabilitation: Proceedings of a Workshop", Federal Highway Administration Report No. FHWA-RD-74-60, June 1974.
3. Austin Research Engineers Inc, "Asphalt Concrete Overlays of Flexible Pavements - Volume 1, Development of New Design Criteria," Federal Highway Administration Report No. FHWA-RD-75-75, June, 1975.
4. McComb, Richard A. and John J. Labra, "A Review of Structural Evaluation and Overlay Design for Highway Pavements," Pavement Rehabilitation: Proceedings of a Workshop--Report No. FHWA-RD-74-60, June 1974.
5. The Design and Construction of Concrete Resurfacing for Old Pavements, PCS, NO. 1S 115.01P, 1965.
6. Design of Concrete Overlays for Pavements, ACI Journal, Vol. 64, 1967.
7. Hutchinson, R., Basis for Rigid Pavement Design for Military Airfields Corps of Engineers, Ohio River Div. Laboratories, Misc. Paper 5-7, May 1966.
8. Austin Research Engineers Inc, "Overlay Design and Reflection Cracking Analysis for Rigid Pavements, Volume 2--Design Procedures," Report FHWA-RD-77-76, August 1977.
9. Austin Research Engineers Inc, "Asphalt Concrete Overlays of Flexible Pavements, Volume 2 - Design Procedures" Report FHWA-RD-75-76, August 1975.
10. McCullough, B. F., "A Pavement Overlay Design System Considering Wheel Loads, Temperature Changes, and Performance," Institute of Transportation and Traffic Engineering Graduate Report, University of California, Berkeley, July 1969.
11. Warren, H. and W. S. Dieckman, "Numerical Computation of Stresses and Strains in a Multiple-Layered Asphalt Pavement System," California Research Company, September 1963.
12. "The AASHTO Road Test, Report 5, Pavement Research," Special Report 61E Highway Research Board, 1962.

13. Treybig, Harvey J., W. R. Hudson, and Adnan Abou-Ayyash, "Application of Slab Analysis Methods to Rigid Pavement Problems," Research Report 56-26, Center for Highway Research, University of Texas, May 1972.
14. Ahlborn, Gale, "Elastic Layered System with Normal Loads," The Institute of Transportation and Traffic Engineering, University of California, Berkeley, California, May 1972.
15. Westergaard, H. M., "Theory of Concrete Pavement Design," Proceedings Highway Research Board, 1927.
16. Pickett, Gerald, M. E. Raville, W. C. Jones, and F. J. McCormick, "Deflections, Movements and Reactive Pressures for Concrete Pavements," Kansas State College Bulletin No. 65, October 1951.
17. Mills, R. E., and R. F. Dawson, "Fatigue of Concrete," Proceedings, Seventh Annual Meeting, Highway Research Board, Washington, D.C., 1928, pp. 160-172.
18. "AASHTO Interim Guide For Design of Pavement Structures," American Association of State Highway and Transportation Officials, 1972.
19. "The AASHTO Road Test Report 3, Traffic Operation and Pavement Maintenance," Special Report 61C, Highway Research Board, Washington, D.C., 1962.
20. Yimprassert, Piti, and B. Frank McCullough, "Fatigue and Stress Analysis Concepts for Modifying the Rigid Pavement Design System," Research Report 123-16, Center For Highway Research, University of Texas at Austin, January 1973.
21. "The AASHTO Road Test, Proceedings of a Conference held May 16-18, 1962, St. Louis, Mo.," Special Report 73, Highway Research Board, Washington, D.C., 1962.
22. Hudson, W. R., and F. H. Scrivner, "AASHTO Road Test Principal Relationships-Performance with Stress Rigid Pavements," Special Report 73, Highway Research Board, Washington, D.C., 1962.
23. Treybig, Harvey J., B. Frank McCullough, and W. Ronald Hudson, "Tests on Existing Pavements and Synthesis of Design Methods," Vol. I, CRC Airfield Pavements, Air Force Weapons Laboratory, December 1973.

24. Vesic, Alexander S., and Surenda K. Saxena, "Analysis of Structural Behavior of Road Test Rigid Pavements, NCHRP Project 1-4 (1), National Cooperative Highway Research Program, 1968.
25. DePuy, G. W., "Highway Applications of Concrete Polymer Materials," Transportation Research Board No. 542, Transportation Research Board, 1975.
26. Kubacka, L. E., J. Fontana, and M. Steinberg, "Polymer Concrete For Repairing Deteriorated Bridge Decks," Transportation Research Board No. 542, Transportation Research Board, 1975.
27. Fowler, David W., James T. Houston, and Donald R. Paul, "Polymer-Impregnation Concrete For Highway Applications," Research Report 114-1, Center For Highway Research, University of Texas at Austin, February 1973.
28. Mehta, H. C., W. F. Chen, J. A. Manson, and J. W. Vanderhoff, "Innovations In Impregnation Techniques For Highway Concrete," Transportation Research Board No. 542, Transportation Research Board, 1975.
29. Parker, Frazier, Jr., "Steel Fibrous Concrete For Airport Pavement Applications," U.S. Army Engineer Waterways Experiment Station, Report No. FAA-RD-74-31, November 1974.
30. Sherman, George B., "Reflection Cracking," Pavement Rehabilitation: Proceedings of a Workshop, Report No. FHWA-RD-74-60, Federal Highway Administration, June 1974.
31. "Preventing Reflection Cracks With An Asphalt Crack - Relief Layer," Construction Leaflet No. 16, The Asphalt Institute, December 1976.
32. Bone, A. J., and L. W. Crump, "Current Practices and Research on Controlling Reflection Cracking," Highway Research Board Bulletin 123, Highway Research Board, 1956.
33. Bone, A. J., and Crump, L. W., and Roggeveen, V. J., "Control of Reflection Cracking in Bituminous Resurfacing over Old Cement-Concrete Pavements." Proceedings, Highway Research Board, Vol. 33 (1954).

34. Davis, M. M., Reflection Cracks in Bituminous Resurfacing. Report 12, Ontario Joint Highway Research Programme, University of Toronto, July 1960.
35. Finn, F. N., K. Nair, and J. Hilliard, "Minimizing Premature Cracking of Asphalt Concrete Pavements," Prepared for 1976 Annual Meeting of the AAPT, Woodward-Clyde Consultants, February 1976.
36. "Pavement Rehabilitation: Materials and Techniques," NCHRP Synthesis of Highway Practice No. 9, Highway Research Board (1972).
37. Way, George, "Prevention of Reflection Cracking in Arizona Minnetonka-East (A Case Study)," Federal Highway Administration Report No. FHWA-AZ-HPR-224, Arizona Department of Transportation-Phoenix, Arizona, May 1976.
38. Kanarowski, Stanley M., "Study of Reflection Cracking in Asphaltic Concrete Overlay Pavements - Phase I" Report No. AFWL-TR-71-142, U.S. Army Engineer Construction Engineering Research Laboratory, Air Force Weapons Laboratory Kirtland AFB, New Mexico, March, 1972.
39. Safford, Mark and Phil McCabe, "Reflection Cracking in Bituminous Overlays," Interim Report No. CDOH-P&R-R&SS-72-1, Colorado Division of Highways - Denver, Colorado, December 1971.
40. McCullagh, Frank R., "Reflection Cracking of Bituminous Overlays on Rigid Pavements," Special Report 16, Engineering Research and Development Bureau, New York State Department of Transportation, February 1973.
41. McGhee, K. H., "Efforts to Reduce Reflective Cracking of Bituminous Concrete Overlays of Portland Cement Concrete Pavements," Virginia Highway & Transportation Research Council, VHTRC 76-R20, November 1975.
42. Brownridge, F. C., "An Evaluation of Continuous Wire Mesh Reinforcement in Bituminous Resurfacing," AAPT Proceedings, Vol. 33 (1964).
43. Tons, E., Bone, A. J., and V. J. Roggeveen "Five Year Performance of Welded Wire Fabric in Bituminous Resurfacing," Highway Research Board Bulletin 290, Highway Research Board, 1961.
44. Roggeveen, V. J., and E. Tons, "Progress of Reflection Cracking in Bituminous Concrete Resurfacing," Highway Research Board Bulletin 131, Highway Research Board, 1956.

45. Wood, William A., "Methods of Minimizing Reflection Cracking In Bituminous Overlays," FHWA Notice N 5140.9, A paper presented at the 34th annual meeting of SASHTO - Myrtle Beach, South Carolina, January 1976.
46. Ludwig, A. C. and Pena, L. N. Jr., "The Use of Sulphur to Control Reflective Cracking," Air Force Civil Engineer, Volume 10, No. 4, November 1969.
47. Kipp, O. L., and C. R. Preus, "Minnesota Practices on Salvaging Old Pavements by Resurfacing," Proceedings, Highway Research Board, Vol. 30 (1950).
48. Lyon, J. W., "Heavy Pneumatic Rolling Prior to Overlay: A 10-Year Project Report," Highway Research Record No. 327, Highway Research Board, 1970.
49. Korfhage, G. R., "The Effect of Pavement Breaker-Rolling on the Crack Reflectance of Bituminous Overlays," Highway Research Record No. 327, Highway Research Board, 1970.
50. Lyon, James W. Jr., "Slab Breaking and Seating on Wet Subgrade With Pneumatic Roller," Highway Research Record 11, Highway Research Board, 1963.
51. Smith, L. L. and W. Gartner, "Welded Wire Fabric Reinforcement for Asphaltic Concrete," Highway Research Board Bulletin No. 322, Highway Research Board, 1962.
52. Velz, P. G., "Effect of Pavement Breaker Rolling on Crack Reflectance in Bituminous Overlays," Highway Research Board Bulletin No. 290, Highway Research Board, 1961.
53. Stackhouse, J. L., "Seating Old Pavements with Heavy Pneumatic-Tired Rollers Before Resurfacing," Highway Research Board Record 11, Highway Research Board, 1963.
54. Billingsley, N. A., "Salvaging Old Pavements by Resurfacing," Highway Research Circular 43, 1966.
55. Vicelja, J. L., "Methods to Eliminate Reflection Cracking in Asphalt Concrete Resurfacing Over Portland Cement Concrete Pavements," Proceedings, AAPT, Vol. 32 (1963).
56. Perry, B. F., "Subsealing of Concrete Pavements," HRB Bulletin No. 322, Highway Research Board, 1962.

57. "Specifications for Undersealing Portland Cement Concrete Pavements With Asphalt," Specification Series No. 6, The Asphalt Institute, December 1966.
58. "Mudjacking-Slabjacking-Limejacking-Subsealing," Maintenance Aid Digest, MAD 2, Federal Highway Administration, April 1971.
59. Fahnestock, T. V., and R. L. Davis, "A New Approach to Subsealing," Highway Research Record No. 11, Highway Research Board, 1963.
60. Slater, Don, "Washington's Shoulder Mud-Jacking Rescues Depressed Pavements," Rural and Urban Roads, January 1977.
61. Carey, Donald E., "Evaluation of Synthetic Fabrics for the Reduction of Reflective Cracking," Report No. 70-1B (B), Research and Development Section, Louisiana Department of Highways - Baton Rouge, Louisiana, April 1975.
62. McDonald, E. B., "Reduction of Reflective Cracking by Use of Impervious Membrane," South Dakota Department of Highways - Pierre, South Dakota.
63. "Reinforcing Fabric For Bituminous Seal Coat," Research Project No. 73-20 (2), Bureau of Materials, Testing and Research, Pennsylvania Department of Transportation.
64. Morris, Gene and Charles McDonald, "Asphalt-Rubber Stress Absorbing Membranes and Recycled Tires," Rural and Urban Roads, August, 1976.
65. Galloway, B. M., "Use of Rubber Aggregate in a Stress Relieving Interlayer for Arresting Reflection Cracking of Asphalt Concrete Pavements," Proceedings, International Symposium on Use of Rubber in Asphalt Pavements, 1971.
66. Copple, F., and L. T. Oehler, "Michigan Investigation of Soil Aggregate Cushions and Reinforced Asphaltic Concrete for Preventing or Reducing Deflection Cracking of Resurfaced Pavements," Highway Research Record No. 239, Highway Research Board, 1968.
67. Stackhouse, J. L., "Preparing Old Pavements for Resurfacing with 50-Ton Compactor," HRB, Proceedings, Vol. 38 (1959).
68. Johnson, Robert D., "Thin Overlay Bituminous Macadam for the Control of Reflex Cracking," Highway Research Record 150, Highway Research Board, 1966.



69. Zube, E., "Wire Mesh Reinforcement in Bituminous Resurfacing," Highway Research Board Bulletin 131, Highway Research Board, 1956.
70. Busching, H. W., Elliott, E. H., and Reyneveld, N. G., "A State of the Art Survey of Reinforced Asphalt Paving," Proceedings, AAPT Vol. 39 (1970).
71. "Wire Mesh Reinforcement of Bituminous Concrete Overlays," Bur. of Phys. Res., Res. Report 66-1, New York State Dept. of Public Works, October 1966.
72. Chastain, W. Jr., and R. H. Mitchell, "Evaluation of Welded Wire Fabric in Bituminous Concrete Resurfacing," Highway Research Record No. 61, Highway Research Board, 1963.
73. Smith, Richard D., "Prevention of Reflection Cracking in Asphalt Overlays with Structofors, Petromat, and Cerex," Project HR-158, Iowa Highway Research Board, May 1977.
74. Tuckett, G. M., Jones, G. M., and Littlefield, G., "The Effects of Mixture Variables on Thermally Induced Stresses in Asphalt Concrete," Proceedings, AAPT, Vol. 39 (1970).
75. Roberts, S. E., "Cracks in Asphalt Resurfacing Affected by Cracks in Rigid Bases," Proceedings, Highway Research Board, Vol. 33 (1954).
76. Wortham, G. R., and L. M. Hatch, "Asbestos Fiber as a Filler in a Plant-Mix Pavement," Research Project No. 24, Idaho Department of Highways, December 1969.
77. Mellott, Dale B., "Asbestos Fibers in ID-2A Bituminous Concrete-Phase II, Research Project No. 70-12, Pennsylvania Department of Transportation, Bureau of Materials, Testing and Research, October 1975.
78. Blackhurst, M. W., Foxwell, J. A., and Kietzman, J. H., "Performance of Asbestos Asphalt Pavement Surface Courses with High Asphalt Contents," Highway Research Record 24, Highway Research Board, 1963.
79. Zuehlke, G. H., "Marshall and Flexural Properties of Bituminous Pavement Mixtures Containing Short Asbestos Fibers," Highway Research Record 24, Highway Research Board, 1963.

80. James, J. G., "A Full Scale Road Experiment with Rubberized Asphalt on Concrete Using Expanded Metal Over the Concrete Joints," Road Research Laboratory Note 3511.
81. Carroll, J. A., and Diller, D. G., "Use of Rubberized Asphalt to Control Reflection Cracking in Asphalt Concrete Overlays," Proceedings, International Symposium on Use of Rubber in Asphalt Pavements, 1971.
82. Gould, V. G., "Summarized Committee Report 1948-1960: Salvaging Old Pavements by Resurfacing," HRB Bulletin No. 290, Highway Research Board, 1961.
83. Van Breeman, William, "Discussion of Possible Designs of Composite Pavements," Highway Research Record 37, Highway Research Board, 1963.
84. Housel, William S., "Design, Maintenance and Performance of Resurfaced Pavements at Willow Run Airfield," Highway Research Board Bulletin 322, Highway Research Board, 1962.
85. Ramsamooj, D. V., "Prediction of Reflection Cracking in Pavement Overlays," Highway Research Record No. 434, Highway Research Board, 1973.
86. Luther, Michael, S., Kamran Majidzadeh, and Che-Wei Chang, "Mechanistic Investigation of Reflection Cracking of Asphalt Overlays," Transportation Research Record No. 572, Transportation Research Board, 1976.
87. Teller, L. W. and Earl C. Sutherland, "The Structural Design of Concrete Pavements," Bureau of Public Roads, November 1935.
88. "Mass Concrete for Dams and Other Massive Structures," Journal of the American Concrete Institute, Proceedings, Vol. 67, April 1970.
89. Timms, A. G., "Evaluating Subgrade Friction-Reducing Mediums for Rigid Pavements," Structural Division, U. S. Bureau of Public Roads.
90. Hudson, W. R., B. F. McCullough, Adam Abou-Ayyash, and Jack Randall, "Design of Continuously Reinforced Concrete Pavements for Highways," Research Project NCHRP 1-15, Center for Highway Research, The University of Texas at Austin, August 1974.

91. Felipe Rivero-Vallejo and B. Frank McCullough, "Drying Shrinkage and Temperature Drop Stresses in Jointed Reinforced Concrete Pavements," Research Report 177-1, Center for Highway Research, The University of Texas at Austin, August 1973.
92. Teller, L. W. and H. L. Bosley, "The Arlington Curing Experiment," Bureau of Public Roads, Vol. 10, No. 12, February 1930.
93. Friberg, Bengt F., "Frictional Resistance Under Concrete Pavements and Restraint Stresses in Long Reinforced Slabs," Proceedings, Vol. 33, Highway Research Board, 1950.
94. Bresler, Boris, Reinforced Concrete Engineering, John Wiley and Sons, 1974.
95. Ferguson, Phil M., Reinforced Concrete Fundamentals, 3rd Edition, John Wiley and Sons, 1973.
96. Asphalt Overlays and Pavement Rehabilitation, Manual Series #17, The Asphalt Institute, November 1969.
97. McLeod, N. W., "Influence of Hardness of Asphalt Cement on Low-Temperature Transverse Pavement Cracking," Proceedings, Canadian Good Roads Association, 1970.
98. Heukelom, W., and A. J. G. Klomp, "Road Design and Dynamic Loading," Proceedings, Association Asphalt Paving Technologist, Vol. 33, 1964.
99. McCullough, B. F., and Harvey J. Treybig, "Determining the Relationship of Variables in Deflection of Continuously Reinforced Concrete Pavement," Departmental Research Report Number 46-4, Texas Highway Department, Aug. 1965.
100. Chang, Hang-Sun, Robert L. Lytton, and Samuel H. Carpenter, "Prediction of Thermal Reflection Cracking in West Texas," Research Report No. 18-3, Texas Transportation Institute, Texas A&M University, December 1975.
101. Tons, Egon and Vincent J. Roggeveen, "Field Testing of Materials for Sealing Cracks and Joints in Bituminous Concrete Resurfacings," HRB Bulletin No. 166, Highway Research Board, 1957.
102. Clary, A. G., "Sealing Cracks in Bituminous Pavements," A paper presented at the AASHTO 55th Annual Meeting in Philadelphia, October 1969.

103. "Asphalt in Pavement Maintenance," Manual Series 16, The Asphalt Institute, December 1967.
104. Tons, Egon, "Reflection Crack Sealing," Research Report 26, Joint Highway Research Project, Massachusetts Institute of Technology, June 1958.
105. Wilson, J. D., "Crack Control Joints in Bituminous Overlays on Rigid Pavements," Highway Research Board Bulletin 322, Highway Research Board, 1962.
106. Treybig, Harvey J., B. Frank McCullough and W. Ronald Hudson, "Continuously Reinforced Concrete Airfield Pavement - Volume I, Tests on Existing Pavement and Synthesis of Design Methods", Report No. FAA-RD-73-33-1, Prepared for Air Force Weapons Laboratory, U.S. Army Engineer Waterways Experiment Station and Federal Aviation Administration, May 1974.
107. "Repair East Runway Randolph Air Force Base", Report No. AF-2, Prepared for Department of the Air Force Headquarters 12th Flying Training Wing (ATC) - Randolph Air Force Base, Texas; Austin Research Engineers Inc, November 1976.
108. Srinarawat, Maitree, "Estimate the Cost Savings That May be Derived from Using a Variable Overlay Thickness Along a Project in Lieu of Designing for Minimum Conditions," Term Paper, Civil Engineering Department, University of Texas, May 1977.
109. McCullough, B. F., and C. L. Monismith, "Application of a Pavement Design Overlay System," Special Report No. 1, Center for Highway Research, The University of Texas at Austin, October 1969.
110. Shelby, M. D. and B. F. McCullough, "Determining and Evaluating the Stresses of an In-Service Continuously Reinforced Concrete Pavement," Report Number 62-1, Texas Highway Department, 1962.
111. Kelley, E. F., "Application of the Results of Research to the Structural Design of Concrete Pavements," Public Roads, August 1939.